DISSERTATION

INTEGRATING TISSUE DOSIMETRY AND MODE OF ACTION TO EVALUATE ATRAZINE DOSE-RESPONSE

Submitted by

Tami S. McMullin

Department of Environmental and Radiological Health Sciences

In partial fulfillment of the requirements

For the Degree of Doctor of Philosophy

Colorado State University

Fort Collins, CO

Summer 2005

COLORADO STATE UNIVERSITY

June 22, 2005

WE HEREBY RECOMMEND THAT THE DISSERTATION PREPARED UNDER OUR SUPERVISION BY TAMI S. MCMULLIN ENTITLED INTEGRATING TISSUE DOSIMETRY AND MODE OF ACTION TO EVALUATE ATRAZINE DOSE-RESPONSE BE ACCEPTED AS FULFILLING IN PART REQUIREMENTS FOR THE DEGREE OF DOCTOR OF PHILOSOPHY

Committee on Graduate Work

Robert J. Handa, PhD.

Colin Clay, PhD.

Marie E. Legare, PhD.

Melvin E. Andersen, PhD.

Advisor, William H. Hanneman, PhD.

Department Head, John D. Zimbrick, PhD.

ABSTRACT OF DISSERTATION

INTEGRATING TISSUE DOSIMETRY AND MODE OF ACTION TO EVALUATE ATRAZINE DOSE-RESPONSE

Atrazine (ATRA) is a widely used chlorotriazine herbicide that causes neuroendocrine effects in animal toxicity studies. Such effects include suppression of the LH surge in estrogen primed female, ovariectomized rats treated with high doses of ATRA. While the mechanism by which ATRA alters neuroendocrine function is not known, previous studies indicated that ATRA had anti-estrogenic properties *in vitro* and *in vivo*. In addition, ATRA is metabolized to chlorinated metabolites by P450 mediated saturable to oxidative metabolism and to non-chlorinated metabolites by GST-mediated GSH conjugation. Accurate determination of the risk of ATRA to exposed human populations is limited by uncertainties in extrapolating the dose-response behavior of a compound using animal toxicity data to predict responses in humans. Knowledge of tissue dosimetry (i.e., the tissue concentrations of ATRA and/or Cl-TRI metabolites that produce neuroendocrine responses) and mode of action (i.e., how ATRA and/or its metabolites interact with tissue constituents to cause these responses), is especially important for determining risk posed by ATRA exposure. The studies presented in this dissertation examined the anti-estrogenic mode of action of ATRA and DACT in brain and the processes that control the

kinetic disposition of ATRA and its metabolites in plasma and target tissue (the brain) under conditions that cause LH surge suppression.

A series of pharmacokinetic models were developed to describe *in vitro* and *in vivo* kinetic data on ATRA and its metabolites. The time-course concentrations of ATRA and the chlorinated metabolites in plasma and brain were regulated by dose-dependent and sequential absorption of compound from gut, oxidative metabolism in the liver and intestine, reactivity with hemoglobin in red blood cells and with plasma proteins, systemic clearance by GST mediated GSH conjugation and urinary elimination. These processes resulted in minimal concentrations of ATRA and retention of the mono-dealkylated metabolites and DACT in plasma and brain. DACT was the major chlorotriazine present in tissue, representing over 95% of total chlorotriazine area under the concentration curve after dosing with ATRA.

In evaluating the neuroendocrine mode of action of Cl-TRIs, we determined that ATRA and DACT suppress the LH surge by mechanisms other than altering binding of estrogen to its cognate receptors in the hypothalamus. Moreover, pituitary responsiveness was altered in animals treated with concentrations of DACT that suppressed the estradiol/progesterone induced LH surge. The high degree of reactivity of DACT with sulfhydryl residues in rat hemoglobin indicate that tissue reactivity of DACT should be considered as a possible mode of action rather than direct interaction, either inhibition or activation, with cellular receptor molecules.

These present studies have improved our understanding of the mechanisms by which chlorotriazines alter the LH surge and the factors that control chlorotriazine tissue dose under conditions where neuroendocrine responses are observed. As such,

these studies should assist low- dose, and to some extent, inter-species extrapolations of the dose-response behavior of chlorotriazines. This research has also identified additional mode of action and kinetic studies that will be required to create a complete model that describes the kinetic and biological effects to support low dose and interspecies extrapolation of risks in humans posed by ATRA.

Tami Sue McMullin
Department of Environmental and Radiological Health Sciences
Colorado State University
Fort Collins, CO 80523
Summer 2005

ACKNOWLEDGEMENTS

I would like to express my appreciation to my graduate committee, Dr. Melvin Andersen, Dr. William Hanneman, Dr. Marie Legare, Dr. Colin Clay and Dr. Robert Handa, for their consistent dedication to my professional and personal development over the past six years.

A special thank you to Dr. Melvin Andersen for the outstanding mentoring I have received during our time working together. His wisdom and approach to solving scientific and life questions will forever remain a part of my character that I hope to carry forward into my professional and personal life. Thank you for hanging in there with me.

My gratitude goes out to Dr. William Hanneman for taking me on board when the water was too deep to jump off the boat. I have greatly appreciated his guidance and encouragement about maneuvering through graduate school and especially his support through the successes and failures of all my animal studies. His personal and down to earth mentoring provided a wonderful and fun atmosphere in which to freely approach science.

I also express my appreciation to Dr. Robert Handa. Without his mentoring and the guidance of many people in his laboratory, I would not have fallen deeply into a beautiful bitter - sweet relationship with hormones and the brain. I am forever

indebted to his laboratory for taking me in as if I was a neuroendocrinologist instead of just one of those "toxicologists".

I especially thank the current and past post-doctorates in Dr. Handa's laboratory. I appreciate their unending patience, time and willingness to answer all my questions. I am grateful for their friendships and insight into life over many hours of conversation together in the laboratory. Wilson Chung spent an extensive amount of time teaching me rat perfusions and working through every possible glitch in immunocytochemistry. Toni Pak assisted me with running and interpreting LH radioimmunoassays and being a mom in science. I am eternally appreciative of Toni and Wilson's generosity in giving me a piece of their office and allowing me to set up baby bed and baby in their space. That was a lot to ask of a bachelor. These last two years would not have been possible without their kindness. I also thank Trent Lund, Wendy Poulliot and Alan Nagahara for all their assistance with my studies and animals.

Thanks to Dr. Marie Legare for keeping me from having to finish my graduate career in the basement of the Physiology building. The time of sharing her office space holds many great memories and moments of tapping into the wealth of knowledge right beside me.

I also want to express my appreciation to all the graduate students in Dr. Handa's and Dr. Hanneman's laboratory that took time out of their day(s) to help me with my extensive and time-consuming animal studies. I hope the beer and pizzas were worth it. I especially thank Marc Walmuth from the animal care facility for all the times he came in on his days off just to help. Thank you to Jill Brzezicki for

faithfully partnering with me during all of those studies until late at night. I will never forget our night goggle and lost rat moments. Perhaps, some lyrics for a song might come out of that.

Thank you to my family and dearest friends for their love, support and listening ears. All those times I said "I quit" and you kept me moving forward and encouraging me. Thank you to Rebecca and Bob Hinkle for spending a wealth of money and time to travel from California to watch my daughter Harmony so I could achieve this goal in my life. My mother always told me to pursue my deepest dreams and persist through the trials to attain those dreams. The pursuit of this degree is a bit of her wisdom at work. Thank you to the Mills family, Mark, Mary, Anna and Alexander, for cooperatively providing emotional and physical support for me by the love and care they gave to Harmony over the past 18 months. I am grateful for my other wonderful friend, Caroyln Yalin. If it wouldn't have been for graduate school and Harmony's arrival into the world, we would have never had a chance to foster such a wonderful friendship. I also want to thank my dearest friend, Tenley French, for the many hours of prayer, encouragement that I received to sustain me in my personal life and in school. The memories we made at CSU and all those outside of the laboratory will never leave me. Thanks for the many hours of dissertation reviewing you provided to help me make it to the finish line.

My deepest gratitude goes to my best friend and husband, Jaymes McMullin., who, after endless hours helping me finish this dissertation, might have thought twice about saying "sure, let's move to Colorado to get your PhD." I am thankful for his dedication to my desire to pursue this degree and his commitment to finding balance

between a meaningful, satisfied life as a family yet working hard to attain personal goals. With the same sense of adventure that brought us here, may the trials and achievements God has faithfully brought us through continue to teach us that we can step into the unknown. Thank you for being my partner on life's adventure over the last 6 years. I look forward to the new beginnings ahead for you, me and Harmony.

DEDICATION

I dedicate this dissertation to my daughter, Harmony Mattie McMullin. May you always be willing to take risks to pursue your dreams.

TABLE OF CONTENTS

LIST OF TABLES

LIST OF FIGURES

CHAPTER 1

GENERAL INTRODUCTION

1. 1. RATIONALE

Atrazine (2-chloro-4-ethylamino-6-isopropyl-amino-s-triazine, CAS# 1912-24-9, ATRA) is a chlorotriazine herbicide. It has been used since 1958 to control broadleaf and some grassy weeds by blocking photosynthesis (Gysin and Knuesli, 1960). Application on corn accounts for 86% of total ATRA usage. The remaining 14% is applied to sorghum, sugarcane, wheat, guavas, hay, and several types of trees. In the United States, 64-75 million pounds of ATRA are applied to crops annually by ground and hand-held sprayers, aircraft, and tractor-drawn spreaders (Hines et al., 2001).

ATRA has low volatility ($3.0x10^{-7}$ mm Hg at 20^0C) and low solubility in water (34.7 ppm at 22 °C). Due to its relative stability in neutral, slightly acidic soil, the half-life of ATRA in soil is approximately 1 year (Stevens and Sumner, 1991; EPA, 2001). These chemical and physical properties of ATRA, in addition to its widespread use, contribute to the prevalence of ATRA in surface and ground water. As such, drinking water is the predominant route of exposure. Other potential exposure routes include dermal and inhalation during the mixing and application process. The frequent environmental occurrence and exposure of ATRA prompted the U.S. EPA to regulate it under the Safe Drinking Water Act (SDWA). This action established a maximum contaminant level of 3 ppb ATRA (EPA, 2001). Indeed,

ATRA has been detected in groundwater at levels that exceed the maximum contaminant level during peak application periods (US EPA, 2001; Hines et al., 2001).

Although epidemiology studies have not provided evidence of a causal relationship between ATRA exposure and toxicity (Mitra et al., 2004), concern of a potential risk to humans from ATRA exposure stemmed from the observations that lifetime administration of high doses of ATRA in feed caused an increase in the incidence and decrease in the latency of mammary tumor formation in female Sprague Dawley rats (Eldridge 1994a, 1999a). However, this tumorigenic effect was strain, sex and species specific (Eldridge et al., 1999a). The results from these studies prompted further investigation into the mode of action by which tumorigenesis in female SD rats was occurring. These studies lead to the discovery that ATRA exposure altered estrous cycling patterns in female SD rats (Eldridge et al., 1994) in a manner that produced a hormonal environment conducive to mammary tumor development (Eldridge et al., 1999a). Such observations consistent with this conclusion included the ability of high oral doses of ATRA to suppress the estrogen primed (Cooper et al., 2000) and proestrus (Eldridge et al., 2001) LH and FSH surge in female rats. More recent studies have also observed delays in pubertal development in male and female offspring of dams exposed to ATRA (Peruzovic et al., 1995; Stoker et al., 1999, 2000, 2002; Laws et al., 2000). Research examining the mode of action by which ATRA causes neuroendocrine toxicity have suggested a potential anti-estrogenic effect of this herbicide. ATRA was weakly anti-estrogenic

in studies examining estrogen mediated uterine responses (Tennant et al., 1994a) and in cellular models (Tennant et al., 1994b; Tran et al., 1996; Connor et al., 1996).

Upon administration, ATRA undergoes extensive hepatic metabolism in the body. In the rat, ATRA is metabolized by P450 mediated oxidation to mono-dealkylated chlorinated metabolites (ETHYL and ISOPROPYL) and subsequently metabolized to the di-dealkylated chlorinated metabolite, diaminochlorotriazine (DACT) (Hanoika et al., 1999a, b; Timchalk et al., 1990). These chlorinated compounds (collectively termed Cl-TRIs) are eliminated in urine or metabolized by glutathione-S-transferase mediated glutathione conjugation to non-chlorinated conjugates. The conjugates are subsequently eliminated into urine and feces (Bakke et al., 1972; Timchalk et al., 1990). Although the majority of ATRA is quickly metabolized and eliminated, radiolabeled studies indicate some accumulation in red blood cells and plasma after multiple doses in rats suggesting reactivity of these compounds with blood proteins (Thede 1987).

The neuroendocrine effects observed after ATRA administration do not occur after exposure to non-chlorinated triazines such as hydroxyatrazine (Eldridge et al., 1994), suggesting that these responses likely result from target tissue exposure to Cl-TRIs rather than the non-chlorinated triazines. Therefore, it has been proposed that health risk assessments for ATRA should be based on net tissue exposure to total Cl-TRIs rather than administered ATRA (U.S.EPA, 2001). Despite this proposal, the limited information on the pharmacokinetic (PK) disposition of ATRA and its chlorinated metabolites *in vivo* and *in vitro* make it difficult to predict tissue

exposures of atrazine and its metabolites after specific oral doses of this herbicide from the existing data.

Evaluating the risk of neuroendocrine disruption in humans by ATRA exposure using animal toxicity data requires extrapolating data from high doses used in animals studies to low, environmentally relevant doses (high-low dose extrapolation) and from animals to humans (interspecies extrapolation). The limited dosimetry data combined with studies indicating anti-estrogenic activity and protein reactivity of Cl-TRIs lead us to examine the pharmacokinetic disposition of Cl-TRIs in plasma and brain (tissue dosimetry) and the relevance of anti-estrogenicity of ATRA on suppression of the LH surge. Combined, these studies provide a consistent and more comprehensive framework from which to link tissue dosimetry and mode of action data to predict risk of ATRA to humans (Andersen 1995a, 2001) (Fig. 1.1).

1.2. RISK ASSESSMENT AND THE DOSE-RESPONSE PARADIGM

Evaluating the risk posed by a chemical to human health requires the complex integration of risk assessment and risk management. The information gathered from these two areas are used to determine the acceptable measures of risk to a human population of concern (NRC, 1983; Roberts and Abernathy, 1996). Risk assessment characterizes the potential adverse health effects of human exposure to hazardous environmental agents while risk management evaluates the regulatory, economic, social and political issues surrounding the responsible agent.

The risk assessment process consists of four steps: (1) hazard identification, (2) dose-response assessment, (3) exposure assessment, and (4) risk characterization.

Hazard identification combines epidemiological and toxicological data to determine a causal association between the compound and an effect. If a causal association exists, a dose-response assessment is performed to quantitatively evaluate the relationship between dose and the effect of concern. Exposure assessment estimates the known or potential concentration of a compound in the human population of interest and risk characterization combines information from exposure assessment and dose-response assessment to determine the risk to human health (NAS, 1983; DHHS, 1985).

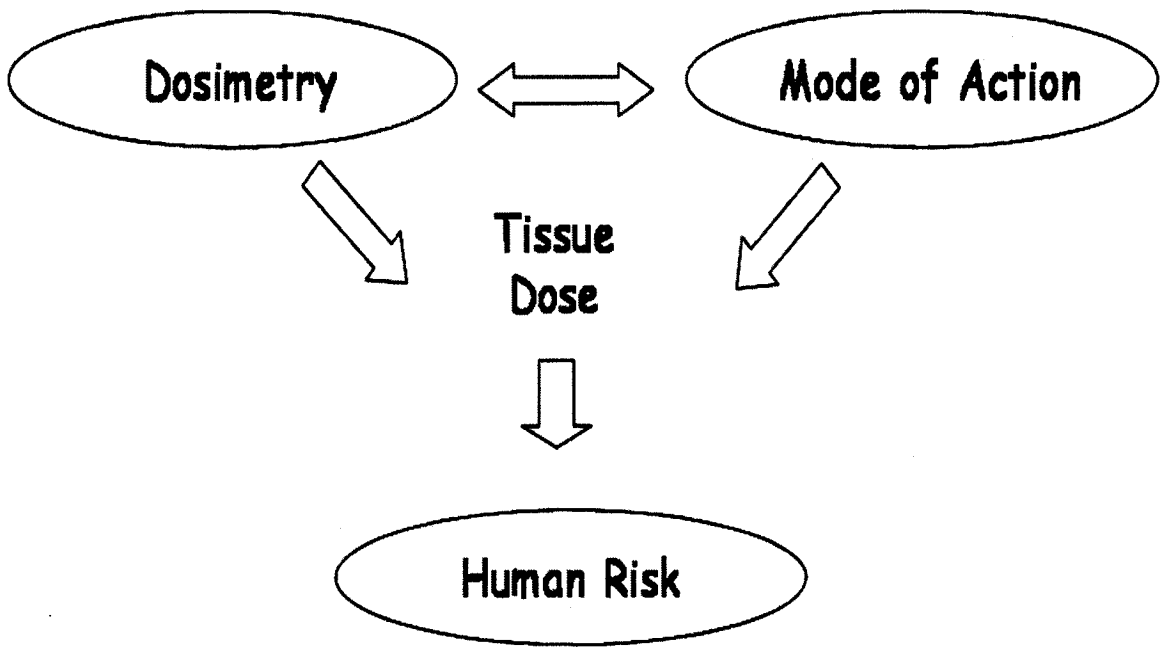

Figure 1.1. A more consistent framework of studies that integrate data on the mode of action and dosimetry of ATRA is needed to improve present estimates of the biological and physicochemical factors that lead chlorotriazine tissue dose and more accurately extrapolate results in animal studies to predict risk to humans.

Appropriate determination of the dose-response relationship of a chemical for specific toxic effects is an area of debate. In the past, estimations of the dose-response relationship related an external measure of dose (i.e. administered dose, concentration in air) to the toxic response (Fig. 1.2). Andersen (1995a) has described this as the black box approach since it neglects the chemical and biological processes that occur upon entrance of the chemical into the body. Ideally, well characterized human epidemiologic and kinetic data would exist to establish the dose-response behavior of a compound. However, predictions about dose-response relationships are typically determined in the absence of human data and therefore necessitate decision making amidst the following uncertainties. These main uncertainties include: (1) extrapolation from high to low dose scenarios (2) Exclusively using animal data to determine the kinetic behavior of a compound in humans (i.e. interspecies extrapolation) and (3) prediction of the behavior of a chemical via different routes of administration (i.e. oral, dermal, inhalation extrapolation). There is a growing awareness of the need to address these uncertainties by integrating mode of action and tissue dosimetry data, thereby developing more biologically motivated risk assessments of chemicals (ILSI, 2001).

1.2.1. Tissue dosimetry

The appropriate dose metric for dose-response assessment depends on the chemical and the response of interest. However, to address the various uncertainties that exist in extrapolation, dose has to be defined appropriately, i.e., as "some measure of the intensity of chemical exposure which is directly linked to the biological processes leading to toxicity or tumor formation" (Andersen, 1981). By

this definition, knowledge of tissue dosimetry and mode of action of a compound are essential components in determining the dose-response for prediction of human risk (Fig. 1.2).

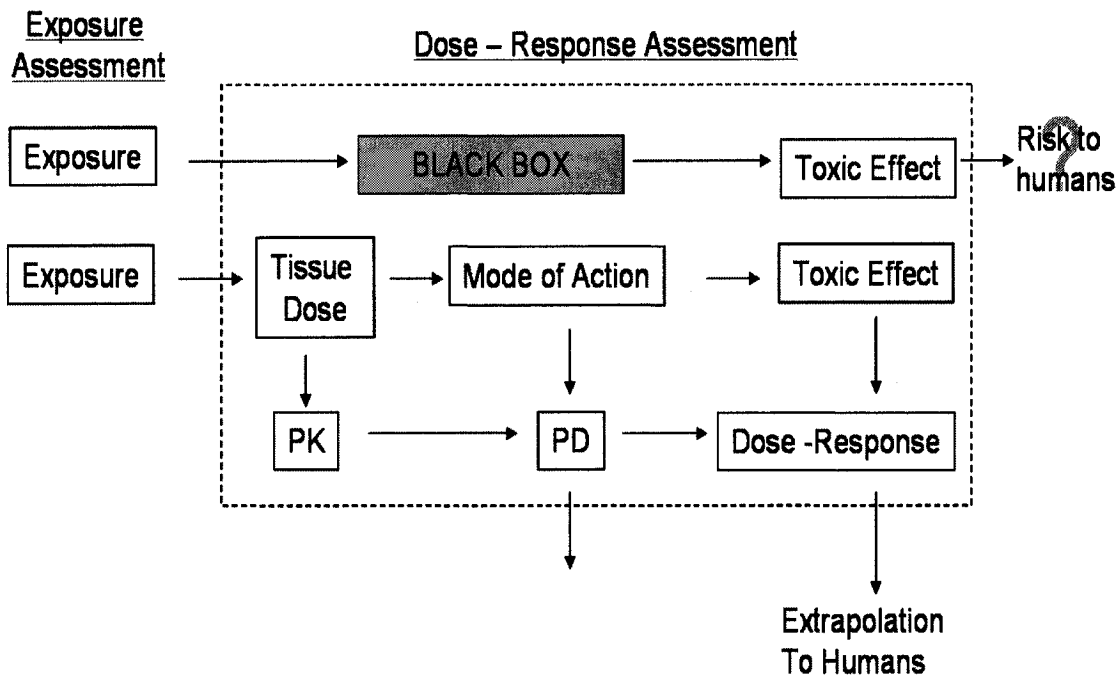

Figure 1.2. In the past, a black box approach was taken to relate exposure to a toxic effect. This essentially neglected the pharmacokinetic and pharmacodynamic processes that occur in the body to result in the toxic effect. As quantitative tools, such as physiologically based pharmacokinetic modeling (PBPK), have arisen to examine these processes, the concepts of tissue dose and mode of action have replaced the black box approach. This evolution has allowed greater consideration of the underlying biological and physicochemical processes that determine the dose-response curve. Approaching risk assessment in this manner reduces uncertainties involved in high dose to low dose, interspecies and route to route extrapolation (Adapted from Andersen 1995a and Barton and Andersen, 1998).

1.2.2. Mode of action

Tissue dose cannot be properly interpreted without an understanding of mode of action. Mode of action refers to the general interactions of a chemical within the body to produce a toxic effect (Andersen and Dennison, 2001). Mode of action data help determine appropriate measures of tissue dose by defining the form of compound contributing to the toxic response, the site of action by which the chemical produces the toxic effect of concern, and the interactions of the chemical with biological processes to cause target tissue responses. Quantitative analysis of mode of action of a chemical for extrapolation in risk assessment is termed pharmacodynamics (PD) (Fig. 1.2) (Barton and Andersen, 1998).

1.3. INTEGRATING TISSUE DOSIMETRY AND MODE OF ACTION TO ASSESS RISK: UTILIZATION OF PHYSIOLOGICALLY BASED PHARMACOKINETIC MODELS

Physiologically based pharmacokinetic (PBPK) modeling arose out of a need to minimize the uncertainties that exist in dose-response assessment. The goal of PBPK modeling is to translate an external measure of dose into a quantitative internal dose metric that more appropriately relates to dose and effect (Dedrick, 1973; Clewell and Andersen 1985). PBPK models are usually developed and refined using an iterative process that includes the utilization of PK studies from the literature and/or addition data gathered in the laboratory to address certain data gaps (Fig 1.3).

These mechanistic based models are computer simulation tools that portray the body as a series of connected tissue compartments with differential equations.

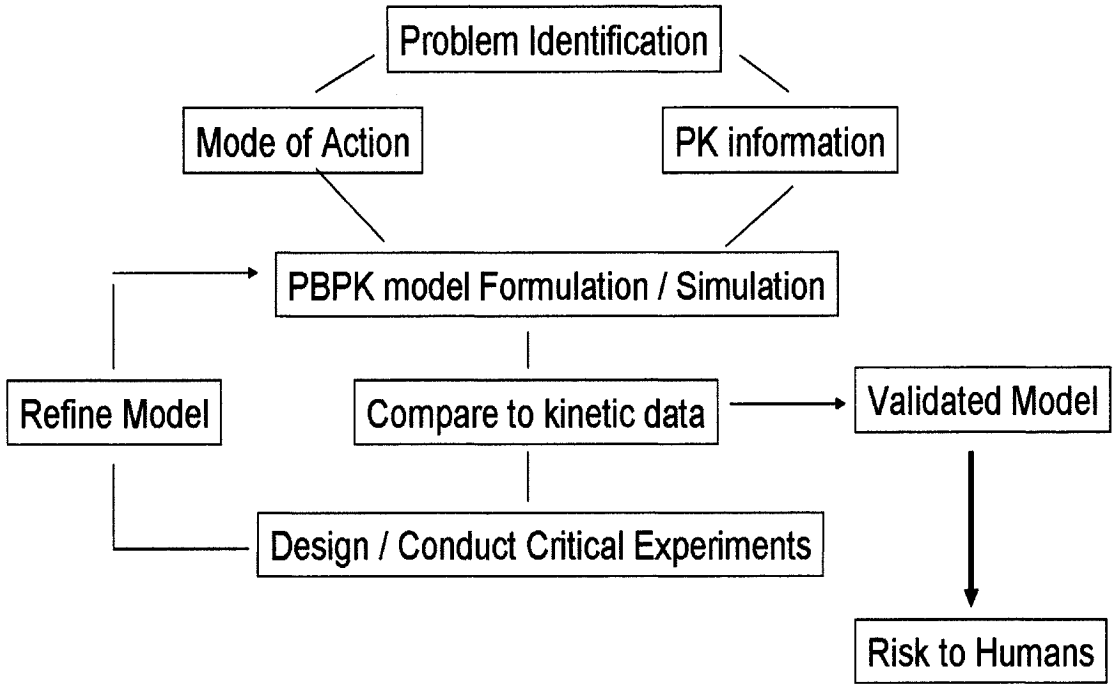

Figure 1.3. Assessing risk to humans requires information on the mode of action and pharmacokinetic disposition of the toxicant. These data can be used to develop PBPK models that assist in estimating risk. The process of PBPK model development assists in refining hypotheses and focusing experimental efforts on critical studies to predict human risk (Adapted from Andersen 1981).

The equations are mathematical descriptions of the underlying biological and physicochemical processes that contribute to the time-course concentrations in plasma and tissue. The transport of a chemical through the compartments is described by physiological and biochemical parameters such as blood flow, tissue volume, protein and macromolecular binding constants, tissue solubility, ventilation rates and metabolic capacity.

PBPK models are valuable tools in designing more hypothesis driven and focused experimentation because the process of developing explicit models of

chemical delivery to tissues often exposes data gaps in the exposure-dose-response paradigm (Andersen 1981; Leung, 1991) (Fig 1.3). The theory and application of PBPK modeling within the risk assessment process has been described in more detail in several review papers (Chen and Blancato, 1987; D'Souza and Boxenbaum, 1988; Andersen 1995a,b,c,d,e; Kedderis and Lipscomb, 2001).

1.4. PHARMACOKINETIC DISPOSITION OF ATRAZINE

The PK disposition of a compound is dictated by absorption, distribution, metabolism and elimination (ADME) processes that result in the circulating free (unbound) plasma concentration. Describing the plasma time-course profile of a compound is important because it also reflects the tissue concentrations (i.e. target tissue). The *in vitro* and *in vivo* PK studies described below examined the general disposition of ATRA.

2.2.1. Absorption

The half-life of absorption of an oral gavage dose of 30 mg [^{14}C]-ATRA/kg b.w. in the rat is 2.6 hrs (Timchalk et al., 1990). Similar absorption rates have been observed in monkeys and humans after oral administration (Ciba –Geigy report). Percutaneous absorption of [^{14}C]-ATRA differs between species. Percent of absorption ranges from 1.2 - 5.6% in man compared 27% for rats (Simoneaux et al.; Ademola et al, 1993).

2.2.2. Distribution

[^{14}C]-ATRA is extensively and rapidly cleared from the body with minimal accumulation in tissue compartments. 72 hours after an oral gavage dose of 30mg [^{14}

C]-ATRA/kg to male F344 rats, 66% of the administered dose was in the urine, 19% in the feces, 1.5% in the skin, 4% in the body, 0.08% in the plasma and 1.24% in red blood cells (Timchalk et al., 1990). Similarly, acute and sub-chronic oral gavage doses of [^{14}C]-ATRA resulted in 4.6 – 7.5% found in body tissues, 18.8% in feces and 73.6% in urine seven days after dosing (Orr et al., 1987). Repeated administration of [^{14}C]-ATRA does not alter the pattern of distribution of radioactivity (Thede, 1987).

The distribution of a chemical is also influenced by biological and physicochemical factors, such as protein (i.e. receptor, blood constituents) binding and/or reactivity, lipophilicity, and solubility. Sulfoxide metabolites of s-triazine compounds such as ametryn and simetryn covalently react with cysteine residue on β-125 of rat hemoglobin *in vitro* (Hamboeck et al., 1981). This binding is species dependent - minimal binding occurs in human red blood cells (RBCs) while the highest binding occurs in rat RBCs. Although minimal compared to the binding observed with sulfoxide derivatives, approximately 6% of radiolabeled ATRA was covalently bound to rat hemoglobin after 24 hours incubation in vitro (Hamboeck et al., 1981). Consistent with covalent RBC reactivity, time-course studies with radiolabeled ATRA indicated that RBC's contained high concentrations of radioactivity. Approximately 1-2% of the radiolabeled dose was retained in red blood cells (RBC's) after single and multiple oral gavage administration in rats at times when unbound plasma concentrations were expected to be small (Miles and Orr, 1987; Orr et al., 1987; Thede, 1987; Timchalk et al., 1990).

The accumulation of radioactive equivalents of ATRA *in vivo* is likely representative of DACT reactivity to hemoglobin (Hb) in RBC's. Incubation of [^{14}C]-DACT with isolated rat hemoglobin caused a dose and time-dependent increase in radioactivity recovered in Hb while [^{14}C]-ATRA showed no binding *in vitro* (Prentiss 2004). MALDI-TOF analysis indicated that DACT did not covalently react with Hb to produce adducts *in vitro*. However, SD rats administered 300mg ATRA/kg for 3 days had high levels of Hb adducts that were identical to those formed after dosing with DACT. These results suggested that adduct formation was dependent on *in vivo* processes that were absent *in vitro*, such as enzymatic processes (Prentiss 2004).

2.2.3. Metabolism

Metabolism is critical to the toxicity of many compounds (Andersen, 1981). Depending on whether or not the toxicity is due to the parent compound or a metabolite, metabolism can either limit toxic responses or lead to the toxic endpoint of concern (Andersen et al., 1980). Most metabolic processes have limited (saturable) capacity because they are regulated by metabolizing enzymes such as glutathione (GSH) and cytochrome P450s. While saturation is unlikely in human exposure scenarios (low-dose ranges), animal toxicity studies are often in the dose range that can deplete metabolizing enzymes, resulting in non-linear tissue dosimetry (D'Souza et al., 1988; Reitz et al., 1988). Since these processes are dose-dependent, their characterization is important for predicting low-dose behavior of a chemical (Andersen et al., 1987; Leung, 1991)

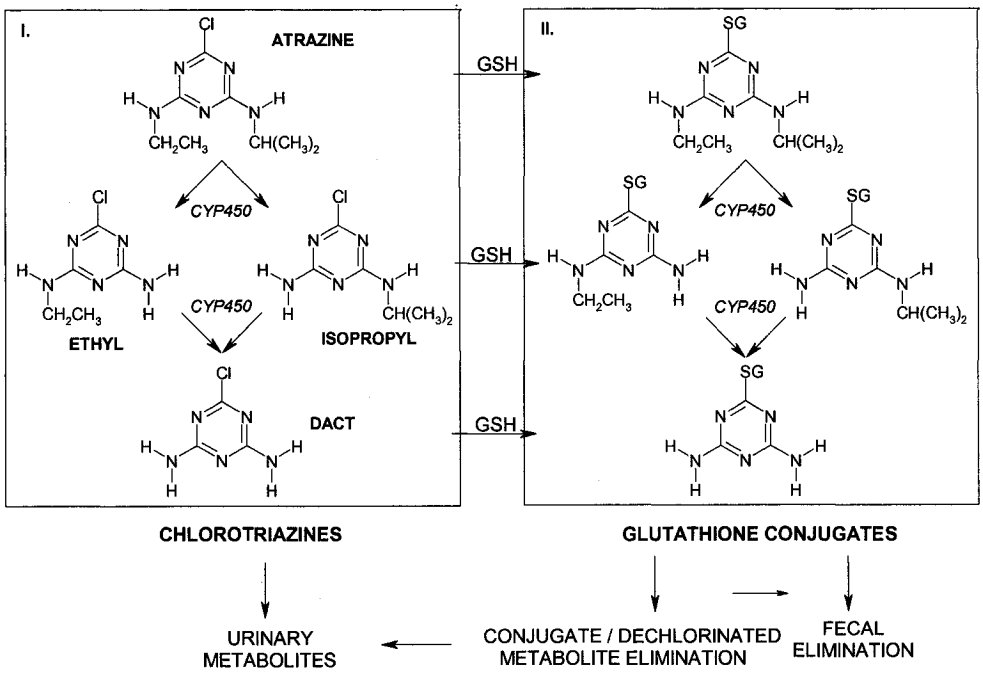

Fig. 1.4. ATRA is metabolized to (I) chlorinated metabolites via oxidative metabolism and to (II) non-chlorinated metabolites via GST mediated GSH conjugation. Chlorotriazines are eliminated in urine and GSH conjugates are eliminated in urine and feces

ATRA is extensively and rapidly metabolized in the liver (Bakke et al., 1972; Meli et al., 1992). *In vitro* and *in vivo* studies indicate that ATRA undergoes N-monodealkylation by cytochrome P450 oxidation to dealkylated, chlorinated metabolites (Timchalk et al., 1990; Hanoika et al., 1999; Hanoika et al., 1999b). ATRA and its chlorinated metabolites are also metabolized by glutathione (GSH) conjugation to form non-chlorinated conjugates that are further metabolized and eliminated in urine and feces (Fig. 1.4). Unmetabolized ATRA was not detected in urine at 24 hours while 2-chloro-4, 6-diamino-1, 3, 5-triazine (DACT) accounted for 70% of total urinary radioactivity. The mono-dealkylated metabolites of ATRA, 2-

chloro-4-amino-6-methylehtylamino-1, 3, 5-triazine (ISOPROPYL) and 2-chloro-4-amino-6-ethylamino-1, 3,5-triazine (ETHYL) were 5% and less than 1.0%, respectively. Mercapturic acids comprised 22% of urinary radioactivity, representing GSH conjugation of the Cl-TRIs (Timchalk et al., 1990).

2.2.4. Elimination

Urine is the principal route of excretion of metabolites of ATRA regardless of route of administration, dosing regimen, species and sex (Orr et al., 1987). High and low dose studies indicate that approximately 66% of orally administered [^{14}C]-ATRA to rats is eliminated in urine and 34% in feces within 72 hours (Miles and Orr, 1987; Timchalk et al., 1990). Orally administered doses ranging from 1-100 mg in rhesus monkeys resulted in 56% of total dose in urine and 27% in feces after 168 hours (Ciba –Geigy, internal report). In man, 90% of an administered dermal dose was in urine by 168 hours (Simoneaux et al., 2001). Intravenous administration to monkeys resulted in 44% of total radioactivity in urine at 12 hours and 84% by 168 hours. Studies on ATRA elimination indicate that oxidative metabolism to chlorinated metabolites is the predominant metabolic pathway. After an oral gavage dose of 30 mg ATRA/kg, chlorinated metabolites made up 75% of total urine radioactivity with DACT representing 67% of this portion. The remaining 25% of radioactivity was comprised of mercapturic acids that represented GSH conjugation products in which the chlorine is lost during glutathione conjugation. In addition to urinary excretion, approximately 50% of mercapturic acids are eliminated in feces (Timchalk et al., 1990). Consistent with other studies, DACT was the major urinary metabolite after acute and sub-chronic dosing of 100 mg/kg/day via oral gavage (Miles and Orr,

1987). Metabolic and elimination patterns are species independent. The profile of urinary metabolites in humans is similar to the rat (Ikonen et al., 1988).

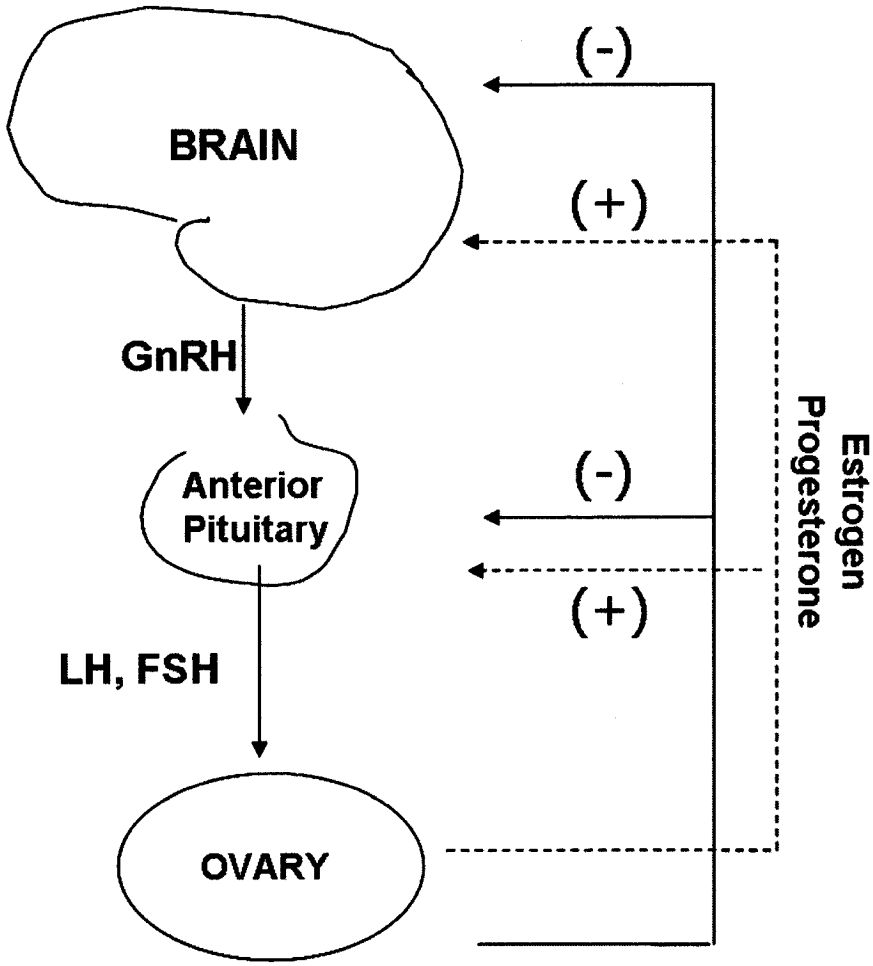

Figure 1.5. Diagram of the regulation of the hypothalamic –pituitary-gonadal (HPG) axis in female rats. Gonadotropin releasing hormone (GnRH) neurons are the central regulators the HPG axis. GnRH released into portal circulation in the median eminence (ME) directly causes synthesis and release of luteinizing hormone (LH) and follicle stimulating hormone (FSH) from gonadotrophes in the anterior pituitary. These circulating hormones bind to receptors on the ovaries to release the sex steroid hormones estrogens (i.e. 17β-estradiol (E_2) and progestins (i.e. progesterone (P_4)). During most of the estrous cycle in the rat, steroids provide a negative feedback onto the brain and pituitary. In the afternoon preceding proestrus, E_2 combined with stimulatory influences from P_4 provide the necessary steroidal environment for initiation of the LH surge and consequent ovulation.

1.5. MODE OF ACTION: NEUROENDOCRINE REGULATION OF REPRODUCTION

The physiological targets of ATRA toxicity have been established. High doses of ATRA and its chlorinated metabolites cause several neuroenodcrine effects such as mammary tumorigenesis, decreased concentrations of steroid hormones in plasma, and reproductive and developmental changes. ATRA also suppresses the proestrous and estrogen induced LH surge, a regularly used marker to assess neuroendocrine toxicity of compounds (Cooper et al., 1999). The processes that control these neuroendocrine effects of ATRA are regulated by the hypothalamic-pituitary-gonadal axis. Hence, the following sections describe the regulation of the HPG axis.

1.5.1. The hypothalamic-pituitary-gonadal (HPG) axis

The synthesis and release of hormones from each tissue that comprises the hypothalamic–pituitary-gonadal axis are critical to normal reproductive function (fig. 1.5). However, GnRH neurons in the hypothalamus provide the central neural control of this axis (Gore 2001). Unlike other neuronal populations, GnRH neurons are sparse in number (800-2000) and their cells bodies are distributed throughout several hypothalamic regions rather than located as a discrete nucleus. In rats, the cell bodies of GnRH neurons that are known to regulate gonadotropin secretion are located primarily in the preoptic area (POA) and organum vasculosum of the lateral terminalis (OVLT) regions of the hypothalamus (Porkka-Heiskanen et al., 1994; Petersen et al., 1996). These neurons synthesize and package the GnRH decapeptide

in storage vescicles that are transported to the nerve terminals. GnRH axons project to the median eminence (ME) where they release GnRH into the portal circulation.

GnRH secretion occurs in discrete pulses that are critical for normal reproductive function and gonadotropin release. For example, continuous infusion of GnRH in ovariectomized (OVX) rhesus monkeys caused suppression of LH whereas intermittent infusion of GnRH produced normal pulsatile LH release (Belchetz et al., 1978). In humans, administration of continuous versus intermittent GnRH analogues produces similar effects on LH (Conn and Crowley, 1991).

GnRH secretion directly regulates gonadotropin synthesis and secretion throughout the estrous cycle in the female rat (Ching et al., 1982; Sarkar et al., 1976; Levine 1982). Upon entering portal blood, GnRH binds to GnRH receptors on the cell surface of gonadotrophes residing in the anterior pituitary (Millar 2004). Before and during proestrus, increased GnRH release up-regulates GnRH receptor mRNA levels to prime the pituitary for the surge in LH (Bauer-Danton et al., 1995). Activation of the GnRH receptor, a G-coupled protein, initiates a cascade of intracellular signal transduction pathways that regulate synthesis and release of the gonadotrophins LH and FSH (Naor 1998).

LH and FSH release from the anterior pituitary circulate in plasma and enter target tissues such as the ovary, where these gonadotrophins bind to their cognate receptors (Hillier 1994). FSH stimulates follicular development in the granulosa cells whereas LH primarily acts to stimulate secretion of estrogen within these cells. The enzyme CYP19 (aromatase) located in granulosa cells is responsible for the conversion of testosterone (T) to estrogen (17β-estradiol; E_2). In females, production

and release of the steroid hormones E_2 and progesterone (P_4) are critical in regulating feedback mechanisms along the HPG axis.

1.5.2. Steroid regulation via nuclear receptors

Steroids primarily exert their effects in various tissues by binding to their cognate receptors, members of the superfamily of nuclear receptors (Evans et al., 1998). These receptors are intracellular transcription factors that reside in the nucleus and/or cytoplasm in an inactive state. Ligand binding causes dimerization of the receptor and translocation of the ligand-receptor complex to specific sequences on DNA, termed hormone response elements. Upon binding, co-regulatory complexes such as co-activators are recruited and aid in additional recruitment of transcriptional machinery required for initiation of gene transcription (for review see Rochette-Egly, 2003; Tsai and O'Malley, 1994).

In females, E_2 is the primary steroid responsible for regulating GnRH release from the brain and gonadotrophin release from the pituitary (Chappel and Levine 2000; Herbison 1998). Estrogen produces cellular responses by binding to its "classical" receptor, estrogen receptor alpha (ERα) (Toft and Gorski, 1966) and the more recently discovered receptor, ERβ (Kuiper et al., 1996) (fig. 1.6). These ERs are encoded by two separate genes and have distinct expression patterns in tissue. For example, ERα and ERβ partially overlap in expression in the brain (Shughrue et al., 1997) while the pituitary primarily expresses ERα (Scully et al., 1997) (for review see Shupnik 2002). Studies using ERα and ERβ knockout mice have demonstrated that ERα is the critical receptor for mediating most reproductive functions, such as LH release (Couse and Korach, 1999; Krege et al. 1998; for review see Hewitt and

Korach, 2003). Couse and Korach (1999) demonstrated that ERα knockout mice had increased levels of LH (due to loss of negative feedback from estrogen) while LH levels in ERβ knockouts were normal.

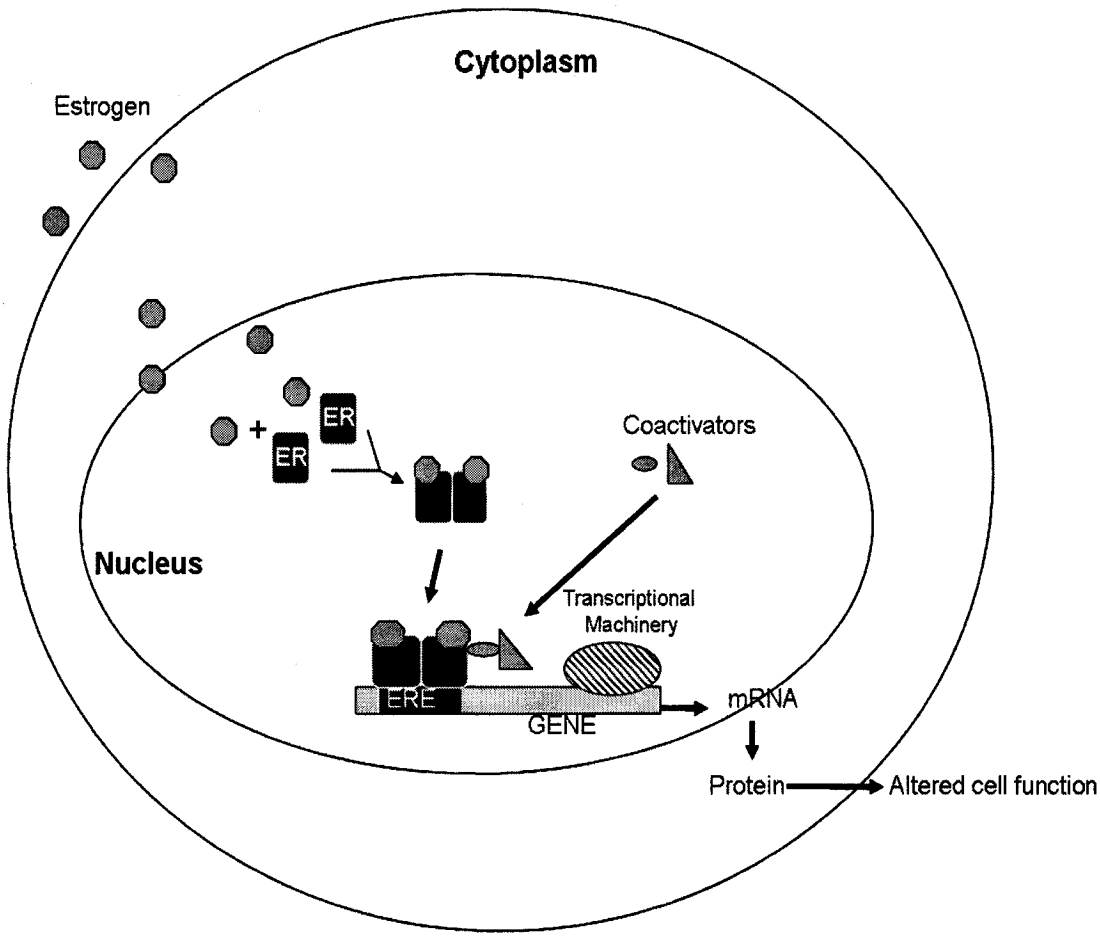

Figure 1.6. Diagram of the classical mechanism by which estrogen (E_2) mediates cellular responses by binding to its nuclear receptors ERα and ERβ. Ligand binding causes dimerization and translocation of the E_2-ER complex to specific sequences on DNA of target genes, called estrogen response elements (ERE). Coactivators are recruited and initiate further recruitment of the general transcriptional machinery required for initiation of gene transcription.

1.5.3. Steroid Feedback

Estrogen is critical in communicating at every level of the HPG axis via feedback mechanisms. Removal of endogenous estradiol by ovariectomy increases levels of GnRH in portal circulation that are rapidly reduced upon infusion of E_2 (Sarkar and Fink 1980), indicating that estrogen exerts a negative feedback onto the GnRH neurons to inhibit basal secretion of GnRH. In contrast to its inhibitory effects, exposure to E_2 for several hours is required to stimulate GnRH secretion for initiation of the LH surge (Sarkar et al., 1976; Ching, 1982; Moenter et al., 1990; Legan et al, 1975). Consistent with studies indicating a bimodal influence of E_2 on GnRH release, GnRH mRNA expression is suppressed throughout the estrous cycle except early in the afternoon prior to the LH surge (Petersen et al., 1995). However, other studies examining GnRH mRNA have produced contradictory results, suggesting that GnRH mRNA expression patterns are likely influenced by multiple signals rather than exclusively by E_2 (reviewed in Petersen et al., 2003). Studies evaluating GnRH heteronuclear RNA, the primary transcript of the GnRH gene have provided a clearer indication that estrogen increases GnRH transcriptional activity in GnRH neurons throughout the OVLT and POA prior to and after the LH surge (Petersen et al., 1996; Jimenez-Linan and Rubin, 2001).

Estrogen feedback on the brain is largely mediated by several neuronal populations within the anteroventroperiventricular (AVPV) nucleus. This nucleus is located adjacent to the third ventricle within the rostral region of the preoptic area (POA) of the hypothalamus. These neurons project to the OVLT, the region that contains sub-population of GnRH neurons responsible for regulating gonadotrophin

release (Gu and Simerly, 1997; Chappel 2002). Early neuroanatomical studies have demonstrated the importance of the AVPV in regulating E_2 mediated LH secretion. OVX rats lesioned in the AVPV region displayed persistent estrus and a loss of the E_2 –P primed LH surge (Wiegand et al., 1980). In addition, OVX rats implanted with estradiol into the AVPV released LH, demonstrating that this region was estrogen responsive (Kalra and McCann, 1975). Consistent with results from these early studies, neurons residing in the AVPV highly express ERα immunoreactivity (Pfaff and Keiner, 1973) and ERα mRNA (Simerly et al., 1990; Simely et al., 1996). These estrogen responsive neuronal populations release neurotransmitters and other peptides that directly act on GnRH cell bodies or neuroterminals to stimulate and/or inhibit GnRH synthesis and release. Moreover, ERβ mRNA (Hrabovszky et al., 2001) and protein are expressed in 50-60% of native GnRH neurons (Kallo et al., 2001), lending to the possibility that this receptor might provide a mechanism for direct regulation of estrogen on GnRH release.

1.5.4. Estrous cyclicity and the LH surge

Female rats undergo a 4 day estrous cycle that is divided into four phases: metestrus, diestrus, proestrus and estrus. During metestrus and diestrus, E_2 produced in developing ovarian follicles exerts a negative feedback onto the hypothalamus and pituitary leads to a basal, pulsatile secretion of LH and FSH. As the follicles mature, they continue to produce increasing amounts of E_2, eventually reaching a critical, circulating concentration of E_2 and P_4. This steroid environment in addition to a central circadian input from the suprachiasmatic nucleus (SCN) (Barbacka-Surowiak et al., 2003) triggers a positive feedback onto the hypothalamus and pituitary. This

stimulatory feedback results in a dramatic surge in GnRH/LH secretion that occurs between 1400 -1600 h on proestrus to initiate ovulation. In the rat, P_4 is required to generate a steroid induced surge that reflects the amplitude of the surge on proestrous (Lee et al., 1990). This stimulatory action of P_4 might be mediated in part, by increasing GnRH neruonal activity (Lee et al., 1990). In addition, E_2 up-regulates progesterone receptors (PR) expression within the AVPV and MPOA to provide additional positive feedback of P_4 during the LH surge (Simerly et al., 1996; Shughrue et al., 1997; Chappell and Levine, 2000).

1.6. MODE OF ACTION: NEUROENDOCRINE EFFECTS OF ATRAZINE

1.6.1. Mammary Tumorigenicity

A review of over 50 studies indicates that ATRA is not genotoxic *in vivo* or *in vitro* (Brusick, 1994). However, results of long -term carcinogenicity studies with ATRA prompted concern for a potential carcinogenic risk to humans. Lifetime dietary exposure of ATRA at or above the MTD (400ppm) caused persistent estrus accompanied by an increase in the incidence of mammary adenocarcinomas and/or fibroadenomas in female Sprague-Dawley (SD) rats (Wetzel et al., 1994; Eldridge et al., 1999; Eldridge et al., 1999; Stevens et al., 1999). However, these responses were strain, sex and tissue specific. They did not occur in male SD rats, female Fischer 344 rats or in three strains of male and female mice (Wetzel et al., 1994; Thakur et al., 1998; Stevens et al., 1999). One interesting finding was that OVX female SD rats receiving doses of ATRA that produced tumor formation in intact SD rats did not form mammary tumors, suggesting that mammary tumorigenesis was mediated by

circulating concentrations of E_2 (Stevens et al., 1999). Based on species specific effects of ATRA and the biological mechanisms that contribute to mammary tumor formation in SD rats, it is generally believed that ATRA acts by a neuroendocrine mode of action to accelerate normal age-related tumorigenesis in female SD rats (Eldridge et al., 1999; Breckenridge et al., 2001). This conclusion prompted a decision by the EPA in 2001 to assess risk of Cl-TRIs based on a neuroendocrine mode of action rather than carcinogenicity (Eldridge et al., 1999; Simpkins et al., 2000; EPA, 2001)

1.6.2. Estrous cyclicity

Several studies indicate that ATRA disrupts ovarian function by altering normal cycling patterns in adult female rats. Lifetime dietary exposure of 400ppm ATRA caused age and dose-dependent persistent estrus in SD rats (Wetzel et al., 1994). Administration of 150mg ATRA/kg/day for 21 days increased time in diestrus in SD and Long Evans (LE) rats (Cooper et al., 1996). Female Fischer 344 rats dosed with 120mg/ATRA/kg/day for 7 days via oral gavage (Simic et al., 1994) displayed extended diestrus. A similar observation has been noted in female pigs fed 1 mg ATRA/kg/day for 19 days in diet (Gojmerac, 1999).

1.6.3. Alterations in hormone profiles in adult female rats

In intact regularly cycling female LE rats, administration of 300 mg/kg/day ATRA produced undetectable serum levels of sex steroids plasma E_2 and P_4, accompanied by low levels of pituitary hormones LH, follicle stimulating hormone (FSH) and prolactin (PRL) (Cooper et al., 1996). Several studies have also assessed the ability of ATRA to alter the proestrous and E_2 primed LH surge in rodent models.

OVX, E_2 primed female LE rats receiving 1 or 3 daily doses of 300mg ATRA/kg demonstrated a suppressed LH and PRL surge. However, LH was not affected in SD rats and PRL was decreased only after 3 doses of 300 mg ATRA/kg/day, suggesting that LE rats might be more sensitive to suppression of the pituitary hormones than SD rats. Sub-chronic administration of at 150 and 300 mg ATRA/ kg/day ATRA (21 days) decreased peak levels of the steroid induced LH and PRL surge in both rat strains. These decreases in serum gonadotrophin levels were accompanied by a significant dose-dependent increase in pituitary tissue concentrations of PRL and an increasing trend in pituitary LH (Cooper et al., 2000). In contract to these results, OVX SD rats administered 150 and 200 mg ATRA kg 3 times /day for 4 days had significantly elevated serum PRL levels (Connor et al., 2000), suggesting that estrogen might be mediating the effects observed on PRL. Long term administration of ATRA also affects LH secretion. Exposure to 400ppm ATRA in feed for 6 months significantly decreased the proestrous and E_2 induced LH surge in adult SD rats (Eldridge et al., 2001). Combined, these data indicate that ATRA clearly alters LH and PRL release in a time and strain specific manner.

In early pregnancy, PRL surges occur twice daily to cause large increases in the concentration of circulating P_4. A combination of high P_4 and E_2 levels provide the hormonal environment necessary for implantation. Wistar dams treated twice daily with 50mg ATRA/kg during post natal days 1-4 displayed a suckling induced decrease in PRL release (Stoker et al., 1999). Consistent with the decreased PRL, another study indicated that ATRA could alter initiation and maintenance of pregnancy, although the results were variable among the different in rat strains.

Diurnal or nocturnal oral gavage dosing of 100 – 200 mg ATRA/kg/day from days 1-8 of pregnancy increased preimplantation loss in F344 rats and postimplantation loss in Holtzman rats on day 9. No implantation loss was observed in LE and SD rats. Strain dependent alterations in P_4, LH and E_2 accompanied these implantation effects (Cummings et al., 2000). In contrast to these results, adult female F344 rats receiving 6 oral gavage doses of 120mg ATRA/kg/day in paraffin oil every 48 hours showed no difference from controls in estrus cycling, mating success and maintenance and delivery of pregnancy despite a significant decrease in body weight. Taken together, these data suggest that ATRA might alter certain aspects of pregnancy that are regulated by PRL.

1.6.4. Effects on pubertal development in female rats

Consistent with a neuroendocrine mediated effect of ATRA, ATRA also delays pubertal development. A dose-dependent delay in vaginal opening (VO) accompanied by irregular cycling patterns occurred in female Wistar rats dosed with 50 – 200 mg ATRA/kg/day during the period of sexual development (post natal days 22- 41) (Laws et al., 2000). While adrenal, kidney, pituitary, ovary and uterine weights were significantly reduced at the highest dose, pair fed studies indicated that VO delay was not due to body weight loss in these animals. No changes were observed in serum levels of thyroid stimulating hormone (TSH), thyroxin (T_4) and triiodothyrinine (T_3), suggesting that thyroid function was normal (Laws et al., 2000). A similar study has also observed a significant delay in VO in both SD and Wistar (Ashby et al., 2002).

In utero exposure to ATRA also alters pubertal development in female offspring. In a cross –fostered study, LE dams were treated with 100 mg ATRA/kg/day during gestational days 15-19. On postnatal day 1, offspring were cross-fostered with control dams or ATRA treated dams to evaluate the effect of post-natal exposure through milk. Offspring exposed during gestation and/or via suckling from an exposed dam had delayed mammary gland development. Suckling exposed and *in utero* + suckling exposed offspring displays a delay in VO. However, VO was not delayed in the *in utero* exposure only group, implying that VO delay might be a PRL mediated effect since pups receive PRL via the dam's milk. These developmental effects occurred in the absence of changes in serum levels of LH, PRL, and TSH and estrous cyclicity (Rayner et al., 2004).

1.6.5. Effects on pubertal development in male rats

Male rats also exhibit treatment related pubertal effects. Oral gavage administration of 50mg ATRA/kg/day or greater during the peripubertal developmental reduces serum, intratesticular testosterone (T) and LH concentrations in to decreasing vesicle and ventral prostate weights (Trentacoste et al., 2001). However, the validity of these effects is unclear since a parallel study restricting the diet of control rats showed similar results (Simic et al., 1994). However, other experiments indicated a clearer cause and effect relationship. Subchronic intraperitoneal (i.p) injections (60 days at 2 times/week) of 60 and 120 mg ATRA/kg decreased epididymis sperm count and motility in male Fischer 344 rats. These effects were accompanied by increased testicular sperm count. Thus, the authors concluded that these effects might be due to altered morphological and structural

changes in testicular tissue causing irregular migration of sperm to the epididymis (Kniewald et al., 2000).

Additional studies have demonstrated that administration of ATRA (Stoker et al., 2000) and/or its chlorinated metabolites (Stoker et al., 2002) during pubertal development caused a dose and time –dependent delay in preputial separation in male Wistar rats, suggesting a treatment related delay in pubertal onset. In addition, intratesticular T was decreased but serum T levels were unchanged. In addition, serum estradiol levels were increased in a dose-dependent manner in these animals (Stoker et al., 2000). These changes in steroid hormone levels accompanied a dose-dependent, but not significant, decrease in LH. Thyroid hormone levels were unaltered (Stoker et al., 2000)

1.6.6. Neuroendocrine mediated effects in non-mammalian species

A few studies have examined neuroendocrine effects in species other than rodents to determine potential ecological risk of ATRA. Some studies suggest that ATRA exposure during development decreased gonadal size and consequent reproduction in frogs (Hayes et al., 2002, 2003; Tavera – Mendoza 2002a, b). An increase in hermaphroditism and demasculinization of the larynges of male African clawed frogs exposed to ecologically relevant concentrations (0.1 - 25μg/L) of ATRA during larval development have also been reported. These effects were accompanied by decreased T levels in high exposed groups (Hayes et al., 2002). However, the results of these studies have been debated. Under similar exposure scenarios, other studies have reported no changes in laryngeal size and sex steroid hormones in ATRA exposed frogs compared to controls, suggesting that reproductive development is not

altered (Carr et al., 2003). To determine if reproductive consequences occurred in frogs as a result of ATRA exposure, a recent study evaluated endpoints such as metamorphosis, sex ratio and morphological changes in gonads. Exposure to E_2 and 5α- dihydrotestosterone (DHT) altered these endpoints while ATRA exposure did not cause any changes (Coady et al., 2004). One caveat of this study was that these effects were examined in a different species of frogs compared to the studies by Hayes et al. (2002, 2003). Therefore, the authors of this study note that such effects as hermaphroditism might be species dependent.

Alligators also show changes in endocrine activity during embryogenesis. Embryonic male alligators exposed to 14 ppm ATRA have elevated gonadal aromatase activity (Crain et al., 1997). While the authors stated that the treatment related elevated aromatase was suggestive of an estrogenic effect of ATRA, further investigation indicated a lack of any estrogenicity. In another study on alligators, treatment with 0.14 – 14 ppm ATRA during the period of reproductive development did not alter masculinization and hepatic aromatase activity under conditions that were altered by E_2. Additionally, reproductive tissues in both males and females were normal (Crain et al., 1999).

1.6.7. Estrogen receptor (ER) mediated effects

Several of the ATRA related neuroendocrine effects, including LH surge suppression, are largely regulated by E_2. Therefore, studies have investigated the estrogen receptor (ER) agonist and antagonist activity of ATRA and its chlorinated metabolites as a potential mechanism by which Cl-TRIs alter neuroendocrine function. Most evidence indicates that Cl-TRIs are not estrogenic by binding to the

ER. ATRA and DACT do not induce ER mediated responses *in vitro* and *in vivo* at doses known to alter neuroendocrine responses (Tennant et al., 1994a; Connor et al., 1996; Ben Jonathan et al., 1999; Oh et al., 2003).

Although ATRA and DACT do not exhibit estrogenic behavior, they are weakly anti-estrogenic *in vitro* and *in vivo*. High doses of ATRA decreased estrogen-stimulated uterine weight, reduced tritiated thymidine incorporation into uterine DNA and suppressed E_2 - induced uterine progesterone receptor (PR) concentrations (Tennant et al., 1994a; Connor et al., 1996). Furthermore, a competition binding assay using uterine cytosolic fraction from treated rats indicated that ATRA and DACT weakly reduced ER binding with [^{3}H]-E_2 (Tennant et al., 1994b). However, these results were only observed if the Cl-TRIs were allowed to preincubate prior to estrogen addition. Moreover, the concentrations required to reduce binding by 50% (IC50) were 4-5 times greater than the IC50 of estradiol. Tennant et al. (1994b) also demonstrated that administration of 50 – 300mg ATRA/kg for 2d could reduce estrogen binding capacity in uterine tissue of OVX rats (Tennant et al., 1994b).

In vitro studies have shown conflicting results relating to the ER mediated anti-estrogenic activity of ATRA. Tran et al. (1996) reported a dose - dependent decrease in estrogen sensitive β- galactosidase reporter activity when ATRA and ETHYL were incubated with sub-maximal (0.5nM) concentrations of E_2. However, ATRA did not inhibit reporter gene activity in the presence of E_2 concentrations that produced maximal responses. Contradictory results have been reported in studies using a similar reporter assay. Graumann et al. (1999) indicated that concentrations of ATRA, ETHYL and ISO ranging from 10^{-9} to 10^{-4}M did not change reporter

activity. In these two assays, differences might have been due to the methods of analysis and the usage of different concentrations of competing E_2. Studies in other cellular models have also indicated a lack of anti-estrogenic action of ATRA and DACT. These compound did not inhibit E_2 induction of cell proliferation and nuclear PR levels in MCF-7 and MCF-7-BUS human breast cancer cell lines (Connor et al., 1996; Oh et al., 2003).

1.6.8. Estrogen receptor (ER) independent effects

While of the neuroendocrine effects of ATRA suggest that ATRA might act by altering estrogen binding to ER, there are other ways in which ATRA could produce anti-estrogenic effects. For example, it is believed that ATRA might alter biosynthesis of aromatase (CYP19), the rate-limiting cytochrome P450 enzyme that catalyzes that conversion of T to estrogen. Some of the tissues with high concentrations of aromatase include placenta, gonads, adipose, mammary tissue, skin and hypothalamic regions in the brain (Simpson et al., 1994; Selmanoff et al., 1977). ATRA and its mono-dealkylated metabolites caused a dose-dependent induction of aromatase activity in JEG-3 placental choriocarcinoma and H295R cells (adrenocortical carcinoma) after 24 hour treatment. ATRA also increased aromatase mRNA similar to the positive control cyclic adenosine monophosphate (cAMP), a molecule involved in aromatase induction *in vivo* (Sanderson et al., 2000; Sanderson et al., 2001). In alignment with increased aromatase, ATRA and its chlorinated metabolites have been shown to inhibit phosphodiesterase (PDE), the enzyme responsible for catalyzing cAMP to 5'-AMP, suggesting that increased aromatase mRNA was due to an increase in cAMP levels (Roberge et al., 2004). In contrast to

these results, Oh et al., 2003 reported that DACT caused a dose-dependent decrease in aromatase activity in the same cell lines while ATRA had no effect.

1.5. Effects on HPG axis

While the mechanism of neuroendocrine disruption by ATRA is unknown, limited studies indicate that ATRA acts on the hypothalamus to cause downstream effects. Cooper et al. (2000) reported a lack of direct pituitary effect in two pituitary experimental models. Using a pituitary perfusion system, direct exposure to ATRA did not suppress LH and PRL secretion. In another experiment, ATRA treated hypophysectomized rats bearing ectopic pituitary autographs (i.e. the pituitary is removed from the direct influence of GnRH neurons) did not alter PRL levels. LH levels were not evaluated in this experiment. The authors also demonstrated that OVX, E_2 primed female rats treated with ATRA and subsequently given exogenous GnRH prior to the expected LH surge had higher levels of LH release compared to ATRA treated rats that did not receive GnRH. A similar study in ATRA treated pigs also indicated that LH release was normal in response to a GnRH challenge (Gojmerac et al., 2004).

Numerous neurotransmitters and neuropeptides participate in control of hypothalamic function. One such key regulator known to inhibit GnRH release is gamma-aminobutyric acid (GABA) (Lamberts et al., 1973; Akema et al., 1990). In a competitive binding assay, ATRA weakly decreased binding of an agonist specific for binding to the benzodiazepine site on $GABA_A$ receptors. However, the mono-dealkylated metabolites and DACT did not alter GABA agonist binding at the same molar concentrations.

Catecholamines norepinephrine and dopamine also regulate GnRH controlled release of LH. Norepinephrine is excitatory on GnRH neurons (Gallo and Drouva; 1979) while dopamine effects tend to be both inhibitory and stimulatory. *In vitro* studies suggest that the Cl-TRIs might act on the CNS by directly altering catecholamine synthesis. Pheochromocytoma (PC12) cells treated with uM concentrations of ATRA caused a dose and time-dependent decrease in intracellular dopamine (DA) and norepinephrine (NE) levels. ATRA also decreased the amount of NE released into the medium (Das et al., 2000). The effects of ATRA metabolites on catecholamine levels varied. Unlike ATRA, ISO and ETHYL increased intracellular DA at concentrations ranging from 50 - 200μM. ISO, but not ETHYL, decreased intracellular NE at 24 hours. Additionally, a decrease in release of NE was observed 24 hours after treatment with ISO and ETHYL. DACT behaved quite differently from the mono-dealkylated metabolites - 18 and 24 hr incubations with 160μM DACT caused a significant increase in intracellular DA and NE accompanied by a dose dependent increase in NE release after 24 hours (Das et al., 2001). In contrast to these in vitro results, an *in vivo* study indicated that ATRA treatment increased intracellular DA and decreased both intracellular levels and the release of NE in the hypothalamus (Cooper et al., 1998). These results suggest that Cl-TRIs might alter catecholamine synthesis and release, but the extent of change is unclear.

1.7. SCOPE OF THESIS

The objective of the work in this dissertation was to address data gaps that exist in understanding the mode of action of the neuroendocrine responses to ATRA

and in the relationship between these neuroendocrine responses and tissue doses of Cl-TRIs. This project tested the hypothesis that **ATRA exposure suppresses the LH surge in rats by acting as an anti-estrogen in the hypothalamic region of the brain and that this neuroendocrine response should be assessed on the basis of circulating concentrations of ATRA and/or ATRA metabolites in blood in order to permit low dose and interspecies extrapolation of risks of Cl-TRIs.** Since the chlorinated compounds rather than the non-chlorinated metabolites cause the neuroendocrine effects such as LH surge suppression, evaluating this effect on the basis of measures of tissue dose rather than administered dose provides a more appropriate estimate of the dose that impairs the hypothalamic – pituitary - gonadal axis and leads to suppression of the LH surge.

Tissue dosimetry was addressed by developing a series of PBPK models for ATRA and the chlorinated metabolites. This work answered the following quantitative questions relating to tissue dose:

- What are the circulating levels of parent compound and metabolites in the plasma and target tissue at external doses of ATRA known to suppress the LH surge?
- What are the biological and physicochemical processes that control the time-course concentrations of Cl-TRIs in tissue after oral administration of ATRA?
- What are the estimated rates of binding of Cl-TRIs to red blood cells (RBC's) and other proteins?

Addressing internal dosimetry provides a clearer context from which the neuroendocrine effects of Cl-TRIs can be examined: The following questions related to mode of action were addressed in this body of work:

- What are the relative potencies of ATRA and DACT, the major chlorotriazine, in terms of altering the steroid induced LH surge?
- Do Cl-TRIs alter binding of E_2 to hypothalamic ERα at doses known to suppress the steroid induced LH surge?
- Is suppression of the surge by ATRA and/or DACT due solely to hypothalamic dysfunction by Cl-TRIs or could these compounds be altering pituitary responsiveness?

In addressing these questions, this research provides a framework to guide risk assessment research with Cl-TRIs.

CHAPTER 2

PHARMACOKINETIC MODELING OF DISPOSITION AND TIME COURSE STUDIES WITH ^{14}C-ATRAZINE

2.1. INTRODUCTION

In the rat, ATRA is metabolized by cytochrome P450 oxidation to dealkylated, chlorinated metabolites (Figure 2.1). ATRA and its chlorinated metabolites undergo glutathione (GSH) conjugation to form non-chlorinated conjugates that are further metabolized and eliminated in urine and feces (Bakke *et al.*, 1971). Although the majority of ATRA is quickly metabolized and eliminated, a disposition study with ^{14}C-ATRA in rats indicated accumulation of radioactivity in red blood cells (RBCs) with multiple dosing (Thede, 1987).

Female Sprague-Dawley (SD) rats fed diet containing 400 ppm ATRA for 24 months exhibited increased incidence and earlier onset of mammary gland tumors (Stevens *et al.*, 1999). These tumors occur because ATRA blocks normal luteinizing hormone (LH) surges and causes persistent estrus with elevated hormone levels that serve to promote mammary cancer in these rats (Eldridge et al., 1999). These carcinogenic effects of ATRA on mammary tissues are species, strain, and gender specific and do not appear to be relevant for human risk assessment (Stevens *et al.*, 1999).

The mode of action underlying the effects of high doses of ATRA on female rats have been well described (Eldridge et al., 1999). High dietary or oral gavage doses of ATRA or other Cl-TRIs alter hypothalamic – pituitary function in rats (Cooper *et al.*, 2000) leading to suppression of the pre-ovulatory LH surge in ovariectomized rats and other neuroendocrine effects (Cooper *et al.*, 1996). The neuroendocrine effects likely result from target tissue exposure to the parent compound, ATRA, and other Cl-TRI metabolites since the toxic responses are not observed after exposure to non-chlorinated triazines (Eldridge *et al.*, 1994). It has been proposed that health risk assessments should be based on net tissue exposure to total Cl-TRI. The US EPA considers ATRA and its chlorinated metabolites to be toxicologically equivalent for human health risk (U.S.EPA, 2001). For this reason, it would be useful to have pharmacokinetic tools that estimate total Cl-TRI exposure of tissues throughout the body after external exposure to ATRA or other Cl-TRI herbicides (for example, simazine, cyanazine, etc.).

Several *in vivo* experiments have been performed with ^{14}C- ATRA to determine its metabolic disposition (Thede, 1987; Timchalk *et al.*, 1990). These data are especially valuable for establishing the relative rates of excretion versus conjugation of the Cl-TRIs and provide ancillary information for developing a kinetic model from these disposition studies with ^{14}C-ATRA.

In this report, the disposition studies with ^{14}C-ATRA were utilized to develop a physiological pharmacokinetic (PPK) model to: (1) provide estimates of net tissue exposures to Cl-TRIs (2) estimate rate constants for filtration and metabolic clearances of the combined pool of Cl-TRIs, and (3) evaluate the binding to blood

constituents based on Cl-TRI reactivity. In addition, a separate time–course study was performed to examine the absorption and metabolic characteristics that contribute to the individual and total Cl-TRI plasma concentrations after a single oral gavage dose of ATRA. This kinetic study with direct determination of ATRA and of the individual chlorinated metabolites served to elucidate the physiological basis of the uptake and clearance rates for the Cl-TRIs estimated in the radioactivity studies.

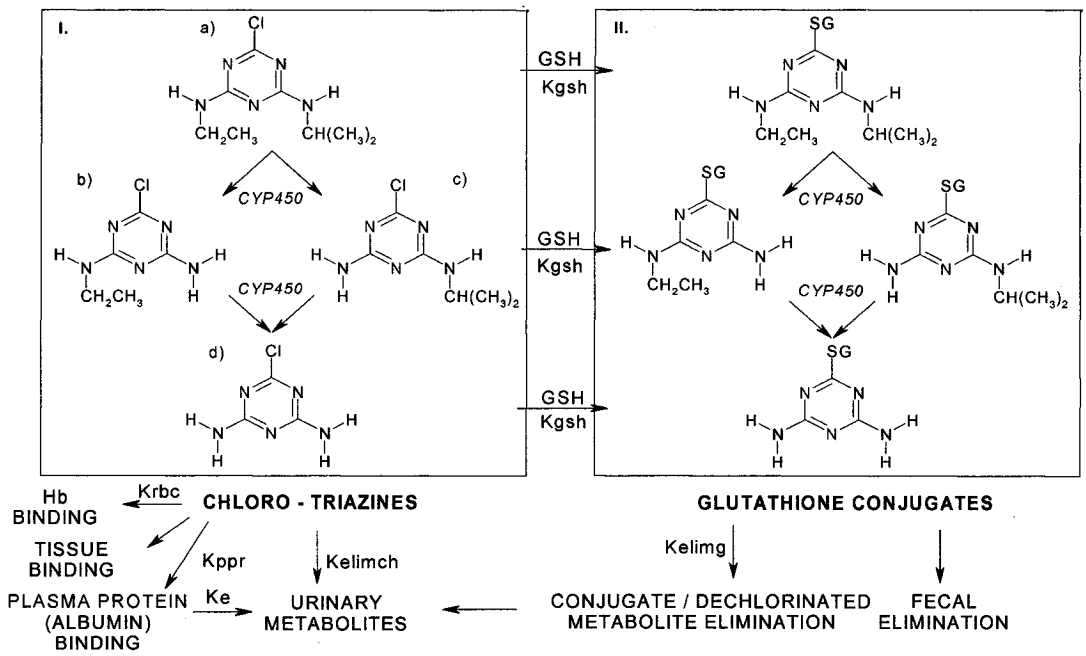

Figure 2.1. Schematic for atrazine metabolism in the rat with incorporation of PPK model parameters. In the model, atrazine metabolism occurs solely in the liver. Cytochrome P450 metabolizes atrazine (Ia) to the chlorinated metabolites, 2-chloro-4-ethylamino-6-amino-s-triazine (Ib) 2-chloro-4-amino-6-isopropylamino-s-triazine (Ic) 2-chloro-4,6-diamino-1,3,5 –s-triazine (DACT) (Id) which are eliminated in the urine. Glutathione (GSH) conjugation produces non-chlorinated metabolites that are eliminated in urine and feces (II). In addition to GSH conjugation and urinary elimination, the free chlorotriazine pool (I) is available to react with red blood cells and plasma proteins.

2.2. MATERIALS AND METHODS

2.2.1. Data Used for Modeling

Single Dose Time-Course Study: Timchalk *et al.* (1990) dosed groups of male Fischer 344 rats with 30 mg radiolabeled ^{14}C-ATRA /kg body weight via oral gavage in an aqueous suspension of 0.5% METHOCEL*F50LV and 0.2% POLYGLYCOL*59-13. Blood time course data were reported as ATRA equivalents (eq). Identified urinary metabolites included ATRA, specific dealkylated triazine metabolites, and several derivatives obtained from processing of GSH conjugates. The determination of individual metabolites in urine was critical in assigning relative rates of GSH-conjugation versus filtration rates for constituents in the Cl-TRI pool. Total cumulative mg – equivalents of ATRA in urine and feces were calculated from data expressed as daily absolute urinary excretion (Table 2.1c). Utilizing these data and assuming that all radiolabeled material in the feces was GSH conjugates, leads to the expectation that 47% of the GSH conjugates formed are excreted in urine and 53% in feces.

Multiple Dose Time-Course Study: Thede (1987) dosed female Sprague–Dawley CD rats weighing 240 – 265 grams daily by oral gavage with ^{14}C-ATRA in a corn starch/polysorbate-80 aqueous suspension. Dose groups received 1,3,7,10,50 or 100 mg/kg body weight/day for 10 days. Each group consisted of only 2 rats. Urine and feces were collected daily. Blood samples were taken at 24, 48, 72, 96, 144, 192, 240, 264 and 288 hours and centrifuged to separate RBCs and plasma for individual analysis. Radioactivity in plasma samples was determined by combustion. RBCs

were lysed, solublized, and decolorized; then, aliquots were added to a liquid scintillation cocktail for radioactivity determination. Concentrations were reported in units of mg-eq/L (Table 2.1a, b). Urine radioactivity was directly measured by liquid scintillation and reported as daily absolute urinary excretion in mg-eq (Table 2.1c).

2.2.2. Model Structure

The tissue compartments in the PPK model (Figure 2.2) were based on the primary site of metabolism (liver) and the site of action (brain), with the remaining volume of distribution accounted for in a lumped body compartment. All compartments are connected by blood circulation. Due to limited data on speciation of metabolites in plasma in the existing ^{14}C-ATRA kinetic studies, individual metabolites are not tracked. The model structure separates total radioactivity data into two pools of compounds (Figure 2.1). First, Cl-TRIs consist of parent ATRA together with all other chlorinated metabolites; the second pool consists of all metabolites derived from glutathione (GSH) conjugation. This strategy for lumping allows the model to calculate concentrations for groups of compounds based on their perceived risks, i.e., the active Cl-TRIs versus the detoxicated conjugates. Free Cl-TRIs in circulation are available to bind plasma proteins and RBCs, become conjugated by GSH, or are eliminated in urine.

GSH conjugates are eliminated through feces and urine. All elimination processes are described as first–order. Model parameters, including units and values, are provided in Table 2.2. An implicit assumption in construction of this total Cl-TRI model was that the individual Cl-TRIs had similar conjugation rates, urinary filtration rates and binding rates with macromolecules in the blood. All model code was

written using Advanced Continuous Simulation Language (ACSL®; Aegis Technologies Group, Inc., Huntsville, AL), a computer software simulation package for integrating differential equations.

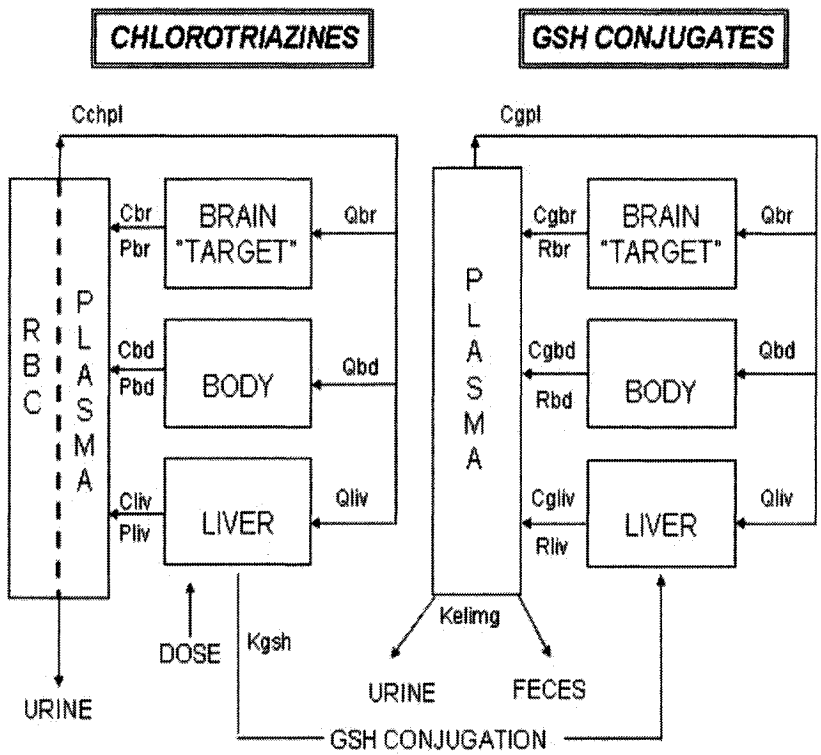

Figure 2.2. The PPK model for atrazine and the two pools of metabolites, chloro-triazines and GSH conjugates, tracked in the model. Abbreviations are defined in Table 2.2.

4.2.3. Macromolecular reactivity of Cl-TRIs

The multi-day disposition studies (see Table 2.1a) indicated persistence of bound radioactivity in RBCs. The PPK analysis also indicated persistent binding in

plasma (see RESULTS). The PPK model equations accounted for this binding by inclusion of reaction pathways for Cl-TRIs with these proteins (either hemoglobin (Hb) in RBCs or generically with plasma proteins) via second-order reactions. The respective rate constants for these reactions are Krbc for the reaction of Cl-TRIs with hemoglobin and Kppr for their reaction with plasma proteins. The multi-day studies included 10 days of dosing and three days after cessation of dosing. In this period there would be little turnover of the RBC pool. Thus, the model for binding to hemoglobin did not include loss of bound material during the 13-day study.

Binding to plasma proteins, however, accounted for protein turnover. Albumin was used as a surrogate protein in developing the binding equations for the plasma because it is present in plasma at high concentrations and its rates of formation and degradation are known (Nguyen, 1999). The rate of change of free albumin and of the covalent product of albumin and Cl-TRIs are described in the following two equations:

$$dCPPR/dt = Kfpp/Vpl - (Kepp*CPPR) - (Kppr*CCHPL*CPPR)$$

$$dCPPRbound/dt = (Kppr*CCHPL*CPPR) - Ke*CPPRbound$$

CPPR is the concentration of free plasma protein (albumin); Kfpp is the synthesis rate of the plasma protein; VPL is the plasma volume; Kepp is the elimination of plasma protein; Kppr is the binding rate of Cl-TRIs to plasma protein; CCHPL is concentration of free Cl-TRI in plasma; Ke is the elimination rate of the triazine plasma protein complex; and CPPRbound is the concentration of the triazine plasma protein complex.

Table 2.1. Time-course data of radiolabeled ATRA-eq in (a) red blood cells (b) plasma (c) urine after 10 daily doses ranging from 1-100 mg/kg/day (Thede, 1987). Data are mean values of two rats. (ND = no data available)

2.1a. Red Blood Cells (mg-eq/L)

Time	1 mg/kg	3 mg/kg	7 mg/kg	10 mg/kg	50 mg/kg	100 mg/kg
24	0.74	3.6	5.8	7.6	43.7	89.7
48	1.4	6.4	13.5	18.3	105.8	212.0
72	2.7	ND	21.5	29.1	153.5	284.19
96	3.1	21.8	28.5	38.3	193.0	390.0
144	4.7	ND	33.9	57.2	323.9	765.4
192	5.8	17.5	46.9	63.9	389.0	612.1
219	10.0	21.2	55.0	83.9	307.8	517.2
240	6.0	18.6	51.4	85.6	324.2	551.4
264	5.4	18.1	46.7	67.8	319.0	605.3
288	5.3	18.5	50.8	41.3	271.5	611.4

Table 2.1b. Plasma (mg-eq/L)

Time	1 mg/kg	3 mg/kg	7 mg/kg	10 mg/kg	50 mg/kg	100 mg/kg
24	0.07	0.22	0.65	1.1	8.8	24.7
48	0.18	0.53	1.5	1.8	8.2	26.0
72	0.44	1.4	3.3	4.1	19.3	49.1
96	0.55	1.8	3.5	4.4	22.9	54.4
144	0.59	2.4	3.8	5.1	24.9	64.6
192	0.61	1.8	3.8	5.0	25.6	46.6
219	0.58	1.4	3.8	5.1	21.4	51.7
240	0.19	0.70	1.6	3.1	26.4	29.6
264	0.14	0.79	1.4	1.7	13.4	17.7
288	0.12	0.34	0.87	1.6	8.3	14.8

Table 2.1c. Daily Absolute Urinary Excretion (mg-eq)

Day	1 mg/kg	3 mg/kg	7 mg/kg	10 mg/kg	50 mg/kg	100 mg/kg
1	0.19	0.47	1.2	1.7	6.5	12.1
2	0.13	0.56	1.4	1.9	8.2	20.1
3	0.22	0.70	1.6	2.5	8.0	13.7
4	0.22	0.63	1.7	2.5	11.2	18.2
5	0.22	0.54	1.4	2.6	9.3	19.9
6	0.21	0.58	1.4	2.4	8.5	20.7
7	0.20	0.57	1.2	2.2	6.0	17.9
8	0.18	0.68	1.3	2.3	10.0	14.9
9	0.20	0.56	1.5	2.3	6.9	24.1
10	0.21	0.48	1.0	1.5	7.3	8.0
11	0.07	0.13	0.33	0.53	5.8	9.1
12	0.02	0.04	0.09	0.27	1.5	3.5

Table 2.2. Physiological and Model Predicted Parameters Used in the PPK Model

Blood Flows [a,b]		
Qpl (L/hr)	Plasma output	3.23
Qliv (L/hr)	Liver	0.81
Qbr (L/hr)	Brain	0.16
Qbd(L/hr)	Body	2.26
Tissue Volumes [a,b]		
Vbl (L)	Blood	0.019
Vliv (L)	Liver	0.010
Vbd (L)	Body	0.191
Vbr (L)	Brain	0.002
Vpl (L)	Plasma	0.011
Vrbc (L)	Red Blood Cells	.008
Rate Constants [a]		
Ka (hr^{-1})	Absorption rate	0.2[c]
Krbc (L/mmole/hr)	Cl-TRI binding rate constant to hemoglobin	0.008[d]
Kelimch (L/hr)	Rate of elimination of Cl-TRIs in urine	0.030[c]
Kelimg (L/hr)	Rate of elimination of glutathione conjugates	0.076[c]
Kgsh (L/mmole/hr)	Rate of glutathione conjugation	0.531[c]
K_0 (mmole/hr)	Glutathione rate of formation	0.021[e]
Keg (hr^{-1})	Glutathione rate of elimination	0.349[e]
Kfpp (mg/hr)	Synthesis rate of plasma protein	11.86[f]
Kepp (hr^{-1})	Elimination rate of unbound plasma protein	0.012[f]
Kppr (L/mg/hr)	Binding rate of chlorotriazines to plasma protein	$1.14x10^{-7}$ [c]
Ke (hr^{-1})	Elimination rate of triazine plasma protein complex	0.01[c]
Partition Coefficients[g]		
Pbd	Body/plasma (chlorinated compounds)	1.7
Prbc	RBC/plasma (chlorinated compounds)	10
Pliv	Liver/plasma (chlorinated compounds)	4
Rbd	Body/plasma (GSH conjugates)	2
Rliv	Liver/plasma (GSH conjugates)	1
Other Constants		
HCT (%)	Hematocrit	41
PU	Proportion of GSH conjugates to urine vs. feces	0.47[c]

[a] All parameters are scaled to body weight of 250g rat.
[b] Physiological parameters were taken from Brown *et al.*(1997).
[c] Estimated from model fit to Timchalk *et al.* (1990) and Thede (1987).
[d] Estimated from model fit to Thede (1987).
[e] Taken from D'Souza *et al.* (1988).
[f] Taken from Nguyen (1999).
[g] model estimated

2.2.4. Glutathione Conjugation and Depletion

ATRA is similar to other chemicals that deplete GSH at high concentrations. Conjugation with GSH is catalyzed by glutathione transferase enzymes, producing stable conjugates that consume a stoichiometric equivalent of GSH (Andersen *et al.*, 1986; Gargas *et al.*, 1995). GSH depletion was incorporated in the model using approaches described by D'Souza *et al.* (1988), in which GSH depletion depends on the second order rate constant for conjugation of the Cl-TRIs with GSH, the initial concentration of GSH, and the rates of GSH synthesis and degradation. The rates of GSH formation and depletion were obtained from D'Souza et al. (1988). In our simulations, initial concentration of liver GSH was 6mmol/L.

2.2.5. Model Parameters

Initial values for tissue volumes, blood flow, and physiological parameters (Table 2.2) are from Brown et al. (1997). The plasma binding rate (Kppr), elimination rates (Kelimch and Kelimg), plasma:body partition coefficient (Pbd), oral absorption rate (Ka) and glutathione conjugation rate (Kgsh) were estimated by fitting the single dose data for time course concentrations of total radioactivity in plasma and urine (Timchalk *et al.*, 1990). The robustness of this set of parameters for predicting results for other dosing situations was tested by using the single dose parameters to predict behavior in the multiple–dose study (Table 2.1). The binding rate constant (Krbc) to Hb was estimated by simulating multiple–dose data on total μg-eq ATRA in RBCs (Thede, 1987). The present estimate of the tissue partition coefficient for the body (Table 2.2) primarily served to constrain the overall volume of distribution for these compounds. Our approach was to estimate the set of parameters that had most

sensitivity for an outcome from specific experiments – oral uptake and total clearance from the oral study of plasma radioactivity, etc. Values for the suite of parameters were estimated here by simple visual comparisons. Sarangapani *et al.* (2002) described a sequential approach to log-likelihood optimization of parameters in more complex PPK models for siloxanes. Dueto the provisional nature of the model for total radioactivity, we did not apply similar statistical approaches in ACSL for formal parameter estimation with this model.

2.2.6. Time – Course Study of Plasma Chlorotriazines

Female Sprague-Dawley rats (200-225 g) were obtained from Charles River Laboratories, Raleigh, NC and kept in Colorado State University's central animal care facility, a fully accredited American Association for Accreditation of Laboratory Animal Care (AAALAC) facility. All animals were housed individually and allowed to acclimate for one week in ventilated cages and maintained on a 12-hr light/dark cycle at a constant temperature of 25°C and humidity of 55%. Rats had free access to certified Teklad NIH-07 rodent diet and tap water prior to beginning the study. Food was withdrawn prior to dosing and returned approximately 12 hours later. ATRA was a gift from the Syngenta Corporation (purity = 97.1%).

Rats were dosed with 90 mg ATRA /kg body weight in 1% methylcellulose (MC). Whole blood (0.2ml) was taken at 0.5, 1, 2, 4, 8, 12, 24, 48 and 72 hours post –dose via indwelling jugular cannulae and centrifuged to separate plasma for analysis. Samples were analyzed for ATRA, des-ethyl ATRA, des-isopropyl ATRA and diaminochloro-s-triazine (DACT) by gas chromatography with detection by mass spectrometry analysis (Cranmer *et al.*, 2002). These data were converted to total Cl-

TRI concentrations and were modeled with a one compartment PK model. Log-likelihood methods in ACSL-MATH were used to estimate an uptake rate constant (hr^{-1}), a Cl-TRI volume of distribution (Liters/kg), and an elimination rate constant (hr^{-1}). The bioavailability of Cl-TRIs in this model was set at 0.53, to account for the elimination of 47 % of dosed ATRA as GSH conjugates.

2.3. RESULTS

One of the main goals in developing this PPK model was to describe plasma Cl-TRIs under various dosing conditions. Several processes, including elimination, distribution to tissues, and RBC reactivity, contribute to the observed total ATRA-eq plasma concentration and to the proportions of Cl-TRIs and GSH conjugates in the plasma. The model for total plasma radioactivity includes these processes with some assumptions about the common reactivity of the various Cl-TRIs. The combination of the single dose results with the multi-dose disposition studies provide an adequate, though limited, data set from which to draw conclusions about the Cl-TRI exposures resulting from oral dosing with ATRA.

2.3.1. Model Description

The single dose urinary data were pivotal to model development because they provided the necessary information regarding individual metabolites in urine to estimate elimination rate constants for urinary excretion of Cl-TRIs (Kelimch) and GSH conjugates (Kelimg) and the glutathione conjugation rate (Kgsh). These rate constants determine the relative time-course amounts of the Cl-TRIs and GSH conjugates in the urine. Twenty-four hours after a single oral gavage dose of 30

mg/kg, the percent of Cl-TRIs in the urine were 72.5% ± 6.0 and GSH conjugates were 27.2% ± 2.9. Approximately 70% of the total urine concentration within 24 hours was DACT. Thus, the oxidation of the alkyl forms of ATRA producing DACT must be more rapid than their elimination into urine. After 72 hours, the urine contained 65.8 ± 1.4% of the total dose, while fecal elimination accounted for 18.7± 1.8% of the total dose (Timchalk *et al.*, 1990).

Utilizing these data, cumulative urinary excretion after single dosing (Figure 2.3) and multiple dosing (Figure 2.4) was described by fitting the rates of glutathione conjugation (Kgsh), Cl-TRI elimination (Kelimch) and conjugate elimination (Kelimg) to give urine radioactivity percentages of 73% Cl-TRIs and 27% GSH conjugates as reported by Timchalk et al. (1990). This parameter set described the plasma radioactivity time course throughout the early period after dosing (Figure 2.5) with the expectation that the plasma radioactivity is over 90% Cl-TRI during this period. This predicted behavior is consistent with rapid blood clearance of GSH conjugates that are produced in liver, distributed to kidney and processed to mercapturic acid and other GSH-conjugate breakdown products (Newton *et al.*, 1986; Schrenk *et al.*, 1988). The estimated large value for the elimination rate constant for removal of GSH conjugates from plasma (Kelimg) was based on known rates of elimination of other GSH conjugates.

2.3.2. Estimating Cl-TRI reactivity toward Hemoglobin

ATRA-derived radioactivity accumulates in the RBCs after single and multiple dose exposures (Thede, 1987; Timchalk *et al.*, 1990). To describe this accumulation of radioactivity, the Cl-TRIs reacted with Hb in RBC's via a second-

order binding rate of 0.008 L/mmole/hr (Krbc). After a single oral gavage dose, the model predicts that there would be 1.5% of the total dose bound to RBC's compared to only 1.2% after 72 hours (Timchalk *et al.*, 1990). The fits to red blood cell radioactivity (Figure 2.6) consistently underestimate the observed radioactivity in red blood cells at these various times after dosing, with the largest discrepancy noted in the 50 mg/kg daily dose groups. While the predicted red blood cell concentration of radioactivity can be increased by relatively small increases (i.e., about 20%) in the second-order rate constant for the reaction of Cl-TRIs with hemoglobin, such an increase would also lead to a correspondingly higher prediction of the amount bound to hemoglobin at 72 hours, i.e., even greater than 1.5 %. Thus, the current value, 0.008 L/mmole/hr, is a compromise parameter that fits single and multiple dose studies adequately, although not perfect for any of the individual data sets.

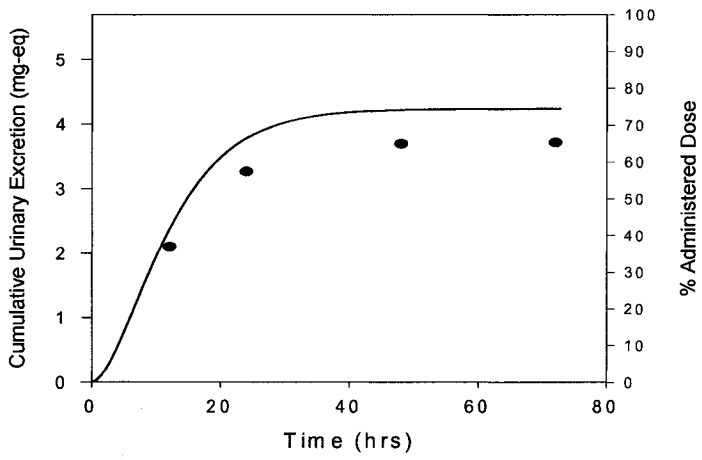

Figure 2.3. Experimental data and model simulation of cumulative urine radioactivity and percent administered dose in rat following a single oral gavage dose of 30 mg radiolabeled ^{14}C –ATRA/kg body weight. Data are from Timchalk *et al.* (1990). Solid line represents model description. Points represent mean values of two animals.

2.3.3. Estimating Plasma Protein Reactivity

Although the model structure with Cl-TRI RBC reactivity described the accumulation of radioactivity in the RBC's after multiple doses, it consistently underestimated the single (Figure 2.5) dose plasma data at longer times. A likely explanation for this discrepancy is that Cl-TRIs also react with plasma proteins, leading to persistence of radioactivity in plasma at later time points. To describe this reaction, plasma protein binding was introduced. In this case, the characteristics of the plasma protein were based on concentration and turnover properties of albumin. Fitting the plasma data for retention of radioactivity for single and multiple dosing (Figures 2.5 & 2.7) resulted in a binding rate constant of 1.14×10^{-7} L/mg/hr with a protein turnover half-life of about 70 hours, similar to albumin's half-life of 60 hours (Allison, 1960).

Once again, it bears emphasis that the fits to the plasma time course curves for total radioactivity for the two rats in Figure 2.7 could be improved by using a larger value of the second-order reaction rate constant between plasma protein and the Cl-TRIs. However, the goal in this exercise was to estimate the plasma reaction rate constant by adjusting the rate constant to describe the single dose time course (Figure 2.5) and then to show that the binding was consistent with the multi-dose study, as it is. The main qualitative points in the simulation and the data (Figure 2.7) are a tendency to have a slight increase in peak concentrations on later days of dosing and a higher magnitude slow phase component after multiple doses compared to the single dose study. Further studies of multi-dose disposition of ATRA with larger number of animals per group could help to refine these second order reaction rate constants.

Nonetheless, the current reaction rate constant parameters for single and multiple dose studies do not differ by more than 25%, a very good agreement for two very diverse studies.

2.3.4. Chlorotriazine Metabolite Time-Course Study

After a single oral gavage dose of 90 mg ATRA/kg body weight, DACT was the major Cl-TRI in the plasma, while ATRA was over 200-fold lower than DACT (Table 2.3). In fact, DACT accounted for about 95% of the total plasma Cl-TRI AUC. Peak des-isopropyl concentration was about 3-fold greater than des-ethyl (i.e. preferential attack of the isopropyl group by cytochrome P450). As expected from the plasma PPK model results with total radioactivity, DACT slowly accumulates in the plasma, peaking at 24 hours post-dose, and remains detectable in the plasma at 72 hours. Plasma DACT concentrations were similar at 0.5, 1.0 and 2.0 hours, indicating a period of rapid absorption (within the first 30 min) followed by slower uptake. Concentrations of the two mono-dealkylated metabolites were high at 0.5 hours and fell off at 2 hours. From 4 to 12 hours they showed evidence of a plateau, indicative of a prolonged constant rate of uptake in this period. These disposition data clearly indicate that a single dose of ATRA yields high tissue exposure to DACT and much lower exposures to the mono-dealkylated Cl-TRIs. The analysis of the total Cl-TRI time-course for this study (Figure 2.8) provided an uptake rate constant of 0.07 hr^{-1}, a volume of distribution of 0.5 L and an elimination rate constant of 0.08 hr^{-1}.

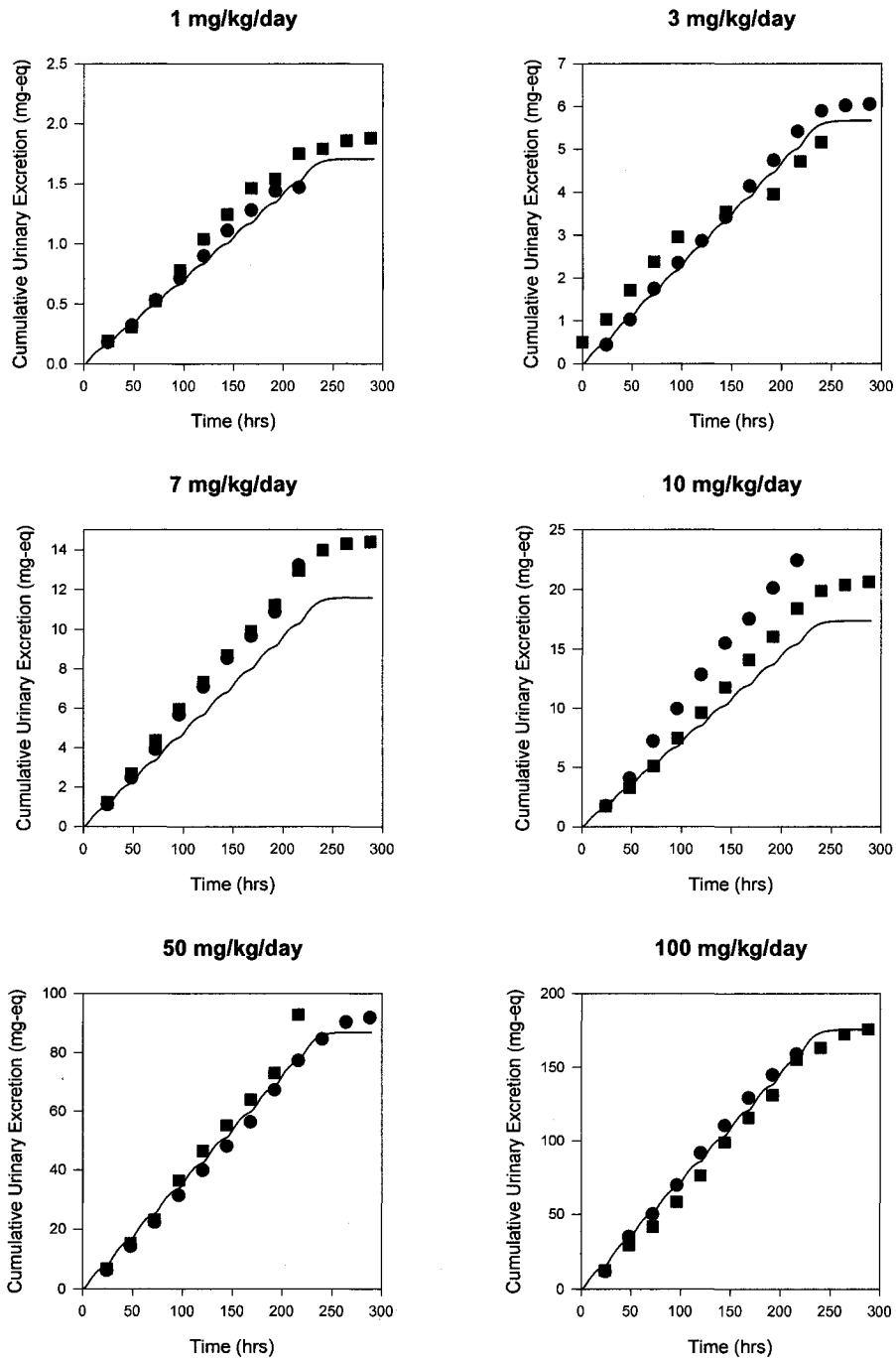

Figure. 2.4. Experimental data and model simulation of cumulative urinary elimination of total ^{14}C –ATRA after 10 daily oral gavage doses (Thede, 1987). Solid line represents model description. Squares and circles each represent data from an individual anima

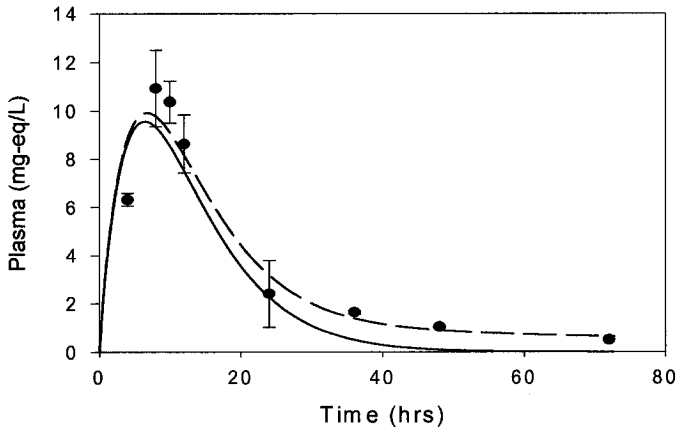

Figure. 2.5. Experimental data and model simulation of plasma time-course concentrations in rat following a single oral gavage dose of 30 mg radiolabeled ^{14}C – ATRA /kg body weight. Data are from Timchalk *et al.*, 1990. Points represent experimental means and standard deviations. Solid line represents model simulation without plasma protein binding. Hatched line represents model simulation with plasma protein binding. Inclusion of plasma protein binding more accurately predicts plasma concentrations at later time points.

Table 2.3. Plasma time-course data of individual chlorotriazines after a single oral gavage dose of 90 mg ATRA/kg body weight. Data are expressed in units of mg/liter as mean ± SEM (n=3).

Time	ATRA	DE - ATRA	DI-ATRA	DACT	Total Cl-TRI
0.5	0.09 ± 0.11	0.26 ± 0	0.80 ± 0.09	1.30 ± 0.14	2.40 ± 0.08
1	0.02 ± 0	0.21 ± 0	0.78 ± 0.26	1.56 ± 0.45	2.56 ± 0.52
2	0.11 ± .17	0.13 ± 0	0.28 ± 0.02	1.74 ± 0.24	2.26 ± 0.23
4	0.02 ± .02	0.17 ± .14	0.50 ± 0.56	2.41 ± 1.48	3.10 ± 1.25
8	0.01 ± 0	0.17 ± 0.13	0.48 ± 0.46	6.29 ± 4.55	6.95 ± 2.91
12	0.02 ± 0	0.20 ± 0.09	0.69 ± 0.38	6.79 ± 3.30	7.70 ± 2.13
24	0.01 ± 0	0.05 ± 0.06	0.07 ± 0.1	7.52 ± 2.87	7.66 ± 1.71
48	0.01 ± 0	0 ± 0	0 ± 0	1.23 ± 0.62	1.25 ± 0.36
72	0 ± 0	0 ± 0	0 ± 0	0.14 ± 0.13	0.14 ± 0.07

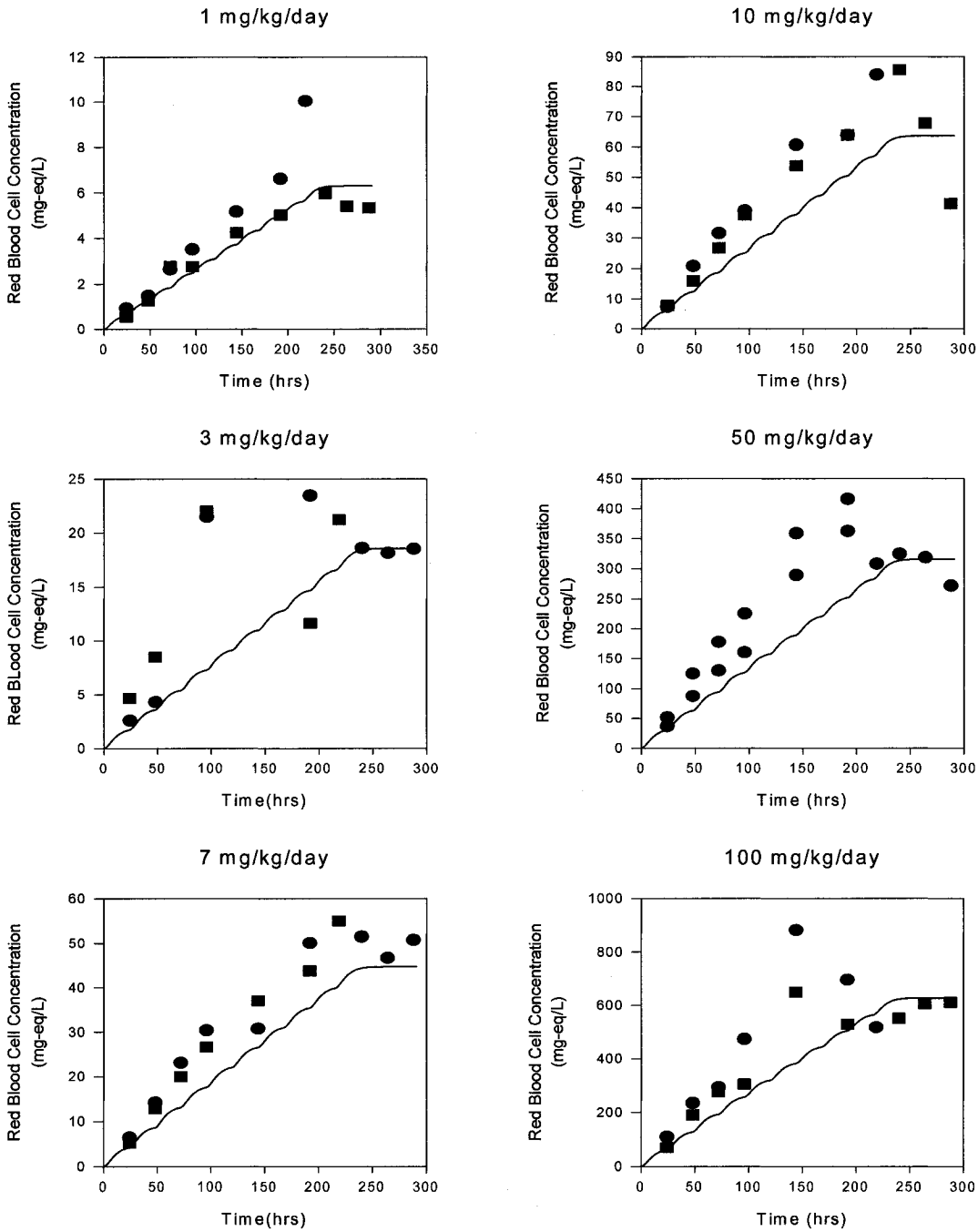

Figure 2.6. Experimental data and model simulation of total ^{14}C –ATRA in red blood cells after 10 daily oral gavage doses from 1 to 100 mg/kg/day (Thede, 1987). The PPK model has irreversible binding of the chlorotriazine pool to hemoglobin in red blood cells with an estimated binding rate constant of 0.008 L/mmole/hr. An estimated 1.5% of the total dose is bound to hemoglobin. Solid line represents model simulation. Squares and circles each represent data from an individual animals.

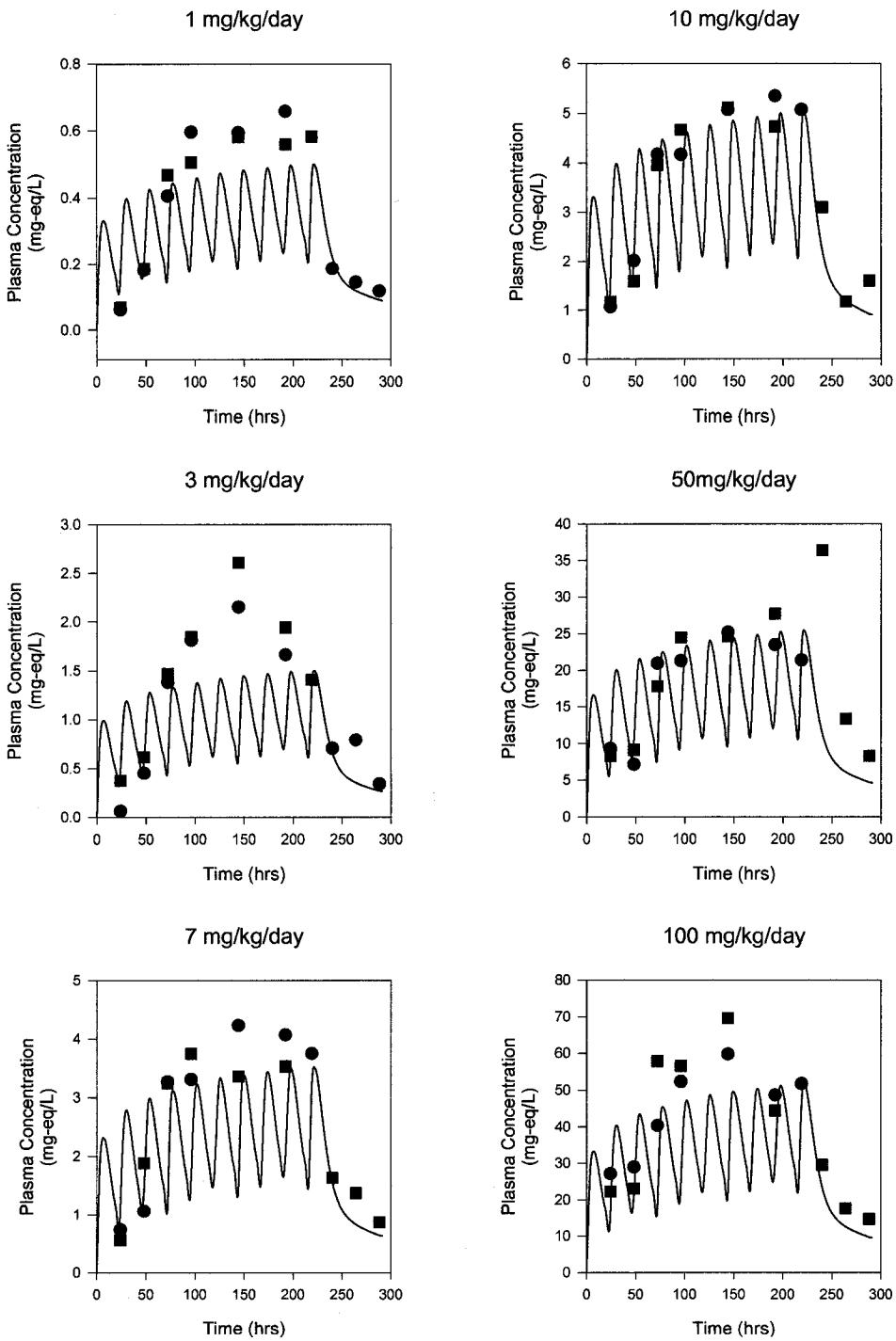

Figure 2.7. Experimental data and model simulation of total ^{14}C –ATRA in plasma after 10 daily oral gavage doses from 1 to 100 mg/kg/day (Thede, 1987). Simulations compare model estimation of plasma concentration with (solid line) and without (hatched line) plasma protein binding. These results indicate chlorotriazine binding to plasma proteins after multiple daily doses. The estimated plasma protein binding rate constant is 1.14×10^{-7} L/mg/hr. Points represent mean of two animals.

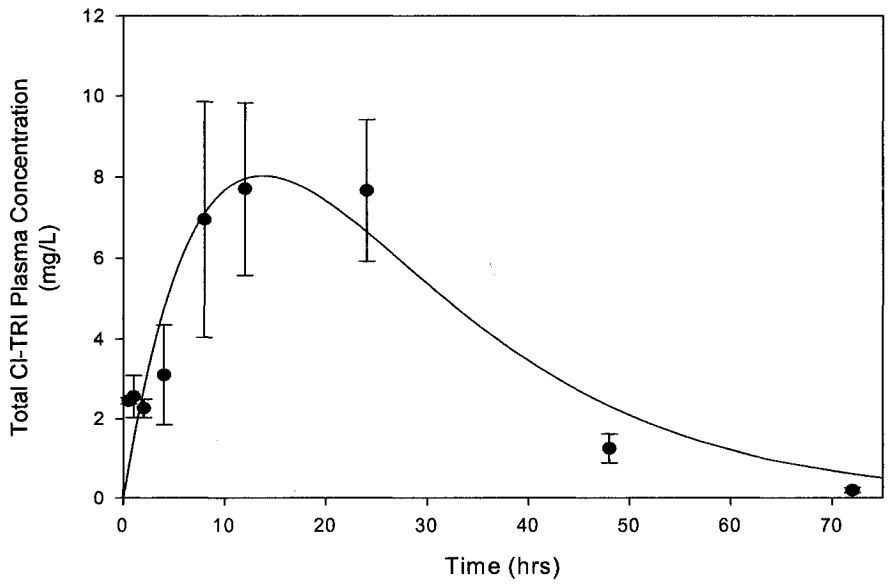

Figure 2.8. Plasma time-course of total Cl-TRI after a single oral gavage dose of 90 mg ATRA/kg body weight. Data points represent the mean ± SEM (n=3) of total Cl-TRIs (see Table 2.3). Solid line represents the log-likelihood best fit to a one-compartment model for Cl-TRI disposition.

2.4. DISCUSSION

Accurately describing the metabolite pharmacokinetics for an extensively metabolized compound like ATRA using total radioactivity data is usually limited because the available data do not differentiate between parent compound and metabolites. The ability to develop a PPK model that described Cl-TRIs and GSH conjugate pools largely relied on the single dose elimination data that provided information on the relative proportions of conjugates and Cl-TRIs in urine and feces. Some of the underlying assumptions in the PPK model were tested in our independent study with unlabeled ATRA which included speciation of the Cl-TRIs in plasma. Comparisons of the absorption and elimination rate constants for the PPK model for

total radioactivity and for the analysis of the plasma time-course metabolite study provide insights into the processes that determine total Cl-TRI time course for these relatively high oral doses of ATRA.

2.4.1. Basic Assumptions

To describe the single dose radiolabeled elimination data, some assumptions about rates of elimination were necessary. First, all Cl-TRIs were assumed to have the same urinary filtration rate and the same conjugation rate. Second, upon GSH conjugation, the Cl-TRI conjugates were assumed to be rapidly eliminated into the urine and feces at an estimated rate (Kelimg = 0.076 L/hr) comparable to known elimination rates of GSH conjugate metabolites of chemicals such as hexachlorobutadiene (Schrenk *et al.*, 1988) and acetaminophen (Newton *et al.*, 1986). The model also assumed that all fecal radioactivity was associated with GSH conjugates and/or their metabolites. Third, the accumulation of radiolabeled material in RBCs and in plasma proteins is due to reactivity with Cl-TRIs. To the extent that these assumptions hold, this model should be an accurate reflection of the disposition of Cl-TRIs and their GSH conjugates in plasma and urine.

2.4.2. Cl-TRI Absorption

PPK modeling results indicated that the rate of ATRA absorption from the gut to the plasma is very slow (Ka = 0.2 hr^{-1}) compared to estimated oral gavage absorption rates of other compounds, especially when these compounds were provided in aqueous vehicles. For instance, the rate constants for oral absorption of styrene, 2-methoxyethanol, and 1,4-dioxane from water or saline vehicles were estimated to be 5.5, 3.0 and 5.0 hr^{-1}, respectively (Ramsey and Andersen, 1984; Hays

et al., 2000; Reitz et al., 1990). This slow uptake could be due to characteristics of transport across gut membranes or to slow dissolution of ATRA from the slurry.

2.4.3. Cl-TRI Reactivity with Proteins

Both the RBC and plasma time-course results with ^{14}C-ATRA are strongly indicative of persistent covalent binding with constituents in these compartments. One possible mechanism for the persistent RBC binding is that the chlorine moiety on Cl-TRI compounds is electron-withdrawing producing a carbon center with a partial positive charge that is prone to nucleophilic displacement of the chlorine. Cysteine residues on hemoglobin or plasma proteins could spontaneously react with Cl-TRIs displacing chloride ion. Many toxicants (Phillips and Farmer, 1994; Rappaport and Yeowell-O'Connell, 1999) and drugs (Kramer and Routh, 1973; Christensen *et al.*, 1980) are capable of forming albumin adducts. The binding in plasma was characterized with a half-life of 70 hours, very similar to that for albumin. Although the data indicate that ATRA exposure leads to strong, likely covalent, binding to RBC's, the rate of hemoglobin binding estimated by the model (0.008 L/mmole/hr) is lower than that for other compounds known to readily form hemoglobin adducts via covalent binding at nucleophilic sites. For instance, the relative rates of reaction with styrene oxide is about 100 fold higher when expressed in similar units (Rappaport *et al.*, 1993).

Hamboeck *et al.* (1981) examined the covalent binding of simetryn sulfoxide and ametryn sulfoxide to Hb from various animal species. These metabolites are formed from the oxidation of the thiomethyl substituent that is present in these two herbicides rather than the chlorine present in ATRA. These metabolites bind

extensively to Hb from rat, mouse and guinea pig *in vitro*. Less rapid binding was found with dog, sheep, cow, and pig Hb. In their assay very little binding occurred with human Hb. In the rat, binding was via a covalent reaction with the I-125 cysteine residue of Hb by nucleophilic displacement with methylsulfoxide serving as the leaving group in the reaction. Much lower binding of radioactivity with Hb was noted with ATRA (See Figure 2.5, (Hamboeck *et al.*, 1981) and virtually none with the parent S-methyl herbicides. The relative binding of ATRA to Hb in various species tracked the species-dependent binding rates noted with ametryn sulfoxide.

Both the RBC and plasma protein binding data, along with these earlier observations in Hb reactivity, indicate some ability of Cl-TRIs to react with proteins in the blood, with chloride being a less favored leaving group than methylsulfoxide. Based on our results from the Cl-TRI metabolite time-course study and the elimination data, the most likely candidate for this interaction would be DACT since it is the predominant Cl-TRI metabolite in the plasma. Binding of DACT to hemoglobin has been confirmed *in vitro* by incubating ^{14}C-DACT with rat hemoglobin and evaluating the accumulation of radioactivity in protein over time (Prentiss, 2004).

2.4.4. Likelihood of GSH depletion

At high concentrations, many chemicals that undergo GSH conjugation deplete GSH stores in the liver and other tissues (D'Souza *et al.*, 1988). GSH depletion at very high doses could potentially alter GSH conjugate and Cl-TRI metabolite plasma profile, leading to increased Cl-TRI area under the curve (AUC). Since the primary detoxification pathway for the Cl-TRIs is GSH conjugation, dose -

dependent GSH depletion was also incorporated into the model to predict the extent of hepatic GSH depletion expected at various doses, including the ranges used in the dosing studies. The model estimated GSH conjugation rate constant was 0.53 L/mmole/hr, a value similar to that for other chemicals that are extensively conjugated by glutathione-s-transferase but smaller than known depleters such as ethylene dichloride (1.2 L/mmole/hr; (D'Souza et al., 1988) and allyl chloride (9.0 L/mmole/hr; (Andersen et al., 1986). Although ATRA is extensively metabolized by GSH, the model estimated depletion of GSH was smaller than expected. In fact, minimal differences in depletion are expected after one or three daily doses and 50% depletion of GSH is estimated to occur only after three daily doses of 500 mg ATRA/kg (simulations conducted, but not shown here).

2.4.5. Comparison of PPK model with Plasma Cl-TRI Metabolite Time- Course Study

The findings from the unlabeled plasma Cl-TRI metabolite time-course study aid in verifying some of the underlying assumptions regarding relative rates of Cl-TRI metabolism used to develop the PPK model. ATRA and the mono-dealkylated metabolites are rapidly converted to DACT, leading to slow accumulation and extended retention of DACT in the plasma. This slow accumulation of DACT appears to be a consequence of the complex absorption characteristics of ATRA. A portion of the intubated ATRA (about 10%) is rapidly absorbed, followed by a slow decline in absorption (Table 2.3; Figure 2.8). These characteristics are likely to be associated with availability of a small portion of dissolved (free) ATRA that is rapidly absorbed from the GI tract followed by slow dissolution of the slurry as a rate-limiting step for most of the uptake. In fact, the total radioactivity plasma time-

course curve reported by Timchalk *et al.* (1990) is similar to the DACT time-course curve and likely represents a composite of two main processes: 1) slow uptake into the body from the dissolution of suspended ATRA in MC used for dosing and 2) rapid metabolic conversion of ATRA to DACT that has a much longer plasma elimination half-life compared to other Cl-TRIs.

Consistent with the PPK model description, the plasma time courses of the individual Cl-TRIs were reflective of the urinary elimination patterns (Figure 2.9). The Cl-TRI elimination patterns largely favor DACT (~67% total radioactivity in urine and the vast majority of the Cl-TRIs in urine) over parent compound and the mono-dealkylated chlorinated metabolites (Figure 2.9). In addition, DACT accounts for over 95% of the total Cl-TRI plasma AUC (Figure 2.9). The correspondence of proportion of Cl-TRI in urine and the plasma AUCs show that the assumption of common filtration rates is valid.

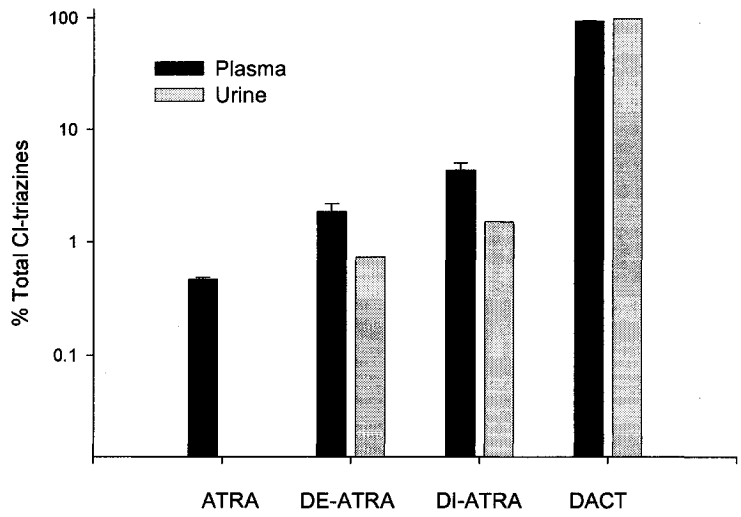

Fig. 4.9. Comparison of individual Cl-TRI metabolites in plasma (90 mg ATRA/kg body weight) and urine (30 mg ATRA /kg body weight ; Timchalk et al., 1990). Plasma data are expressed as percent total Cl-TRI AUC. Urine data are expressed as percent total Cl-TRI mass at 24 hours post – dose.

2.4.6. One Compartment Model for Total Plasma Cl-TRIs

The parameters for absorption in the simple one compartment model correspond well with the parameters from the PPK model for total radioactivity. Compared to Timchalk et al. (1991), our rats were dosed with 100 rather than 30 mg ATRA/kg. To the extent that uptake consists of both rapid absorption of dissolved ATRA and slower dissolution of the slurry, the higher dose should exhibit slower rate constants for absorption as was observed (0.07 hr^{-1} versus 0.2 hr^{-1}). In each model the terminal elimination phase was similar and is simply related to the fact that the all radioactivity at longer times represents a single compound, DACT. The comparison of the radiolabeled study and our study with speciated Cl-TRIs was most useful for uncovering the processes involved in absorption. The time course data on individual metabolites (Table 2.3) should be useful for developing a more comprehensive PBPK model for the entire suite of Cl-TRIs.

2.4.7 Summary

The majority of pharmacokinetic studies with commercially important pesticides are conducted with radiolabeled material. Such data are far from optimum for developing PPK models for the disposition of the compound and its metabolites. Our limited PPK model describing the disposition of Cl-TRIs in plasma using ^{14}C-ATRA data was informative regarding persistent binding and overall Cl-TRI time courses. The success with using single uptake and elimination rates occurred because DACT is the predominant plasma Cl-TRI throughout the time course and slow dissolution of ATRA with rapid dealkylation regulated DACT appearance in the plasma. The ability to estimate the multiple oral gavage dosing data without any

parameter adjustments from the single dose data give some degree of confidence in the predictions from the model. Because ATRA and the chlorinated metabolites are all believed to contribute to the observed toxicity seen in rats, this pharmacokinetic model and the metabolite time course plasma data are the first steps in providing a more appropriate estimate of target tissue dosimetry for assisting in dose-response assessment in the animal studies. Improved protocols for collecting PK and disposition data with radiolabeled compounds should be developed to reduce current testing requirements while providing specific information to develop PBPK models that could aid in many aspects of pesticide risk assessments (ILSI, 2001). The difficulties in providing unambiguous identification of rate processes with the ATRA total radioactivity studies attests to the need for improved PK testing protocols for studies with pesticides in general. Such studies would couple evaluation of residue levels after dosing with radiolabeled compounds with time courses of the parent compound and major metabolites. A strategy that can now be pursued with ATRA using the analytical chemistry methods developed for the Cl-TRI compounds (Cranmer et al., 2002) and used for the first time in our time course study here.

CHAPTER 3

ESTIMATING CONSTANTS FOR METABOLISM OF ATRAZINE IN PRIMARY RAT HEPATOCYTES BY KINETIC MODELING

3.1. INTRODUCTION

To date, ATRA metabolism has been evaluated in rat liver microsomes (Dauterman and Mueke, 1973; Hanoika et al., 1999Lang *et. al.,* 1996). Data from microsomal studies are useful for determining P450 mediated product formation rates and comparing inter-species differences in metabolism. However, kinetic data from microsomal preparations may not completely reflect the metabolic processes occurring *in vivo* (Billings *et. al.*, 1977). *In vitro* studies using freshly isolated primary hepatocytes have provided kinetic parameters that more accurately correlate with *in vivo* metabolism (Chenery *et. al.,* 1991, Sirica and Pitot, 1980, Thurman and Kauffman, 1979). The *in vivo* metabolism of chemicals such as benzene (Cole et al., 2001), furan (Kedderis et al, 1993), and almokalant, an antiarrhythmic drug (Andersson et al., 2001), have been successfully described with physiologically based pharmacokinetic (PBPK) models that incorporated *in vitro* metabolic parameter data resulting from time-course studies with primary hepatocyte suspensions.

Quantitative *in vivo* physiological descriptions of the kinetic disposition of ATRA and its metabolites has been limited. A preliminary *in vivo* physiological pharmacokinetic model for ATRA was developed (McMullin et al., 2003) that used existing radioactivity and urinary data to estimate total Cl-TRI's in plasma, red blood

cells and urine. Due to the lack of time-course data on the individual compounds, this model was based on an aggregate estimate of total Cl-TRIs rather than tracking individual compounds separately. This kinetic analysis indicated the need to more thoroughly examine the oxidative metabolic behavior of ATRA that leads to the total Cl-TRI time-course in order to provide information about the disposition of individual Cl-TRIs. Since the evaluation of these studies tracking total ATRA derived radioactivity, kinetic studies have been conducted to evaluate the time course of individual Cl-TRIs after dosing by oral gavage in female Sprague Dawley (SD) rats (Brzezicki et al., 2003). While these *in vivo* studies provided useful data for developing a physiologically based pharmacokinetic (PBPK) model to evaluate total Cl-TRI tissue dose (Chapter 6), other approaches are needed to estimate kinetic parameters for the oxidative metabolism of ATRA separate from *in vivo* time course studies. For this reason, this research determined *in vitro* kinetic parameters for ATRA oxidative metabolism from time –course studies using incubations with primary rat hepatocytes. A series of kinetic models were generated to describe the dose and time - dependent kinetic behavior of ATRA and the Cl-TRI metabolites. These data provide values of kinetic parameters that serve as initial estimates for metabolic clearance pathways *in vivo.*

3.2 MATERIALS AND METHODS

The following methods and time-course data used in this kinetic analysis are from the thesis of Hatfield – Berube, 2004.

3.2.1. Chemicals

ATRA (97.1% purity), ETHYL (97.1% purity), ISO (97.1% purity) and DACT (96.8% purity) were generously provided by Syngenta Corporation (Greensboro, NC). Earles' balanced salt solution without $CaCl_2$ and $MgCl_2$ (EBSS) was obtained from Sigma Chemical Co. (St. Louis, MO). Hepatocyte Wash Buffer was from GIBCO. Dimethylsulfoxide (DMSO), distilled diethyl ether (EE), Optima grade acetone, n-hexane, iodomethane (stabilized 99%), and tetra-butyl-ammonium hydroxide (TBAOH) were from Fisher Chemical Company (Houston, TX). Cyanazine (CYA; 99% purity) was from Sigma Chemical Company (St. Louis, MO).

Standards of ATRA, ETHYL, ISO, and CYA (all at 4.6 mM) were prepared in acetone. DACT was prepared in DMSO at 6.87 mM. Stock solutions were diluted to working concentrations of 4.6 and 46.3 and 463 μM in acetone.

3.2.2. Hepatocyte Preparations

Female Sprague-Dawley (SD) rats (200-300g) were obtained from Charles River laboratories and held at Colorado State University Laboratory Animal Research facility. All procedures were approved by Colorado State University Animal Care and Use Committee. The isolation of hepatocytes followed the procedure by Seglen (1976) with some modifications. Upon anesthetizing the animal and catheterizing the portal vein, the liver was perfused with Buffer A (500ml EBSS, 7.5 mM HEPES, 100 nM Dexamethasone, 0.75mM EGTA) and 5 ml Penicillin-Streptomycin (Pen-Strep) for 5 min and subsequently perfused with Buffer B (500ml EBSS, 10 mM HEPES, 2.5 mM $CaCl_2$, 100 nM Dexamethasone, 5 ml Pen - Strep, and 0.04% Collagenase) for 5 min. The liver was removed and washed with Hepatocyte Wash Buffer with

gentle stirring for 1.5 min. Only perfused lobes were used for subsequent hepatocyte isolation.

Cells were filtered to remove tissue debris and placed in 50 ml conical vials. Hepatocyte Wash buffer was added to bring the volume to 50 ml. The cellular suspension was centrifuged at 500 rpm (IEC HN-SII centrifuge) for 2 min. After removal of the supernatant, the pellet was re-suspended in Hepatocyte Wash Buffer and centrifuged 2 additional times (500 rpm). This process insures <10% contamination by non-hepatocyte cells (Berry and Friend, 1969). The final pellet was reconstituted to 50 ml with Hepatocyte Wash Buffer and gently mixed. Isolations yielding ≥80% viability, as determined by the trypan blue exclusion assay, were used for metabolism studies.

3.2.3. Incubation procedure and time –course study

Hepatocytes ($2x10^6$ cells/ml) were added to flasks containing 10ml EBSS fortified with 2% bovine serum albumin (BSA). The flasks were continuously shaken at 37^0C under 5%CO_2 in air. After a 15 min. acclimation period, ATRA was added directly to the flasks at concentrations of 1.74, 44, 98, and 266 μM in 0.01% DMSO. Aliquots (100μl) of the media were collected at 0, 30, 60, and 90 min. to monitor the disappearance of ATRA and simultaneous appearance of ISO, ETHYL and DACT. Metabolism was terminated by addition of 500μL saturated sodium sulfate. Samples were spiked with 40nM CYA (surrogate standard) and stored at -20°C until analysis. To monitor possible cytotoxicity due to DMSO, a control flask containing 0.01% DMSO was used in parallel with the samples. To verify daily method performance, control hepatocytes (100μl) were spiked with an internal standard mixture of ATRA,

ETHYL, ISO, DACT and CYA (surrogate standard) and analyzed within each set of unknown time-course samples. Four separate time course experiments were run for 1.74 and 44 μM ATRA. Two separate experiments were run for 98 and 266μM ATRA. Results are plotted as the mean ± SD of all studies at each concentration.

3.2.4. Analysis of Time-Course Samples

Frozen control and time-course samples were analyzed following methods by Brzezicki et al. (2003). Each sample was thawed and extracted over EE (3x2ml) with gentle mixing at RT for 10 min. and followed by centrifugation (2min.) to separate the EE phase. Extracted samples were placed in glass culture tubes (6ml) and evaporated to complete dryness under a steady stream of nitrogen. Acetone (100 μl) in azeotrope residual water was added to the sample and evaporated under nitrogen for 20 min.

Derivatization of all analytes in the samples and standards was performed by adding DMSO (100μl), tetrabutyl ammonium hydroxide (5μl), n-hexane (500μl), and methyl iodide (30μl). Tubes were capped and rotated @ RT for 30 min. After rotation, deionized water (1ml) and n-hexane (2ml) were added to all tubes and shaken for 2 min. The methylated analytes were extracted into the n-hexane phase (3x). Extracts were dried to <100μl under nitrogen. Sample volumes were brought to100μl with n-hexane.

Extracts were analyzed by GC-MS (Hewlett Packard 5890 Gas Chromatograph equipped with a Model 5972 mass-selective detector). Concentrations were quantified using calibration curves. Analyte recoveries were +/- 20% of mean recovery values obtained during daily method validation.

3.2.5. In Vitro Kinetic Model Development

A series of kinetic models were developed in order to analyze the hepatocyte kinetic data while accounting for changes in time-course concentrations of substrate and product. The kinetic analysis included several partial models for metabolism up to the most complete description depicted in Fig.ure 3.1. These models were used to estimate the *in vitro* metabolic rate parameters (V_{max} and K_M) for the saturable, P450 mediated oxidative metabolism of ATRA to its chlorinated metabolites.

The oxidative metabolism of ATRA, ETHYL and ISO is presumed to be catalyzed by the same CYPP450 enzyme. ATRA is metabolized via saturable oxidative metabolism to ETHYL and ISO. Appearance of ETHYL and ISO in the incubation system is determined by the rate of metabolism of ATRA and the fraction metabolized to each mono-dealkylated metabolite (frac). Formation of DACT occurs from oxidative metabolism of the mono-dealkylated metabolites to DACT. In the final model, competitive inhibition of oxidative metabolism influenced the time-course concentrations of each compound (see modeling approach and parameterization in METHODS).

Although it did not improve the ability to describe these *in vitro* results, a, first-order loss rate was initially included to account for non-oxidative clearance such as glutathione conjugation and/or production of non-chlorinated products (katra, kethyl, kiso, kdact). At least in these *in vitro* settings, clearance of these Cl-TRIs is predominantly via oxidative metabolism.

Model code was written using Berkeley-Madonna (B-M) modeling software (version 8.0.1 for Windows). The multiple curve-fitting routine in B-M, which

minimizes the root mean square deviation between the data points and the model output, was used to optimize the various model structures to the time-course data with the 4 compounds at 4 concentrations.

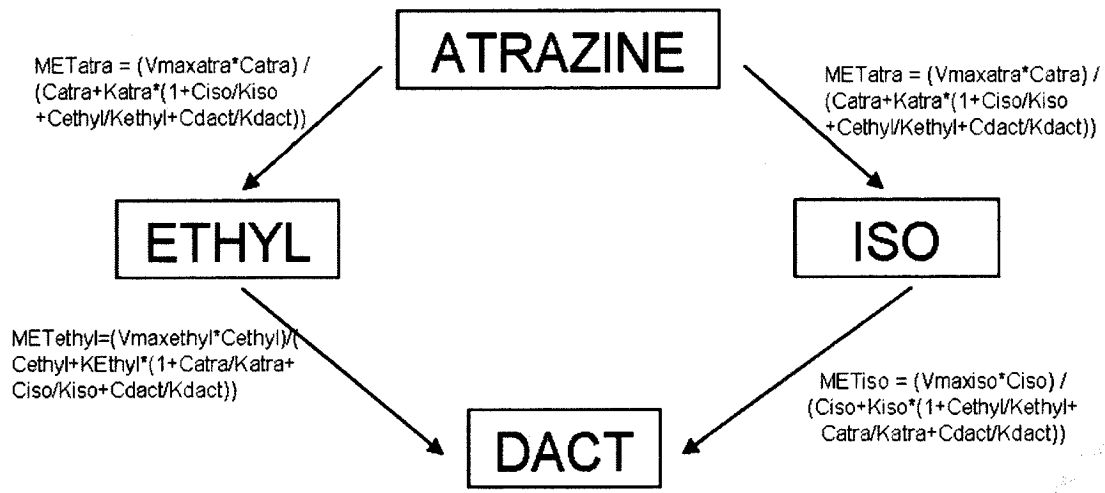

Figure 3.1. Diagram of the kinetic model describing oxidative metabolism of ATRA to ETHYL and ISO and subsequent metabolism to DACT in a hepatocyte incubation system. Equations describe the metabolism of each Cl-TRI where each compound acts as a competitive inhibitor of metabolism on the other compounds.

3.2.6. Model Parameterization

Our first attempt to parameterization utilized a global approach to fit all parameters simultaneously with a single model. Without a strategy for parameter estimation by curve fitting, the constants obtained from the global fit gave extremely low values for Michaelis-Menten (M-M) constants that were biologically unrealistic

and inconsistent with previously published results (Hanoika et al., 1998, 1999a; Hanoika et al., 1999b).

Instead of using an unconstrained fitting procedure for estimating the kinetic constants, we next applied a sequential parameterization process based on the dose-dependent kinetic behavior of the compounds. Three different kinetic models were used. In the first model for the lowest concentration (1.7μM) the kinetics was described by first-order elimination, with a single first-order rate constant $V_{max}atra/K_Matra$. After establishing this rate constant for metabolism for ATRA to the mono-dealkylated metabolites, a second model was developed to estimate the M-M constants under conditions with higher substrate concentration. The data from the 44μM ATRA incubation resulted in peak DACT concentrations, indicating that metabolism of ATRA was approaching the maximal velocity of the enzyme ($V_{max}atra$). Therefore, metabolism of ATRA to the mono-dealkylated metabolites at this concentration was limited by $V_{max}atra$. Using saturable M-M kinetics that included enzyme inhibition by ATRA to describe these data, the second model provided initial estimates of both Vmax and Km, constrained by the value of the first-order constant from the first model. $V_{max}atra$ was estimated by fitting while holding all other parameters constant. K_Matra was estimated using the equation $V_{max}atra/K_Matra$ = first - order transition rate (determined in the first-order model). Initial values of K_Methyl and K_Miso were set to equal K_Matra and then initial estimates of $V_{max}ethyl$ and $V_{max}iso$ were estimated by fitting the 44μM incubation data set. These two models together served as a constraint on the Vmax and Km values utilized in the third model.

This third model was used to describe the entire data set. The data at the higher concentrations (98μM and 266μM) indicated that DACT production was complexly related to the initial ATRA concentration peaking at 44μM and falling at higher incubation concentrations. Therefore, the final kinetic parameter values were determined based on the dose-response curve for DACT at 90 min and then assessed for their ability to simulate all data sets. V_{max} and K_M values for ETHYL and ISO were initially fixed at the values determined in the previous model. The dose-response for DACT at 90 min (Figure 3.3) was visually fit by varying V_{max}atra and $K_M$atra. To account for reduced conversion to DACT at the higher ATRA concentrations, this final model included competitive inhibition between the substrates, as noted in the following equations:

dMETatra/dt = (Vmaxatra*Catra) / (Catra+Katra*(1+Ciso/Kiso+Cethyl/Kethyl+ Cdact/Kdact))

dMETiso/dt = (Vmaxiso*Ciso) / (Ciso+Kiso *(1+Cethyl/Kethyl+Catra/Katra+ Cdact/Kdact))

dMETethyl /dt= (Vmaxethyl*Cethyl)/(Cethyl+Kethyl *(1+Catra/Katra+Ciso/Kiso +Cdact/Kdact))

METatra, METiso and METethyl are the rates of metabolism of ATRA, ISO and ETHYL, respectively. V_{max}atra is the maximal velocity of the enzyme metabolizing ATRA to ETHYL and ISO. V_{max}ethyl and V_{max}iso are the maximal velocities of the enzymes converting the mono-dealkylated metabolites to DACT. Katra, Kiso and Kethyl are the binding affinities that act as competitive inhibitor parameters of ATRA, ISO and ETHYL, respectively.

3.3 RESULTS

3.3.1. Time Course Study

At all incubation concentrations, heteroatom dealkylation of ATRA by CYP450 preferentially attacked the isopropyl group, resulting in ETHYL concentrations up to 6 times higher than ISO. Depletion of ATRA from the solution and production of the mono-dealkylated metabolites ETHYL and ISO were time and dose - dependent over the entire monitoring period (Table 3.1 and Figure 3.2a-c). Unlike the mono-dealkylated metabolites, peak DACT production occurred at 44μM and decreased with increasing substrate concentrations (Figure 3.2d). This non-linear characteristic of ATRA metabolism with respect to DACT indicated that competitive inhibition was likely occurring in the incubation system and was examined in the kinetic analysis.

3.3.2. Kinetic Analysis

The step-wise kinetic analysis was performed to determine *in vitro* metabolic parameters in a system where substrate and product concentrations were time-dependent. This modeling approach also evaluated competitive inhibition as a possible explanation for the non-linear formation of DACT at 98μM and 266μM ATRA (see modeling approach and parameterization in METHODS). A model that described metabolism using M-M kinetics with no inhibition simulated the data at the lowest concentrations but greatly overestimated DACT concentrations at 98μM and 266μM (Fig.ure 3.3a). Competitive inhibition by all Cl-TRis was tested as a plausible explanation for this behavior. Inclusion of inhibition on metabolism accurately estimated the dose-dependent time-course concentrations of ATRA, ETHYL and ISO

while simultaneously describing the non-linear behavior of DACT (Figure 3.3 and Figure 3.4-3.7). Model estimated parameters used in the final kinetic model that includes multi – substrate competitive metabolic inhibition are listed in Table 3.2. Although the final model accounted for competition by all Cl-TRIs for the same metabolizing enzyme, ATRA and the mono-dealkylated metabolites mainly contributed to the overall inhibition since DACT concentrations were minimal relative to the other Cl-TRIs in all these incubations.

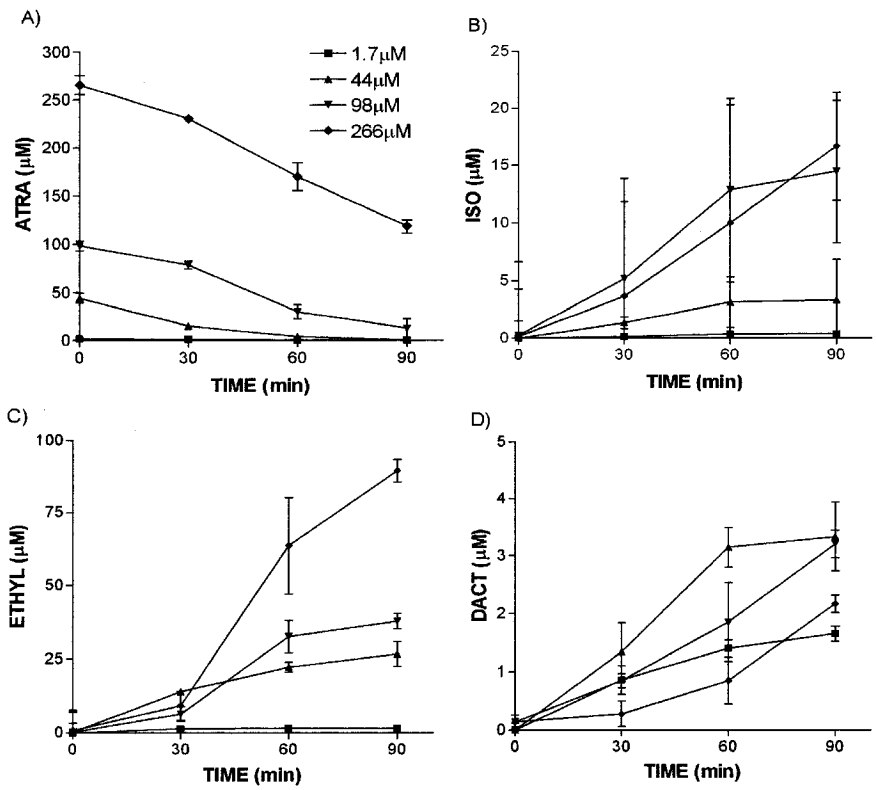

Figure 3.2. Time-course concentrations of (a) ATRA (b) ISO (c) ETHYL and (d) DACT in media after incubation with 1.7, 44.98 and 266 μM ATRA

Table 3.1. Time-Course data of ATRA, ISO, ETHYL and DACT after incubating hepatocytes with a) 1.7μM ATRA b) 44μM ATRA c) 98μM ATRA and d) 266μM ATRA[a,b].

a) 1.7 μM

Time (min)	ATRA	ISOPROPYL	ETHYL	DACT
0	1.74 ± 0.12	0 ± 0.12	0 ± 0.16	0 ± 0.12
30	1.18 ± 0.05	0.13 ± 0.03	1.36 ± 0.05	0.86 ± 0.24
60	0.37 ± 0.12	0.37 ± 0.12	1.5 ± 0.12	1.40 ± 0.15
90	0.11 ± 0.22	0.39 ± 0.01	1.49 ± 0.13	1.65 ± 0.13

b) 44 μM

Time (min)	ATRA	ISOPROPYL	ETHYL	DACT
0	44.1 ± 5.0	0 ± 1.5	0.23 ± 3.0	0 ± 0.05
30	15.1 ± 1.3	1.5 ± 0.51	13.0 ± 0.25	1.3 ± 0.5
60	4.3 ± 1.4	3.1 ± 2.2	22.2 ± 1.6	3.1 ± 0.3
90	0.31 ± 2.5	4.2 ± 3.5	26.6 ± 4.2	3.3 ± 0.6

c)98 μM

Time (min)	ATRA	ISOPROPYL	ETHYL	DACT
0	98.1 ± 5.0	0.28 ± 4.0	0.2±7.0	0.14 ± 0.05
30	78.3 ± 4.0	5.2 ± 6.7	6.5±2.5	0.84 ± 0.12
60	29.8 ± 7.5	12.9 ± 8.0	32.5±5.5	1.8 ± 0.68
90	12.6 ± 10.0	14.5 ± 6.2	37.7±2.5	3.2 ± 0.24

d) 266 μM

Time (min)	ATRA	ISOPROPYL	ETHYL	DACT
0	265 ± 10	0.14 ± 6.5	0.76 ± 7.0	0.14 ± 0.12
30	230 ± 2.3	3.7 ± 10.2	9.2 ± 4.9	0.28 ± 0.22
60	170 ± 14.5	10 ± 10.3	63.5 ± 16.5	0.84 ± 0.4
90	118 ± 6.8	16.7 ± 4.7	89.4 ± 3.9	2.2 ± 0.15

[a] Data are expressed as mean ± SD.
[b] Taken from Hatfield-Berube, 2004

Additional clearance from the incubation system due to GSH conjugation or production of other metabolites not monitored in this study was also considered. However, the mass balances for the time course studies and the subsequent kinetic

analysis indicated that this loss was negligible compared to oxidative metabolic clearance.

While the model structure describing metabolism with competitive substrate inhibition provided a good estimate to the majority of the data sets, the final model structure underestimated the 1.7μM DACT data. This incubation required analysis of the lowest concentrations of the Cl-TRI and in this study the sum of ATRA and all chlorinated products during the incubations was frequently greater than the initial ATRA concentration. This data set was most important for assessing the first-order clearance of ATRA from the incubation media and to determine the proportion of ETHYL and ISO produced by ATRA oxidation.

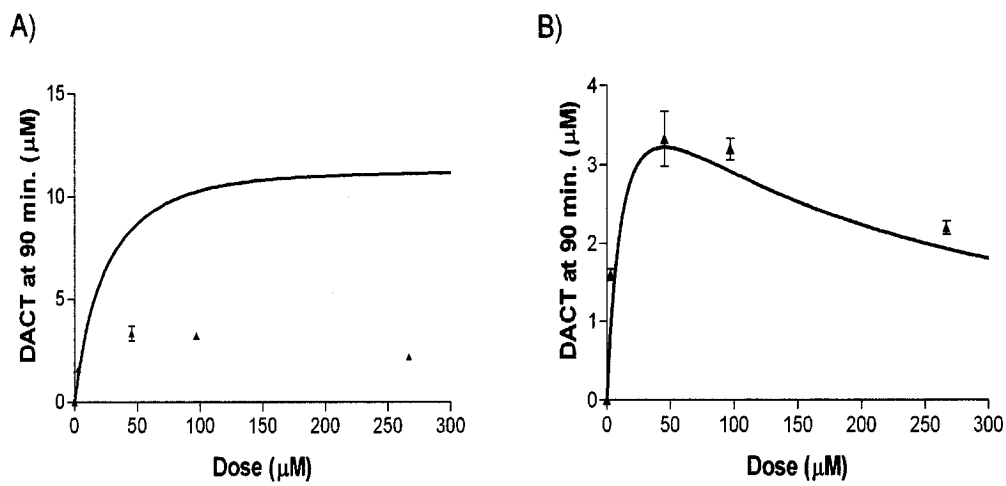

Figure 3.3. DACT dose-response at 90 minutes comparing model simulations (a) without and (b) with competitive metabolic inhibition terms. The non-linear behavior of DACT formation could only be simulated with a model that included competitive inhibition of oxidative metabolism. Lines represent model simulations. Points represent data means ± SD.

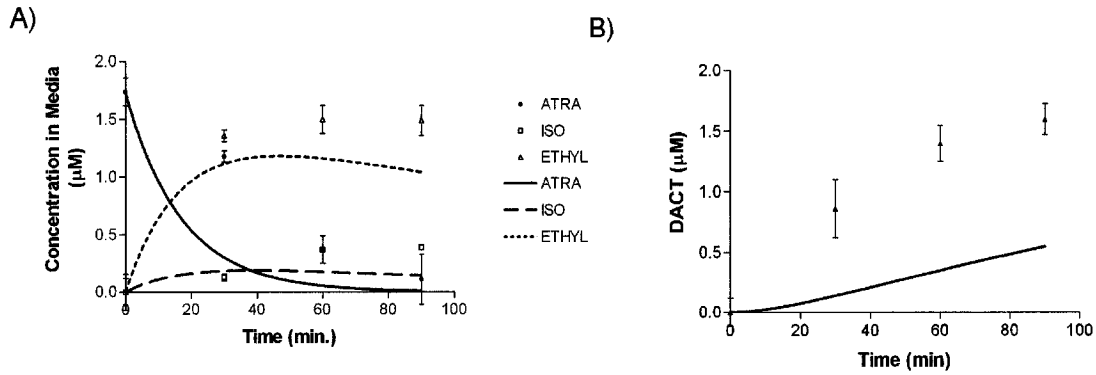

Figure 3.4. Experimental data and competitive inhibition model simulations of (a) ATRA, ETHYL, ISO and (b) DACT after 1.74μM ATRA treatment. Lines represent model simulations. Points represent data means ± SD.

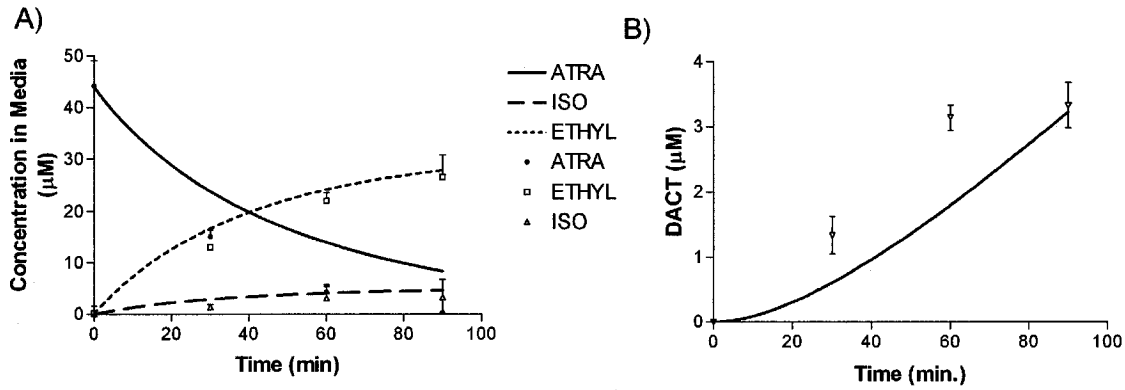

Figure 3.5. Experimental data and competitive inhibition model simulations of (a) ATRA, ETHYL, ISO and (b) DACT after 44μM ATRA treatment. Lines represent model simulations. Points represent data means ± SD

Mono-dealkylated metabolite formation depended on the rates of oxidative metabolic clearance of ATRA and the proportion of ATRA metabolized to ISO and ETHYL. ATRA oxidation produced 85% ETHYL and 15% ISO metabolites. The DACT time-course concentrations were then dependent on the metabolic rates of

oxidation of the mono-dealkylated metabolites. The estimates of the parameters for the model indicated that the oxidative metabolic clearance of ATRA to the mono-dealkylated metabolites ($V_{max}atra/K_Matra = 0.06\ hr^{-1}$) was greater than the rates of oxidative metabolism of ETHYL and ISO to DACT ($V_{max}ethyl/K_Methyl = 0.005\ hr^{-1}$, $V_{max}iso/K_Miso = 0.009\ hr^{-1}$) (Table 3.2).

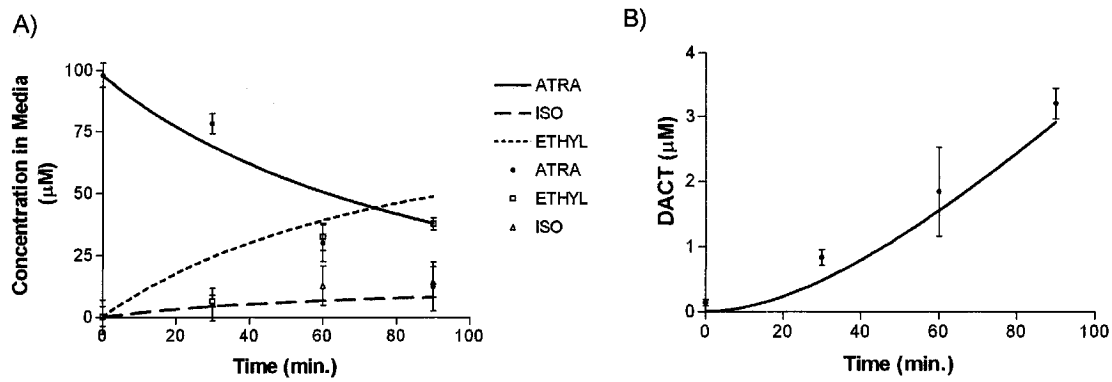

Figure 3.6. Experimental data and competitive inhibition model simulations of (a) ATRA, ETHYL, ISO and (b) DACT after 98μM ATRA treatment. Lines represent model simulations. Points represent data mean ± SD.

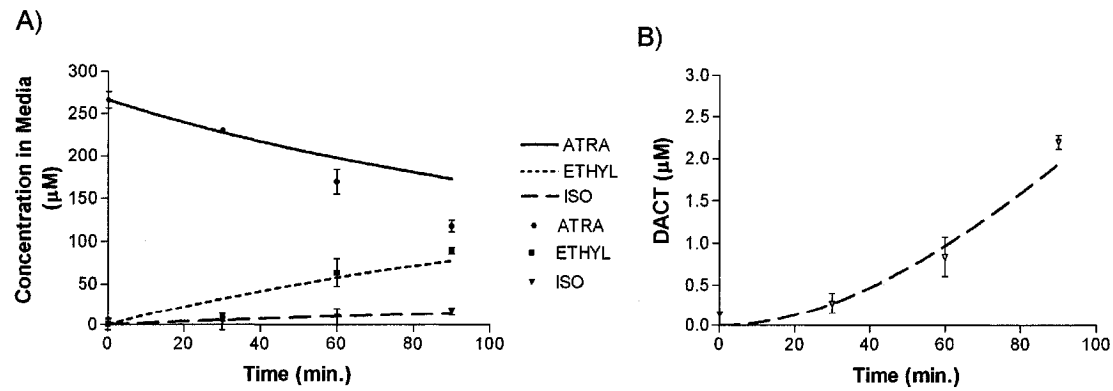

Figure 3.7. Experimental data and competitive inhibition model simulations of (a) ATRA, ETHYL, ISO and (b) DACT after 266μM ATRA treatment. Lines represent model simulations. Points represent data means ± SD.

Table 3.2. Model estimated parameters used in the final kinetic model that accounts for multi – substrate competitive metabolic inhibition

Parameter		Value
V_{max}atra (μM/min)	Maximum metabolic rate of ATRA to ETHYL and ISO	1.6
V_{max}ethyl (μM/min)	Maximum metabolic rate of ETHYL to DACT	0.07
V_{max}iso (μM/min)	Maximum metaboic rate of ISO to DACT	0.12
$K_M$atra (μM)	Micaelis-Menten constant for ATRA	25.0
$K_M$ethyl(μM)	Micaelis-Menten constant for ETHYL	13.3
$K_M$iso (μM)	Micaelis-Menten constant for ISO	13.3
$K_M$dact (μM)	Micaelis-Menten constant for DACT	10000
Frac	Fraction of ATRA metabolized to ISO	0.15

3.4. DISCUSSION

A quantitative description of the oxidative metabolism of ATRA is necessary for predicting net tissue dose to Cl-TRIs for exposure to ATRA in the environment. This study utilized a sequential kinetic modeling approach from data generated in primary rat hepatocytes to determine metabolic kinetic parameters for oxidative metabolism of ATRA to its chlorinated metabolites. Hepatocytes were incubated with concentrations of ATRA that resulted in dose- dependent kinetic behaviors of the Cl-TRIs over 90 min.

3.4.1. Oxidative Metabolism of ATRA in Rat Hepatocytes

The preferential metabolism of ATRA to ETHYL over ISO is consistent with results obtained from microsomal *in vitro* studies where the clearance of ATRA due to oxidative metabolism to ETHYL was ten-fold greater than oxidative metabolic clearance to ISO (Hanoika et al., 1999a; Hanoika et al., 1999b). Similar metabolic behavior occurs *in vivo*. Peak ETHYL concentrations were approximately 3-fold greater than ISO after an oral gavage dose of 150 mg ATRA/kg b.w. (Brzezicki et al.,

2003). This kinetic behavior is most likely due to preferential attack by the P450 oxidative enzyme on the CH group adjacent to the nitrogen in the ISO side-chain rather than the methylene group adjacent to the nitrogen in the ETHYL side chain.

Unlike the constants obtained from the initial global fit, the metabolic constants estimated in the final model are similar to previous estimates from microsomal studies. Using the fraction of ATRA metabolism to ISO of 0.15 and converting the *in vitro* values to common *in vivo* units, V_{max} values for ATRA to ISO and ETHYL determined in our hepatocyte incubation system are 0.028mmol/hr/kg and 0.156 mmol/hr/kg, respectively. Hanoika et al. (1999a, b) report similar V_{max} values for ATRA metabolism to ISO of 0.01 – 0.012mmol/hr/kg and ATRA metabolism to ETHYL of 0.12 – 0.15mmol/hr/kg. However, the K_M value for ATRA metabolism to ETHYL and ISO determined in microsomes is approximately 2 times greater than the value reported here.

DACT is produced from the oxidative metabolism of the mono-dealkylated metabolites. While our time-course results indicate DACT production after ATRA incubation, DACT was not detected in a microsomal study by Hanoika *et al.* (1999). The lack of DACT production in this microsomal study was likely due to the incubation conditions where high concentrations of ATRA (up to 200μM) were incubated for 20min rather than 90 min in our study. The results from the present work indicate that DACT formation would be minimal due to inhibition of oxidation of ETHYL and ISO by high concentrations of ATRA.

To evaluate the contribution each mono-dealkylated metabolite has in formation of DACT, *in vitro* and *in vivo* time-course studies using each mono-

dealkylated metabolite as a substrate have previously been performed. In all previous studies, oxidative metabolism of ISO resulted in significantly more DACT than metabolism of ETHYL (Dauterman and Mueke, 1973; Brzezicki et al., 2003). The kinetic analysis performed in this study similarly predicted a larger contribution of DACT formation from ISO metabolism, as estimated by V_{max}/K_M.

3.4.2. Evaluation of Competitive Metabolic Inhibition

Mechanistic kinetic models provide useful tools to examine possible mechanisms responsible for the kinetic behaviors of compounds (i.e. different metabolic interactions). An interesting outcome here was the observation that the greatest DACT production occurred at 44μM and subsequently decreased with increasing substrate concentration. This behavior indicated a dose-dependent suppression of oxidative metabolism consistent with substrate inhibition (Figure 3.3). This hypothesis was tested by use of a kinetic model that included competitive inhibition by all Cl-TRIs. Inclusion of competitive metabolic inhibition by all Cl-TRIs was necessary to describe every data set, including the non-linear characteristics of DACT while providing an internally consistent and biochemically realistic set of model parameters. Although competitive metabolic inhibition occurs at high substrate concentrations within this *in vitro* system, this phenomenon still needs to be examined for its relevance *in vivo*.

Dose-dependent inhibition of product formation has been observed *in vitro* and *in vivo* with compounds in which both the parent compound and metabolite(s) are extensively metabolized by the same enzyme. For example, hexane is metabolized to methyl-n-butyl ketone (MNBK) with further metabolism of MNBK to hexanedione

(HD) by the same oxidative enzyme. Increasing hexane expsoure saturates the rate of metabolism to MNBK, causing inhibiton of HD formation at exposure concentrations greater than 100ppm (Baker and Rickert, 1981). This kinetic behavior was described in a PBPK model that included dose-dependent competitive metabolic inhibition of HD by hexane (Andersen and Clewell, 1983). Benzene displays similar dose-dependent behavior to hexane. Schlosser *et al.* (1993) developed an *in vitro* kinetic model to determine kinetic parameters for oxidative metabolism of benzene to phenol and the subsequent metabolism of phenol to hydroquinone and catechol from data obtained in mouse and rat microsomes. The kinetic disposition of each compound was successfully simulated by describing metabolism with competitive inhibition of phenol to hydroquinone as benzene concentrations increased.

3.4.3. Summary

The kinetic analysis used to evaluate the time-course behavior of ATRA and the Cl-TRI metabolites in rat hepatocytes demonstrates the utility of kinetic modeling in determining *in vitro* kinetic parameters and in testing plausible mechanisms to describe kinetic behaviors of compounds (i.e. competitive inhibition). Previous studies have successfully integrated parameters determined in primary hepatocytes into PBPK models to simulate in vivo biotransformation of compounds that are primarily metabolized in the liver (Kedderis et al. 1993, 1996; Andersson *et al.*, 2001). Similarly, the V_{max} for ATRA determined in this study can be extrapolated to an *in vivo* value assuming $128x10^6$ hepatocytes/g liver (Seglen, 1976). This extrapolation provides a V_{max} for oxidative metabolism of ATRA to the mono-dealkylated metabolites of 0.116 mmol/hr/kg. While the Km values can be reliably

used to estimate the kinetics *in vivo*, determination of accurate rates of oxidative metabolism of the mono-dealkylated metabolites to DACT (V_{max}ethyl and V_{max}iso) may require future kinetic studies in a hepatocyte incubation system using the mono-dealkylated metabolites as substrates. The *in vitro* kinetic parameters determined in freshly isolated heptocytes should be useful for developing a PBPK model to describe the oxidative metabolism of ATRA that contributes to total Cl-TRI tissue dose.

CHAPTER 4

A PHSYIOLGICAL MODEL TO DESCRIBE ABSROPTION AND OXIDATIVE METABOLISM OF ATRAZINE AND ITS CHLOROTRIAZINE METABOLITES IN RAT

4.1. INTRODUCTION

Risk assessments for human exposures to ATRA should be based on an understanding of the concentrations of ATRA and/or active metabolites that reach target tissues. Until recently, *in vivo* kinetic descriptions of plasma Cl-TRI concentrations were limited to studies using [^{14}C]-ATRA (Thede, 1987; Timchalk et al., 1990). While useful in understanding the overall disposition of ATRA, these radiolabeled studies did not differentiate between parent compound and metabolite in tissue. However, the data from these studies combined with limited data on the concentrations of ATRA and its metabolites in urine permitted development of a preliminary physiological pharmacokinetic (PPK) model describing Cl-TRI plasma dosimetry in the rat after single and multiple oral gavage exposures (Chapter 2). From this PK analysis, relative first-order rates of oxidation of Cl-TRIs and for GSH conjugation could be adjusted in order to account for total Cl-TRI time-course disposition in the rat. This approach, though far from optimal, could describe the kinetics of Cl-TRIs separate from non-chlorinated species such as GSH conjugates. The analysis of the data sets with this PK model showed that the time-course of radiolabeled material in the plasma was dependent on several processes: relatively slow uptake of ATRA from the gut, extensive metabolic and excretory clearance

processes, and Cl-TRI reactivity with red blood cells and plasma proteins. However, it was difficult to extrapolate this initial model to other doses, dose-routes or species in the absence of information on the disposition of individual Cl-TRIs.

To evaluate the kinetic behavior of individual Cl-TRIs, *in vivo* and *in vitro* studies have been performed in our laboratory to determine the rates of oxidative metabolism of ATRA to the mono and di-dealkylated chlorinated metabolites (Hatfield - Berube, 2004; Brzezicki, 2003). *In vitro* time-course studies using primary rat hepatocytes incubated with ATRA examined the dose-dependent metabolic behavior of ATRA and the Cl-TRI metabolites. These data were used to develop a kinetic model that estimated Michaelis-Menten (M-M) parameters for the oxidative metabolism of ATRA to the chlorinated metabolites (Chapter 3).

By integrating the metabolic parameters determined *in vitro* and using previously determined time-course plasma data on individual Cl-TRIs (Brzezicki, 2003), the goal of this work was to develop a more comprehensive PBPK model to assess the rates of processes such as absorption and oxidative metabolism that contribute to the pharmacokinetic behavior of individual Cl-TRIs in the rat. Additionally, this chapter also includes estimates of brain concentrations of Cl-TRIs and the inclusion of this data into an *in vivo* PBPK model. The brain concentrations are particularly important since brain regions in the hypothalamus or pituitary are proposed to be targets for the neuroendocrine responses of laboratory rats to these Cl-TRIs.

4.2 MATERIALS AND METHODS

4.2.1. Animals

ATRA (97.1% purity), ETHYL (97.1% purity), ISO (97.1% purity) and DACT (96.8% purity) were generously provided by Syngenta Corporation (Greensboro, NC). Female Sprague-Dawley (SD) rats (200-225 g) were obtained from Charles River Laboratories (Raleigh, NC) and kept in the central animal care facility at Colorado State University . All studies were approved by the Animal Care and Use committee at Colorado State University. Rats had free access to certified Teklad NIH-07 rodent diet and tap water prior to beginning the study. Food was withdrawn before dosing and returned approximately 12 hours later.

4.2.2. Time- Course Studies used for modeling

Plasma time-course studies. The plasma time-course data of individual Cl-TRIs after dosing with each Cl-TRI were determined by Brzezicki (2003). Female SD rats were administered equal molar amounts of Cl-TRIs: (a)150mg ATRA/kg b.w. (b) 121.5 mg ETHYL/kg b.w. (c)132 mg ISO, kg b.w. or (d)100.2 mg DACT/kg.b.w. in 1% carboxymethylcellulose (CMC) (dosing volume = 0.5ml ATRA/100g) between 0800 – 0900 by oral gavage. Whole blood samples were taken via indwelling jugular cannulae from two groups of animals (n=3/group) that received identical treatment regimens but were alternately bled at different times post-dose (group A = 0.5, 2, 8, 24, 72 hrs; Group B = 1, 4, 12, 48 hrs). Whole blood was centrifuged to separate plasma and stored at -20°C until analysis. Samples were analyzed for ATRA, ETHYL, ISO and DACT by gas chromatography with detection by mass spectrometry as described by Brzezicki *et al.* (2003).

Brain Time - Course Study. This study determined Cl-TRI time-course concentrations in plasma and whole brain samples (target tissue) after dosing with ATRA. Female SD rats (n=12) were gavaged with 150 mg ATRA /kg b.w. in 1.0% CMC (dosing volume = 0.5ml ATRA/100g) at 0900. The animals consisted of four groups (n=3/group) that received identical treatment regimens but were killed at different times (0.5, 2, 24, 72 hr). Sacrifice times were chosen to span the absorption phase, the peak concentrations of DACT and the elimination phase based on the previous Cl-TRI plasma time - course studies. At the designated time points, rats were deeply anesthetized by isoflourane and whole blood was collected via cardiac puncture. Blood was centrifuged to separate the plasma for analysis. Whole brains were removed and rapidly frozen in liquid nitrogen. Tissue and plasma were stored at -20°C until analysis. Samples were analyzed for ATRA, ETHYL, ISO and DACT by gas chromatography with detection by mass spectrometry.

4.2.3 Model Structures

The models consisted of four compartments - the gut (absorption), liver (primary site of metabolism), brain (target tissue) and a lumped body compartment (remaining volume of distribution). Mass balance differential equations were included to describe the time-course concentrations of each Cl-TRI in plasma and brain. All model equations were solved using Berkeley Madonna™ software package. The models were developed in a sequential manner beginning with development of a model to describe the time-course of DACT after dosing with DACT, followed by modeling the time course of the mono-dealkylated metabolites

with the DACT parameters held constant. The Berkeley-Madonna code for these models is available on CD from the author (TSM).

DACT model. Absorption of DACT from the gut into the body compartment was described by a first -order rate of uptake from the gut. Clearance of DACT occurred by a first-order elimination process that represented a composite rate including both GSH conjugation and urinary elimination (Figure 4.1a).

ETHYL and ISO models. The uptake of the mono-dealkylated metabolites into the body could not be accurately described with a single first - order absorption rate. Instead, the administered doses of ETHYL and ISO had to be apportioned between a first –order and a zero-order uptake process. Upon administration into the gut, each mono-dealkylated metabolite also underwent pre-systemic metabolism prior to entering circulation. Plasma clearance of the mono-dealkylated metabolites occurred by saturable, oxidative metabolism in the liver to DACT and a first – order clearance process that represented GSH conjugation and urinary elimination (Figure 4.1b, 1c). Time-course concentrations of DACT were dependent on oxidative metabolism of the respective substrate and loss of DACT due to first-order clearance processes.

ATRA model. To describe the observed time courses of Cl-TRIs following oral gavage with ATRA it was necessary to invoke a more complex absorption process than that used for the mono-dealkylated metabolites. The initial dose was divided into three portions that were absorbed by rapid first - order uptake, slower first order uptake and a third zero -order uptake process (Figure 4.1d). Oxidative metabolism of ATRA to the mono-dealkylated metabolites and subsequent

metabolism of the mono-dealkylated metabolites to DACT occurred in the liver and GI tract. Hepatic oxidative metabolism was described by saturable M-M kinetics with inclusion of dose-dependent competitive metabolic inhibition among the Cl-TRIs. Metabolic inhibition was included to evaluate *in vitro* observations that showed competitive metabolic inhibition among the Cl-TRIs at high incubation concentrations of ATRA (Chapter 5). Inhibition of ISO and ETHYL metabolism to DACT by ATRA (see APPENDIX C) was included in model development and its relative importance depended on the concentrations of the Cl-TRIs available for metabolism at any particular time.

The ATRA time –course study indicated less bioavailability of ATRA and greater ISO and ETHYL plasma concentrations than could initially be predicted when assuming that all absorbed compound reached the liver as parent ATRA. With metabolism only in liver, the simulations consistently underestimated time-course concentrations of ETHYL and ISO while ATRA plasma concentrations were overestimated after ATRA administration. Several compounds are known to be metabolized by oxidative enzymes in the GI tract prior to absorption into portal blood (Gibaldi et al., 1971; Wacher et al., 1998; Pang et al., 1986; Doherty and Pang, 2000; Kaminsky and Zhoung, 2003). In evaluating the optimal model structure needed to describe the ATRA uptake data, intestinal metabolism of ATRA to mono-dealkylated metabolites was included to determine if this second pre-systemic clearance pathway might be significant for ATRA.

Intestinal metabolism was included by addition of first - order rate of oxidative metabolism in the gut (krxn).

A

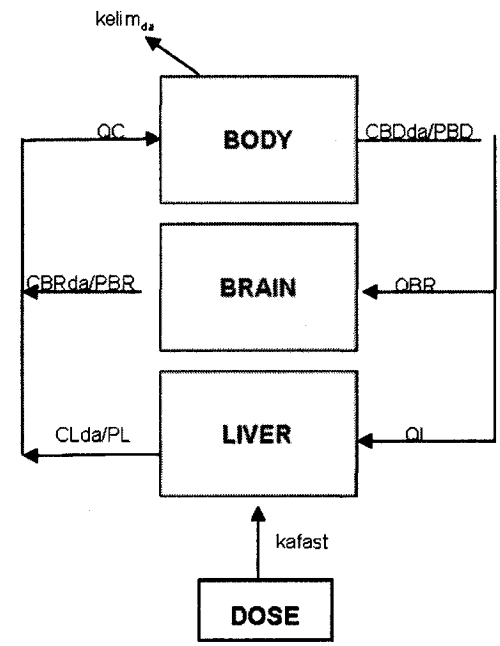

B

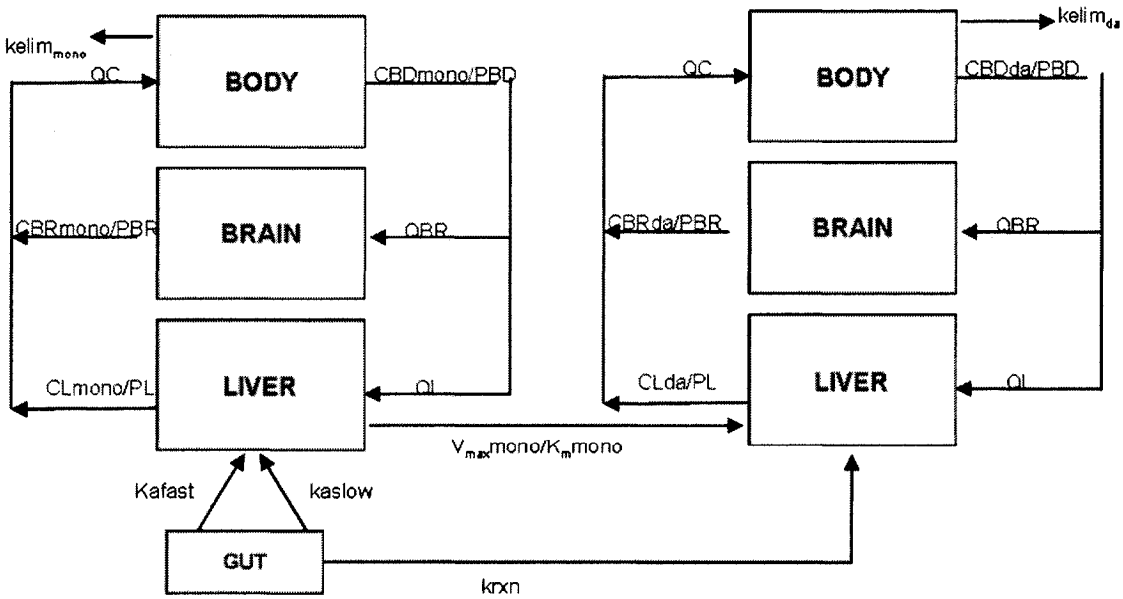

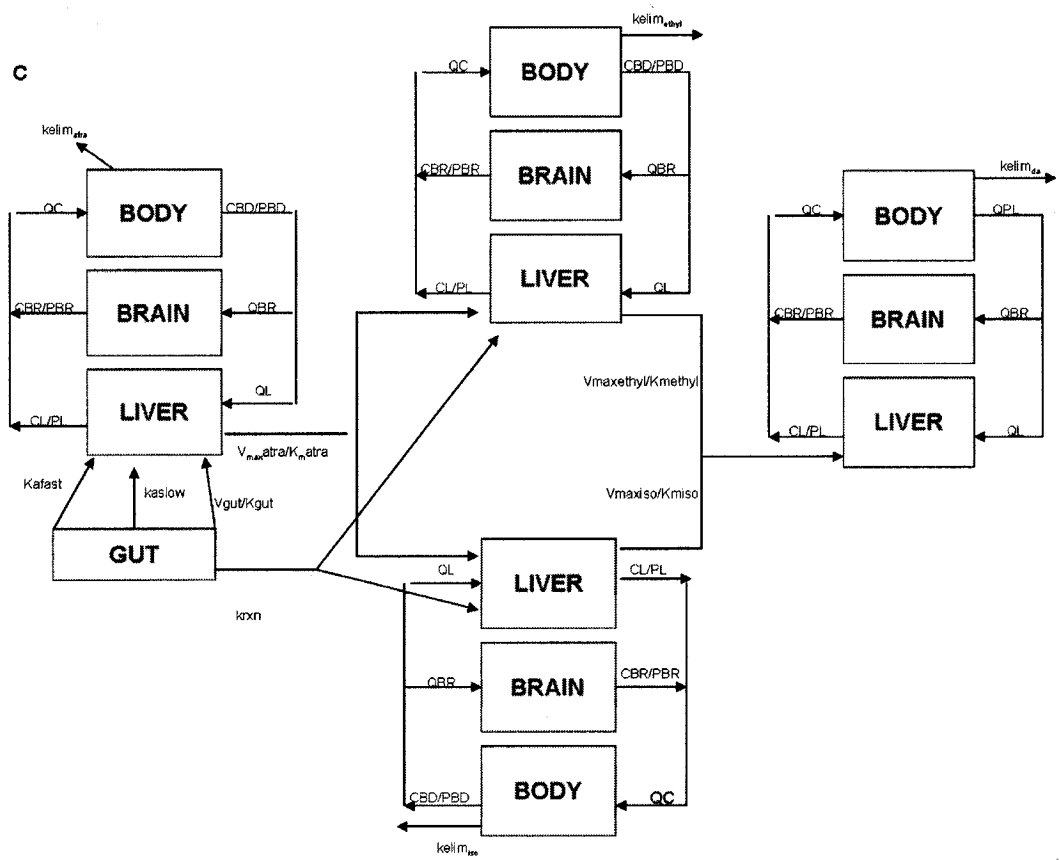

Figure 4.1. Structure of the PPK models describing time-course concentrations of a) DACT after dosing with DACT b) the mono-dealkyalated metabolites (mono = ETHYL or ISO) and DACT after dosing with ETHYL or ISO c) ISO and DACT after dosing with ISO and c) ATRA, ETHYL, ISO and DACT after dosing with ATRA. Values of the parameters are provided in Table 4.1 and 4.2.

Upon absorption of ATRA by each uptake process (fast first-order, slow first-order, zero-order), the absorbed compound could either be swept away in blood to liver or undergo metabolism in the GI tract tissues. Thus, a portion of the absorbed dose of ATRA would be metabolized in the GI tract to ETHYL and ISO.

The following equations described the fraction of ATRA metabolized by the intestines to the mono-dealkylated metabolites and subsequent uptake of ATRA, ETHYL and ISO from the gut prior to entering circulation:

Proportion of ATRA unchanged

(1) (PROPatra) = Ka/(Krxn+Ka)

Proportion of ATRA metabolized in intestine to ETHYL (PROPethyl)

(2) (1-frac)*(Krxn/(Krxn+Ka))

Proportion of ATRA metabolized in intestine to ISO (PROPiso)

(3) frac*(Krxn/(Krxn+Ka))

Uptake rate of administered ATRA

(4) PROPatra x (total uptake rate from gut)

Uptake rate of ETHYLproduced from intestinal metabolism of ATRA

(5) PROPethyl x (total uptake rate from gut)

Uptake rate of ISO produced from intestinal metabolism of ATRA

(6) PROPiso x (total uptake rate from gut)

Ka is the absorption rate of Cl-TRIs that is specific for each uptake process. AGUT is the amount of ATRA in the gut compartment; Frac is the fraction of ATRA metabolized to ETHYL versus ISO; Krxn is the first-order rate of oxidative metabolism in the gut. In this formalism, the proportion metabolized depends of the ratio of the rates of intestinal metabolism (krxn) and absorption (ka). For slower absorption processes, occurring at longer times after dosing with ATRA, there would be greater pre-systemic clearance related to intestinal metabolism (since the ka term operative with the slowest uptake would be small).

The percentage of administered ATRA that was removed from blood by oxidative metabolism, intestinal metabolism and elimination and the rate equations that described each of these processes were determined by the following equations:

Hepatic oxidative metabolism of ATRA

(7) rate of amt. ATRA metab. to ISO = frac*(V_{max}atra*CLatra/PL)/($K_M$atra + CLatra/PL)

(8) rate of amt. ATRA metab. to ETHYL = (1-frac)*(V_{max}atra*CLatra/PL)/($K_M$atra + CLatra/PL)

(9) % ATRA metabolized to iso = (amt. ATRA metabolized to ISO/dose)*100

(10) % ATRA metabolized to ethyl = (amt. ATRA metabolized to ETHYL/dose)*100

Frac is the fraction of administered ATRA metabolized to ISO; V_{max}atra is the maximal velocity of ATRA metabolism to ISO and ETHYL; K_M is the binding affinity of the P450 oxidative enzyme to ATRA; CLatra is the concentration of ATRA in liver; PL is the liver:plasma partition coefficient.

First-order elimination of ATRA =

(11) rate of amt. ATRA eliminated = kelimatra*ALatra

(12) % ATRA eliminated = (amt. ATRA eliminated/dose)*100

kelimatra is the first-order rate constant for elimination of ATRA from the body; ALatra is the amount of ATRA in liver

Intestinal oxidative metabolism of ATRA = see equations 1-6

(12) % ATRA cleared by intestinal metabolism: = 100 – (eq. 9 + eq. 10+ eq. 12)

Additional plasma clearance of ATRA occurred via a non-specific first -order elimination representing processes such as GSH conjugation and urinary elimination (Figure 4.1d). The kinetic behavior of the mono-dealkylated metabolites and DACT in modeling the ATRA time course studies were controlled by the same processes that affected clearance of these compounds when they were administered directly.

4.2.4. Model Parameterization

Figure 4.2 illustrates the sequential parameterization process used to develop an integrated description of the time-course concentrations of all Cl-TRIs after administration of ATRA. This approach minimized the number of parameters required to be optimized simultaneously, while still providing a single set of parameters for all data sets for dosing with the four Cl-TRIs. Values for tissue volumes, blood flows, and physiological parameters were from Brown *et al.* (1997). The liver: body partition coefficient (PL) was taken from McMullin *et al.* (2003)

(Chapter 3). Optimum absorption and elimination constants and the brain to plasma partition coefficient were estimated using the curve fitting routine in B-M™ that minimized the root mean square deviation between the data points and the model output. *In vitro* estimates of V_{max} and K_M metabolic constants (Chapter 3) were used as starting values for kinetic constants in the ETHYL, ISO and ATRA models. Model parameters, including units and values, are in Table 4.1.

DACT model. Simulation of the plasma time-course data for DACT provided values for the volume of distribution (vbd) and the first-order elimination rate of DACT (kelimda) that were integrated into the other models.

ETHYL and ISO models. Both *in vitro* estimated V_{max} and K_M (Chapter 3) values for ETHYL and ISO were initially incorporated into the mono-dealkylated models. However, integrating both parameters and keeping the DACT parameters constant caused an underestimation of the DACT time-course concentrations. Because K_M values determined *in vitro* are unlikely to be different *in vivo*, these values were utilized in the models. Absorption rates, V_{max} and first-order elimination rates were estimated by fitting the time course data for the mono-dealkylated Cl-TRIs and DACT using the parameter estimation module in Berkeley-Madonna.

ATRA model. The chemical specific parameters estimated in the DACT, ETHYL and ISO models, the volume of distribution determined in the DACT model and the hepatic oxidative metabolic parameters for ETHYL and ISO were incorporated directly into the ATRA model. *In vitro* estimated parameters for hepatic oxidative metabolism of ATRA to the mono-dealkylated metabolites (V_{max}atra, $K_M$atra) were also used directly in the ATRA model.

DACT concentrations were significantly greater than the concentrations of other Cl-TRIs after dosing with ATRA. Global parameter estimations using a non-weighted fitting algorithm repeatedly fit the DACT concentrations and provided poor fits to the other Cl-TRIs. To achieve fits to all 4 Cl-TRI time courses after dosing with ATRA, a more targeted approach to parameterization was used that was based on the knowledge of the underlying processes occurring during each part of the time-course curve. Initial fitting by trial and error adjustments of absorption parameters and the fraction of ATRA metabolized to ETHYL and ISO indicated the presence of phases of rapid uptake and subsequent plateaus with the mono-dealkylated metabolites after dosing with ATRA. Optimized values for these respective uptake rate constants were obtained by formal fitting of the time course curves for ATRA, ISO and ETHYL. Once absorption was adequately described, the rate constant of intestinal metabolism of ATRA to the mono-dealkyalted metabolites and the rate constant of non-specific first-order elimination of ATRA were determined by simultaneously optimizing the model predictions to the ATRA, ETHYL, ISO and DACT time-course data. The data on the time-course concentrations of Cl-TRIs in brain were simulated by adjusting the brain:plasma partition coefficient.

4.3. RESULTS

These PPK models examined the absorption and oxidative metabolic clearance processes regulating blood and tissue concentrations of Cl-TRI in rat after oral gavage administration of ATRA. The plasma time course data combined with

the previously estimated *in vitro* oxidative metabolic parameters provided a comprehensive data set for development of these models.

Using these data, four models were successively developed to describe the time-course profiles of each individual compound after dosing with DACT, ETHYL, ISO and ATRA. This approach restricted the number of parameters that needed to be estimated simultaneously in each model and provided a common set of biologically realistic compound specific values that described the individual Cl-TRI plasma profiles following each dosing situation (Figure 4.2 and Table 4.1).

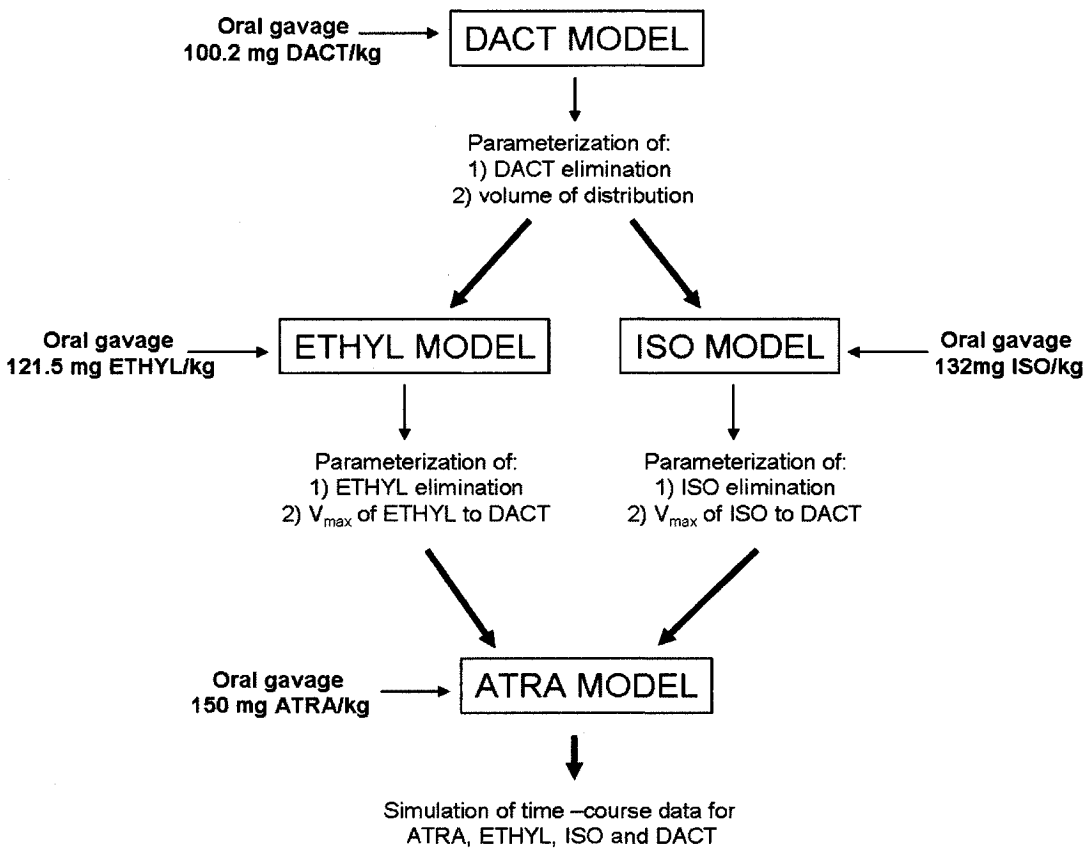

Figure 4.2. Schematic representation of the sequential parameterization process used in the development of the chlorotriazine PPK models.

Table 4.1. Physiological and Model Estimated Parameters used in the DACT, ISO, ETHYL and ATRA PBPK models

Parameter		Model			
		MODEL			
		DACT	ISO	ETHYL	ATRA
Physiological Parameters[a]					
Blood Flows					
QCC	Cardiac Output (L/hr/kg$^{.74}$)	9.0	9.0	9.0	9.0
QLC	Fraction of blood flow to liver (L/hr/kg$^{.74}$)	0.25	0.25	0.25	0.25
QBR	Fraction of blood flow to brain (L/hr/kg$^{.74}$)				
Tissue Volumes					
VL	Volume of Liver (L/kg)	0.04	0.04	0.04	0.04
VBR	Volume of Brain (L/kg)	0.008	0.008	0.008	0.008
VBD	Volume of body (L/kg)	1.77[f]	1.77[f]	1.77[f]	1.77[f]
Partition Coefficients					
PBD	body:plasma for Cl-TRIs	1.0	1.0	1.0	1.0
PL[b]	liver:plasma	4.0	4.0	4.0	4.0
PBR	brain:plasma	--	--	--	2.25
Elimination Rate Constants					
kelimcatra[c]	Non-specific elimination of ATRA (/hr/kg $^{0.7}$)	---	---	---	450
kelimciso[d]	Non-specific elimination of ISO (/hr/kg $^{0.7}$)	---	38	---	38
kelimcethyl	Non-specific elimination of ETHYL (/hr/kg $^{0.7}$)	---	---	12.6	12.6
kelimcda[f]	Non-specific elimination of DACT (/hr/kg $^{0.7}$)	0.41	0.41	0.41	0.41
Absorption Rate Constants					
kaslow	Slow first-order absorption from gut (hr^{-1})	---	---	---	0.05
kafast	Fast first-order absorption from gut (hr^{-1})	0.85	6.0	5.0	1.75
Vgut	Zero-order absorption (mmol/hr)	---	.012	0.005	0.005
Kgut	Zero-order absorption (mmol)	---	.006	0.012	0.005
Intestinal Metabolism Rate Constant					
krxn	intestinal metabolism rate (hr^{-1})	---	0.129	0.029	1.4

--- Parameter not included in model
[a] Based on Brown et al. (1997)
[b] taken from McMullin et al.(2003) (Chapter 3) model estimations
[c] Determined from fitting the ATRA model to the ATRA time course data
[d] Determined from fitting the ISO model to the ISO time-course data
[e] Determined from fitting the ETHYL model to the ETHYL time-course data
[f] Determined from fitting the DACT model to the DACT time-course data

4.3.1. Absorption of chlorotriazines

Plasma time- course concentrations of DACT after dosing with DACT followed first-order absorption and elimination kinetics (Figure 4.3). Simulation of these data provided an estimated volume of distribution (1.77 L) and an elimination rate constant for DACT (0.41/hr) that were subsequently used in the ISO, ETHYL and ATRA models.

Oral administration of ISO and ETHYL produced peak plasma concentrations of these compounds at 0.5 hours followed by a rapid decline over 2 hours. A second, smaller plasma peak occurred at 2 hours that extended until 24 hours before concentrations fell below the detection limit (Figure 4.4a, 4.5a). Similar time-course profiles have been observed after oral administration of drugs and xenobiotics (Semino et al., 1997; Lilly et al., 1998; Schultz et al., 1999). This behavior has frequently been attributed to varying rates of absorption of chemical during transit through the GI tract. Our model structure described this behavior by including two uptake processes, a rapid absorption phase for a portion of the dose followed by zero-order absorption over a more extended period of time (Table 4.2) for the remainder of the dose.

The fitting processes indicated that 58% of administered ETHYL was absorbed by a rapid first order uptake process from the GI tract ($kafast_{ethyl}$ = 5.0/hr) that accounted for the initial peak and rapid decline of blood concentrations. The rapid first-order uptake rate constant for ISO was similar to ETHYL (6.0/hr). The later peak and plateau of ETHYL and the longer retention of DACT plasma concentrations were described with a zero-order rate of uptake for the remaining 42%

of the administered dose (Figure 4.4a, b). The second plasma peak of ETHYL was slightly underestimated by this model prediction – a compromise that was necessary to fit the time-course concentrations of DACT (Figure 4.4a). Plasma ISO concentrations were maintained at a relatively high concentration over a longer period of time compared to ETHYL (Figure 4.5a, b). Consequently, with ISO, a greater percentage of administered dose was absorbed by the zero-order uptake process (74% versus 42%, respectively) than with ETHYL.

Although ATRA was more rapidly and extensively removed from plasma compared to the mono-dealkylated compounds, similar kinetic behaviors of each Cl-TRI were observed after ATRA administration. ATRA concentrations peaked at early times and fell within 2 hours. A second, smaller peak of ATRA occurred after several hours and extended for over 24 hours (Figure 4.6a). The time-course concentrations of ETHYL, ISO and DACT all reflected this multiple peak behavior (Figure 4.6 b-d). A rapid initial peak of each metabolite occurred at 0.5 hours followed by a slower and smaller peak at 4 hours that persisted for up to 24 hours. To adequately describe this more complex absorption behavior with ATRA, three absorption processes were included: two linear processes and a zero-order pathway. Absorption of 30% of the administered dose of ATRA occurred by rapid first-order uptake ($kafast_{atra}$ = 1.75 /hr). This rapid phase simulated the early peaks for ATRA, ISO and ETHYL and allowed for the rapid removal of ATRA from circulation. The rapid absorption was also consistent with the shoulder at 1 hr noted with DACT. The slower second plasma peak and long retention of the compounds required both a slow first-order absorption process ($kaslow_{atra}$= 0.05/hr) of 45% of administered ATRA

and zero-order absorption process of 30% of administered ATRA that began 2 hrs post –dose (Figure 4.6).

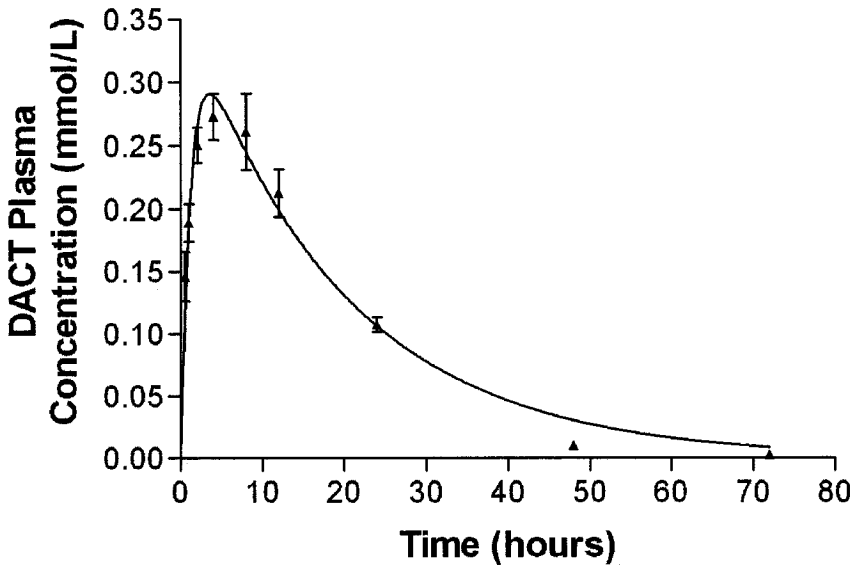

Figure 4.3. Plasma DACT concentration time profiles and model simulations following an oral gavage dose of 100.2mg DACT/kg b.w. in 1% carboxymethylcellulose vehicle. Points represent experimental data (mean ± SEM; n=5). Solid line represents least squares best-fit model simulation.

Table 4.2. Model estimated percentages of administered dose of Cl-TRI absorbed from the gut via different rate processes

Cl-TRI model	%Rapid first – order	%Slow first – order	% Zero-order
DACT	---	100	----
ISOPROPYL	26	----	74
ETHYL	58	----	42
ATRA	25	45	30

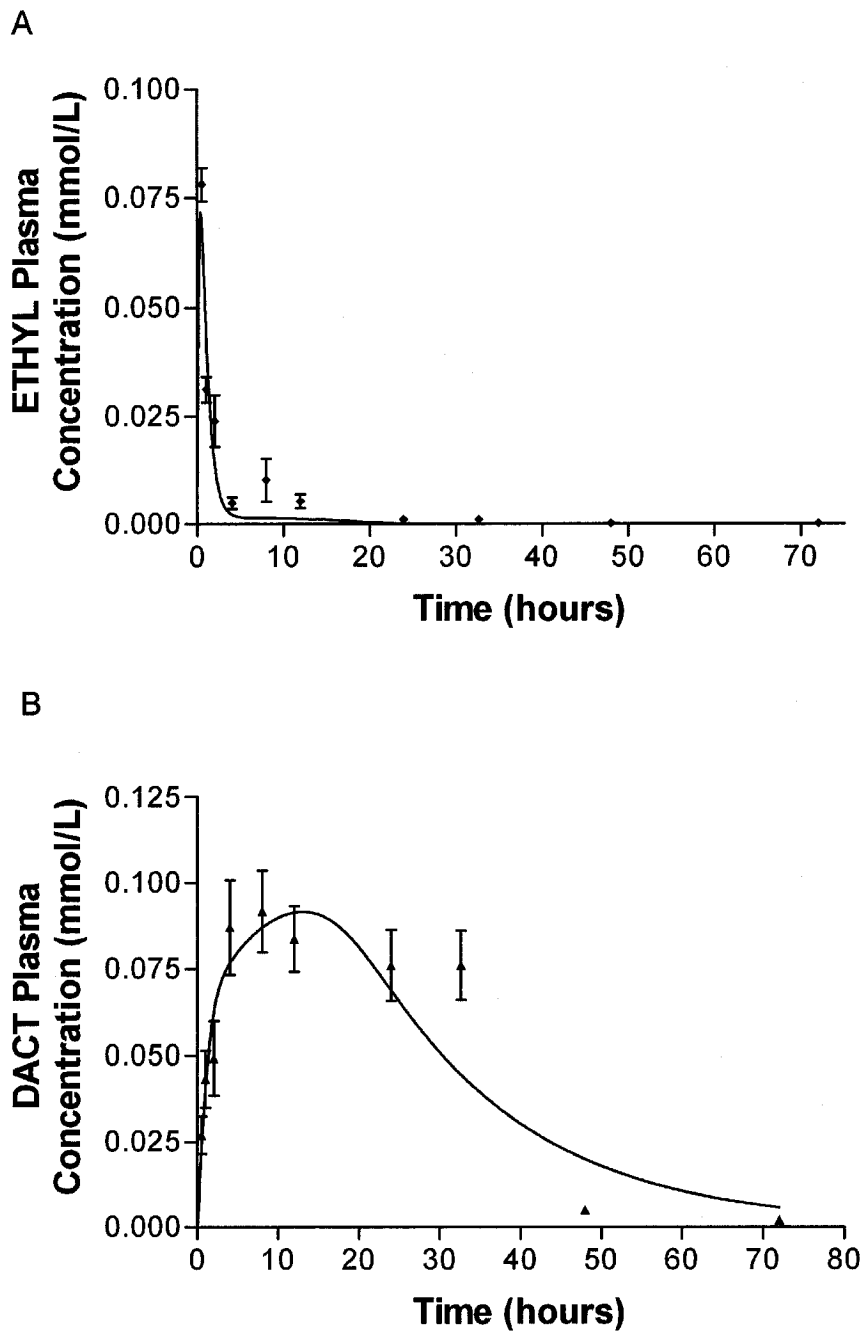

Figure 4.4. Plasma concentration time profiles and model simulations of (a) ETHYL and (b) DACT following an oral gavage dose of 121.5 mg ETHYL/kg b.w. in 1% carboxymethylcellulose vehicle. Points represent experimental data (mean ± SEM; n=3). Solid lines represent least squares best-fit model simulation.

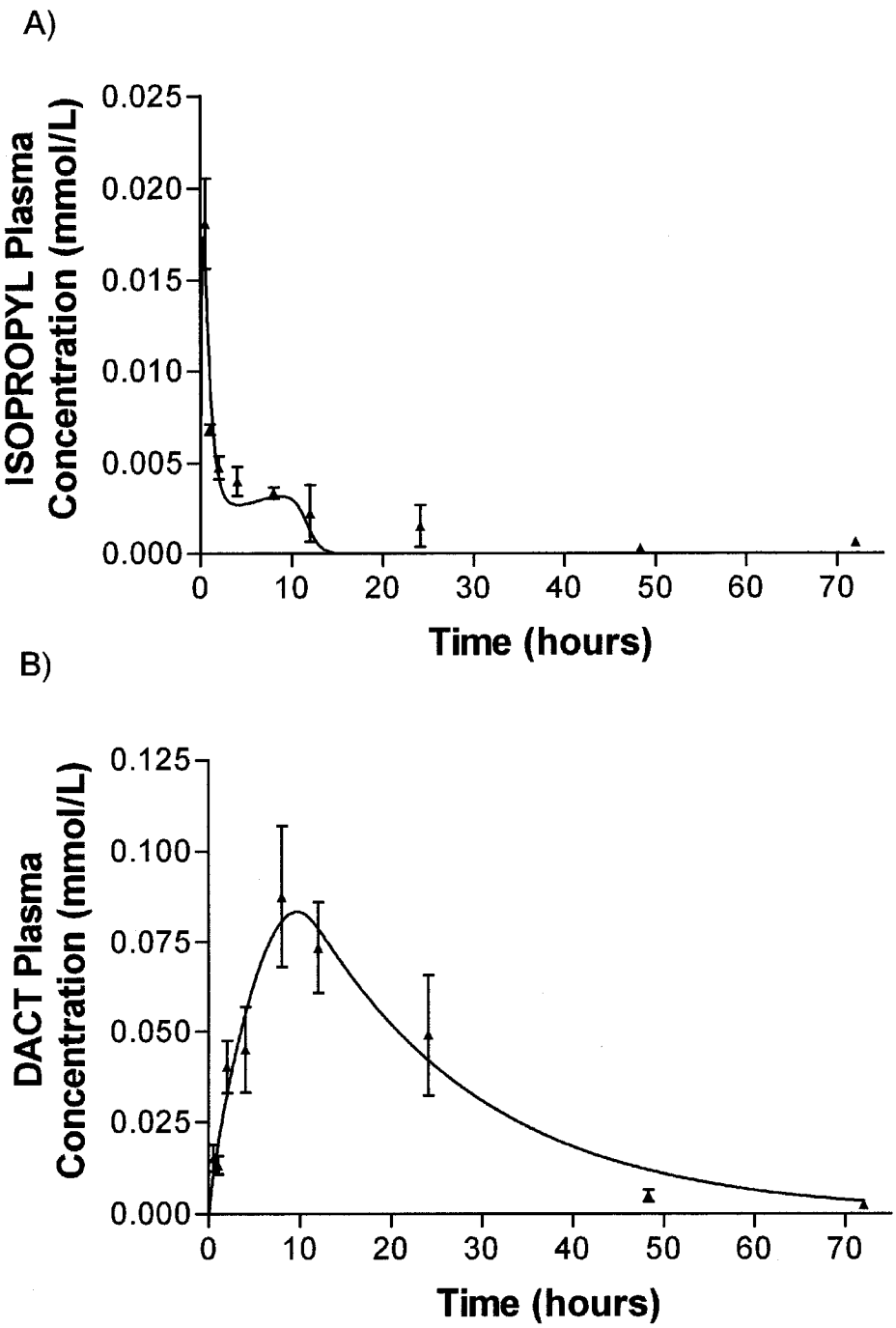

Figure 4.5. Plasma concentration time profiles and model simulations of (a) ISOPROPYL and (b) DACT following an oral gavage dose of 132.5 mg ISOPROPYL/kg b.w. in 1% carboxymethylcellulose vehicle. Points represent experimental data (mean ± SEM; n=3). Solid lines represent least squares best-fit model simulation

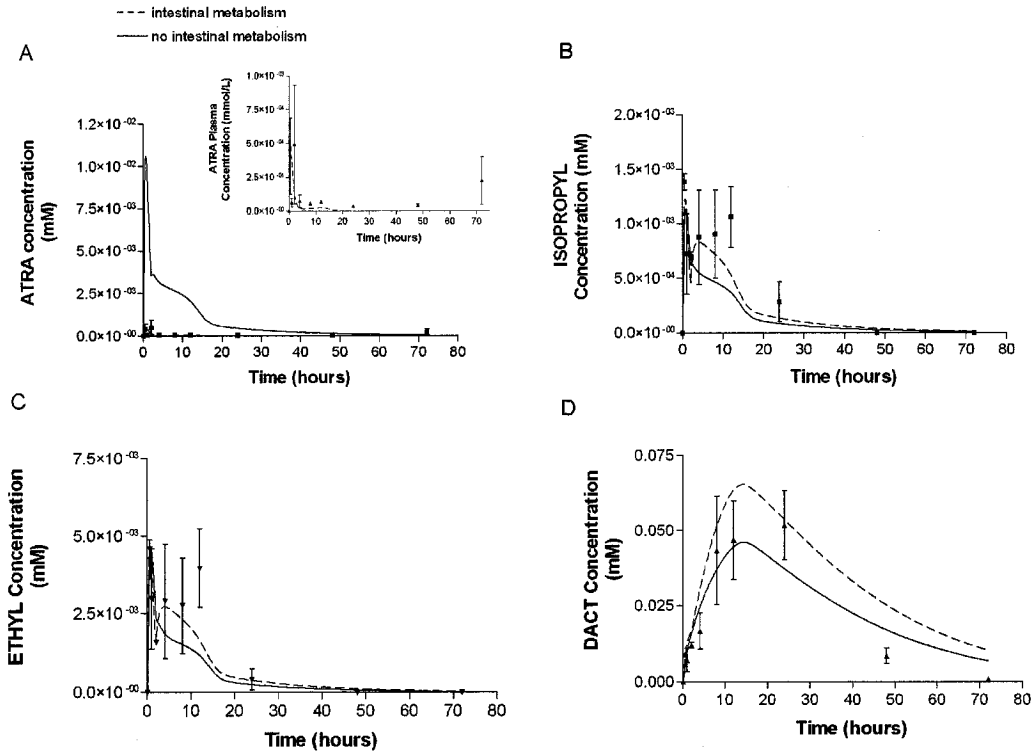

Figure 4.6. Experimental data and model simulations of plasma time-course concentrations of (a) ATRA (b) ISOPROPYL (c) ETHYL and (d) DACT following an oral gavage dose of 150 mg ATRA/kg b.w. in 1% carboxymethylcellulose vehicle. Points represent experimental data (mean ± SEM; n=3). Solid lines represent least squares best-fit model simulation without intestinal metabolism. Hatched lines represent model simulation with intestinal metabolism.

4.3.2. Hepatic oxidative metabolism of chlorotriazines

One of the goals in this modeling work was to determine if it would be possible to use *in vitro* estimated metabolic parameters to describe oxidative metabolism of the Cl-TRIs *in vivo*. *In vitro* K_M values were incorporated as fixed inputs into the mono-dealkylated models and the values for V_{max} of ETHYL and ISO metabolism to DACT were predicted from simulation of the mono-dealkylated data sets. Using this approach V_{max} values for ETHYL and ISO were predicted to be

0.021 mmol/hr and 0.002 mmol/hr and metabolic clearances (V_{max}/K_M) of 1.61 L/hr and 0.15 L/hr, respectively. Hepatic oxidative metabolism of ATRA to the mono-dealkylated metabolites was described by integrating the V_{max} and K_M constants determined *in vitro*. Oxidative metabolic clearance of ATRA (1.64 L/hr) was similar to ETHYL, metabolic clearance of ISO to DACT was 7 times lower (Table 4.3).

Table 4.3 Cl-TRI Hepatic Oxidative Metabolic Parameters and Clearance Values

	V_{max} (mmol/hr)[a]	K_M (mmol/L)[b]	Cl (L/hr)
ATRA	0.041[b]	0.025	1.64
ETHYL	0.021[c]	0.013	1.61
ISOPROPYL	0.002[d]	0.013	0.15

[a] Vmax values were converted to mmol/hr from mmol/hr/kg$^{0.7}$ assuming 0.22 kg body weight
[b] Parameter determined *in vitro* (Chapter 3)
[b] Determined from fitting the ETHYL model to the ETHYL time-course data
[e] Determined from fitting the ISO model to the ISO time-course data

Table 4.4. Model estimated percentages of hepatic and GI metabolic clearance and clearance by additional elimination processes 72 hours after administered Cl-TRI dose

Cl-TRI model	% Hepatic Oxidative Metabolic Clearance	% Intestinal Metabolic Clearance	% Additional Clearance
DACT	0	0	100
ISOPROPYL	4	29	67
ETHYL	41	7	52
ATRA	0.75	80	19.3

4.3.3. GI tract oxidative metabolism of chlorotriazines

An initial model where liver was the only site for oxidative metabolism of ATRA consistently under-estimated plasma time-course concentrations of ETHYL and ISO during the plateaus while over-estimating ATRA (Figure 4.6). Increasing

body: plasma partition coefficients of the mono-dealkylated compounds and decreasing the partition coefficient of ATRA in body successfully adjusted for this behavior but did not explain the biological phenomena underlying this behavior. Increasing V_{max} for hepatic oxidative metabolism of ATRA to the mono-dealkylated metabolite partially compensated for this behavior by decreasing ATRA concentrations and slightly increasing concentrations of the mono-dealkylated metabolites (Figure 4.7). However, as stated earlier, one the main goals in this model development was to evaluate the ability of *in vitro* metabolic parameters to describe *in vivo* metabolism. Therefore, GI tract metabolism of ATRA to the mono-dealkylated metabolites was examined as a potential underlying mechanism that produced the higher than predicted concentrations of mono-dealkylated metabolites and the extendend plasma profiles of theses compounds at the longer time points. Addition of GI metabolism of ATRA adequately simulated the time-course behaviors of the Cl-TRIs by lowering the bioavailability of ATRA and increasing plasma concentrations of the mono-dealkylated metabolites, especially at the longer time points during the second peak and plateau (Figure 4.6a-c). The model description using the *in vitro* kinetic parameters and including GI metabolism of ATRA to the mono-dealkylated metabolites predicts that GI metabolism contributes to 80% of clearance of the administered dose of ATRA (Table 4.3).

Because the same biological processes likely occur after administration of the mono-dealkylated metabolites, GI metabolism was also added to these models. Unlike ATRA, GI metabolism contributed to 7% of total clearance of administered ETHYL and 29% of clearance of ISOPROYL (Table 4.4).

4.3.4. Brain Time-Course Study

After administration of 150 mg ATRA/kg b.w., mean Cl-TRI brain concentrations ranged from 1-4 times the plasma concentrations (Table 4.5). Peak brain concentrations of DACT at 24 hours were 1.7 times higher than peak plasma concentrations. Initial ISO brain concentrations were 2 times greater than plasma but dropped below plasma concentrations at 24 hrs. ETHYL brain and plasma concentrations were similar at all time points. While ATRA concentrations were much smaller than the other Cl-TRIs, they were consistently greater in brain than plasma. DACT was the major Cl-TRI in both tissues. Peak DACT concentrations in brain were 165 times higher than ATRA brain concentrations. ETHYL was 2-3 times higher than ISO.

Overall, the ATRA model predicted the general time-course concentrations of Cl-TRIs in brain and plasma from this independent study. Simulation of the brain concentrations of Cl-TRIs required a brain:plasma partition coefficient of 2.25. DACT concentrations in brain were well predicted at all time points but plasma concentrations of DACT were slightly underpredicted at 24 hours. The largest discrepancy was for the prolonged elevations in brain ATRA observed in the study that were not predicted by the optimized PK model for absorption of ATRA into the body from oral dosing. The model underpredicted brain and plasma concentrations of ATRA, ETHYL and ISO at 24 hours (Figure 4.8a-c) but provided accurate simulations of the initial time points when multi-phasic absorption was occurring (see insert Figure 4.8b,c). These initial conclusions about brain uptake were estimated

from flow-limited descriptions of the tissues. It might be of some value to assess expected behavior for tissue descriptions that were diffusion limited.

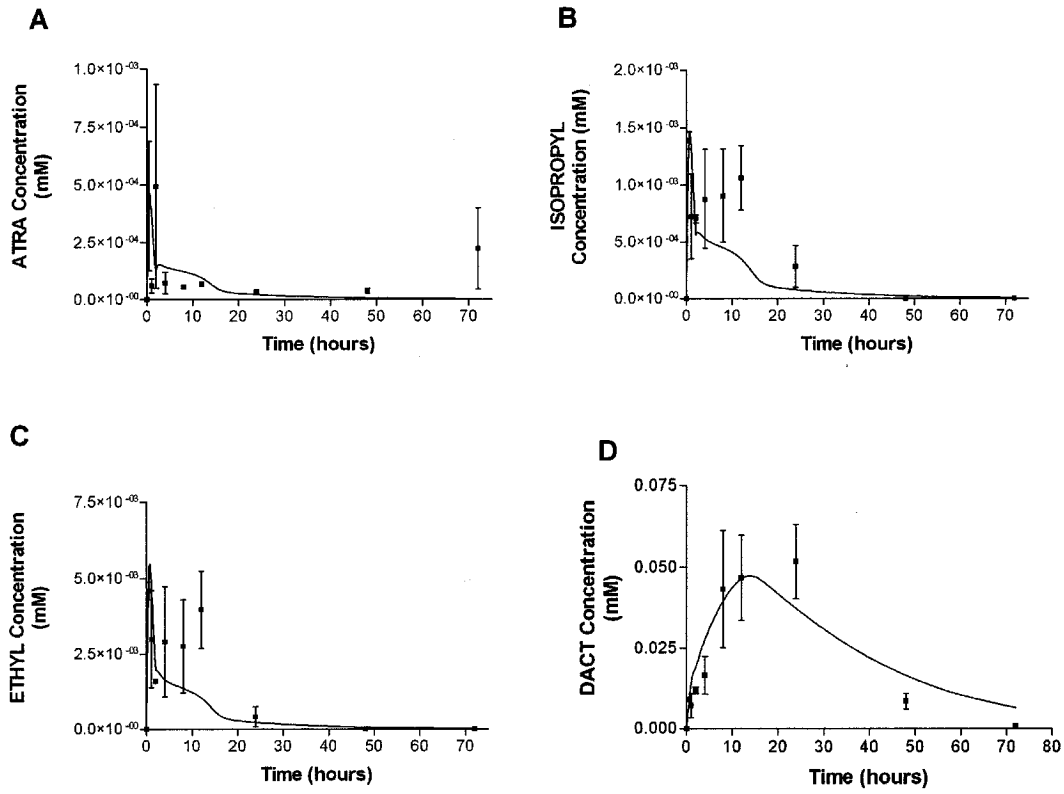

Figure 4.7. Model simulations and plasma time-course concentrations of (a) ATRA (b) ISOPROPYL (c) ETHYL and (d) DACT using a model with no intestinal metabolism and incorporation of the model estimated $Vmax_{atra}$ (2.26 mmol/hr) to describe hepatic oxidative metabolism rather than the V_{max} estimated *in vitro*. Points represent experimental data (mean ± SEM; n=3). Solid lines represent least squares best-fit model simulation.

Table 6.5. Brain and plasma time-course data of indivdual chlorotriazines after an oral gavage dose of 150mg/kg b.w.

Time(hrs)	DACT		ETHYL		ISOPROPYL		ATRA	
	BRAIN	**PLASMA**	**BRAIN**	**PLASMA**	**BRAIN**	**PLASMA**	**BRAIN**	**PLASMA**
0.5	0.005±0.001	0.005±0.001	0.004±001	0.003±0.001	0.002±0	0.001±0	0.0005±0	0.0002±0
2.0	0.018±0.001	0.013±0.002	0.007±0.001	0.007±0.002	0.002±0	0.001±0	0.0008±0	0.0002±0
24	0.132±0.03	0.078±0.004	0.004±0.001	0.004±0.001	0.001±0.001	0.002±0	0.0006±0	0.0004±0
72	0.002±0	0.001±0	0±0	0±0	0±0	0±0	0 ±0	0.0002±0.0001

Note. Data are expressed in units of mM as mean ± SEM (n=3).

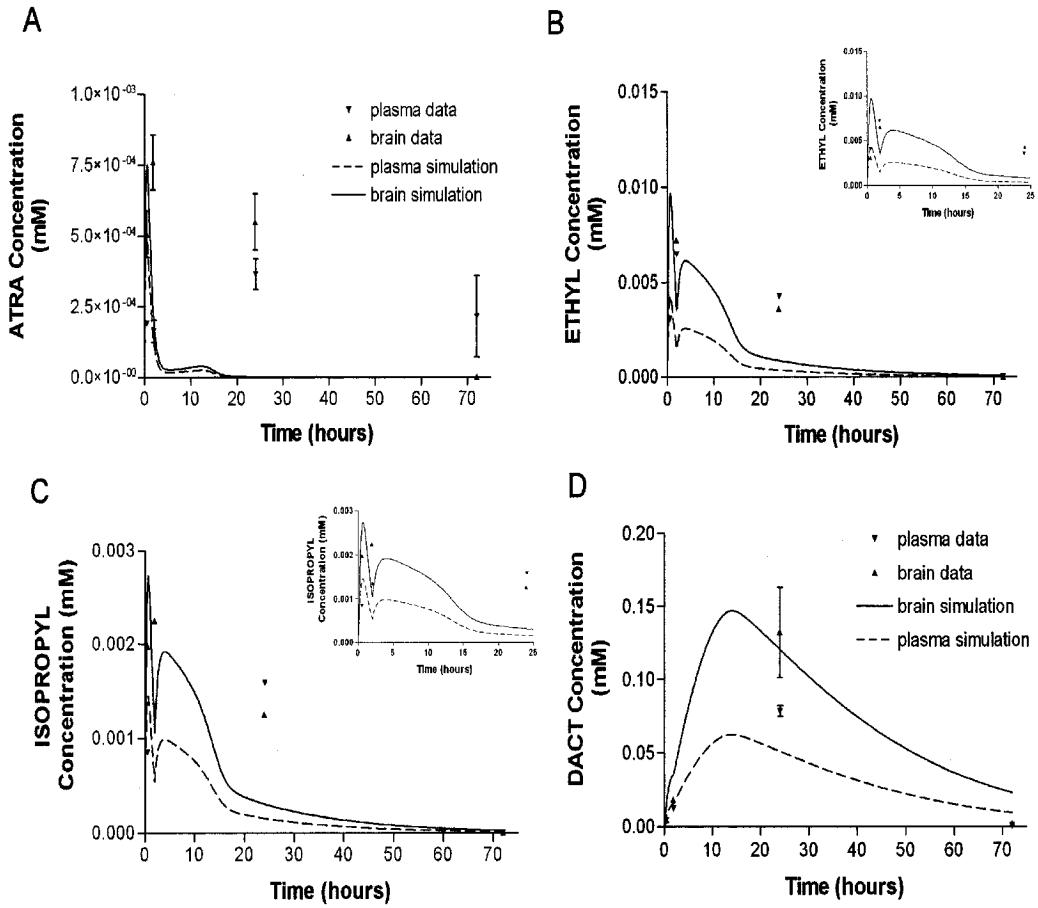

Figure 4.8. Brain and plasma concentration time profiles and model simulations of (a) ATRA (b) ETHYL (c) ISOPROPYL and (d) DACT following an oral gavage dose of 150 mg ATRA/kg b.w. in 1% carboxymethylcellulose vehicle. Points represent experimental data (mean ± SEM; n=3). Solid lines represent least squares best-fit model simulation.

Table 4.6. Estimated percentages of administered ATRA dose absorbed by rapid and slow uptake processes

ATRA (mg/kg)	% Rapid uptake	% Slow uptake
150	25	75
100	37.5	62.5
50	75	25
20	100	0
5	100	0

4.4. DISCUSSION

Prior to these studies, existing time-course data for ATRA only provided information from which to estimate relative rates of oxidative metabolic versus non-oxidative metabolic clearance (Chapter 2). The time-course studies presented in this chapter and the oxidative metabolic parameters determined by *in vitro* studies with hepatocytes (Chapter 3) provided additional data to develop this PK model. Using these data, this model addressed some of the existing data gaps regarding rates of oxidative metabolism of ATRA to the mono-dealkylated metabolites and examined the absorption and clearance processes that contribute to Cl-TRI disposition in the rat.

4.4.1. Describing complex absorption behavior of the chlorotriazines after oral administration

Complex plasma time-course profiles of ISO, ETHYL and ATRA were observed after oral administration of these compounds. While the general PK disposition of initial uptake of ATRA and the mono-dealkyated metabolites could be described using a single first-order absorption rate, this approach did not accurately fit the double peaks and the longer plateau of compound in plasma consistently observed in each time-course study. This behavior is likely a reflection of limited compound solubility in the gut and sequential absorption of compound along the GI tract. The high doses of Cl-TRIs used in these kinetic studies and studies that observed neuroendocrine effects required preparation of ATRA as a suspension in a vehicle such as carboxymethylcellulose. Initial rapid stomach absorption of dissolved material followed by slower, delayed first-order and zero-order absorption along the intestinal mucosa of material that was initially present in suspension would produce

results consistent with the observed double peaking and prolonged retention. Based on these general ideas, the percent of ATRA absorbed by rapid first-order uptake processes would be dose-dependent (Table 4.6). At lower doses, more material would be in solution rather than suspension. Thus, a larger proportion of the dose would be rapidly absorbed and plasma retention of compound from continuous slow absorption would be less important than at the higher doses.

Multiple plasma peaks and compound retention have been frequently observed after oral administration of many drugs and some environmental chemicals. Several kinetic models and experimental analyses have identified certain physicochemical and biological processes in the GI tract that produce these atypical absorption profiles. Similar to this model description of absorption, dissolution-limited absorption of other drugs has resulted in plasma time-course concentrations that were well described by a first-order input followed by a zero-order input (Zhou et al., 2003). Experimental analysis of plasma and intestinal concentrations after oral administration of some drugs has revealed that dose-dependent solubilization of compound along the GI tract can produce multiple peaks in plasma concentration (Parguet et al., 1985).

Several GI tract PK models have been developed to examine discontinuous plasma behavior observed after oral administration of compounds. GI tract sub-models linked to a PBPK model have empirically explained the multiple peaks in the blood and exhaled breath time-course concentrations of volatile organic compounds such as carbon tetrachloride (CCl4) and bromodichloromethane (BCDM) following oral gavage in corn oil and Emulphor (water-like) vehicles. In these models, portions

of compound were sequentially transported through multiple GI sub-compartments at various first order rates for specified periods of time prior to entering the plasma compartment. Describing the uptake of these VOC's in corn oil vehicle required slower rates and more compartments than were needed to describe the profiles of the compounds when administered in Emulphor vehicle. While not experimentally determined, the authors suggested that the initial peaks reflected rapid absorption of compound from the stomach while later peaks represented absorption of compound during transit through the small intestine (Gallo et al., 1993; Semino et al., 1997; Lilly et al., 1998). Similarly, discontinuous absorption of compound in the stomach and intestinal tract has been hypothesized to account for multiple plasma peaks after oral administrations of other xenobiotics and drugs such as di-halogenated acetates, halomethanes, cimiteidine and ranitidine (Schaiquevich et al., 2002; Schultz et al., 1999; Suttle et al., 1992, 1995).

Consistent with studies on other compounds, the necessary inclusion of an initial rapid first-order uptake rate followed by a slow first-order and zero-order uptake process after a 2 hour lag time implies that a complex pattern of Cl-TRI absorption was likely occurring as a result of compound solubility and sequential absorption of high oral gavage doses of Cl-TRIs along the GI tract. However, additional studies would need to be performed to evaluate this hypothesis in more detail. Comparisons of the plasma area under the curves after oral and intravenous administration of ATRA would clarify some of the underlying mechanisms responsible for the multiple peak behavior and aid in prediction of kinetic behavior expected at low environmentally relevant doses.

4.4.2. Describing Clearance of Chlorotriazines

One of the main goals in developing the PK model to describe ATRA and its chlorinated metabolites was to integrate oxidative metabolic parameters determined *in vitro* to predict *in vivo* hepatic metabolism of the Cl-TRIs. Incorporation of both the *in vitro* V_{max} and K_M values for ETHYL and ISO metabolism to DACT into mono-dealkylated models did not adequately simulate the time-course concentrations of these compounds and DACT. Therefore, the *in vitro* K_M values were kept constant and V_{max} for ETHYL and ISO were determined by model fitting. The model fitted V_{max} value for *in vivo* hepatic oxidative metabolism of ISO to DACT was consistent with the value estimated *in vitro* but the *in vivo* model estimated V_{max} describing ETHYL metabolism to DACT was 10 times greater than the value estimated *in vitro* (Table 4.7). Direct determination of *in vitro* V_{max} and K_M values for ETHYL and ISO metabolism to DACT should be pursued to address this discrepancy between ETHYL and ISO. Incubating each mono-dealkylated metabolite in a primary rat hepatocyte suspension and monitoring loss of substrate and DACT formation would provide experimental values for V_{max} and K_M of ETHYL and ISO metabolism to DACT that could be integrated into these models to replace the current model estimated values.

One of the more interesting findings from this kinetic analysis was the consistent underestimation of the mono-dealkylated time-course concentrations and the overestimation of ATRA plasma concentration following administration of ATRA using a model that described metabolic clearance of ATRA occurring solely in liver via saturable, oxidative metabolism (Figure 4.6).

Table 4.7. Comparison of V_{max} values used in the *in vitro* and *in vivo* models

	In vivo V_{max} (mmol/hr) [a]	*In vitro* V_{max} (mmol/hr) [a]
ISOPROPYL	0.002	0.003
ETHYL	.021	0.002
ATRA	0.04	0.04

[a] V_{max} values were converted to mmol/hr from mmol/hr/$kg^{0.7}$ assuming 0.22 kg body weight

Increasing the V_{max} value of ATRA metabolism to the mono-dealkyalted metabolites from the value estimated *in vitro* partly accounted for the inability of the model to predict the time course behaviors of ATRA and the mono-dealkylated metabolites (Figure 4.7). However, the model predicted value (V_{max}atra = 0.78 mmol/hr) was 20 times greater than the value determined from the *in vitro* studies. Even using a higher rate of hepatic oxidative metabolism, this model description could not adequately simulate the later time points when the mono-deaklyated metabolites were retained in plasma and ATRA was extensively removed.

Additional pre-systemic clearance of ATRA and retention of ETHYL and ISO were included by addition of GI metabolism of ATRA to the mono-dealkylated metabolites prior to absorption. Intestinal metabolism was also included in the mono-dealkylated metabolite models. However, inclusion of intestinal metabolism was not required to simulate the mono-dealkylated data sets. These data sets could be adequately simulated by setting the intestinal metabolic rate constant (krxn) to 0 and fitting for V_{max}ethyl and V_{max}iso in liver. This description was considered less realistic, since intestinal metabolism was necessary for ATRA it was also likely to be needed for ISO and ETHYL. The final model values for V_{max} and krxn of each

mono-dealkylated compound were determined by simultaneously fitting these rate constants to the mono-dealkylated data sets. However, this fitting approach resulted in very different values for the V_{max} and krxn constants of ETHYL and ISO and hence, different percentages of clearance of these compounds via intestinal and hepatic oxidative metabolism (Table 4.4). The accuracy of the predicted values for V_{max} and krxn of ETHYL and ISO is limited since V_{max} and krxn have similar effects on the time course curves for plasma concentrations of the absorbed compounds.

Intestinal metabolism contributes to the bioavailability of many orally administered environmental toxicants and drugs (Gibaldi et al., 1971; Leu and Huang, 1995; Lown et al., 1997; Wacher et al., 1998; Pang et al., 1986; Doherty and Pang, 2000). Enterocytes, largely located in the small intestine, contain several phase I and II metabolic enzymes. Most notable in rat are the P450 isoforms CYP1A2, 2C, 2E1 and 3A (Kaminsky and Zhang, 2003). Some xenobiotics induce intestinal P450 isoforms (Traber et al., 1988) and are metabolized by these enzymes. Polycyclic aromatic hydrocarbons are extensively metabolized by Caco-2 cells (an enterocyte cell line) (Cavret and Feidt, 2005).

Although the GI tract is thought to be a minor contributor to pre-systemic clearance of compounds compared to the liver, intestinal metabolism exceeds hepatic metabolism at high doses for some compounds. At high doses, intestinal conjugation of phenol exceeds hepatic metabolism (Cassidy and Houston, 1984). A PBPK model simulating saturable metabolism of ethanol in the intestine by alcohol dehydrogenase determined that 26% of the administered dose of ethanol was metabolized by the intestine compared to 12.6% by the liver (Pastino and Conolly, 2000).

While intestinal metabolism can exceed hepatic metabolism, the contribution of intestinal metabolism to ATRA clearance seems quite high. Model simulations predicted that 80% of administered ATRA was metabolized in the GI tract prior to entering systemic circulation. In this model description, the contribution of hepatic oxidative metabolism to total ATRA clearance was limited by the values of V_{max} and K_M that were determined *in vitro* and the remaining pre-systemic clearance was accounted for by intestinal metabolism. If the larger model predicted value for hepatic V_{max} was used rather than the *in vitro* estimated value, intestinal and hepatic oxidative metabolism would have accounted for 12.4% and 50% of ATRA clearance, respectively. While these percentages are more similar to those observed with other compounds, the extent of GI metabolism to total Cl – TRI clearance cannot be quantified without being assessed experimentally.

To address the relative contributions of intestinal and hepatic oxidative metabolism and GSH and urinary clearance of these Cl-TRIs, additional studies are needed that will provide rates of these processes. Time-course studies that monitor the urinary and fecal accumulation of individual Cl-TRIs or *in vitro* studies that determine Cl-TRI conjugation rates to non-chlorinated metabolites could address the uncertainty that still exists regarding relative rates of P450 oxidative and GST mediated metabolism. *In vitro* time-course studies using metabolically active immortalized enterocyte cell lines such as Caco-2 cells (Cavret amd Feodt, 2005; Gan and Thakker, 1997; Carriere et al., 2001), freshly isolated enterocytes (Carriere et al., 2001) or intestinal tissue slices (De Kanter et al., 2002) incubated with the individual

Cl-TRIs would provide a useful, rapid and inexpensive means of preliminarily examining the role intestinal metabolism has on the bioavailability of Cl-TRIs.

Another model assumption that should be further addressed was the need to include metabolism of the fraction of administered dose that is rapidly absorbed. The hypothesis used to develop this model was that the rapidly absorbed portion represented dissolved material being absorbed from the stomach or the proximal portions of the intestinal tract. If the absorption of Cl-TRIs occurred in the stomach, the need to have pre-systemic loss prior to liver would be questionable because the metabolic activity in stomach lumen is low relative to small intestine (Ding and Kaminsky, 2003). However, intestinal metabolism of the rapidly absorbed portion would likely occur if this portion represents rapid absorption from the proximal regions of the intestine since the proximal portions of the small intestine have the greatest metabolic capacity of all regions in the GI tract (Hall et al., 1999).

4.4.3. Evaluating Competitive Metabolic Inhibition

Dose-dependent inhibition of DACT occurred after incubation of ATRA in primary rat hepatocytes (Chapter 3). This kinetic behavior was adequately described by competitive substrate inhibition of oxidative metabolism. The high doses used in *in vivo* studies to examine the toxicity of a compound could cause saturation of metabolic enzymes and lead to altered kinetic profiles that may not be relevant at lower doses. However, inclusion of competitive inhibition terms to describe oxidative metabolism of the Cl-TRIs did not improve the model fit to these *in vivo* studies (data not shown). Competitive interactions are not expected due to the low

concentrations of ATRA achieved *in vivo* following oral dosing, even following a dose of 100 mg/kg.

4.4.4. Evaluating Concentrations of Chlorotriazines in brain

Consistent with a previous study that examined the urinary profiles of metabolites (Timchalk et al., 1990) and with the other plasma time-course study presented in this chapter, the time-course profiles of Cl-TRIs in brain indicate that DACT is the major contributor to internal Cl-TRI tissue dose after administration of the mono-dealkylated metabolites or ATRA.

Without any parameter adjustments, this model simultaneously predicted the initial uptake and peak concentrations of all Cl-TRIs in brain and plasma from all studies. However, the model consistently underpredicted the concentrations of ATRA and the mono-dealkylated metabolites at 24 hours in this study compared to the other studies. It is unlikely that the differences are solely due to variations in analysis of samples since the underpredictions only occurred at the 24 hour time point. While a more accurate simulation of this retention in brain and plasma could have been performed by increasing clearance of these compounds from the body (kelimc), this adjustment would have compromised the parameterization approach and overpredicted ATRA and the mono-dealkylated compounds for the other plasma time-course studies.

Higher peak Cl-TRI concentrations and total Cl-TRI AUC occurred in brain relative to plasma. DACT reacts with macromolecules such as hemoglobin *in vitro* and *in vivo* after dosing with ATRA (Prentiss 2004). Previous modeling work also suggested that Cl-TRIs react with proteins. Specific and/or non-specific reactivity of

Cl-TRIs with brain proteins might be contributing to greater concentration and retention in brain compared to plasma. The molecular targets for ATRA remain unknown. One possibility for the mode of action of Cl-TRI may be the ability of DACT to react with specific tissue nucleophiles, such as sulfhydryl residues.

4.4.5. Comparison of model descriptions for individual Cl-TRIs and total Cl-TRI radiolabeled equivalents

The previous PPK model utilized existing [^{14}C]-ATRA plasma disposition data and urinary data on the speciation of metabolites to estimate total Cl-TRI dose separate from the non-chlorinated GSH conjugated metabolites (Chapter 2). This model was limited in its predictive abilities because the relative rates of GSH conjugation and oxidative metabolism were indirectly estimated from the radiolabeled data. Still, some similarities exist between these studies. The kinetic disposition of the plasma total radioactivity data was similar to the DACT time-course behavior. These current studies provide evidence that ATRA and the mono-dealkylated metabolites are rapidly cleared from plasma, resulting in the majority of plasma Cl-TRI consisting of DACT. Since DACT accounted for over 95% of the AUC after dosing with ATRA, the total radioactivity data likely reflected DACT, especially at the later time points when the other Cl-TRIs had been cleared from plasma.

Total radioactivity data indicated persistence of radiolabeled material in the plasma up to 72 hrs post - dose. This behavior was accurately simulated with a second-order reaction rate constant between plasma protein and Cl-TRIs, indicating covalent interactions between the Cl-TRIs and plasma proteins. Retention of

radiolabeled triazine was also observed in red blood cells and was described by covalent reactivity of Cl-TRIs with these macromolecules (Chapter 2). In the present time –course studies, individual Cl-TRIs were rapidly and extensively removed from the plasma, resulting in levels of ATRA and the mono-dealkylated metabolites below limits of detection after 24 hours. The lack of retention of Cl-TRIs in plasma compared to the radiolabeled study provides further evidence that the retention of radiolabeled material in the plasma after dosing with [^{14}C]-ATRA represented a reaction product between Cl-TRIs and plasma proteins. Although reactivity of Cl-TRIs with plasma proteins has not been experimentally tested, binding to hemoglobin (Hb) has now been shown to be derived from adduction of a 110 dalton fragment that is consistent with binding of DACT after loss of chlorine with the cys-125 residue of the β-chain of rat hemoglobin. After three daily doses of 100 mg/kg, over 15% of the total Hb had reacted to form this adduct (Prentiss 2004, unpublished data from J. Tessari laboratory). Triazine plasma protein adducts would not have been detected by the methods employed in these current time-course studies and thus, retention of compound at the later time points was not expected.

4.4.6. Summary

Overall, this PK modeling analysis determined a general suite of parameters to describe plasma and brain time-course concentrations of individual Cl-TRIs and evaluated the biological and physicochemical processes that lead to total Cl-TRI tissue dose. These studies indicate that Cl-TRI internal dosimetry is driven by complex dose-dependent absorption processes from the GI tract, rapid and extensive pre-systemic clearance via oxidative metabolism in the gut and liver and additional

clearance by GSH conjugation and urinary elimination. The conclusions about complex absorptive processes and likely intestinal loss of absorbed ATRA were made possible by development of this quantitative PBPK model for ATRA and its Cl-TRI metabolites. Although studies need to be performed to examine some of the processes hypothesized in this model development, these models provide initial tools to improve predictions of the kinetic disposition of total Cl-TRIs after administration of ATRA.

CHAPTER 5

EVIDENCE THAT ATRAZINE AND DIAMINOCHLOROTRIAZINE INHIBIT THE ESTROGEN/PROGESTERONE INDUCED SURGE OF LH IN FEMALE SPRAGUE-DAWLEY RATS WITHOUT CHANGING ESTROGEN RECEPTOR ACTION

5.1. INTRODUCTION

The mechanism by which ATRA suppresses the LH surge is not known. While multiple neuroendocrine signals and neurotransmitters affect LH release from the pituitary, it is largely regulated by estrogen binding to estrogen receptor (ER) in various hypothalamic nuclei (Legan et al., 1975; Kalra, 1993; Herbison, 1998). Increasing circulating estrogen levels on the morning of proestrus initiate a positive feedback response which drives gonadotropin releasing hormone (GnRH) release and results in an LH surge. *In vitro* and *in vivo* studies suggest that ATRA is not estrogenic (Eldridge et al., 1994a). However, ATRA exhibits anti - estrogenic properties in rat uterus (Tennant et al., 1994a), in estrogen responsive MCF-7 cell lines (Tran et al., 1996) and decreases estrogen binding to ER in uterine cytosol (Tennant et al., 1994b). The importance, if any, of anti-estrogenic actions of the triazines for toxic responses in the intact animal remains a topic of current debate.

Once in the body, ATRA is extensively metabolized to the mono- and di-dealkylated chlorinated metabolites and to non-chlorinated, glutathione conjugate metabolites. Although limited, studies show that Cl-TRIs can elicit common neuroendocrine effects. This is exemplified by studies in male Wistar rats that show

alterations in puberty and thyroid function (Stoker et al., 2002). As a result of these and other data, US EPA risk assessment guidelines for triazines consider ATRA and its Cl-TRI metabolites to be toxicologically equivalent in terms of their effects on the neuroendocrine system.

Our group has recently shown that DACT is the major chlorinated metabolite in the plasma after dosing with ATRA, accounting for over 95% of the total chlorotriazine plasma area under the curve (AUC). Twenty –four hours after dosing with 300 mg ATRA/kg, the AUC for ATRA is 2.93 mg/L-hr whereas the AUC for DACT is 486.09 mg/L-hr (McMullin et al., 2003; Chapter 2). These data indicate that *in vivo* treatment with ATRA produces minimal tissue concentrations of ATRA and high tissue concentrations of DACT, making exposure of the brain to ATRA unlikely. Although the brain is most likely being exposed to DACT, not ATRA, there is limited information on the mechanistic behavior of DACT.

In this study the relative potency of DACT was compared to ATRA in terms of its ability to suppress the estradiol benzoate (EB)/progesterone (P) induced LH surge and in altering pituitary and/or hypothalamic function. Additionally, we examined the ability of these compounds to interfere with estrogen binding to ERalpha (ERα) *in vitro* and *in vivo*. *In vivo*, changes in estrogen mediated responses in the hypothalamus were examined. These changes included evaluation of unoccupied levels of ER and estrogen induced progesterone receptor (PR) mRNA expression in two estrogen responsive hypothalamic nuclei associated with reproductive function, the anteroventral periventricular nucleus (AVPV) and the

medial preoptic nucleus (MPOA). The results of these studies indicate that ATRA and DACT are inhibiting LH via mechanisms other than estrogen antagonism.

5.2. MATERIALS AND METHODS

5.2.1. ***Animals and Treatment regimen***

Female SD rats (225-275g; Charles River Laboratories, Raleigh, North Carolina) were shipped to Colorado State University and housed in the animal care facility with a 12hr light/12 dark (0600/1800) photoperiod. Food and water were available *ad libitum*. All surgical and experimental procedures were approved by Colorado State University Animal Care and Use Committee.

Technical grade ATRA (2-chloro, 4-ethylamino, 6-isopropylamino – s-triazine) of 97.1% purity and DACT of 96.8% purity (generously provided by Syngenta Corporation, Greensboro, NC).

5.2.2. Effects of ATRA, or its metabolite DACT, on the LH surge in adult, female OVX rats.

Estrogen Priming. Rats were treated with either 300mg ATRA /kg b.w. in a 0.5% carboxymethylcellulose (CMC) suspension or an equal volume of 0.5% CMC via oral gavage between 0900h to 1000h for 5 consecutive days. Rats were bilaterally OVX on day 0. On day 4, an indwelling right atrial catheter was inserted via the jugular vein and exteriorized at the nape of the neck similar to previous protocols (Levine and Ramirez, 1982; Jongen and Norman, 1987) . This procedure was followed by insertion of a Silastic capsule containing 17β-estradiol (5mm long, 0.078" i.d., 0.125" o.d.) into the subcutaneous (sc) pocket. On the fifth and sixth day

of dosing, serial blood samples (0.3ml) were collected at 1200, 1400, 1500, 1600, 1700, 1800, 1900h into heparinized syringes. Serial blood samples were collected remotely via the indwelling right atrial catheters connected to PE50 tubing to allow the animals to remain in their home cage. Animals were heparinized with 14units of sodium heparin prior to sampling. The samples were centrifuged and plasma was removed and frozen at -20°C until assayed for LH. To maintain hematocrit, red blood cells (RBCs) were re-suspended in saline and re-infused into each animal prior to the subsequent bleed. After completion of the experiment, rats were anesthetized and decapitated.

EB/P priming in OVX female rats. These studies determined if exposure to ATRA or DACT alters the LH surge. To mimic the endogenous hormonal milieu prior to an LH surge, adult female rats were primed with both EB and P. Bilaterally OVX and right atrial cannulated adult, female SD rats were purchased from Charles River Laboratories and acclimated for one week prior to dosing. Animals were exposed to 300, 100, 30, or 0 mg ATRA/kg or 77 mg DACT/kg in a 0.5% CMC suspension or via oral gavage between 0900h to 1000h for 5 consecutive days. The rats were injected s.c. with EB dissolved in safflower oil vehicle (10μg/100g bw) for three consecutive days (day 2-4) simultaneously with dosing of ATRA or DACT. On day 5, P (2mg/animal in safflower oil vehicle) was injected s.c. between 1030h and 1100h. Serial blood samples were collected remotely via the indwelling right atrial catheters connected to PE50 tubing to allow the animals to remain in their home cage. Animals were heparinized with 14 units of sodium heparin prior to sampling. Samples (0.3ml) were collected at 1200, 1400, 1500, 1600, 1700, 1800, 1900, 2000h.

To maintain hematocrit, RBCs were re-suspended in saline and re-infused into each animal prior to the subsequent bleed. The samples were centrifuged and plasma was separated and frozen at -20°C until assayed for LH. After completion of the experiment, rats were euthanized with CO_2.

5.2.3. LH Radioimmunoassay (RIA). Plasma LH levels were determined by RIA using methods previously described (Pak et al., 2001). All samples were run in duplicate in a single assay. rLH RP-3 and rLH-S11 were obtained from the National Hormone and Peptide Program and used as the RIA standard and primary antibody, respectively. oLH was iodinated by the Colorado State University peptide analysis facility using the chloramine-T method and used as the trace hormone. The detection limit of the assay was 1.2 ng/ml. The intrassay and interassay coefficients of variation were 5.2% and 8.3%, respectively.

*5.2.4. **Effect of DACT on Pituitary LH release afterGnRH challenge***

The purpose of this experiment was to examine pituitary function, as indicated by its ability to release LH in response to GnRH, under dosing conditions of DACT which suppress the EB/P primed LH surge. Hormone priming and dosing with DACT were identical to that described for the EB/P primed animals. Serial blood samples were collected remotely via the indwelling right atrial catheters connected to PE50 tubing to allow the animals to remain in their home cage. Animals were heparinized with 14 units of sodium heparin prior to sampling. Beginning at 1200, serial blood samples (0.2ml) were collected every 10 minutes. Two baseline samples were collected prior to an intravenous bolus injection of 100ng GnRH /100g b.w. (Peninsula Laboratories, Inc.; Lot # 036833) and six samples were taken every 10

minutes thereafter. Plasma was analyzed for LH via RIA. The samples were centrifuged and plasma was separated and frozen at -20°C until assayed for LH as described above. Upon completion of the experiment, rats were euthanized with CO_2.

5.2.5. The Effect of ATRA or DACT on Estradiol Binding to ER in vitro

Previous studies indicate that ATRA has anti-estrogenic properties. To further investigate the mode of action by which ATRA and DACT might be suppressing the LH surge, the ability of ATRA or DACT to alter binding of estradiol to estrogen receptor alpha (ERα) was evaluated.

Chemicals and Reagents. Solutions of ATRA were prepared in absolute ethanol (solubility= 83.3mM) at a concentration of 6mM. Primary stock solutions of DACT were in DMSO at a concentration of 6mM. Previous studies using GC/MS were used to verify that these concentrations were in solution. TEGM stock buffer (10mM Tris; 1.5mM EDTA; 10% glycerol; 25mM molybdate; pH 7.4 on ice) was stored at 4°C. TEGMD buffer was made the morning of the assay by adding 1.0mM dithiothreitol to TEGM buffer. All buffer reagents were purchased from Sigma – Aldrich Co., Saint Louis, MO. [^{3}H]estradiol stock (New England Nuclear; NET-317; 71 Ci/mmol) was diluted with ethanol to 25ml and stored at -70°C until further diluted in TEGMD to the appropriate concentration for the binding study.

Uterine cytosolic ER binding assay. Uteri from two adult, OVX female SD rats (Charles River Laboratories) were dissected and fat was removed. Uteri were minced and homogenized in 6 ml of ice cold TEGMD buffer with a glass homogenizer (Dounce Co., Vineland, NJ). Homogenates were centrifuged at 100,000 x *g* in an ultracentrifuge (Beckman Coulter, Inc., Palo Alto, CA) with a fixed angle

rotor (Sorvall TI 60, Dupont-Sorvall, Wilmington, DE) for 15 min at 4°C to prepare a cytosolic fraction. To evaluate dose dependent binding, 100µl of uterine cytosol were incubated with increasing concentrations of ATRA (0 to 0.75mM) in TEGMD buffer. ATRA was allowed to incubate in the cytosolic mixture for either 0, 15, 30 or 60 minutes prior to addition of [^{3}H]estradiol in order to examine the ability of ATRA to inhibit [^{3}H]estradiol binding to ER. After the appropriate pre-incuabtion period, 1nM [^{3}H]estradiol was added to each tube. The tubes were capped, vortexed, and incubated for 2 additional hours at RT. To determine non-specific binding, parallel incubation tubes also included a 200-fold excess of diethylstilbesterol (DES). All incubations were performed in triplicate.

Free and bound radioligand were separated using 1ml lipophilic Sephadex LH-20 columns as previously described (Handa et al., 1986). 200ul of TEGMD buffer was added to the top of each column to equilibrate and allowed to drip dry. 127.5 µl of each sample was placed on a Sephadex column, allowed to enter the column and then followed by 100 µl of TEGMD. After 30 minutes incubation on the column, each column was flushed with 600µl (2 x 300µl) of TEGMD. Scintillation vials were placed under each column and each column was allowed to drip dry overnight at 4°C. 4ml of scintillation fluid (Packard Ultima Gold Scintillation Fluid) were added to each vial. Vials were capped, shaken, and counted (5 minutes/vial) on a 2900 TR Packard scintillation counter (Packard Bioscience, Meriden, CT).

ERα binding assay. Full length rat ERα was translated from a DNA template (pcDNA ERα; RH Price, UCSF) using the TnT® Coupled Reticulocyte Lysate translation procedure (Promega Corporation; Madison, WI) with T7-RNA

polymerase, during a 90 minute reaction at 30°C. Translation reaction mixtures were stored at -80°C until further use.

Briefly, ATRA and DACT at increasing concentrations (0 - 1.0 mM) were incubated with 1.0 nM of [^{3}H]estradiol in 100µl of ERα with an equal protein concentrations per tube. All tubes were brought to a total volume of 150µl with TEGMD buffer. All tubes were capped, vortexed, and incubated for 3 hours at RT. Separation of free and bound were as described above.

5.2.6. ***Effects of ATRA exposure on Estrogen-Mediated Effects in Two Estrogen Responsive Hypothalamic Nuclei***

Two indicators of ER activity in the hypothalamus were investigated to evaluate the ability of ATRA to interfere with ER mediated hypothalamic effects under dosing conditions that suppressed the EB/P primed LH surge. These endpoints included examination of changes in unoccupied ER levels and PR mRNA expression in estrogen responsive hypothalamic regions associated with regulation of LH release.

Rats were bilaterally OVX on day 0. Animals were dosed with 300mg ATRA/kg in a 0.5% CMC suspension or an equal volume of 0.5% CMC via oral gavage between 0900h to 1000h for 5 consecutive days (days 2-6). At 0900h on days 4-6, rats were injected sc with corn oil vehicle or EB (10µg/100g b.w.) dissolved in oil. This resulted in four groups of rats (n=6/group): 1) 0.5% CMC + OIL 2) ATRA + OIL 3) EB + ATRA 4) EB+0.5% CMC. Rats were decapitated and brains were collected, frozen on dry ice, and stored in -80°C until sectioned.

Slide Preparation: Serial coronal sections (20µm) were cut on a 1720 Digital cryostat (Leitz Corp.) maintained at -20°C and thaw –mounted, then immediately

snap frozen on a cold metal platform at -20°C. Slides were stored desiccated at -80°C until analyzed for changes in hypothalamic ER binding and PR mRNA expression.

Changes in unoccupied ER levels following treatment with ATRA. To examine the effects of ATRA on hypothalamic estradiol binding, ER levels were assayed using an *in vitro* ER exchange assay procedure similar to previously described protocols (Walters et al., 1993; Yuan et al., 1995). Briefly, all slides were transferred from -80°C freezer to a 4°C cold room. Each slide was covered with 100µl of TEGBD incubation buffer (10mM Tris HCl, 1.5mM EDTA, 10% glycerol, 1mM dithiothreitol, 0.5mM Bacitracin, and 0.1mg/ml protamine sulfate, pH 7.4 @ 4°C; Sigma – Aldrich Co., Saint Louis, MO) and either a) 2nM [^{3}H]estradiol to evaluate specific binding or b) 2nM [^{3}H]estradiol + 1uM moxestrol to evaluate non-specific binding and incubated at 30°C for 45 minutes. After incubation, the sections were returned to 4°C and rinsed in cold circulating PM rinse buffer (3.0mM $MgCl_2$, 1.0mM KH_2PO_4) with protamine sulfate (1 mg/ml) to remove all unbound estrogen. Tissue sections were fixed with 4% paraformaldehyde in 0.1M phosphate buffer for 5 minutes. Slides were washed (3x5 minute in cold, circulating PM buffer with Triton X-100 (0.1%) and 2x5 minute in cold PM buffer), dipped in double deionized water and air dried overnight. Slides were placed on high resolution autoradiographic film (Amersham's 3H sensitive film) and developed for 21 days.

Evaluation of PR mRNA. In situ hybridization was performed to examine effects of ATRA treatment on estrogen induced expression of PR mRNA. A 320 base pair rat PR complementary DNA (cDNA) was obtained from Dr. Junzo Kato (U. Tokyo). cRNA probes generated from this cDNA recognize both the A and B form

of the progesterone receptor (Hagihara et al., 1992). The rat PR cDNA was linearized with *Hin*dIII and a cRNA probe was transcribed with T7 RNA polymerase in the presence of 35S-UTP.

In situ hybridization for PR mRNA was carried out as previously described (Handa et al., 1993). Briefly, brain sections were brought to room temperature, the sections were fixed in 10% formalin, acetylated with 0.25% acetic anhydride, dehydrated with ethanol (50-100%) washes and delipidated with chloroform. $2x10^6$ cpm/μl of 35S labeled riboprobe in hybridization solution of 0.1% sodium thiosulfate, 100mM DTT, and 0.5% SDS in formamide and hybridization buffer mix (1200 nM NaCl; 20mM Tris-HCl, pH7.5; 0.04% Denhart's; 2mM EDTA,pH 8.0; 0.02% SSD-DNA; 0.10% Total Yeast RNA; 0.01% yeast tRNA; 20% dextran sulfate) was placed on each slide and slides were coverslipped and placed in a humidified incubator (60°C) overnight. Following hybridization, slides were consecutively washed with 2xSSC (0.3M NaCl, 0.03 M sodium citrate; pH 7.0), treated with RNase A (20μg/ml at 37°C for 30 min), rewashed in 0.5 and 0.1xSSC. Sections were then dehydrated with increasing concentrations of ethanol (50 - 100%). For autoradiography, sections were apposed to x-ray film (Hyperfilm betamax; Amersham, Lake Forest, IL) for 11 days. Hypothalamic regions sampled for PR mRNA levels were the AVPV and the MPOA.

Image Analysis. For analysis of PR mRNA and unoccupied ER, film autoradiograms were used to evaluate the intensity of the hybridization signal under brightfield illumination using a computer-based imaging system using NIH Image software, version 1.61. The density of the hybridization signal within the AVPV and

MPOA were measured by blind analysis using a template of fixed size. The intensity from two samples of two sequential sections per animal was subtracted from background. For evaluation of unoccupied ER, the intensity of the signal was converted to pmol/mg tissue section protein using a [^{3}H]estradiol standard curve. Specific binding was assessed by subtracting non-specific binding from total binding. For PR mRNA levels, the intensity of the signal was converted to nCi/mg tissue section protein from a ^{14}C standard curve.

5.2.7. Statistics

For the LH surge studies, two - way ANOVA with repeated measures for treatment time was used to compare differences between treatment group and treatment time followed by Fisher's PLSD post hoc test. Estrogen mediated effects in the hypothalamus were also evaluated with two-way ANOVA for treatment and group effects and interactions. Differences were considered significant when $P<$ 0.05. Numerical values are reported as the mean ± SEM. The computer program StatView 5.0.1 (SAS Institute Inc., Cary, NC USA) was used for statistical analysis. Graphs were plotted with GraphPad Prism version 3.05 (GraphPad Software, San Diego California USA).

5.3. RESULTS

5.3.1. Effects of ATRA, or its metabolite DACT, on the LH surge in adult, female OVX rats.

The aim of these experiments was to characterize the dose-dependent LH surge suppression after ATRA exposure and to evaluate the relative potency of

DACT compared to ATRA. To date, LH suppression by ATRA has only been evaluated after priming rats with EB (Cooper *et al.*, 2000). To further characterize the ability of ATRA to suppress the LH surge, treatments with both EB and P were used to generate an LH surge. Priming with EB and P produced a peak LH surge approximately three times higher than EB priming alone (Figure 5.1, 5.2a). The EB/P induced LH surge was significantly suppressed by ATRA in a dose-dependent manner with 300 mg ATRA/kg/day abolishing the LH surge (Figure 5.2a, b). Body weight loss occurred but was not significant until day 5 with the 300 mg ATRA/kg/day dose level (data not shown).

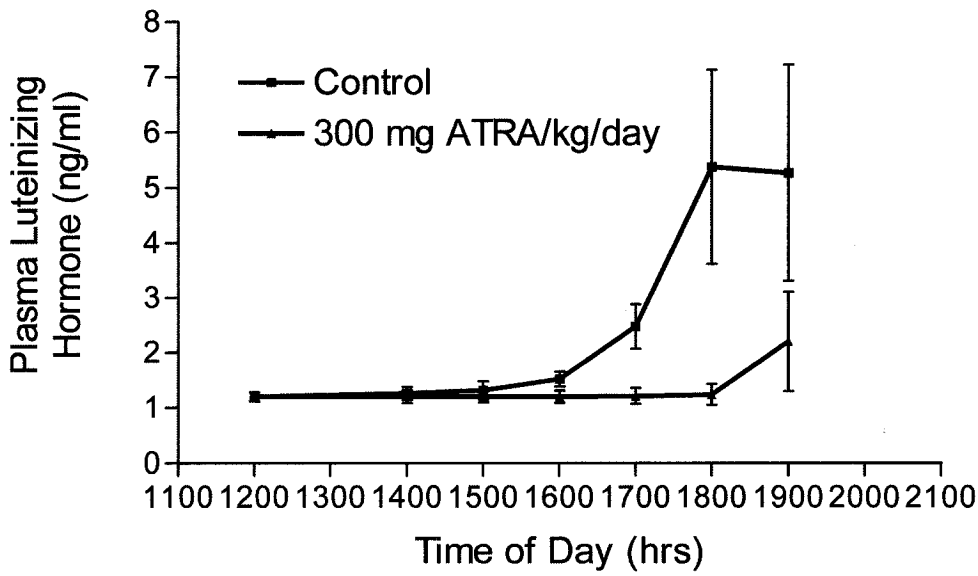

Figure 5.1. Suppression of the estrogen induced LH surge by five daily doses of 300 mg ATRA/kg/day in adult ovariectomized Sprague-Dawley rats. Peak LH levels in controls and ATRA treated animals were 5.37 ± 1.76 ng/ml and 2.20 ± 0.906 ng/ml, respectively. Points and bars represent mean ± SEM.

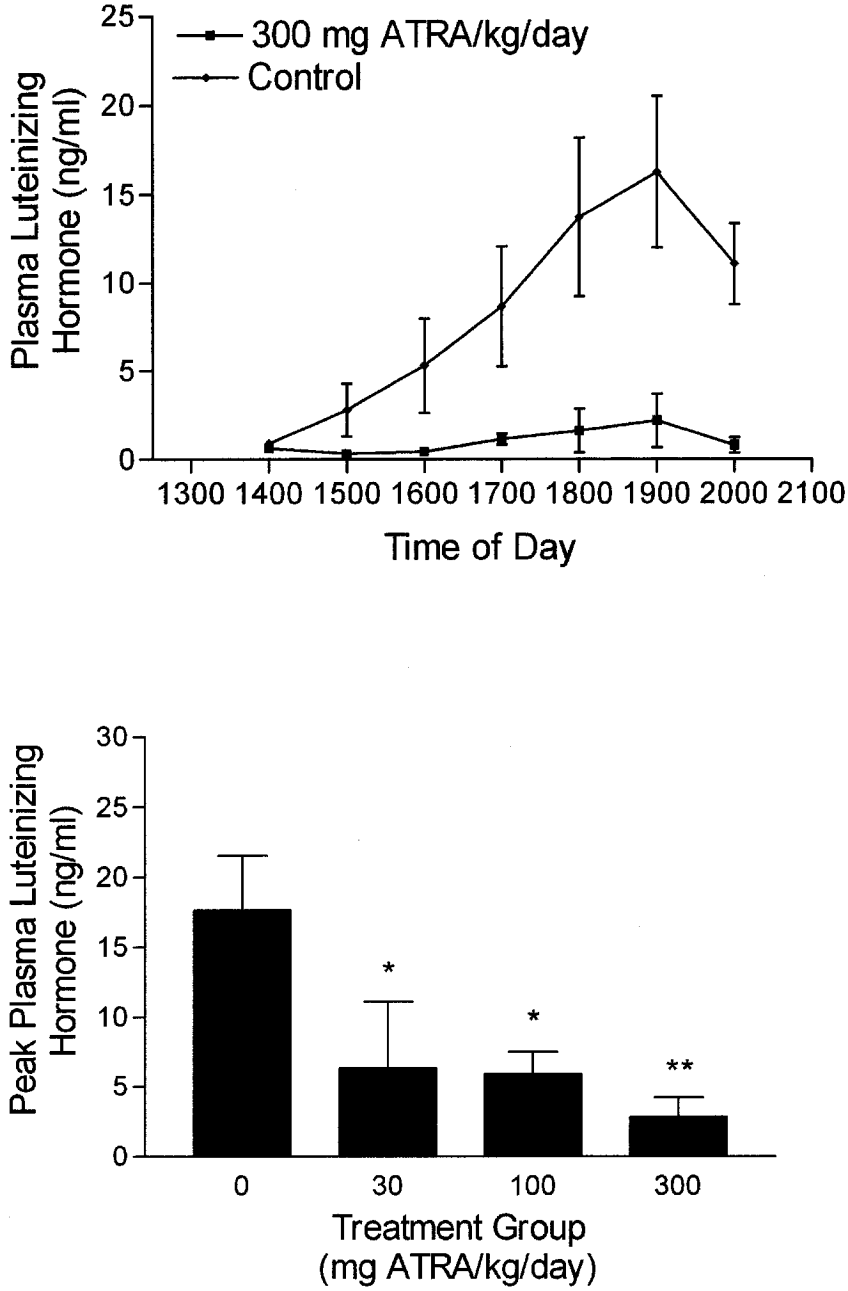

Figure 5.2. Dose - dependent suppression of 300, 100, or 30 mg ATRA/kg/day for five days on the estrogen and progesterone primed LH surge in adult female ovariectomized Sprague Dawley rats. a) a representative time-course of the LH surge for 300 mg ATRA/kg/day and control groups. 300 mg ATRA/kg/day completely blocked the LH surge. b) ATRA suppresses peak plasma LH concentrations in a dose-dependent manner. Points and bars represent mean ± SEM. * = $p<0.05$ compared to controls; ** = $p< 0.001$ compared to controls

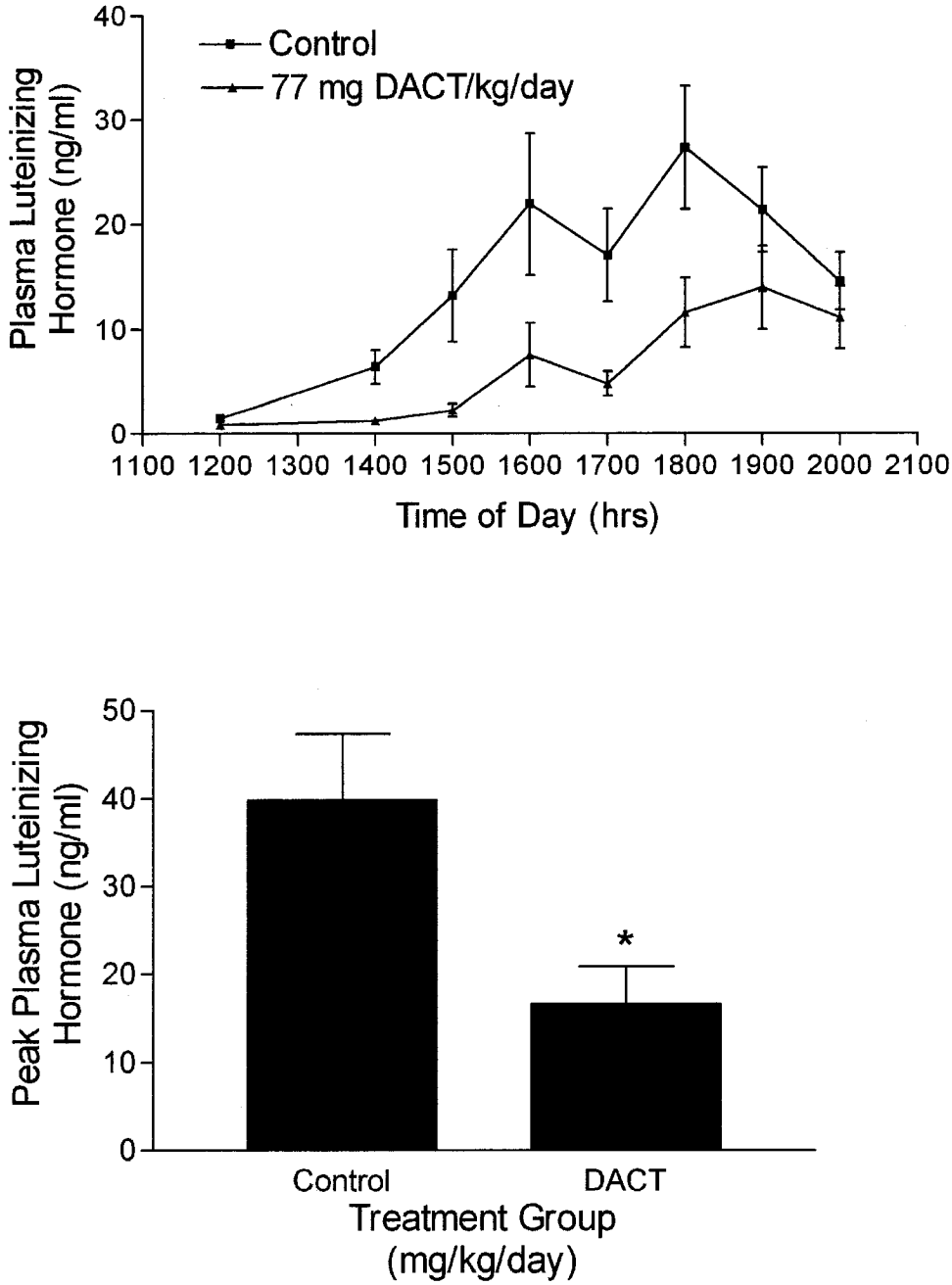

Figure 5.3. Dosing with 77 mg DACT/kg/day (the equivalent AUC concentration as dosing with 300 mg ATRA/kg/day) causes a) suppression of the amplitude of the LH surge and b) produces a 58% decrease in the peak LH surge levels in adult female ovariectomized Sprague-Dawley rats primed with EB and P. Points and bars represent mean ± SEM. * = $p<0.05$ compared to controls

To gain insight into the ability of the chlorinated metabolites to suppress the LH surge, animals were dosed with DACT, the major chlorinated metabolite in plasma after dosing with ATRA. The concentration of DACT chosen was based on kinetic studies in our laboratory where 300 mg ATRA/kg/day produced a plasma AUC of DACT equivalent to dosing of 77 mg DACT/kg/day. Although to a lesser degree than ATRA, DACT significantly suppressed the total plasma LH AUC and peak LH surge levels in EB/P primed animals by 60% and 58%, respectively (Figure 5.3 a, b).

5.3.2. ***Effect of DACT on Pituitary LH release after GnRH challenge***

This study examined the effect of DACT on pituitary responsiveness to exogenous GnRH. DACT treatment attenuated the LH response by 47% compared to control (31.5 ± 4.8 ng/ml versus 59.4 ± 15.03 ng/ml, respectively) (Figure 5.4a). Total plasma LH secretion over the entire 60 minutes (AUC) was reduced by 37% compared to control (174.7 ± 16.2 ng/ml/min versus 274.0 ± 40.0 ng/ml/min, respectively) (Figure 5.4b).

5.3.3. The Effects of ATRA or DACT on Estradiol Binding to ERα in vitro

Initial binding studies were performed with uterine cytosolic ER to determine the ability of ATRA to interfere with estradiol binding to this receptor. In addition, we also determined whether pre-incubation of ATRA with the receptor would lead to greater reduction of estradiol-binding than noted on short incubations. At all time points examined, ATRA decreased [^{3}H]estradiol binding to uterine cytosol, independent of pre-incubation conditions (Figire 5.5). The apparent Ki of ATRA is 0.02 mmol compared to 0.13nmol for estradiol.

To examine the direct binding of ATRA to ERα, ATRA was incubated simultaneously with [^{3}H]estradiol and *in vitro* transcribed ERα. ATRA reduced [^{3}H]estradiol binding to ERα in a dose-dependent manner (Figure 5.6). Since DACT is the major chlorinated metabolite in the plasma after dosing with ATRA, the ability of DACT to reduce estradiol binding to ERα was also investigated. DACT, at the molar equivalent concentration of ATRA, had no effect on [^{3}H]estradiol binding to ERα, with an apparent Ki 10x greater than ATRA (Ki = 0.2mmol vs. 0.02mmol) (Figure 5.6).

5.3.4. ***Effects of ATRA Exposure on Estrogen-Mediated Effects in Two Estrogen Responsive Hypothalamic Nuclei***

Changes in unoccupied ER levels after in vivo treatment with ATRA. To determine the ability of *in vivo* ATRA exposure to alter binding of estrogen to hypothalamic ER, unoccupied ER levels were evaluated in AVPV and MPOA, two hypothalamic nuclei that are responsive to estrogen and contain high levels of ER. The ligand bound (occupied) receptor can be discriminated from the unoccupied receptor by incubation conditions (Yuan et al., 1995). While CMC + EB treatment significantly decreased unoccupied ER levels compared to oil controls, treatment with ATRA + EB under dosing conditions that suppress the LH surge did not alter AVPV and MPOA unoccupied ER levels compared to EB treatment group (Figure 5.7).

Evaluation of changes in progesterone receptor mRNA expression. EB treatment significantly increased PR mRNA expression in the AVPV and MPOA. However, ATRA + EB did not alter the AVPV and MPOA PR mRNA expression compared to the EB-alone group (Figure 5.8).

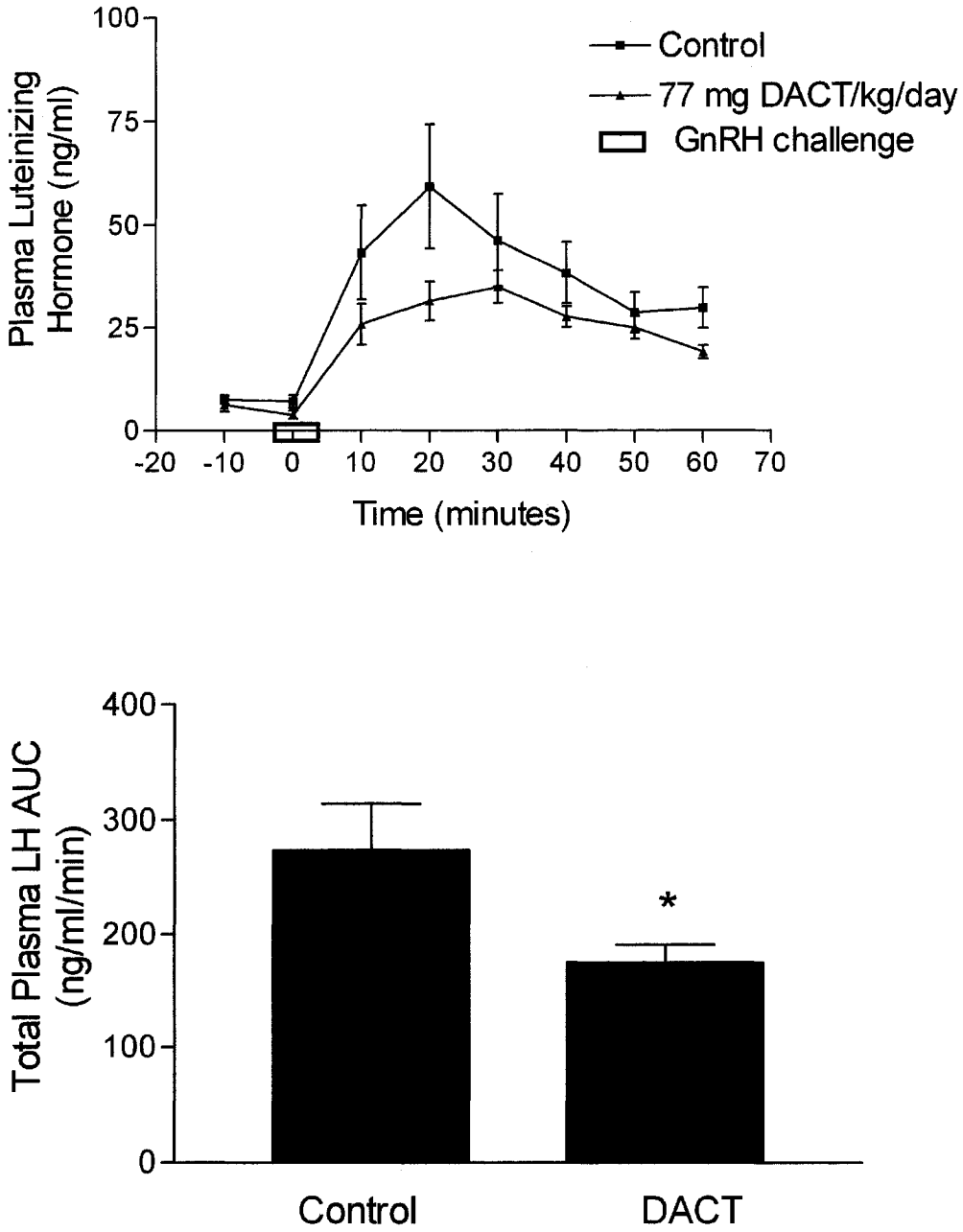

Figure 5.4. DACT, under conditions which suppress the LH surge, decrease release of LH from the pituitary. a) Plasma LH time course of DACT and control andimals after i.v. injection of 100ng GnRH /100g b.w. b) Total LH secretion over 60 minutes, as indicated by area under the curve (AUC), from DACT and control animals. Points and bars represent mean ± SEM. * = $p<0.05$ compared to controls.

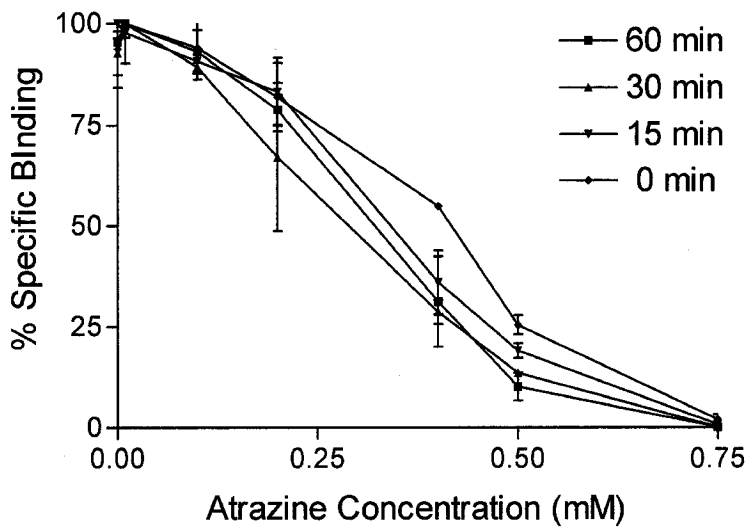

Figure 5.5. Independent of *in vitro* pre-incubation time, ATRA inhibits binding of [^{3}H] estradiol to uterine cytosol in a dose-dependent manner. Each curve represents various pre-incubation times of ATRA in the cytosolic incubation mixture prior to addition of [^{3}H]estradiol. Points and bars represent mean ± SD of three determination performed in triplicate.

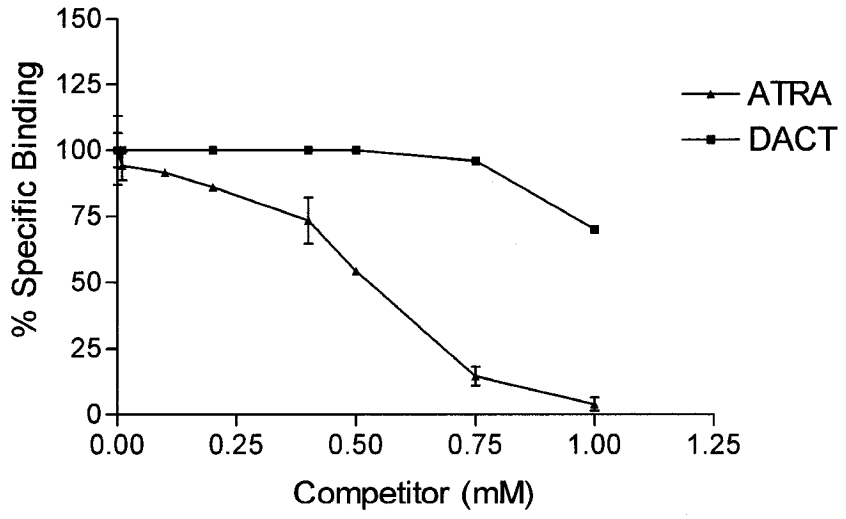

Figure 5.6. ATRA and DACT were incubated simultaneously with [^{3}H]estradiol and *in vitro* transcribed ERα. ATRA reduces [^{3}H] estradiol binding to ERα in a dose-dependent manner. DACT, at the molar equivalent concentration of ATRA, has no effect on [^{3}H]estradiol binding to ERα under equilibrium conditions. Points and bars represent mean ± SD of three determinations.

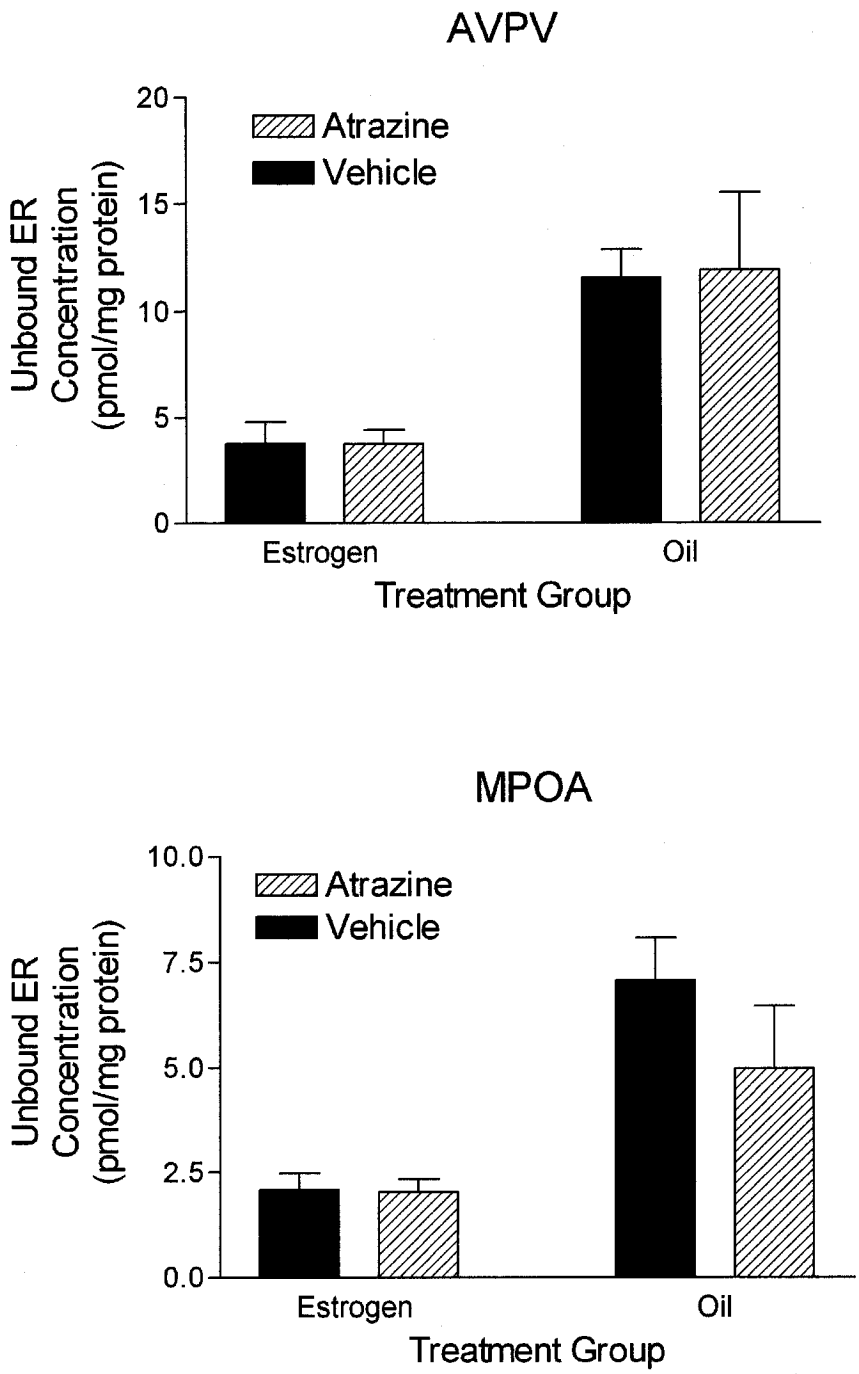

Figure 5.7. 300 mg ATRA/kg/day for 5 days does not alter levels of unoccupied ER in various estrogen responsive hypothalamic nuclei a) anteroventroperiventricular region (AVPV) b) medial preoptic area (MPOA) in adult, ovariectomized EB primed female SD rats compared to EB primed controls. Bars represent mean ± SEM.

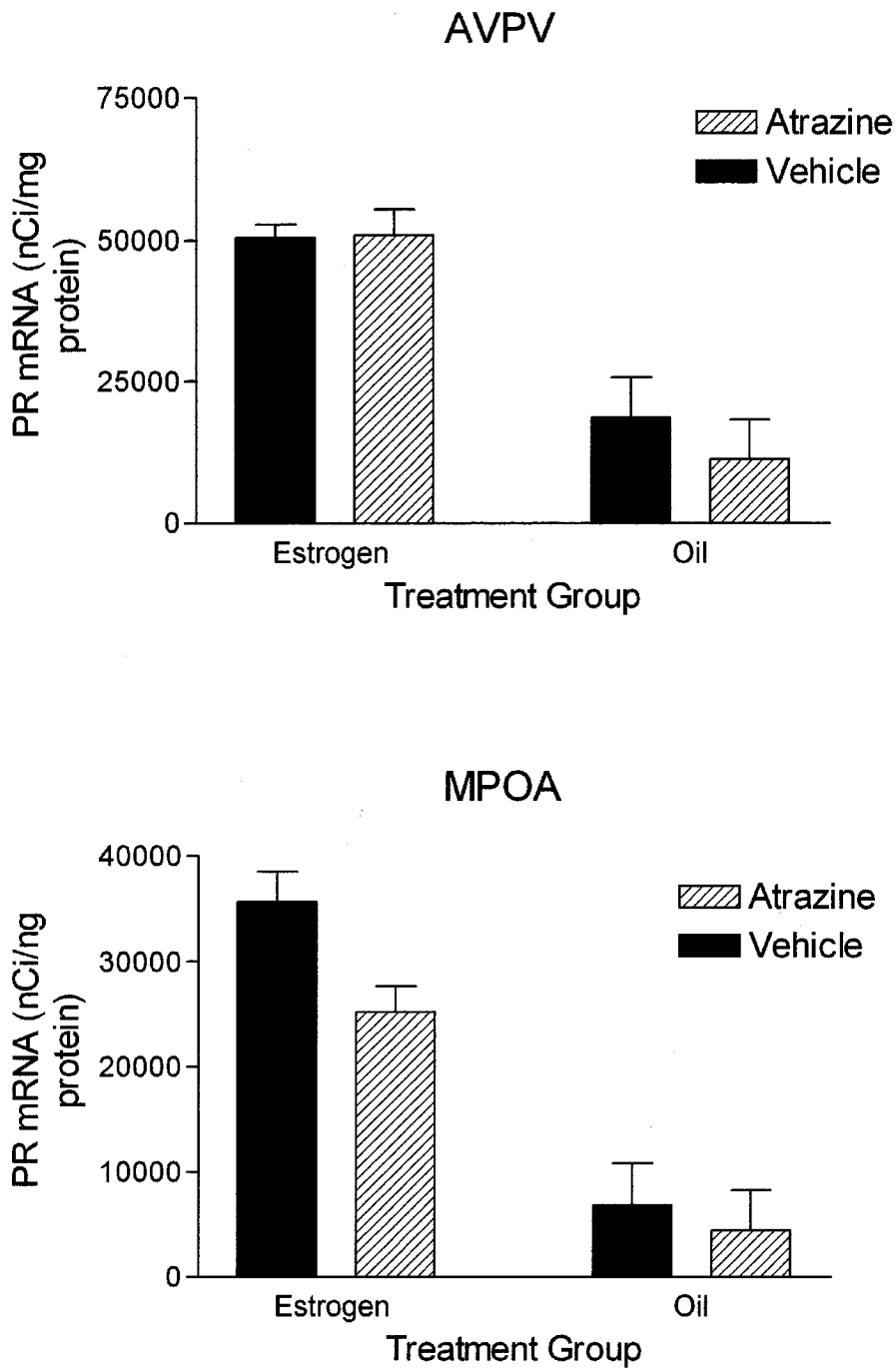

Figure 5.8. In adult, ovariectomized female SD rats primed with EB, five daily doses of 300 mg ATRA/kg/day does not alter estrogen induced PR mRNA upregulation in various estrogen responsive hypothalamic nuclei compared to controls. a)anteroventroperiventricular region (AVPV) b) medial preoptic area (MPOA) compared to EB primed controls. Bars represent mean ± SEM.

5.4. DISCUSSION

LH surge suppression in adult, female OVX rats due to high doses of ATRA is indicative of large scale neuroendocrine disruption. This effect is critical in determining risk of Cl-TRI to humans. However, only limited mechanistic data are available with which to draw conclusions on the human relevance of this effect. Because ATRA is extensively metabolized, plasma (Brzezicki et al., 2003) and brain (McMullin, unpublished data,2003) Cl-TRI concentrations after ATRA treatment are largely DACT, the di-dealkylated chlorinated metabolite of ATRA. Yet, the ability of DACT to alter neuroendocrine function has not been directly evaluated. Therefore, these studies were important to investigate the mechanism by which the Cl-TRI are acting to suppress the LH surge and to understand the significance of DACT in contributing to this effect.

5.4.1. ATRA and DACT Decreased the EB/P Primed LH Surge Response in Adult, Female OVX SD Rats

ATRA suppressed the EB/P LH surge in a dose dependent fashion, almost completely abolishing the surge when administered at the highest dose for 5 days. Although slightly different dose regimens have been examined by others, these results are consistent with the suppression of the EB induced LH surge by ATRA as reported by Cooper *et al.* (2000). However, these studies evaluated the LH surge under conditions of estrogen priming only. While this hormonal condition may be sufficient to observe treatment differences, priming with P in addition to EB enhances the LH surge, producing conditions more realistic of the *in vivo* hormonal environment prior to the LH surge (Lee et al., 1990). This observation is

substantiated by our current studies where EB/P priming in OVX rats produced a peak LH surge approximately 3 times greater than did priming with EB alone (Figure 5.1, 5.2a). Additionally, these priming conditions allowed for greater sensitivity for the dose-response studies and for clearer comparisons of potency between ATRA and DACT.

As noted above, DACT is the primary chlorotriazine metabolite. DACT also suppressed the LH surge in OVX, EB/P primed female SD rats (Figure 5.3). The percent of peak LH suppression after dosing with DACT was only 58% while ATRA dosing at the equivalent plasma AUC completely abolished the LH surge. This may be due, in part, to the different kinetic behaviors between ATRA and DACT. One difference in kinetic behavior is the rate of clearance by phase II processes, primarily glutathione-conjugation, where the total clearance of alkyltriazines by conjugation must be almost as large as their oxidative clearance (McMullin et al., 2003). Additionally, *in vivo* time-course studies indicate that direct dosing with DACT at the molar equivalent of ATRA produces peak DACT plasma concentrations approximately four times greater than when dosing with ATRA, also suggesting different rates of absorption and clearance (Brzezicki et al., 2003). Due to these differences, further work will be requird to assess relative potency of these compounds based on some consistent measure of target tissue dose or at least a measure of plasma concentrations of triazines and their metabolites.

5.4.2. DACT decreased pituitary LH release after GnRH challenge

In order to further examine the site of action of the Cl-TRI, pituitary function was evaluated using the EB/P priming model and dosing conditions of DACT that

suppress the LH surge in our studies. DACT significantly decreased the peak LH concentrations and the overall output of pituitary LH release compared to controls. This behavior indicates that under these conditions, DACT decreases pituitary responsiveness to GnRH.

A previous study indicated that the pituitaries of OVX, estrogen primed female Long Evans rats receiving three daily doses of 300 mg ATRA/kg/day were capable of releasing normal levels of LH after exogenous GnRH administration (Cooper et al., 2000). The observed differences between ATRA and DACT may be due to differences in experimental design. For instance, in our study, animals were primed with EB and P instead of EB alone and animals were challenged with 50% greater GnRH. EB/P priming elevated LH levels 10x greater than EB priming alone. Cooper and co-workers determined that, in the presence of exogenous GnRH, the pituitaries of ATRA treated animals are capable of releasing LH. However, our study indicates that, while the pituitaries of DACT treated animals are able to release LH in response to a GnRH challenge, the response is significantly reduced compared to controls. The differences between ATRA and DACT on pituitary release of LH after GnRH administration may also be due to differences in kinetic behaviors of the Cl-TRI. Such differences could lead to greater exposure of the pituitary and/or hypothalamus to DACT in DACT treated animals than from ATRA treatment, resulting in altered pituitary function.

While it may be possible for all Cl-TRI to elicit neuroendocrine effects at high doses, our kinetic results (Brzezicki et al., 2003) indicate that DACT, not ATRA itself, is most likely responsible for disruption leading to suppression of the LH surge.

The possible role of glutathione conjugates formed from ATRA and the two mono-de-alkylated metabolites remains unknown.

5.4.3. ATRA and DACT alter Estrogen Binding to ER in vitro but not in vivo

To investigate the mechanism by which exposure to ATRA or DACT leads to altered LH release, we examined changes in ER activity *in vitro* after ATRA and DACT treatment and modulation of estrogen responses in the hypothalamus of ATRA exposed animals. *In vitro*, ATRA reduced [^{3}H]estradiol binding to uterine cytosolic ER (Figure 5.5) and reduced binding of [^{3}H]estradiol to ERα in a dose-dependent manner (Figure 5.6). In contrast to a previous report (Tennant *et al.*, 1994a), there was no effect of pre-incubation in determining the extent of reduction in [^{3}H]estradiol binding caused by ATRA. Perhaps these differences may be attributed to the different range of concentrations and incubation times used. Due to the rapid metabolism of ATRA to the mono and di-dealkylated chlorinated metabolites, a single dose of 300 mg ATRA/kg is expected to produce an *in vivo* peak plasma concentration of ATRA of only 0.50 mg/L (McMullin et al., 2003). This concentration is approximately 400–fold lower than the highest dose of ATRA used in the *in vitro* binding studies (216 mg/L), making it unlikely that brain concentrations of ATRA after *in vivo* dosing would approach the high end of *in vitro* doses used in this study. However, the range of *in vitro* concentrations in the binding studies with DACT (0 – 146 mg/L) are more similar to the estimated *in vivo* peak plasma concentrations of DACT after dosing with ATRA (28 mg/L) or dosing directly with DACT at the molar equivalent to ATRA (80 mg/L). Even at these high concentrations, DACT does not inhibit binding of [^{3}H] estradiol to ERα. Tennant *et*

al. (1994b) showed that ATRA and DACT were capable of binding ER in uterine cytosol in a binding study when allowed to pre-incubate for 30 minutes prior to addition of [^{3}H] estradiol. Therefore, DACT, unlike ATRA, may require pre-incubation to bind to purified ERα. In conclusion, high concentrations of ATRA, but not DACT, can inhibit [^{3}H] estradiol binding to ERα *in vitro*. The steepness of the binding curve of ATRA suggests that ATRA likely binds ERα and inhibits binding of estradiol through non-competitive, rather than competitive binding and should be further investigated.

In vitro findings and previous studies with ATRA indicated that a possible direct anti-estrogenic effect of ATRA may occur *in vivo* to produce the suppression of the LH surge (Tennant *et al.*, 1994a; Tennant *et al.*, 1994b). However, many known anti-estrogens are tissue specific in their ability to act as either an estrogen agonist or antagonist. Therefore, our studies, which evaluated ER activity in the target tissue after ATRA treatment, were significant in determining the relevance of ATRA's anti-estrogenic properties to suppression of the LH surge.

EB treatment of OVX rats causes significant increases in PR mRNA expression in various estrogen responsive hypothalamic nuclei (Simerly et al., 1996; Shughrue et al., 1997; Chappell and Levine, 2000). This stimulation is a direct effect of estradiol on PR gene expression and estrogen antagonists such as tamoxifen and raloxifene decrease PR mRNA expression in the hypothalamus (Shughrue et al., 1997). ATRA, however, did not alter the estradiol induced PR mRNA expression in the AVPV and MPOA of the hypothalamus. Additionally, ATRA did not alter the binding of estrogen to ER in these same hypothalamic regions. It is worth noting that

compounds that have an *in vitro* affinity and potency similar to estradiol, such as tamoxifen and raloxifene, require *in vivo* concentrations 100 to 1000-fold higher than *in vitro* to produce an anti-estrogenic effect on PR mRNA in the hypothalamus (Shughrue et al., 1997). Similarly, ATRA and DACT may be binding ER *in vivo*, but their anti-estrogenic activity is not potent enough to compete with estradiol under *in vivo* conditions.

These studies also highlight the importance of proper design of *in vitro* mechanistic studies to study pituitary and hypothalamic effects of Cl-TRIs. Such studies should consider the treatment regimen in the context of the *in vivo* kinetic behavior of ATRA. While it is challenging to design a proper *in vitro* study that directly compares with the *in vivo* scenario, direct treatment with DACT or, potentially, other metabolites, is essential for allowing more appropriate interpretation between *in vitro* and *in vivo* effects. *In vivo* treatment with DACT eliminates many variables due to metabolism, allowing for a more direct interpretation of the mechanism by which Cl-TRIs are altering the LH surge and aiding in more appropriate risk assessment.

CHAPTER 6

GENERAL DISCUSSION

Atrazine (ATRA) is the most widely used herbicide in corn production in the United States. Runoff from application into the watershed is the main route of exposure for humans and wildlife species (EPA 2001). Concern over the human health risks from ATRA exposure initially resulted from rodent studies that indicated an increase in mammary tumors and decrease in time to tumor development after lifetime exposure to ATRA to female Sprague –Dawley rats (Eldridge et al., 1999). Further research demonstrated that ATRA altered estrous cyclicity in these rats, leading to high levels of circulating estrogen that produced an environment conducive to tumor formation (Eldridge et al., 1999). Moreover, ATRA also decreases release of the steroid primed luteinizing hormone (LH) surge from the pituitary in several rat strains, suggesting that this herbicide acts by a more general mechanism of disrupting neuroendocrine function (Cooper et al., 1996; Eldridge et al., 2001; Cooper et al., 2000).

Despite the large amount of data accumulated from examining animal models, it is still difficult to estimate the risk of neuroendocrine toxicity to humans from ATRA exposure using a biologically based approach (EPA 2001). Such an approach reduces the uncertainties in assessing the dose-response of a compound by integrating data on the interaction between the compound and/or its metabolites with tissue constituents (mode of action) and the kinetic disposition of the compound and/or its

metabolites in the body under conditions that cause key endpoints of toxicity (tissue dosimetry). The uncertainties regarding the dose-response behavior of ATRA mediated neuroendocrine effects include extrapolating the effects observed in animal models to humans (i.e. inter-species extrapolation) and at high doses to low, environmentally relevant exposure levels (i.e. high-low dose extrapolation). As such, research that examines the mode of action and tissue dosimetry of ATRA and its chlorinated metabolites (collectively termed Cl-TRIs) is essential to further establish a biologically based approach to determining ATRA risk to humans. This current research was intended to address these data gaps by (1) examining the processes that control exposure of plasma and brain (possible target tissue) to ATRA and its metabolites using a series of predictive kinetic models (Chapter 2-4) and (2) evaluating the ability of ATRA and its primary chlorinated metabolite, DACT, to cause disrupt the LH surge by altering estrogen binding to its cognate receptor, ERα, in the hypothalamus (Chapter 6).

6.1. DEVELOPMENT OF PBPK MODELS TO EXAMINE CHLOROTRIAZINE TISSUE DOSE

In the body, ATRA is extensively metabolized to chlorinated metabolites (desethyl and desisopropyl triazine and subsequent metabolism of these dealkylated intermediates (Hanoika et al., 1999a, b). ATRA and the chlorinated metabolites (collectively termed Cl-TRIs) are also metabolized to non-chlorinated metabolites (Bakke et al., 1972; Timchalk et al., 1990). Neuroendocrine effects are not observed after exposure to non-chlorinated triazines (Eldridge et al., 1994), suggesting that

these toxic responses likely result from target tissue exposure to Cl-TRIs rather than the non-chlorinated metabolites. U.S. EPA proposed to conduct the health risk assessments for ATRA based on net tissue exposure to total Cl-TRIs rather than administered ATRA (U.S.EPA, 2001). Prior to the pharmacokinetic studies presented in Chapters 2-4, there was no appropriate data to develop models to assist in extrapolating across dose levels and across species, such as low level human exposures. To address this deficiency we developed a series of physiologically based pharmacokinetic (PBPK) models to address this need for quantitative methods of predicting tissue dose of Cl-TRIs based on biological understanding of the major determinants of Cl-TRI within the body. These models examined the biological and physiochemical processes that regulate the distribution and accumulation of Cl-TRI in plasma and tissues after oral administration of ATRA in rat. Analysis of these studies indicated that the time-course behavior of Cl-TRIs is controlled by complex absorption processes, extensive oxidative metabolism in the liver and possibly intestines, reactivity with hemoglobin and plasma proteins and systemic clearance by GST mediated GSH conjugation and urinary elimination. These processes, working in concert, are responsible for rapid clearance of ATRA and the slower accumulation and extended retention of DACT in the plasma. *In vivo*, at doses usually used in toxicity studies, we found that the vast majority of tissue Cl-TRI exposure is due to DACT rather than the alkylated precursors. The differential tissue exposure is due to more rapid metabolic clearance of ATRA, desethyl and desisopropyl triazines, compared to DACT.

6.1.1. Extensive oxidative metabolism limits tissue exposure to ATRA while producing high tissue concentrations of DACT

One of the main goals in developing these PBPK models was to quantitatively describe the oxidative metabolism of ATRA and its chlorinated metabolites in the body in order to assess total Cl-TRI tissue dose separate from the non-chlorinated compounds. Previously, oxidative metabolic parameters describing oxidative metabolism of ATRA to the mono-dealkylated metabolites and subsequent metabolism to DACT were estimated from time-course studies using freshly isolated rat hepatocytes (Hatfield-Berube, 2004). Incorporation of these *in vitro* values into the PBPK models provided a fairly good representation of kinetics in the rat (Chapter 3), indicating the value of collecting these kinetic constants to estimate equivalent *in vivo* metabolism of a compound.

Extrapolation of these PBPK models to predict time-course concentrations of Cl-TRIs in humans will require integrating human metabolic parameters into these existing models. Our success in describing the *in vivo* metabolism of ATRA to the mono-deaklyated metabolites using *in vitro* estimated values suggests that these *in vitro* metabolism systems will be useful for predicting metabolism in humans based on in vitro analysis of ATRA metabolism in human hepatocytes. Studies in which ATRA and the mono-dealkylated metabolites are incubated in a human microsomes or ideally, primary hepatocytes, and loss of substrate and formation of metabolites are monitored over time would provide experimental parameters that could be integrated into these existing models to describe the oxidative metabolism of Cl-TRIs in humans.

6.1.2. Systemic availability of ATRA also appeared to be limited by oxidative metabolism in the GI tract

An interesting finding from our kinetic analyses was the requirement to include oxidative metabolism of ATRA in the GI tract in addition to hepatic metabolism to describe the uptake and bioavailability of absorbed ATRA (Figure 4.6). The extent to which GI tract metabolism contributes to limited tissue exposure of ATRA obviously needs to be experimentally verified. To examine this possibility, time-course studies using metabolically active immortalized enterocyte cell lines such as Caco-2 cells (Cavret and Feodt, 2005; Gan and Thakker, 1997; Carriere et al., 2001), freshly isolated enterocytes (Carriere et al., 2001) or intestinal tissue slices (DeKanter et al., 2002) incubated with the individual Cl-TRIs need to be performed. Determination of the rates of oxidative metabolism of the Cl-TRIs in enterocytes from *in vitro* studies could be easily incorporated into the existing PBOK model structures in order to determine the relative contribution of intestinal metabolism on the bioavailability of Cl-TRIs after oral administration.

6.1.3. Complex dose-dependent absorption causes slow uptake of Cl-TRIs from the gut

The studies examining the individual time-course concentrations of ATRA and its chlorinated metabolites after oral gavage administration of ATRA showed that absorption of Cl-TRIs into the blood was complex (Chapter 4). The multiple peak behavior of Cl-TRIs in plasma is likely a reflection of limited compound solubility in the gut and continuing absorption of more slowly dissolving compound along the GI tract. To give quantitative structure to this mechanistic hypothesis for absorptive

processes for triazines, our PBPK models were modified to describe the absorption characteristics with availability of a small portion of dissolved (free) ATRA in the gavage dose that was rapidly absorbed from the GI tract followed by slow dissolution of the remaining slurry as a rate-limiting step for most of the uptake (Chapter 2 and 4). These absorption characteristics are also consistent with the observed kinetic behavior for oral absorption of several other chemicals, especially compounds that are administered in suspension (Zhou et al., 2003; Gallo et al., 1993; Semino et al., 1997; Lilly et al., 1998). Future studies comparing the plasma area under the curves after oral and intravenous administration of ATRA will be necessary to clarify some of the underlying mechanisms responsible for this multiple peak behavior and thereby, aid in prediction of the expected kinetic behavior of Cl-TRIs at low environmentally relevant doses.

6.1.4. Reactivity of Cl-TRIs with blood proteins likely causes dose-dependent accumulation in red blood cells and plasma

Modeling the accumulation of radioactivity in red blood cells and plasma required addition of a second-order reaction rate between Cl-TRIs and hemoglobin and albumin. The necessity to incorporate this reaction to describe the time-course profiles of ^{14}C-ATRA suggested that Cl-TRIs might react with constituents in red blood cells and plasma (Chapter 2). Based on our results from the Cl-TRI metabolite time-course study (Chapter 4) and previous urinary elimination studies (Timchalk et al., 1990), the most likely candidate for this interaction would be DACT since DACT is the predominant Cl-TRI metabolite in the blood after dosing with ATRA. Consistent with this hypothesis, recent studies from other scientists at

Colorado State University have determined that DACT reacts to hemoglobin (Hb) in a dose-dependent manner after three daily doses ranging from 10 – 300mg/kg (Prentiss 2004). Examination of adducted hemoglobin showed formation of an adduct weighing 110 daltons that was consistent with displacement of chloride ion from DACT and binding with the cysteine-125 residue of the β-chain of rat Hb (Dooley G. and Tessari J., unpublished observations).

A previous study examined the covalent binding of two other chloro-s-triazine herbicide metabolites, simetryn sulfoxide and ametryn sulfoxide to Hb from various animal species. *In vitro* incubation of these metabolites with Hb indicated that reactivity of these metabolites with Hb was species dependent. Simetryn sulfoxide and ametryn sulfoxide extensively reacted to Hb from rat, mouse and guinea pig while minimal binding occurred with human Hb. This study also determined that the binding in the rat was via a covalent reaction with the cysteine-125 residue of Hb by nucleophilic displacement with methylsulfoxide serving as the leaving group in the reaction. The reactivity of DACT to rat Hb is likely much higher than that in humans since human Hb does not contain a cysteine-125 residue on its β-chain, suggesting that adduct formation of DACT with Hb might not be a good a marker of Cl-TRI reactivity and exposure in humans.

In our model, retention of radioactivity in plasma was described by the binding of Cl-TRIs to albumin. Many toxicants (Phillips and Farmer, 1994; Rappaport and Yeowell-O'Connell, 1999) and drugs (Kramer and Routh, 1973; Christensen *et al.*, 1980) are capable of forming albumin adducts. As such, albumin adduct formation might prove to be a better marker of Cl-TRI exposure in humans

than Hb adducts since albumin can react with protein residues that are less species specific. Future studies to assess time and dose dependent binding of Cl-TRIs to plasma proteins such as albumin will provide experimental rates of binding that can be incorporated into these PBPK models.

8.1.5. The kinetic disposition of Cl-TRIs in brain reflects plasma

Prior to this research and development of the PBPK models, the time-course disposition of Cl-TRIs in brain (possible target tissue) was not known. Evaluation of the time-course profiles of Cl-TRIs in brain indicated that administration of ATRA results in total Cl-TRI brain concentrations that are predominantly DACT (Chapter 4). Moreover, peak Cl-TRI concentrations and total Cl-TRI area under the curve was higher in brain relative to plasma. Since DACT reacts with macromolecules such as hemoglobin *in vitro* and *in vivo* after dosing with ATRA (Prentiss, 2004), specific and/or non-specific reactivity of DACT with brain proteins might also produce the higher brain concentrations and retention in brain compared to plasma. This possibility is consistent with our original hypothesis on the anti-estrogenic actions of ATRA that ATRA and its chlorinated metabolites could react with residues on receptors to form an inactive adduct in a similar manner to the reaction of DACT with rat hemoglobin or with albumin. Eventually, studies might be pursued in target tissues (either hypothalamus or pituitary) to examine Cl-TRI adduction with proteins that are associated with GnRH signaling and neuroendocrine responses. These molecular reactions could be integrated into the existing PBPK model with equations that describe the time and dose dependent interaction of Cl-TRIs (or only DACT) with specific sites on cellular targets in the brain as depicted in Figure 6.1.

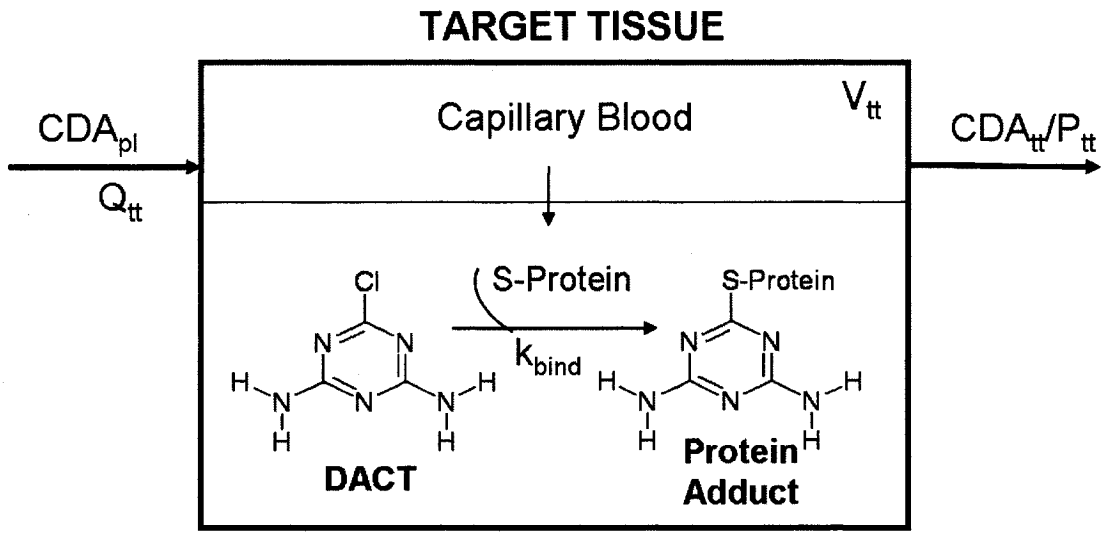

CDA_{pl} = free concentration of DACT in plasma (mmol/L)
Q_{tt}= blood flow to target tissue (L/hr)
K_{bind} = irreversible second-order binding rate of DACT with target protein (L/mmol/hr)
CDA_{tt} = free concentration of DACT leaving target tissue (mmol/L)
P_{tt} = partition coefficient in target tissue
V_{tt} = volume of target tissue (L)

(1) The rate of change of amount DACT bound in target tissue:

$$dADAbound_{tt}/dt = K_{bind} \times CCl_{tt} \times C_{tt} \times V_{tt}$$
$$CDAbound_{tt} = ADAbound_{tt}/V_{tt}$$

(2) Circulating free concentration of DACT in target tissue:

$$dADA_{tt/dt}/dt = Q_{tt} \times (CDApl - CDA_{tt}/P_{tt}) - (dADAboundtt/dt)$$
$$CDA_{tt} = ADA_{tt}/V_{tt}$$

Figure 6.1. A schematic and mathematical description of the possible reactivity of DACT with cysteine residues on target tissue proteins. Using the equations described in the figure, this interaction can be included into the existing PBPK models to describe concentrations of free and bound DACT in target tissue under conditions that suppress the LH surge.

6.1.6. Summary: Assessing tissue dosimetry

This research that quantitatively examined the kinetic disposition of Cl-TRIs using PBPK models is the first step in providing tools that will permit more accurate

estimation of target tissue dosimetry and be useful for assisting in dose-response assessment in the animal studies. Ideally, the PBPK models should be linked to pharmacodynamic (PD) models that quantitatively describe mode of action of Cl-TRIs in target tissues. Combined, the PK and PD models could provide a more biologically based approach to analyzing the dose-response behavior of Cl-TRIs under different exposure conditions in different species. While specific recommendations can be provided for steps to improve the PBPK model and extrapolation of the model across species, it is less clear where to focus attention on examining the toxicity of these compounds. The difficulty of determining the mode of action resides in a continuing challenge to understand the molecular targets of ATRA/DACT that produces the variety of neuroendocrine responses observed in animal models.

6.2. EVALUATING NEUROENDOCRINE MODE(S) OF ACTION

To determine human risk from ATRA exposure using a biologically based approach, it becomes imperative to understand the manner in which the toxic compound(s) interact with the biological system to cause adverse responses (Andersen 1995c; Andersen and Dennison 2001). Earlier studies indicated that ATRA caused anti-estrogenic responses in uterine tissue (Tennant et al., 1994a) and decreased binding of estrogen to ER *in vitro* (Tran et al., 1996; Tennant et al. 1994b; Connor et al., 1996). Therefore, we hypothesized that the most likely candidate to be targeted by Cl-TRIs was ERα expressed in cells within hypothalamic nuclei responsible for regulating the GnRH/LH surge. The main objective of our studies

was to further examine the site of action of ATRA/DACT mediated suppression of the steroid induced LH surge, an indicator of disruption of neuroendocrine disruption.

6.2.1. Chlorotriazines decrease LH release by altering pituitary function

Release of gonadotropin release hormone (GnRH) from GnRH neurons in the hypothalamus is the primary regulator of pituitary release of LH. One of the more interesting observations from the current work was the inability to recover the diminished LH surge after DACT administration by infusion of GnRH into the animal (see Chapter 5, Fig. 5.4). These results clearly demonstrated that DACT exposure decreases the ability of the pituitary to respond to a GnRH challenge with a normal release of LH. Previous studies indicated that ATRA suppressed the LH surge at the level of the hypothalamus rather than directly acting on the pituitary (Cooper et al., 2000). Two experiments by Cooper et al. (2000) supported this hypothesis. In a similar experiment to our study, the authors examined the circulating levels of LH after administration of exogenous GnRH in OVX, estrogen-primed female Long Evans rats treated with ATRA. This study showed that GnRH infusion stimulated an LH surge in treated animals. Based on this observation, the authors concluded that the pituitary was responsive and the site of action was the hypothalamus. However, the authors did not compare the amplitude of the GnRH induced LH surge in treated animals to that of a GnRH induced surge in untreated animals. In light of our results that indicated the presence, but reduced amplitude, of an LH surge response compared to untreated animals receiving GnRH, I would argue that the previous study by Cooper et al. (2000) does not conclusively show that pituitary function was normal. However, it is also plausible that design differences between our study and

that of Cooper et al. (2000) might have contributed to the differing results. Such differences include examination of the responses after DACT versus ATRA treatment, the use of different strains of rats (SD vs. LE) known to have different sensitivities in LH release in response to ATRA treatment (Cooper et al., 2000) and the use of estrogen and progesterone to induce an LH surge in our study versus only estrogen to induce a surge in the animals used in the study by Cooper et al. (2000).

In another experiment, Cooper et al. (2000) directly examined release of LH from pituitaries incubated with 100μM ATRA and challenged with GnRH. Under these conditions, ATRA treatment did not decrease LH release compared to control pituitaries, suggesting that the pituitary functioned normally to release LH. This *in vitro* study has the potential to be misleading. In the intact rat after oral dosing, tissues are exposed primarily to DACT with very low tissue levels of the other three Cl-TRIs (Chapter 6). Although the pituitary has limited oxidative metabolic capacity, tissue concentrations of Cl-TRIs were not measured to assess the extent of metabolism that might have occurred to produce DACT. Additionally, time and dose-response studies were not performed to assess if an effect would have been observed at higher incubation concentrations or longer incubation times. Future studies need to be performed to clarify the discrepancies observed between our studies and those of Cooper et al. (2000). One such experiment might include a pituitary perfusion study where pituitaries from animals dosed with ATRA or DACT at concentrations that suppressed the LH surge are placed in perfusion chambers and GnRH induced LH release is measured from the pituitaries. Results from such a

study would determine if Cl-TRIs directly alter LH release from the pituitary under *in vivo* conditions that cause neuroendocrine toxicity.

Pulsatile secretion of GnRH into the median eminence followed by binding of GnRH to its receptor residing in the gonadotrophes of the anterior pituitary regulates release of LH (Clayton et al., 1988; Sealfon et al., 1997). The pulse patterns of GnRH highly regulate GnRH receptor concentration and mRNA levels (Savoy-Moore et al., 1980, 1981; Bauer-Dantoin et al., 1995; Kaiser et al., 1997). Receptor concentrations are also regulated by exposure to steroid hormones such as estrogen (Duncan et al., 1986; Yasin et al., 1995), as during the time of the LH surge. Activation of the GnRH receptor by GnRH initiates a cascade of signaling mechanisms that result in *de novo* synthesis of LH and secretion of this gonadotrophin from secretory vesicles within the cell (Stojilkovic et al., 1994, 1995; Naor 1998; Kraus et al., 2001) (Figure 6.2). Based on our results showing that DACT alters release of LH from the pituitary in response to GnRH, the GnRH receptor might be a possible cellular target for further study (Figure 6.2). Future *in vivo* experiments that evaluate treatment related changes in number and affinity of GnRH receptor or GnRH receptor mRNA expression would determine if the pituitary cannot normally respond to GnRH because receptor concentration or synthesis of receptor is decreased. Furthermore, *in vitro* binding studies would be valuable in assessing the ability of Cl-TRIs to react with GnRH receptors in a manner that causes inhibition of GnRH binding.

Independent of altering GnRH receptor function, DACT could decrease LH release from the pituitary by modifying intracellular signaling mechanisms that occur

in response to binding of GnRH to its receptor (Clayton et al., 1988; Stojilkovic and Catt 1995; Naor et al., 1998) (Figure 6.2). Studies using αT3-1 cells, an immortalized murine anterior pituitary derived cell line that expresses GnRH receptors (Windle et al., 1990; Kaiser et al., 1997), have been largely responsible for elucidating the pituitary signaling mechanisms that control synthesis and release of LH. Experiments in these cells indicate that GnRH binding to its cognate receptor, a G coupled protein (Sealfon et al., 1997), activates a series of signaling cascades within the gonadotrope to amplify and regulate LH release. Ligand binding of the GnRH receptor activates the G proteins Gqα and G11α (Shah et al., 1994). These proteins stimulate phospholipase C within the cell which in turn activates second messengers, specifically inositol -1, 4, 5-triphyosphate (IP_3) and diacylglycerol (DAG). Assessing activation status of these second messenger proteins as a result of DACT treatment would assist in identifying possible sites of Cl-TRI interaction within the cell that regulate the downstream release LH.

Ca^{2+} is one of the critical intracellular signals that controls gene expression and release of LH within the pituitary. Increased cytoplasmic Ca^{2+} levels occur in response to activation of the second messenger IP_3. IP_3 causes a rapid mobilization of stores of Ca^{2+} from the endoplasmic reticulum (Naor 1990). Additional increases in intracellular Ca^{2+} also result from influx of extracellular Ca^{2+} via activation of L-type Ca^{2+} channels on the plasma membrane of gonadotrophes. This influx is mediated by the presence of high concentrations of GnRH and estrogen during the time of the LH surge (Naor et al., 1990; Bulayeva et al., 2004). The large mobilization of free intracellular Ca^{2+} initiates the protein kinase C (PKC)-mitogen activated protein

kinase (MAPK) signaling cascade, resulting in highly regulated synthesis and release of gonadotrophins from the pituitary (Naor et al., 1998; Kraus et al., 2001; Seger and Krebs 1995) (Figure 6.2). Recently, *in vitro* studies have demonstrated that picomolar to nanomolar concentrations of several estrogenic organochlorine pesticides can induce rapid increases in cytoplasmic Ca^{2+} levels via activation of the L-type Ca channels in addition to initiating MAPK activation via non-genomic estrogen mediated pathways (Bulayeva et al., 2004; Wozniak et al., 2005). Therefore, it would be interesting to examine the ability of DACT to similarly act on certain signals that are responsible for increasing intracellular Ca^{2+}.

Activation of this MAPK cascade phosphorylates and activates downstream phospholipases such as phospholipase A_2 (PLA_2). Phosphorylated PLA_2 releases arachidonic acid (AA) into the gonadotrope (Naor 1991; Shraga-Levine et al., 1996). AA is a precursor for synthesis of several leukotrienes via lipoxygenase metabolic pathway. One lipoxygenase product of AA that is of particular interest with respect to GnRH induce LH release is leukotriene C_4 (LTC_4). LTC_4 is a cysteine containing leukotriene synthesized from AA by leukotriene C_4 synthase and glutathione-s-transferase mediated GSH conjugation (Samuelsson et al., 1987; Funk et al. 2001). *In vitro* and *in vivo* studies indicate that GnRH stimulates AA release and production of LTC_4 in the pituitary (Dan-Cohen et al., 1992; Kiesel et al., 1991). Moreover, LTC_4 appears to act as a second messenger within the gonadotrope to stimulate release of LH (Hulting et al., 1985), possibly by cross-talk with PKC (Naor et al., 1990; Stojilkovic et al., 1994; Ben-Mehahem et al., 1992). Recent evidence that DACT reacts with cysteine residues on proteins (Dooley G., unpublished data) makes LTC_4 a

possible target for Cl-TRI neuroendocrine toxicity that should be considered (Figure 6.2). One such study to address this possibility would include assessing LTC_4 levels within the pituitary after *in vivo* and/or *in vitro* DACT/ATRA exposure.

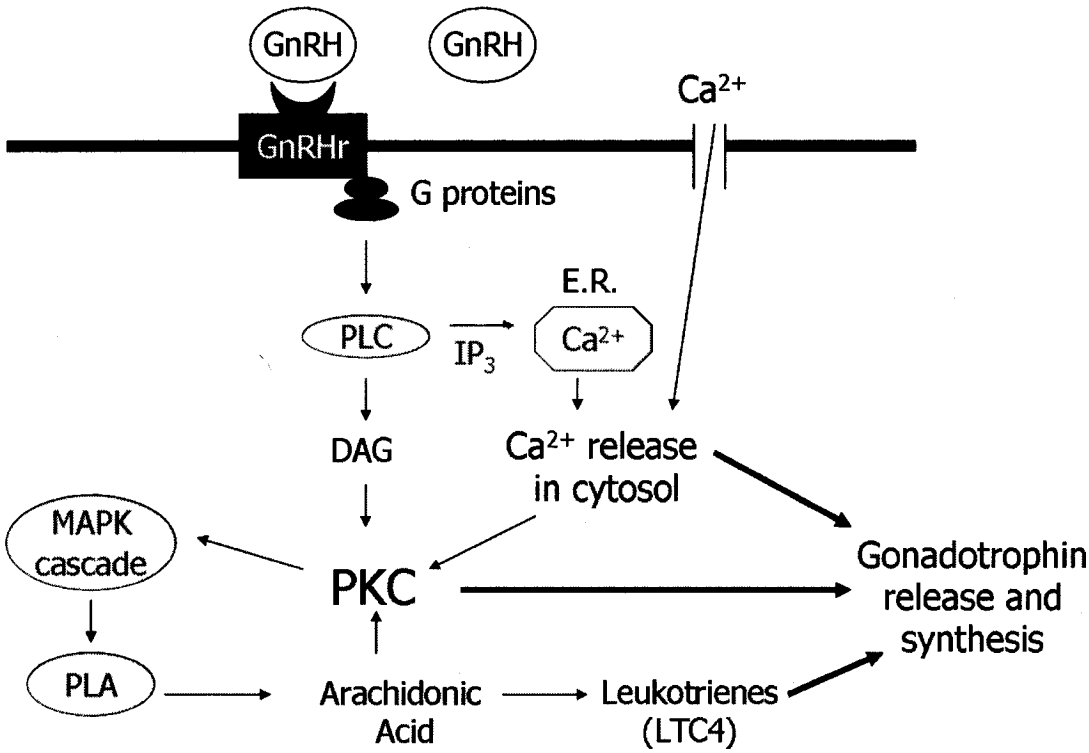

Figure 6.2. A diagram of some of the well-characterized signaling pathways within the anterior pituitary gonadotrophes that mediate synthesis and release of LH (adapted from Naor 1998).

6.2.2. Cl-TRIs might act on hypothalamic signaling mechanisms to decrease GnRH mediated LH release

Although the current data indicate that DACT alters pituitary responsiveness to exogenous GnRH, the possibility that Cl-TRIs interfere with centrally mediated

mechanisms controlling LH release cannot be entirely excluded. Binding of estrogen to its nuclear receptor ERα in specific nuclei within the medial preoptic area of the hypothalamus has long been established as necessary for stimulation of the LH surge (Goodman RL, 1978; Goodman and Knobil, 1981). Our experiments, however, have demonstrated that ATRA does not suppress the LH surge by interfering with binding of estrogen to nuclear ERα within the medial preoptic area and another estrogen responsive region, the anteroventroperiventricular (AVPV) nucleus (Figure 5.7 and 5.8). However, ATRA could suppress the LH surge by reacting with other cellular constituents within the hypothalamus responsible for regulating LH synthesis and secretion from the pituitary.

Do Cl-TRIs alter GnRH neuronal function? LH is directly regulated by the secretory patterns of GnRH from GnRH neurons (Lu and Yen, 1980; Levine et al., 1991; McCann et al., 2001; Gore 2002). Any disruption of critical hypothalamic signaling mechanisms that regulate LH release would also alter GnRH neuronal function during the time of the LH surge. Thus, it would be prudent to examine GnRH neuronal function in ATRA treated animals to determine if ATRA exposure prevents adequate communication between the GnRH neurons and the anterior pituitary. Although monitoring release patterns of GnRH in portal circulation in rodent models would be ideal, studies of this type can be difficult due to the procedures necessary to collect blood from portal circulation in the rat. Therefore, other markers of GnRH neuronal activity during the steroid induced LH surge have frequently been examined. FOS, the protein product of the *c-fos* gene, is an immediate early gene product that has been widely used to study the transcriptional

and secretory activity of GnRH neurons under various experimental conditions (Hoffman et al., 1993; Hoffman and Lyo, 2002). A body of literature has consistently demonstrated that a subpopulation of GnRH neurons express FOS in direct correlation with LH release during the time of the pre-ovulatory LH surge (Lee et al., 1990; Wang et al., 1995; Eyigor and Jennes 2000) and during the steroid induced LH surge (Hoffman et al., 1990; Eyigor and Jennes 2000) while FOS expression in these neurons is minimal to undetectable at other times. Indeed, examination of FOS expression in GnRH neurons of DACT treated animals was attempted in this thesis research and is still in progress.

Additional studies to assess changes in GnRH transcriptional activity might also provide some insight into GnRH neuronal function after Cl-TRI exposure. Several laboratories have evaluated GnRH mRNA levels during the surge. Results from these studies have demonstrated that GnRH mRNA might not be the most reliable indicator of GnRH transcriptional activation for several reasons. First, GnRH mRNA levels are not highly up-regulated during the LH surge (Sagrillo et al., 1996) and studies assessing mRNA levels in OVX estrogen/progesterone primed rat models have frequently observed different results due, in large part, to variations in steroid environments, methods used to evaluate mRNA expression (Gore and Roberts 1997). Moreover, GnRH mRNA expression is highly regulated by the time of day and is region specific (Petersen et al., 1995). In contrast to GnRH mRNA expression, GnRH heteronuclear RNA, the primary transcript of GnRH gene, has a clearer expression pattern that correlates with the LH surge. For example, GnRH heteronuclear RNA levels within the OVLT and POA substantially increase in the

early morning prior to the estrogen induced LH surge in OVX rats (Petersen et al., 1996; Jimenez-Linan and Rubin, 2001). As such, *in situ* hybridization experiments to examine GnRH heteronuclear RNA transcript in specific GnRH neuronal populations of ATRA treated animals would be an appropriate marker to assess if ATRA might decrease transcriptional activity of the GnRH neurons prior to the onset of the expected steroid induced LH surge.

In vitro studies utilizing the immortalized GnRH neuronal cell line (GT1 cells) might assist in determining if Cl-TRIs directly alter GnRH neuronal function. Previous dose-response studies in this cell line suggested that the organochlorine pesticides chlorpyrifos and methoxychlor might cause neuroendocrine toxicity by directly altering GnRH transcription and peptide levels (Gore 2002). Although the GT1 cell line is widely used to study GnRH neuron physiology because it retains many of the characteristics of intact GnRH neurons, (Mellon et al., 1990), there are some concerns with the use of this cell line that may make it difficult to extrapolate results from these studies to the *in vivo* situation. These cells were derived from the olfactory placode in developing mice (Mellon et al., 1990) and therefore, might more similarly represent properties of GnRH neurons during development rather than in adulthood (Selmanoff 1997). GT1 cells express ERα (Shen et al., 1998; Butler et al., 1999) yet there is no conclusive evidence that ERα is expressed in native GnRH neurons (Legan and Tsai 2003; Hrabovsky et al., 2000, 2001; Skynner et al., 1999). Moreover, it is believed that there are marked differences in the regulation of biosynthesis of GnRH among hypothalamic GnRH neurons and GT1 cells (for review see Gore and Roberts, 1997). Although an awareness of the limitations of this

cellular model is necessary, dose-response studies utilizing these neuronal cells could assist in determining possible direct action of DACT on GnRH synthesis and/or release.

In order to draw meaningful conclusions from any *in vitro* data, experiments will need to be performed under exposure conditions that most similar represent the *in vivo* situation that causes the neuroendocrine effects. Such studies include evaluating *in vitro* responses after incubation with DACT at concentrations that are observed in target tissue during suppression of the LH surge. The target tissue concentrations can be estimated using tools such as the PBPK models presented in this dissertation and/or by using existing GC/MS methods (Brzezicki et al., 2003 and Chapter 4) to directly determine concentrations of the Cl-TRIs in plasma during the time of the suppressed LH surge.

Do Cl-TRIs alter signaling pathways that regulate GnRH synthesis and release?

Several neuronal signaling pathways within the medial preoptic area (MPOA) are integrated by the GnRH neurons to produce species, sex and age dependent secretion patterns of GnRH release (Gore 2002; Herbison 1998; Fink 2000) (Figure 6.3). Many of the neurosecretory cells in this region project directly to the GnRH neurons (Gu and Simerly 1997) and regulate the GnRH induced LH surge. For example, lesioning of the AVPV, a critical nucleus within the POA, ablates the LH surge and induces persistent estrus (Wiegand et al., 1980). Therefore, possible reactive residues in receptors on specific neuronal populations within the AVPV that control the GnRH/LH surge response might be likely hypothalamic targets for Cl-TRI endocrine toxicity (Table 6.1)

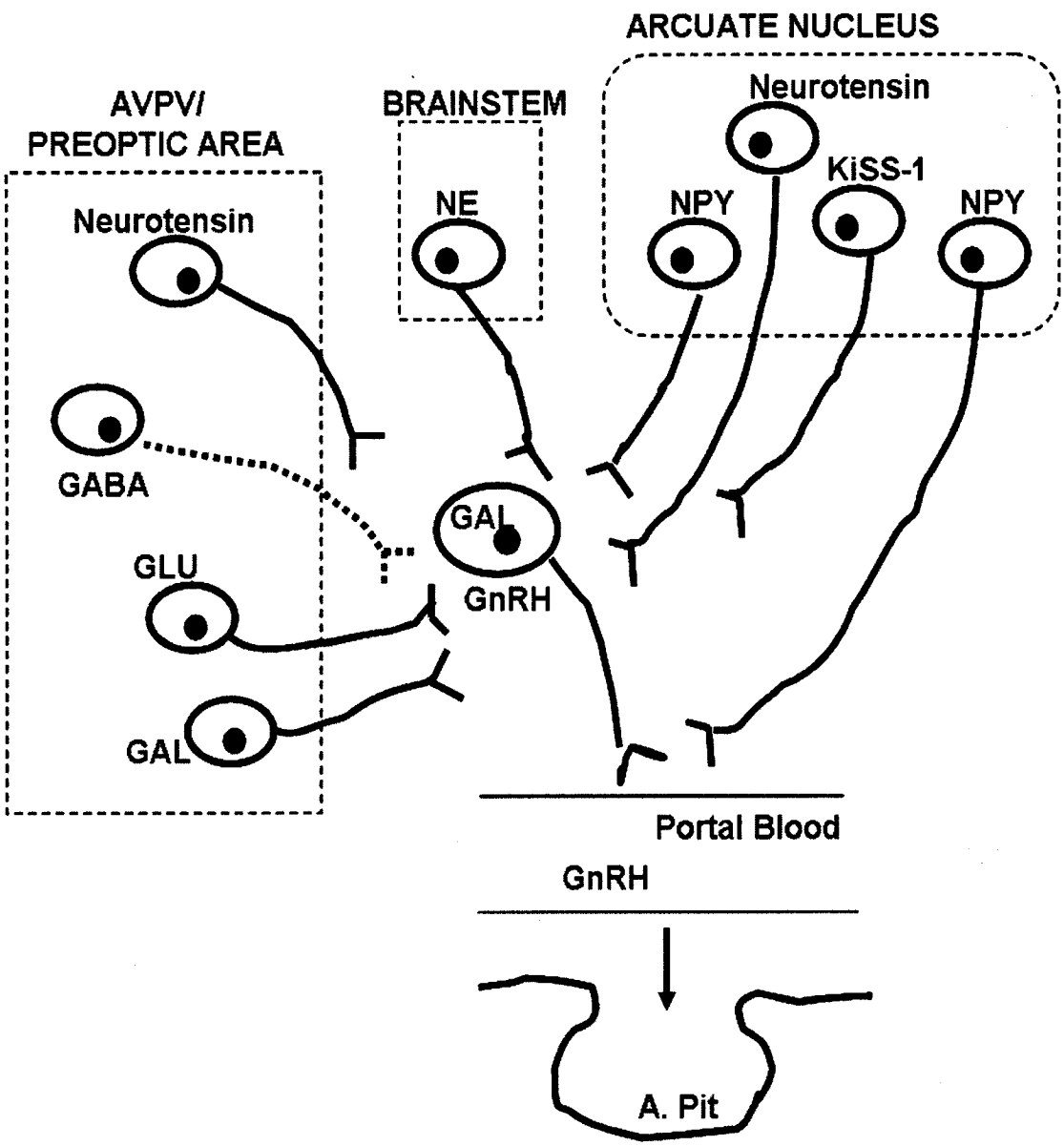

Figure 6.3. Many neuronal populations within the hypothalamus stimulate (solid line) and inhibit (dotted line) release of GnRH from GnRH neurons and modulate the LH surge. Some neuronal populations alter LH release by direct and indirect action on the anterior pituitary (a. pit.). These selected populations all regulate GnRH and LH by binding to their receptors and therefore, might be possible hypothalamic targets for Cl-TRIs. (See Gore, 2001 for an extensive list on all regulators of GnRH.)

Table 6.1. Some of the well characterized hypothalamic signals that regulate GnRH release via receptor binding and that are necessary for appropriate release of LH in rats

Neurotransmitter/ Amino acid	Receptor	Effect on GnRH/LH release	Reference
GABA	$GABA_A$	Inhibitory	Lamberts et al. (1983)
Neuropeptide Y	NPY	Stimulatory	Woller et al.(1991), Sahu et al. (1987), Xu et al. (2000); O'Connor et al. (1993)
Glutamate (GLU)	NMDA and non-NMDA	Stimulatory	Liaw J-J and Barrachlough (1993); Brann and Mahesh (1991); Lopez et al. (19990)
Kisspeptins (i.e. KISS-1)	GRP54	Stimulatory	Seminara and Kaiser (2005); Irwig (2004); Navarro et al. (2004)
Norepinephrine (NE)	α-adrenergic	Stimulatory[a]	Gallo and Drouva (1979)
Galanin (GAL)	GAL-R1/2	Stimulatory	Lopez et al. (1991)
Neurotensin (NT)		Stimulatory	Ferris et al. (1984); Akema et al. (1987)

[a] NE can inhibit LH release in the absence of estrogen (Pau and Spies, 1986)

6.2.3. Cl-TRIs might react with cysteinyl containing leukotrienes that mediate LH secretion

Previous *in vitro* and *in vivo* studies have indicated an ability of DACT to react with cysteinyl proteins such as hemoglobin to form inactive adducts (Prentiss, 2004 and G.Dooley unpublished data). Arachidonic acid (AA) and its cysteinyl containing lipoxygenase product leukotriene C_4 (LTC_4) have been implicated as second messengers in pituitary gonadotrope release of LH (see section 6.2.2.). A series of studies have also indicated that AA and LTC_4 are produced in the

hypothalamus and median eminence (Lindgren et al., 1984). In fact, one study examining LTC_4 and GnRH expression via immunohistochemical techniques indicated some co-localization of these two proteins, suggesting that LTC_4 protein is located in GnRH neurons (Hulting et al., 1985). Further research has demonstrated that AA and LTC_4 assist in the release of GnRH from GnRH neuroterminals (Gerozissis et al., 1991; Saadi et al., 1990) likely via activation by nitric oxide (NO) pathway (Rettori and McCann, 1998). Moreover, physiological concentrations of LTC_4 are capable of inducing a rapid release of LH from rat pituitary cells (Przylipiak et al., 1990; Keisel et al., 1987, 1991) and increasing gene transcription of LH in αT3-1 cell models (Ben-Menahem et al., 1994). LTC_4 antagonists decrease GnRH induced LH release in these *in vitro* models (Przylipiak et al., 1996), further suggesting that this cysteinyl leukotriene mediates GnRH action on LH secretion in addition to acting as a second messenger within the gonadotrope. Combined, these studies suggest that LTC_4 is a likely candidate for Cl-TRI targets of neuroendocrine toxicity. An initial in vitro experiment co-incubating LTC_4 and DACT for a period of time and determining adduct formation would provide insight into Cl-TRI reactivity with these cellular targets while in vivo studies to assess LTC_4 formation and relative concentrations of AA versus LTC_4 would assist in determining if Cl-TRIs are altering the enzymatic pathway by which this leukotriene is formed.

6.2.4. Cl-TRIs might produce anti-estrogenic responses by reacting with estrogen receptors other than nuclear ERα

Estrogen is the primary regulator of GnRH neuronal activity and is necessary for the GnRH/LH surge to occur (Herbison 1998; Legan et al., 1975; Moenter et al., 1990). Until recently, it was believed that estrogen regulated the HPG axis and other reproductive functions at the level of the brain and pituitary only by binding of estrogen to nuclear ERα. New research has found evidence for other nuclear and membrane receptors that bind estrogen within the hypothalamus and pituitary (Fig 6.4). In fact, many known exogenous estrogenic compounds, such as phytoestrogens and organochlorine pesticides, have now been shown to mimic estrogen mediated responses by other signaling mechanisms (Wozniak et al., 2005). Interestingly, these compounds have very weak affinities for ERα compared to estrogen yet can produce effects on estrogen regulated signaling pathways at extremely low concentrations (Wozniak et al., 2005). Our results did indicate an ability of ATRA to bind, although weakly, to ERα. However, ATRA did not alter binding of estrogen to nuclear ERα in the hypothalamus. Therefore, it would be valuable to establish if ATRA or DACT were able to bind more strongly with other forms of ER and hence, modify signaling mechanisms of estrogen apart from the classical genomic action of this steroid.

For many years it has been generally accepted that estrogen mediated effects on GnRH were via indirect mechanisms. This prevailing belief was due to the absence of detected ER- α co-localized with GnRH neurons (Herbison and Theodosis, 1992; Herbison et al., 1995; Lehman and Karsch, 1993). However, the discovery of another biologically active ER isoform, ER-β, has caused a rethinking of the mechanisms of action of estrogen (Kuiper et al., 1996; for review see Herbison and Pape, 2001). ER-β belongs to the superfamily of nuclear receptors and binds estrogen

with an affinity similar to ERα (Kuiper et al., 1996). ER-β is localized in GnRH neurons in rodents (Hrabovsky et al., 2001, Kallo et al., 2001; Sharifi et al., 2002; Butler and Coen, 1999), sheep (Skinner and Dufourny, 2005) and primates (Densmore and Urbanski, 2004). In addition to its presence in GnRH neurons, ERβ mRNA and protein are also expressed in cells residing in hypothalamic regions that regulate reproduction, such as the MPOA (Shughrue et al., 1996, 1999). Moreover, it has recently been demonstrated that estrogen and ER-β selective agonists stimulate expression of galanin (a potent stimulator of GnRH release) mRNA within GnRH neurons, suggesting that ER-β functionally mediates GnRH neuronal activity via estrogen (Merchenthaler et al., 2005). At this time, there is no information on the interactions between ER-β and these Cl-TRIs. Given that other compounds, such as phytoestrogens, have a much greater affinity for ERβ than ERα (Kuiper et al., 1998), investigations into the ability of Cl-TRIs to alter estrogen binding to ER-β would elucidate a possible novel role for the anti-estrogenicity of these compounds. However, the extent to which estrogen binding to ERβ regulates the GnRH/LH surges is still unclear.

Estrogen produces many rapid physiological and cellular effects within tissues that cannot be accounted for by the genomic actions of estrogen binding to ERα (Importa-Brears et al., 1999). Recent evidence indicates these rapid effects might be mediated by a non-genomic action of estrogen via receptors residing outside of the nucleus. Emerging data have identified the presence of functional plasma membrane estrogen receptors that can activate cell signaling pathways upon estrogen binding (Bjornstrom and Sjoberg, 2002; Hewitt et al., 2005; Wozniak et al., 2005) (for

reviews see Kelly and Levin 2001; Levin 2001). In fact, several estrogenic organochlorine pesticides induce rapid increases in intracellular signals in a rat prolactinoma cell line (GH3/B6/F10) expressing membrane bound ER.

In addition to membrane localized ERs, the discovery of a G-protein coupled receptor, GPR30, in several breast carcinoma cell lines (Carmeci et al., 1997) that can bind estrogen (Revankar et al., 2005) has further demonstrated that estrogen produces cellular responses through non-genomic mechanisms. GPR30 has been detected at different locations within *in vitro* cell lines depending on the cell type investigated. Thomas et al. (2005) detected GPR30 expression in the plasma membrane of breast carcinoma cell lines. In a study by Revankar et al. (2005), embryonic kidney cells that do not natively express nuclear ER of GPR30 were transfected with fluorescent labeled GPR30 and the localization of this receptor was examined. Results from this study indicated that GPR30 was localized in the endoplasmic reticulum rather than the plasma membrane. In addition, these authors demonstrated that estrogen mediated activation of this receptor mobilized intracellular Ca^{2+} similar to ER activation but GPR30 and ER likely regulated cell signaling responses through distinct pathways (Revankar et al., 2005). Although this receptor can bind estrogen, it should be noted that the affinity of GPR30 for estrogen is 6.6nM, approximately 50 fold less than that of ERα for estrogen (Revankar et al., 2005). While GPR30 holds potential for new pathways by which estrogen can exert its effects, the physiological relevance and detection of this protein within the body, or specifically within the regions of the brain responsible for LH release is yet to be determined. Despite the complexities of these estrogen mediated signal transduction pathways, a non-genomic

action of Cl-TRIs would be a novel way by these endocrine active compounds might cause anti-estrogenic effects in rodent models.

6.2.4 Summary: Assessing Mode of Action

Our original hypothesis regarding action of ATRA as a weak anti-estrogen by altering estrogen binding to ERα in the hypothalamus was not validated by our research. The complexity of the neuroendocrine pathways involved in regulating LH release made it difficult to determine unequivocally the exact mechanism by which Cl-TRIs alter neuroendocrine function. Independent of the specific target of toxicity, the underlying mechanism by which Cl-TRIs modulate these neuroendocrine signaling pathways is still uncertain. While many hypotheses were discussed in this section, immediate studies should be targeted at evaluating the reactivity of DACT with specific sites on proteins or peptides, rather than on interactions of these Cl-TRIs with specific neurotransmitter and other regulatory pathways. Our PBPK model descriptions of covalent reactivity of Cl-TRIs with cysteine containing hemoglobin and albumin and other recent studies verifying that DACT reacts with cysteine-125 on hemoglobin (Dooley G. and Tessari J., unpublished observations) suggests that cellular constituents containing cysteinyl residues are the most plausible targets of Cl-TRI action within the pituitary and/or brain (see Figure 6.1).

6.3. POTENTIAL NEUROENDOCRINE EFFECTS OF ATRAZINE IN FARM PRODUCTION ANIMALS

Conception rates in dairy and beef cattle (heifers) have dropped by at least 10% since the 1970's (Studer, 1998). Between 11-48% of dairy cows are diagnosed

as anovulatory at the start of breeding season (Rhodes et al., 2003), usually due to extended post-partum infertility (Garverick et al., 1993). Infertility in these animals is associated with inhibition of both tonic and surge release of GnRH from the hypothalamus and reduced LH or FSH secretion (Nett 1987). These reproductive effects are the main factors limiting production efficiency in cattle (Short 1990) and therefore, are primary economic concerns in the field of farm animal production.

Several environmental factors such as nutritional status and suckling time are known to alter LH levels in heifers (Steiner et al., 1983; Stillo, 1992; Richards et al., 1989). However, the potential for environmental contaminants to contribute to reduced fertility and altered estrous cyclicity has not been addressed. Corn grain is the primary nutritional supplement in the diet of a dairy cow (Dado 1999). The extensive application of ATRA on corn and the neuroendocrine effects observed in our rodent models and previous studies makes it plausible that ATRA could contribute to the reduced fertility observed in cattle. Although the work presented in this dissertation has primarily been targeted to assessing the risk of Cl-TRIs in humans, a similar exposure-dose-response paradigm can be applied to non-human species such as farm production animals.

Studies to determine concentrations of ATRA in food residues and the plasma levels of Cl-TRIs in these animals would be the first step needed to assess any possible associations between acyclicity and ATRA exposure. Methods employed in this dissertation, such as PBPK modeling, will be valuable tools to assess the relationship of Cl-TRI exposure to acyclic effects in these animals. Further elucidation of the mechanisms affecting Cl-TRI targets, such as the pituitary, will also

aid in determining if similar mechanisms exist in rodents and cattle to alter neuroendocrine function. Another interesting association between infertility in cattle and ATRA is the inability of exogenous administration of GnRH to effectively treat all cows (Short et al., 1990). This observation is consistent with our results that indicate a pituitary mode of action of Cl-TRIs.

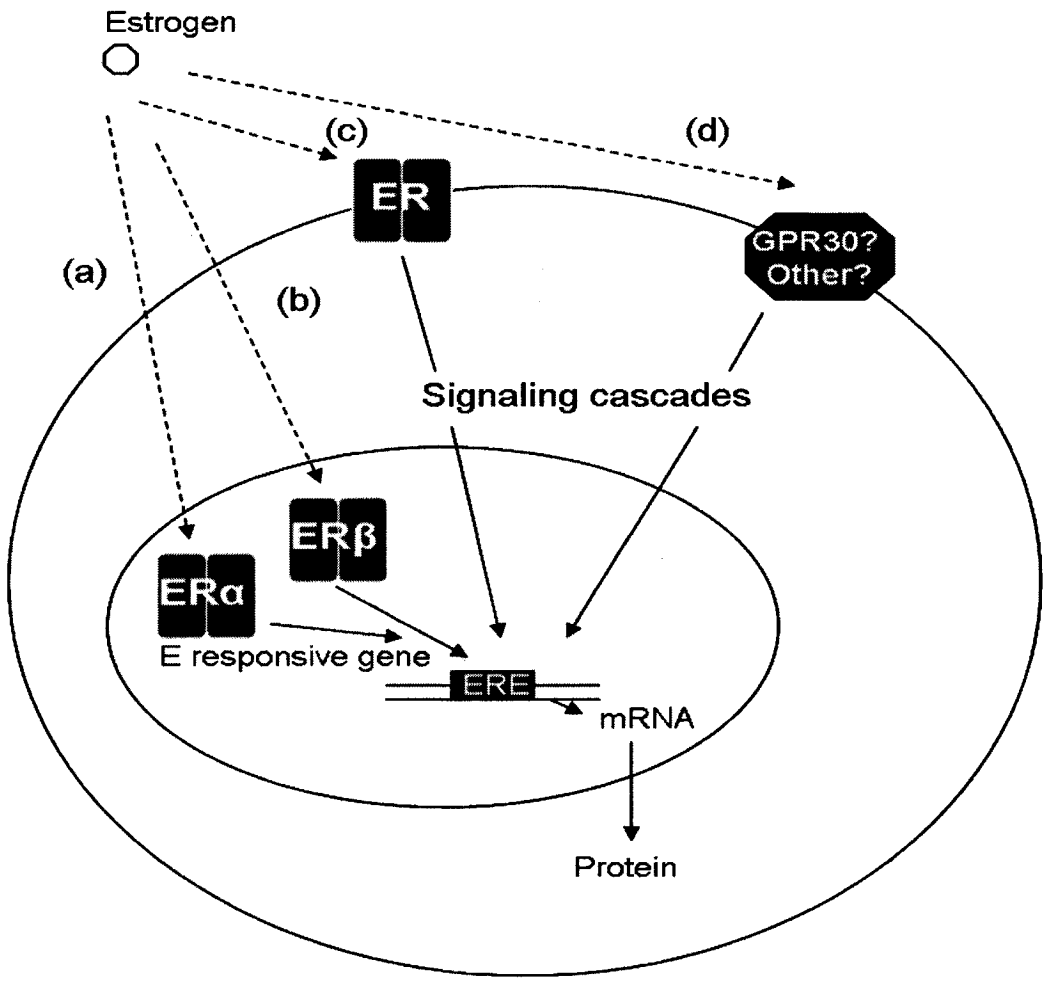

Figure 6.4. Recent evidence indicates other genomic and non-genomic actions of estrogen apart from the (a) "classical" pathway by which estrogen binds to nuclear receptor ERα to initiate transcriptional regulation of estrogen responsive genes. (b) Estrogen binds with high affinity to ERβ, another nuclear transcription factor, estrogen also mediates activation of several intracellular signaling cascades within the cell by binding to (c) membrane bound ERs and possibly (d) non-ER proteins. However, the in vivo consequences of these alternative estrogen receptors are still largely unknown.

6.4. CONCLUSIONS

These present studies have provided an initial framework for combining mode of action and kinetic data to quantitatively extrapolate Cl-TRI risk across species and dose while integrating both *in vitro* and *in vivo* studies of metabolism. The predominance of DACT in plasma and brain tissue after ATRA administration and the indication of neuroendocrine targets other than the hypothalamus represent important findings for extending our knowledge of ATRA toxicity in experimental animals. In conclusion, the most important areas of future research should be related to reactivity of DACT with cellular constituents within the pituitary, development of kinetic parameters for metabolism of ATRA and the Cl-TRI metabolites in human hepatocytes/liver microsomes, and experiments that will allow the extension of the current PBPK models to lower doses where ATRA is present in solution rather than in suspension.

REFERENCES

Ademola, J. L., Sedik LE, Wester RC, Maibach HLFile (1993). In Vitro Percutaneous Absorption and Metabolism in Man of 2-Chloro-4-Ethylamino-6-Isopropylamine-S-Triazine (Atrazine). *Arch Toxicol* **67**: 85-91.

Akema, T., Praputpittaya, C., and Kimura, F. (1987). Effects of preoptic microinjection of neurotensin on luteinizing hormone secretion in unanesthetized ovariectomized rats with or without estrogen priming. *Neuroendocrinology* **46**, 345-9.

Allison, A. C. (1960). Turnovers of erythrocytes and plasma proteins in mammals. *Nature(London)* **188**: 37-40.

Andersen, M. E., Thomas, O. E., Gargas, M. L., Jones, R. A. and Jenkins, L. J., Jr. (1980).The Significance of Multiple Detoxification Pathways for Reactive Metabolites in the Toxicity of 1,1-Dichloroethylene. *Toxicol Appl Pharmacol* **52**(3): 422-32.

Andersen, M. E. (1981). Saturable Metabolism and Its Relationship to Toxicity. *Crit Rev Toxicol* **9**: 105-150.

Andersen , M. E. (1981). Tissue Dosimetry in Risk Assessment, or What's the Problem Here Anyway? Drinking Water and Health, Pharmacokinetics in Risk Assessment. Washington D.C., National Acadamy Press. **8:** 8-23.

Andersen, M.E. and Clewell, H.J.,3rd. (1983). Pharmacokinetic Interactions of Mixtures. Proceedings of the 14th Annual Conference on Environmental Toxicology, Dayton, Ohio. AFAMRL-TR-83-099: 226-238

Andersen, M. E., Clewell, H. J., 3rd, Gargas, M. L., and Connolly, R. B. (1986). A physiologic pharmacokinetic model for hepatic glutatione (GSH) depletion by inhaled halogenated hydrocarbons. *Toxicologist* **6**:148.

Andersen, M. E., Clewell, H. J., 3rd, Gargas, M. L., Smith, F. A., and Reitz, R. H. F. (1987). Physiologically based pharmacokinetics and the risk assessment process for methylene chloride. *Toxicol Appl Pharmacol* **87**, 185-205.

Andersen, M. E., Clewell, H. J., 3rd, Gargas, M. L., Smith, F. A. and Reitz, R. H. (1987).Physiologically Based Pharmacokinetics and the Risk Assessment Process for Methylene Chloride. *Toxicol Appl Pharmacol* **87**(2): 185-205.

Andersen , M. E. (1995a). What do we mean by...dose? *Inhalation Toxicology* **7**, 909-915.

Andersen , M. E. (1995b). Physiologically based pharmacokinetic (PB-PK) models in the study of the disposition and biological effects of xenobiotics and drugs. *Toxicol Lett* **82-83**, 341-8.

Andersen , M. E. (1995c). Development of physiologically based pharmacokinetic and physiologically based pharmacodynamic models for applications in toxicology and risk assessment. *Toxicol Lett.* **79**, 35-44.

Andersen , M. E., Clewell, H. J. 3rd., and Frederick, C. B. (1995d). Applying simulation modeling to problems in toxicology and risk assessment--a short perspective. *Toxicol Appl Pharmacol.* **133**, 181-7.

Andersen , M. E., Clewell, H. J. 3rd, and Krishnan, K. (1995e). Tissue dosimetry, pharmacokinetic modeling, and interspecies scaling factors. *Risk Anal.* **15**, 533-7.

Andersen, M. E. and Dennison, J. (2001)..Mode of Action and Tissue Dosimetry in Current and Future Risk Assessments. *Sci. Total Environment* **274**(1-3): 3-14.

Andersson T.B, Sjoberg H, Hoffmann K.J, Boobis A.R, Watts P, Edwards R.J, Lake B.G., Price R.J., Renwick A.B., Gomez-Lechon M.J., Castell J.V., Ingelman-Sundberg M, Hidestrand M, Goldfarb P.S., Lewis D.F., Corcos L, Guillouzo A, Taavitsainen P, Pelkonen O. (2001). An assessment of human liver-derived in vitro systems to predict the in vivo metabolism and clearance of almokalant. *Drug Metab Dispos.* **29**(5):712-20.

Aschner, M. (2000).Neuron-Astrocyte Interactions: Implications for Cellular Energetics and Antioxidant Levels. *Neurotoxicology* **21**(6): 1101-7.

Ashby, J., Tinwell, H., Stevens, J., Pastoor, T. and Breckenridge, C. (2002).The Effects of Atrazine on the Sexual Maturation of Female Rats. *Regul Toxicol Pharmacol* **35**(3): 468.

Bakke, J., Robbins, J., and Feil, V. (1971). Metabolism of 2-methoxy-4-ethylamino-6-sec-butylamino-s-triazine. *J.Agr.Food Chem.* **19**: 462-466.

Bakke, J. E., Larson, J. D. and Price, C. E. (1972).Metabolism of Atrazine and 2-Hydroxyatrazine by the Rat. *J. Agr. Food Chem* **20**(3): 602-607.

Baker T.S., Rickert D.E. (1981). Dose-dependent uptake, distribution, and elimination of inhaled n-hexane in the Fischer-344 rat. *Toxicol Appl Pharmacol.* 61(3):414-22.

Barton, H. A. and Andersen, M. E. (1998).Endocrine Active Compounds: From Biology to Dose Response Assessment. *Crit Rev Toxicol* **28**(4): 363-423.

Bauer-Dantoin, A. C., Weiss, J., and Jameson, J. L. (1995). Roles of estrogen, progesterone, and gonadotropin-releasing hormone (GnRH) in the control of pituitary GnRH receptor gene expression at the time of the preovulatory gonadotropin surges. *Endocrinology* **136**, 1014-9.

Belchetz, P. E., Plant, T. M., Nakai, Y., Keogh, E. J., and Knobil, E. (1978). Hypophysial responses to continuous and intermittent delivery of hypopthalamic gonadotropin-releasing hormone. *Science* **202**, 631-3.

Ben Jonathan, N., Cooper, R. L., Foster, P., Hughes, C. L., Hoyer, P. B., Klotz, D., Kohn, M., Lamb, D. J. and Stancel, G. M. (1999). An Approach to the Development of Quantitative Models to Assess the Effects of Exposure to Environmentally Relevant Levels of Endocrine Disruptors on Homeostasis in Adults. *Environ.Health Perspect.* **107 Suppl 4**: 605-611.

Ben-Menahem, D., Shraga-Levine, Z., Limor, R., and Naor, Z. (1994). Arachidonic acid and lipoxygenase products stimulate gonadotropin alpha-subunit mRNA levels in pituitary alpha T3-1 cell line: role in gonadotropin releasing hormone action. *Biochemistry* **33**, 12795-9.

Berry M.N., Friend D.S. (1969). High-yield preparation of isolated rat liver parenchymal cells: a biochemical and fine structural study. *J Cell Biol.* 43(3):506-20.

Billings R.E., McMahon R.E., Ashmore J, Wagle S.R. (1997). The metabolism of drugs in isolated rat hepatocytes. A comparison with in vivo drug metabolism and drug metabolism in subcellular liver fractions. *Drug Metab Dispos.* 5(6):518-26.

Brown, R. P., Delp, M. D., Lindstedt, S. L., Rhomberg, L. R., and Beliles, R. P. (1997). Physiological parameter values for physiologically based pharmacokinetic models. *Toxicol. and Ind. Health* **13**: 407-484.

Breckenridge, C. B., Stevens, J. T., Simpkins, J. W., Eldridge, J. C., Tyrey, L., Sielken, R. L. J. and valdez-Flores, C. F. (2001).Mechanism Underlying the Occurence of Mammary Ademnocarcinomas and Fibroadenomas in Female Spregue - Dawley Rats Exposed to Atrazine: A Staistical Evaluation of Risk Factors. *The Toxicologist*

Brusick, D. J. (1994). An Assessment of the Genetic Toxicity of Atrazine: Relevance to Human Health and Environmental Effects. *Mutat.Res.* **317**(2): 133-144.

Brzezicki, J. M., Andersen, M. E., Cranmer, B. K. and Tessari, J. D. (2003).Quantitative Identification of Atrazine and Its Chlorinated Metabolites in Plasma. Journal of *Analytical Toxicology* **27**: 1-5.

Bulayeva, N. N., Wozniak, A. L., Lash, L. L., and Watson, C. S. (2005). Mechanisms of membrane estrogen receptor-alpha-mediated rapid stimulation of Ca2+ levels and prolactin release in a pituitary cell line. *Am J Physiol Endocrinol Metab* **288**, E388-97.

Carr, J. A., Gentles, A., Smith, E. E., Goleman, W. L., Urquidi, L. J., Thuett, K., Kendall, R. J., Giesy, J. P., Gross, T. S., Solomon, K. R., and Van Der Kraak, G. (2003). Response of larval Xenopus laevis to atrazine: assessment of growth, metamorphosis, and gonadal and laryngeal morphology. *Environ Toxicol Chem.* **22**, 396-405.

Carriere, V., Chambaz, J., and Rousset, M. (2001). Intestinal responses to xenobiotics. *Toxicol In Vitro.* **15**, 373-8.

Cassidy, M. K., and Houston, J. B. (1984). In vivo capacity of hepatic and extrahepatic enzymes to conjugate phenol. *Drug Metab Dispos.* **12**, 619-24.

Cavret, S., and Feidt, C. (2005). Intestinal metabolism of PAH: in vitro demonstration and study of its impact on PAH transfer through the intestinal epithelium. *Environ Res.* **98**, 22-32.

Chappell, P. E. and Levine, J. E. (2000).Stimulation of Gonadotropin-Releasing Hormone Surges by Estrogen. I. Role of Hypothalamic Progesterone Receptors. *Endocrinology* **141**(4): 1477-85.

Chen, C. W. and Blancato, J. N. (1987). Role of Pharmacokinetic Modeling in Risk Assessment:Perchloroethylene as an Example. Drinking Water and Health, Pharmacokinetics in Risk Assessment. Wahsington, D.C., National Academy Press. **8:** 369-390.

Chenery, R.J., Keogh, J.P., Rath, L.C., and McWilliams, P. (1991). *In vitro-in vivo* extrapolation of xenobiotic metabolism. Symposium: *In Vitro* Toxicology: Mechanisms and New Technology. p. 135-143.

Ching, M. (1982). Correlative surges of LHRH, LH and FSH in pituitary stalk plasma and systemic plasma of rat during proestrus. Effect of anesthetics. *Neuroendocrinology* **34**, 279-85.

Christensen, J. H., Andreasen, F., and Jensen, E. B. (1980). The binding of thiopental to serum proteins determined by ultrafiltration and equilibrium dialysis. *Acta Pharmacol. Toxicol. (Copenh)* **47**: 24-32.

Clayton, R. N. (1988). Mechanism of GnRH action in gonadotrophs. *Hum Reprod* **3**, 479-83.

Clewell, H. J., III and Andersen , M. E. (1985).Risk Assessment Extrapolations and Physioloigcal Modeling. *Toxicol Ind Health* **1**: 111-112.

Cole C.E., Tran H.T., Schlosser P.M. (2001). Physiologically based pharmacokinetic modeling of benzene metabolism in mice through extrapolation from *in vitro* to *in vivo*. *J Toxicol Environ Health A.* **62**(6):439-65.

Conn, P. M., and Crowley, W. F., Jr. (1991). Gonadotropin-releasing hormone and its analogues. *N Engl J Med* **324**, 93-103.

Connor, K., Howell , J., Chen, I., Liu, H. and Berhane, K. (1996).Failure of Chloro-S-Triazine-Derived Compounds to Induce Estrogen Receptor -Mediated Responses in Vivo and in Vitro. *Fundamental and Applied Toxicology* **30**: 93-101.

Coady, K., Murphy, M., Villeneuve, D., Hecker, M., Jones, P., Carr, J. A., Solomon, K. R., Smith, E., Van Der Kraak, G., Kendall, R., and Giesy, J. (2004). Effects of atrazine on metamorphosis, growth, and gonadal development in the green frog (Rana clamitans). *J Toxicol Environ Health A.* **67**, 941-57.

Cooper, R. L., Goldman, J. M. and Rehnberg, G. L. (1986).Neuroendocrine Control of Reproductive Function in the Aging Female Rodent. *Geriatric Bioscience* **34**: 735-751.

Cooper, R. L., Stoker, T. E., Goldman, J. M., Parrish, M. B., and Tyrey, L. (1996). Effect of atrazine on ovarian function in the rat. *Reprod. Toxicol.* **10**(4) : 257-264.

Cooper, R. L., Stoker, T. E., McElroy, W. K. and Hein, J. (1998).Atrazine (Atr) Disrupts Hypothalamic Catecholamines and Pituitary Function. *Toxicologist* **42**: 160.

Cooper, R. L., Stoker, T. E., Tyrey, L., Goldman, J. M., and McElroy, W. K. (2000). Atrazine disrupts the hypothalamic control of pituitary-ovarian function. *Toxicol.Sci.* **53** (2): 297-307.

Couse, J. F., and Korach, K. S. (1999). Estrogen receptor null mice: what have we learned and where will they lead us? *Endocr Rev* **20**, 358-417.

Crain, D., Guilette, L., Jr., Rooney, A. and Pickford, D. (1997).Alterations in Steroidogenesis in Alligators (Alligator Mississippiensis) Exposed Naturally and Experimentally to Environmental Contaminants. *Environ Health Perspect* **105**: 528-533.

Crain, A., Spiteri, D. and Guillette, L. (1999).The Functional and Structural Observations of the Neonatal Reproductive System of Alligators Exposed Inovo to Atrazine, 2,4 - D, or Estradiol. *Toxicology and Industrial Health* **15**: 180-185.

Cranmer, B. K., Brzezicki, J. M., Tessari, J. D., and Andersen, M. E. (2002). Quantitative identification of atrazine (ATRA) and diaminochlorotriazine (DACT) in rat whole blood utilizing GC/MS/SIM. *The Toxicologist* **66**:65.

Cummings, A. M., Rhodes, B. E. and Cooper, R. L.(2000).Effect of Atrazine on Implantation and Early Pregnancy in 4 Strains of Rats. *Toxicol.Sci.* **58**(1): 135-143.

Dado, R. G. (1999). Nutritional benefits of specialty corn grain hybrids in dairy diets. *J Anim Sci* **77 Suppl 2**, 197-207.

Dan-Cohen, H., Sofer, Y., Schwartzman, M. L., Natarajan, R. D., Nadler, J. L., and Naor, Z. (1992). Gonadotropin releasing hormone activates the lipoxygenase pathway in cultured pituitary cells: role in gonadotropin secretion and evidence for a novel autocrine/paracrine loop. *Biochemistry* **31**, 5442-8.

Das, P., McElroy, W. and Cooper, R.L (2001). Alteration of catecholamines in pheochromocytoma (Pc12) cells in vitro by the metabolites of chlorotriazine herbicide. *Toxicological Sciences* **59**: 127 - 137.

Das, P. C., McElroy, W. K. and Cooper, R. L. (2000). Differential modulation of catecholamines by chlorotriazine herbicides in pheochromocytoma (Pc12) cells in Vitro. *Toxicol.Sci.* **56**(2): 324-331.

Dauterman, W. and Mueke, W. (1973). In vitro metabolism of atrazine by rat liver. *Pesticide Biochemistry and Physiology* **4**: 212-219.

Dedrick, R. L. (1973).Animal scale-up. *Biopharm.* **1**: 435-461.

DeKanter, R., De Jager, M. H., Draaisma, A. L., Jurva, J. U., Olinga, P., Meijer, D. K., and Groothuis, G. M. (2002). Drug-metabolizing activity of human and rat liver, lung, kidney and intestine slices. *Xenobiotica.* **32**, 349-62.

DHHS. (1985). Risk Assessment and Risk Management of Toxic Substances: A Report to the Secretary, Department of Health and Human Services from the Executive Committee, DHHS Committe to Coordinate Environmental and Related Programs (CCERP), DHHS.

Densmore, V. S., and Urbanski, H. F. (2004). Effect of 17beta-estradiol on hypothalamic GnRH-II gene expression in the female rhesus macaque. *J Mol Endocrinol* **33**, 145-53.

Ding, X., and Kaminsky, L. S. (2003). Human extrahepatic cytochromes P450: function in xenobiotic metabolism and tissue-selective chemical toxicity in the respiratory and gastrointestinal. *Annu Rev Pharmacol Toxicol.* **43**, 149-73.

Doherty, M. M., and Pang, K. S. (2000). Route-dependent metabolism of morphine in the vascularly perfused rat small intestine preparation. *Pharm Res* **17**, 291-8.

Dringen, R., and Hirrlinger, J. (2003). Glutathione pathways in the brain. *Biol Chem* **384**, 505-16.

D'Souza, R. W. and Boxenbaum, H. (1988).Physiological pharmacokinetic models: some aspects of theory, practice and potential. *Toxicol Ind Health* **4**: 151-171.

D'Souza, R. W., Francis, W. R. and Andersen, M. E. (1988).Physiological model for tissue glutathione depletion and increased resynthesis after ethylene dichloride exposure. *J. Pharmacol. Exp. Ther.***245**(2): 563-568.

Duncan, J. A., Barkan, A., Herbon, L., and Marshall, J. C. (1986). Regulation of pituitary gonadotropin-releasing hormone (GnRH) receptors by pulsatile GnRH in female rats: effects of estradiol and prolactin. *Endocrinology* **118**, 320-7.

Eberhardt, I., Kiesel, L., Rosenberg, K., Klinga, K., and Runnebaum, B. (1991). Characterization of leukotriene C4 binding in anterior pituitary membrane preparations. *Prostaglandins* **41**, 185-99.

Eldridge, J., Tennant, M., Wetzel, L., Breckenridge, C. and Stevens, J. (1994a).Factors Affecting Mammary Tumor Incidence in Chlorotriazine-Treated Female Rats: Hormonal Properties, Dosage, and Animal Strain. *Environmental Health Perspectives* **102**(11): 36.

Eldridge, J., Fleenor - Heysor, D. G., Extrom, P. C., Wetzel, L. T., Breckenridge, C. B., Gillis, J. H., Luempert III, L. G., and Stevens, J. T. (1994b). Short - term effects of chlorotriazines on estrous in female Sprague-Dawley and Fischer 344 Rats. *J. Toxicol. Environ. Health* **43**: 155-167.

Eldridge, J. C., Wetzel, L. T., Stevens, J. T., and Simpkins, J. W. (1999a). The mammary tumor response in triazine-treated female rats: a threshold-mediated interaction with strain and species-specific reproductive senescence. *Steroids* **64** (9): 672-678.

Eldridge, J. C., Wetzel, L. T., and Tyrey, L. (1999b). Estrous cycle patterns of Sprague-Dawley rats during acute and chronic atrazine administration. *Reprod.Toxicol.* **13**(6): 491-499.

Eldridge, J.C., Minnema, D., Breckenridge, CB., McFarland, JE. and Stevens, JT. (2001). Effect of 6 months of atrazine or hydroxyatrazine on the leutinizing hormone surge in female Sprague - Dawley and Fischer 344 rats. *The Toxicologist*

Eyigor, O., and Jennes, L. (2000). Kainate receptor subunit-positive gonadotropin-releasing hormone neurons express c-Fos during the steroid-induced luteinizing hormone surge in the female rat. *Endocrinology* **141**, 779-86.

Ferris, C. F., Pan, J. X., Singer, E. A., Boyd, N. D., Carraway, R. E., and Leeman, S. E. (1984). Stimulation of luteinizing hormone release after stereotaxic microinjection of neurotensin into the medial preoptic area of rats. *Neuroendocrinology* **38**, 145-51.

Funk, C. D. (2001). Prostaglandins and leukotrienes: advances in eicosanoid biology. *Science* **294**, 1871-5.

Gallo, R. V., and Drouva, S. V. (1979). Effect of intraventricular infusion of catecholamines on luteinizing hormone release in ovariectomized and ovariectomized, steroid-primed rats. *Neuroendocrinology* **29**, 149-62.

Gan, L. S., Moseley, M. A., Khosla, B., Augustijns, P. F., Bradshaw, T. P., Haendren, R. W., and Thakker, D. R. (1996). CYP3A-like cytochrome P450-mediated metabolism and polarized efflux of cyclosporin A in Caco-2 cells. *Drug Metab Dispos* **24**, 344-9.

Gargas, M. L., Andersen, M. E., Teo, S. K., Batra, R., Fennell, T. R., and Kedderis, G. L. (1995). A physiologically based dosimetry description of acrylonitrile and cyanoethylene oxide in the rat. *Toxicol. Appl. Pharmacol.* **134** (2): 185-194.

Garverick, H. A., and Smith, M. F. (1993). Female reproductive physiology and endocrinology of cattle. *Vet Clin North Am Food Anim Pract* **9**, 223-47.

Gerozissis, K., Bommelaer-Bayet, M. C., Wisner, A., Saadi, M., Ramassamy, C., and Dray, F. (1991). Prostaglandin E2 and leukotriene C4-induced luteinizing hormone-releasing hormone release from immature and adult male rat median eminences in vitro: eicosanoid formation and binding parameters. *Prostaglandins* **41**, 345-57.

Gibaldi, M., Boyes, R. N., and Feldman, S. (1971). Influence of first-pass effect on availability of drugs on oral administration. *J Pharm Sci.* **60**, 1338-40.

Gojmerac, T. (1999).Reproductive Distrubance Casued by an S-Triazine Hebicide in Pigs. *Acta Veterinaria Hungarica* **47**(1): 129-135.

Gojmerac, T., Pleadin, J., Zuric, M. and Rajkovic-Janje, R. (2004).Serum Luteinizing Hormone Response to Administration of Gonadotropin-Releasing Hormone to Atrazine -Treated Gilts. *Vet Human Toxicol* **46**(5): 245-7.

Goodman, R. L. (1978). The site of the positive feedback action of estradiol in the rat. *Endocrinology* **102**, 151-9.

Goodman, R. L., and Knobil, E. (1981). The sites of action of ovarian steroids in the regulation of LH secretion. *Neuroendocrinology* **32**, 57-63.

Gore, A. C. and Roberts, J. L. (1997). Regulation of Gonadotropin-Releasing Hormone Gene Expression in Vivo and in Vitro. *Front Neuroendocrinol* **18**(2): 209-45.

Gore, A. C. (2001).Gonadotropin-Releasing Hormone Neurons, Nmda Receptors, and Their Regulation by Steroid Hormones across the Reproductive Life Cycle. Brain *Res Brain Res Rev* **37**(1-3): 235-48.

Gore, A. C. (2002). *GnRH: The master molecule of reproduction.* Kluwer Academic Publishers, Boston.

Graumann K, B. A., Jungbauer A. (1999).Monitoring of Estrogen Mimics by a Recombinant Yeast Assay:Synergy between Natural and Synthetic Compunds? *The Science of the Total Environment* **225**: 69-79.

Gu, G. B., and Simerly, R. B. (1997). Projections of the sexually dimorphic anteroventral periventricular nucleus in the female rat. *J Comp Neurol* **384**, 142-64.

Gysin, H. and Knuesli, E. (1960). Chemistry and Herbicidal Properties of Triazine Derivatives. Advances in Pest Control Research. R. Metcalf. New York, NY, Wiley (Interscience). **3:** 289-358.

Hagihara, K., Hirata, S., Osada, T., Hirai, M. and Kato, J. (1992).Distribution of Cells Containing Progesterone Receptor Mrna in the Female Rat Di- and Telencephalon: An in Situ Hybridization Study. *Brain Res Mol Brain Res* **14**(3): 239-49.

Hall, S. D., Thummel, K. E., Watkins, P. B., Lown, K. S., Benet, L. Z., Paine, M. F., and Mayo, R. R. (1999). Molecular and physical mechanisms of first-pass extraction. *Drug Metab Dispos.* **27**, 161-6.

Hamboeck , H., Fischer, W., Di Iorio, E. E., and Winterhalter, K. H. (1981). The binding of s-triazine metabolites to rodent hemoglobin appears irrelevant to other species. *Mol. Pharmacol.* **20**: 579-584.

Handa, R. J., Reid, D. L. and Resko, J. A. (1986).Androgen Receptors in Brain and Pituitary of Female Rats: Cyclic Changes and Comparisons with the Male. *Biol Reprod* **34**(2): 293-303.

Handa, R. J., Nunley, K. M. and Bollnow, M. R. (1993).Induction of c-Fos mRNA in the Brain and Anterior Pituitary Gland by a Novel Environment. *Neuroreport* **4**(9): 1079-82.

Hanioka N, Jinno H, Kitazawa K, Tanaka-Kagawa T, Nishimura T, Ando M, Ogawa K. (1998). In vitro biotransformation of atrazine by rat liver microsomal cytochrome P450 enzymes. *Chem Biol Interact.* **116**(3):181-98.

Hanoika, N., Jinno, H., Tanaka - Kagawa, T., Nishimura, T. and Ando, M. (1999a). In vitro metabolism of simazine, atrazine and propazine by hepatic cytochrome P450 enzymes of rat, mouse and guinea pig, and oestrogenic activity of chlorotriazines and their main metabolites. *Xenobiotica* **29**(12): 1213-1226.

Hanoika, N., Jinno, H., Tanaka-Kagawa, T., Nishimura, T. and Ando, M. (1999b). In Vitro Metabolism of Chlorotriazines:Chracterization of Simazine, Atrazine, and Propazine Metabolism Using Liver Microsomes from Rats Treated with Various Cytochrome P450 Inducers. *Toxicol Appl Pharmacol* **156**: 195-205.

Hatfield -Berube, A. (2004). An Investigation of Atrazine metabolism in rat hepatocytes. In Department of Environmental and Radiological Health Sciences, p. 60. CSU, Fort Collins.

Hayes, T. B., Collins, A., Lee, M., Mendoza, M., Noriega, N., Stuart, A. A. and Vonk, A. F. (2002). Hermaphroditic, Demasculinized Frogs after Exposure to the Herbicide Atrazine at Low Ecologically Relevant Doses. *Proc Natl Acad Sci U S A* **99**(8): 5476-80.

Hayes, T., Haston, K., Tsui, M., Hoang, A., Haeffele, C., and Vonk, A. (2003). Atrazine-induced hermaphroditism at 0.1 ppb in American leopard frogs (Rana pipiens): laboratory and field evidence. *Environ Health Perspect.* **111**, 568-75.

Hays, S. M., Elswick, B. A., Blumenthal, G. M., Welsch, F., Conolly, R. B., and Gargas, M. L. (2000). Development of a physiologically based pharmacokinetic model of 2-methoxyethanol and 2-methoxyacetic acid disposition in pregnant rats. *Toxicol. Appl. Pharmacol.* **163**: 67-74.

Herbison, A. E. (1997).Noradrenergic Regulation of Cyclic Gnrh Secretion. *Rev Reprod* **2**(1): 1-6.

Herbison, A. E. (1998).Multimodal Influence of Estrogen Upon Gonadotropin-Releasing Hormone Neurons. *Endocr Rev* **19**(3): 302-30.

Herbison, A. E., and Pape, J. R. (2001). New evidence for estrogen receptors in gonadotropin-releasing hormone neurons. *Front Neuroendocrinol* **22**, 292-308.

Hewitt, S. C., and Korach, K. S. (2003). Oestrogen receptor knockout mice: roles for oestrogen receptors alpha and beta in reproductive tissues. *Reproduction* **125**, 143-9.

Hewitt, S. C., Deroo, B. J., and Korach, K. S. (2005). Signal transduction. A new mediator for an old hormone? *Science* **307**, 1572-3.

Hines, C. J., Deddens, J. A., Tucker, S. P. and Horung, R. W. (2001).Distribution and Determinants of Pre-Emergent Herbicide Expsorues among Custom Applicators. *Ann Occup Hyg* **45**(3): 227-239.

Hoffman, G. E., Lee, W. S., Attardi, B., Yann, V., and Fitzsimmons, M. D. (1990). Luteinizing hormone-releasing hormone neurons express c-fos antigen after steroid activation. *Endocrinology* **126**, 1736-41.

Hoffman, G. E., Smith, M. S., and Verbalis, J. G. (1993). c-Fos and related immediate early gene products as markers of activity in neuroendocrine systems. *Front Neuroendocrinol* **14**, 173-213.

Hoffman, G. E., and Lyo, D. (2002). Anatomical markers of activity in neuroendocrine systems: are we all 'fos-ed out'? *J Neuroendocrinol* **14**, 259-68.

Hrabovszky, E., Shughrue, P. J., Merchenthaler, I., Hajszan, T., Carpenter, C. D., Liposits, Z., and Petersen, S. L. (2000). Detection of estrogen receptor-beta messenger ribonucleic acid and 125I-estrogen binding sites in luteinizing hormone-releasing hormone neurons of the rat brain. *Endocrinology* **141**, 3506-3509.

Hrabovszky, E., Steinhauser, A., Barabas, K., Shughrue, P. J., Petersen, S. L., Merchenthaler, I., and Liposits, Z. (2001). Estrogen receptor-beta immunoreactivity in luteinizing hormone-releasing hormone neurons of the rat brain. *Endocrinology* **142**, 3261-4.

Hulting, A. L., Lindgren, J. A., Hokfelt, T., Eneroth, P., Werner, S., Patrono, C., and Samuelsson, B. (1985). Leukotriene C4 as a mediator of luteinizing hormone release from rat anterior pituitary cells. *Proc Natl Acad Sci U S A.* **82**, 3834-8.

Ikonen, R., Kangas, J. and Savolainen, H. (1988).Urinary Atrazine Metabolites as Indicators for Rats and Human Exposure to Atrazaine. *Toxicol Lett* **44**: 109-112.

ILSI (2001). *Developing Straegies for Agricultural Chemical Safety Evaluation.* Washington, DC, ILSI Health and Environmental Sciences Institute **pp.**1-52.

Improta-Brears, T., Whorton, A. R., Codazzi, F., York, J. D., Meyer, T., and McDonnell, D. P. (1999). Estrogen-induced activation of mitogen-activated protein kinase requires mobilization of intracellular calcium. *Proc Natl Acad Sci U S A* **96**, 4686-91.

Infurna, R., Levy, B., Meng, C., Yau, E., Traina, V., Rolofson, G., Stevens, J. and Bernett, J. (1988).Teratological Evaluations of Atrazine Technical, a Triazine Herbicide, in Rats and Rabbits. *J Toxicol Environ Health* **24**(3): 307-319.

Irwig, M. S., Fraley, G. S., Smith, J. T., Acohido, B. V., Popa, S. M., Cunningham, M. J., Gottsch, M. L., Clifton, D. K., and Steiner, R. A. (2004). Kisspeptin activation of gonadotropin releasing hormone neurons and regulation of KiSS-1 mRNA in the male rat. *Neuroendocrinology* **80**, 264-72.

Jimenez-Linan, M., and Rubin, B. S. (2001). Dynamic changes in luteinizing hormone releasing hormone transcriptional activity are associated with the steroid-induced LH surge. *Brain Res* **922**, 71-9.

Jongen, M. J. and Norman, A. W. (1987).A Simplified Cannulation Procedure for Pharmacokinetic Experiments in Rats. *J Pharmacol Methods* **17**(3): 271-5.

Kaiser, U. B., Jakubowiak, A., Steinberger, A., and Chin, W. W. (1997). Differential effects of gonadotropin-releasing hormone (GnRH) pulse frequency on gonadotropin subunit and GnRH receptor messenger ribonucleic acid levels in vitro. *Endocrinology* **138**, 1224-31.

Kalra, S. P. and Kalra, P. S. (1983).Neural Regulation of Luteinizing Hormone Secretion in the Rat. *Endocr.Rev.* **4**(4): 311-351.

Kalra, S. P. (1993).Mandatory Neuropeptide-Steroid Signaling for the Preovulatory Luteinizing Hormone-Releasing Hormone Discharge. *Endocr Rev* **14**(5): 507-38.

Kaminsky, L. S. and Zhang, Q. (2003). The small intestine as a xenobiotic-metabolizing organ. *Drug Metab Dispos* **31**, 1520-5.

Karsch, F. J., Bowen, J. M., Caraty, A., Evans, N. P., and Moenter, S. M. (1997). Gonadotropin-releasing hormone requirements for ovulation. *Biol Reprod* **56**, 303-9.

Kedderis G.L, Carfagna M.A., Held S.D., Batra R, Murphy J.E., Gargas M.L. (1993). Kinetic analysis of furan biotransformation by F-344 rats in vivo and in vitro. *Toxicol Appl Pharmacol.* **123**(2):274-82.

Kedderis G.L, Held S.D. (1996). Prediction of furan pharmacokinetics from hepatocyte studies: comparison of bioactivation and hepatic dosimetry in rats, mice, and humans. *Toxicol Appl Pharmacol.* **140**(1):124-30.

Kedderis, G. L., and Lipscomb, J. C. (2001). Application of in vitro biotransformation data and pharmacokinetic modeling to risk assessment. *Toxicol. and Indust. Health* **17**, 315-321.

Kelly, M. J., and Levin, E. R. (2001). Rapid actions of plasma membrane estrogen receptors. *Trends Endocrinol Metab* **12**, 152-6.

Kiesel, L., Przylipiak, A. F., Habenicht, A. J., Przylipiak, M. S., and Runnebaum, B. (1991). Production of leukotrienes in gonadotropin-releasing hormone-stimulated pituitary cells: potential role in luteinizing hormone release. *Proc Natl Acad Sci U S A* **88**, 8801-5.

Kniewald, J., Jakominic, M., Tomljenovic, A., Simic, B., Romac, P., Vranesic, D. and Kniewald, Z. (2000).Disorders of Male Rat Reproductive Tract under the Influence of Atrazine. *J.Appl.Toxicol.* **20**(1): 61-68.

Kniewald, J., Milder, P. and Kniewald, Z. (1979).Effects of S-Triazine Herbicides on Hormone-Receptor Complex Formation, 5a-Reductase and 3a-Hydroxysteroid Dehydrogenase. *J Steroid Biochem* **11**: 833-838.

Kniewald, J., Peruzovic, M., Gomerjic, T., Milkovic, K. and Kniewald, Z. (1987).Indirect Influence of S-Triazines on Rat Gonadotropic Mechanism at Early Postnatal Period. *J Steriod Biochem* **27**(4-6): 1095-1100.

Kramer, E., and Routh, J. I. (1973). The binding of salicylic acid and acetylsalicylic acid to human serum albumin. *Clin. Biochem.* **6**(2): 98-105.

Kraus, S., Naor, Z., and Seger, R. (2001). Intracellular signaling pathways mediated by the gonadotropin-releasing hormone (GnRH) receptor. *Arch Med Res* **32**, 499-509.

Krege, J. H., Hodgin, J. B., Couse, J. F., Enmark, E., Warner, M., Mahler, J. F., Sar, M., Korach, K. S., Gustafsson, J. A., and Smithies, O. (1998). Generation and reproductive phenotypes of mice lacking estrogen receptor beta. *Proc Natl Acad Sci U S A* **95**, 15677-82.

Kuiper, G. G., Enmark, E., Pelto-Huikko, M., Nilsson, S., and Gustafsson, J. A. (1996). Cloning of a novel receptor expressed in rat prostate and ovary. *Proc Natl Acad Sci U S A* **93**, 5925-30.

Kuiper, G. G., Lemmen, J. G., Carlsson, B., Corton, J. C., Safe, S. H., van der Saag, P. T., van der Burg, B., and Gustafsson, J. A. (1998). Interaction of estrogenic chemicals and phytoestrogens with estrogen receptor beta. *Endocrinology* **139**, 4252-63.

Lang D, Criegee D, Grothusen A, Saalfranck R.W, Bocker R.H. (1996). In vitro metabolism of atrazine, terbuthylazine, ametryne, and terbutryne in rats, pigs, and humans. *Drug Metab Dispos.* **24**(8):859-65.

Lavgeveld, C. H., Schepens, E., Jongenelen, C. A., Stoof, J. C., Hjelle, O. P., Ottersen, O. P. and Drukarch, B. (1996).Presence of Glutathione

Immunoreactivity in Cultured Neurones and Astrocytes. *Neuroreport.* **7**(11): 1833-6.

Laws, S. C., Ferrell, J. M., Stoker, T. E., Schmid, J. and Cooper, R. L. (2000).The Effects of Atrazine on Female Wistar Rats: An Evaluation of the Protocol for Assessing Pubertal Development and Thyroid Function. *Toxicol.Sci.* **58**(2): 366-376.

Lee, W. S., Smith, M. S. and Hoffman, G. E. (1990). Progesterone Enhances the Surge of Luteinizing Hormone by Increasing the Activation of Luteinizing Hormone-Releasing Hormone Neurons. *Endocrinology* **127**(5): 2604-6.

Legan, S. J., Coon, G. A. and Karsch, F. J. (1975). Role of Estrogen as Initiator of Daily LH Surges in the Ovariectomized Rat. *Endocrinology* **96**(1): 50-6.

Legan, S. J., and Tsai, H. W. (2003). Oestrogen receptor-alpha and -beta immunoreactivity in gonadotropin-releasing hormone neurones after ovariectomy and chronic exposure to oestradiol. *J Neuroendocrinol* **15**, 1164-70.

Leung, H. (1991).Development and Utilization of Physiologically Based Pharmcokinetic Models for Toxicological Applications. *Journal of Toxicology and Environmental Health* **32**: 247-267.

Levin, E. R. (2001). Cell localization, physiology, and nongenomic actions of estrogen receptors. *J Appl Physiol* **91**, 1860-7.

Levine, J. E., Bauer-Dantoin, A. C., Besecke, L. M., Conaghan, L. A., Legan, S. J., Meredith, J. M., Strobl, F. J., Urban, J. H., Vogelsong, K. M. and Wolfe, A. M. (1991).Neuroendocrine Regulation of the Luteinizing Hormone-Releasing Hormone Pulse Generator in the Rat. *Recent Prog Horm Res* **47**: 97-151; discussion 151-3.

Levine, J. E. and Ramirez, V. D. (1982).Luteinizing Hormone-Releasing Hormone Release During the Rat Estrous Cycle and after Ovariectomy, as Estimated with Push-Pull Cannulae. *Endocrinology* **111**(5): 1439-48.

Levine, J. E. (1997). New concepts of the neuroendocrine regulation of gonadotropin surges in rats. *Biol Reprod* **56**, 293-302.

Lilly, P. D., Andersen, M. E., Ross, T. M. and Pegram, R. A. (1998).A Physiologically Based Pharmacokinetic Description of the Oral Uptake, Tissue Dosimetry, and Rates of Metabolism of Bromodichloromethane in the Male Rat. *Toxicol Appl Pharmacol* **150**(2): 205-17.

Lin, J. H., Sugiyama, Y., Awazu, S. and Hanano, M. (1982).Physiological Pharmacokinetics of Ethyoxybenzamide Based on Biochemical Data Obtained

in Vitro as Wall as on Physiological Data. *J. Pharmacokin. Biopharm.* **10**: 649-661.

Lindgren, J. A., Hokfelt, T., Dahlen, S. E., Patrono, C., and Samuelsson, B. (1984). Leukotrienes in the rat central nervous system. *Proc Natl Acad Sci U S A* **81**, 6212-6.

Lopez, F. J., Merchenthaler, I., Ching, M., Wisniewski, M. G., and Negro-Vilar, A. (1991). Galanin: a hypothalamic-hypophysiotropic hormone modulating reproductive functions. *Proc Natl Acad Sci U S A* **88**, 4508-12.

Lu, K. H., and Yen, S. S. (1980). The effect of an antiserum to luteinizing hormone-releasing hormone on the progesterone-induced luteinizing hormone surge in ovariectomized,estrogen-primed rats. *Endocrinology* **106**, 867-70.

Martins - Afferri, M. P., Ferreira-Silva, I. A., Franci, C. R., and Anselmo-Franci, J. A. (2003). LHRH release depends on Locus Coeruleus noradrenergic inputs to the medial preoptic area and median eminence. *Brain Res Bull* **61**, 521-7.

McCann, S. M., Karanth, S., Mastronardi, C. A., Dees, W. L., Childs, G., Miller, B., Sower, S. and Yu, W. H. (2001). Control of Gonadotropin Secretion by Follicle-Stimulating Hormone-Releasing Factor, Luteinizing Hormone-Releasing Hormone, and Leptin. *Arch Med Res* **32**(6): 476-85.

McMullin, T. S., Brzezicki, J. M., Cranmer, B. K., Tessari, J. D. and Andersen, M. E. (2003). Pharmacokinetic modeling of disposition and time-course studies with [^{14}C]atrazine. *J Toxicol Environ Health A.* **66**(10): 941-64.

McMullin, T.S., Andersen M.E, Nagahara A, Lund T.D, Pak T, Handa R.J, Hanneman W.H. (2004.) Evidence that atrazine and diaminochlorotriazine inhibit the estrogen/progesterone induced surge of LH in female Sprague-Dawley rats without changing estrogen receptor action. *Toxicol Sci.* **79**(2):278-86.

Meli, G., Bagnati, R., Fanelli, R., Benfenati, E. and Airoldi, L. (1992).Metabolic Profile of Atrazine and N-Nitrosoatrazine in Rat Urine. *Bull Environ Contam Toxicol* **48**(5): 701-8.

Mellon, P. L., Windle, J. J., Goldsmith, P. C., Padula, C. A., Roberts, J. L., and Weiner, R. I. (1990). Immortalization of hypothalamic GnRH neurons by genetically targeted tumorigenesis. *Neuron* **5**, 1-10.

Merchenthaler, I., Hoffman, G. E., and Lane, M. V. (2005a). Estrogen and estrogen receptor-{beta} (ER{beta})-selective ligands induce galanin expression within gonadotropin hormone-releasing hormone-immunoreactive neurons in the female rat brain. *Endocrinology* **146**, 2760-5.

Merchenthaler, I. (2005b). Estrogen stimulates galanin expression within luteinizing hormone-releasing hormone-immunoreactive (LHRH-i) neurons via estrogen receptor-beta (ERbeta) in the female rat brain. *Neuropeptides*.

Millar, R. P., Lu, Z. L., Pawson, A. J., Flanagan, C. A., Morgan, K., and Maudsley, S. R. (2004). Gonadotropin-releasing hormone receptors. *Endocr Rev* **25**, 235-75.

Miles, J. B. and Orr, G. R. (1987). Characterization and Identification of Atrazine Metabolites from Rat Urine. Greensboro, NC, Ciba - Geigy Corporation: 1-32.

Moenter, S. M., DeFazio, R. A., Pitts, G. R., and Nunemaker, C. S. (2003). Mechanisms underlying episodic gonadotropin-releasing hormone secretion. *Front Neuroendocrinol* **24**, 79-93.

Naor, Z. (1991). Is arachidonic acid a second messenger in signal transduction? *Mol Cell Endocrinol* **80**, C181-6.

Naor, Z., Shacham, S., Harris, D., Seger, R., and Reiss, N. (1995). Signal transduction of the gonadotropin releasing hormone (GnRH) receptor: cross-talk of calcium, protein kinase C (PKC), and arachidonic acid. *Cell Mol Neurobiol* **15**, 527-44.

Naor, Z., Harris, D., and Shacham, S. (1998). Mechanism of GnRH receptor signaling: combinatorial cross-talk of Ca2+ and protein kinase C. *Front Neuroendocrinol* **19**, 1-19.

Navarro, V. M., Fernandez-Fernandez, R., Castellano, J. M., Roa, J., Mayen, A., Barreiro, M. L., Gaytan, F., Aguilar, E., Pinilla, L., Dieguez, C., and Tena-Sempere, M. (2004). Advanced vaginal opening and precocious activation of the reproductive axis by KiSS-1 peptide, the endogenous ligand of GPR54. *J Physiol* **561**, 379-86.

Nett, T. M. (1987). Function of the hypothalamic-hypophysial axis during the post-partum period in ewes and cows. *J Reprod Fertil Suppl* **34**, 201-13.

Newton, J. F., Hoefle, D., Gemborys, M. W., Mudge, G. H., and Hook, J. B. 1986. Metabolism and excretion of a glutathione conjugate of acetaminophen in the isolated perfused rat kidney. *J. Pharmacol. Exp. Ther.* 237(2): 519-524.

Nguyen, H. T. (1999). Transport Proteins. The Clinical Chemistry of Laboratory Animals. W. F. Loeb and F. W. Quimby. Philidelphia, Taylor and Francis: 309-311.

NRC. (1983). The Nature of Risk Assessment. Risk Assessment in the Federal Government: Managing the Process. Wahington D.D., National Acadamy Press: 17-50.

Oh, S., Shim, S. and Chung, K. (2003).Antiestrogenic Action of Atrazine and Its Major Metabolites in Vitro. *Journal of Health Science* **49**(1): 65-71.

Orr, G. R., Simoneaux, B. J. and Davidson, I. W.(1987). Disposition of Atrazine in the Rat: 1-51.

Pak, T. R., Lynch, G. R. and Tsai, P. S. (2001).Testosterone and Estrogen Act Via Different Pathways to Inhibit Puberty in the Male Siberian Hamster (Phodopus Sungorus). *Endocrinology* **142**(8): 3309-16.

Pang, K. S., Yuen, V., Fayz, S., te Koppele, J. M., and Mulder, G. J. (1986). Absorption and metabolism of acetaminophen by the in situ perfused rat small intestine preparation. *Drug Metab Dispos* **14**, 102-111.

Parquet, M., Metman, E. H., Raizman, A., Rambaud, J. C., Berthaux, N., and Infante, R. (1985). Bioavailability, gastrointestinal transit, solubilization and faecal excretion of ursodeoxycholic acid in man. *Eur. J. Clin. Invest.* **15**, 171-8.

Peruzovic, M., Kniewald, J., Capkun, V. and Milkovic, K. (1995).Effect of Atrazine Ingested Prior to Mating on Rat Females and Their Offspring. *Acta Physiol Hung.* **83**(1): 79-89.

Peters, J. W. and Cook, R. M. (1973).Effects of Atrazine on Reproduction in Rats. *Bulletin of Environmental Contamination and Toxicology* **9**(5): 304.

Petersen, S. L., McCrone, S., Keller, M., and Shores, S. (1995). Effects of estrogen and progesterone on luteinizing hormone-releasing hormone messenger ribonucleic acid levels: consideration of temporal and neuroanatomical variables. *Endocrinology* **136**, 3604-10.

Petersen, S. L., Gardner, E., Adelman, J., McCrone, S., Porkka-Heiskanen, T., Urban, J. H., Turek, F. W., and Levine, J. E. (1996). Examination of steroid-induced changes in LHRH gene transcription using 33P-and 35S-labeled probes specific for intron 2 Gene expression in a subpopulation of luteinizing hormone-releasing hormone (LHRH) neurons prior to the preovulatory gonadotropin surge. *Endocrinology* **137**, 234-9.

Petersen, S. L., Ottem, E. N., and Carpenter, C. D. (2003). Direct and indirect regulation of gonadotropin-releasing hormone neurons by estradiol. *Biol Reprod* **69**, 1771-8.

Pfaff, D. W. and Keiner, M. (1973). Atlas of Estradiol-Concentrating Cells in the Central Nervous System of the Female Rat. *J Comp Neurol* **151**: 121-158.

Phillips, D. H., and Farmer, P. B. (1994). Evidence for DNA and protein binding by styrene and styrene oxide. *Crit. Rev. Toxicol.* **24 Suppl:** S35-46.

Porkka-Heiskanen, T., Urban, J. H., Turek, F. W., and Levine, J. E. (1994). Gene expression in a subpopulation of luteinizing hormone-releasing hormone (LHRH) neurons prior to the preovulatory gonadotropin surge. *J Neurosci* **14**, 5548-58.

Prentiss, P. L. (2004). Hemoglobin adducts as biomarkers of exposure to chlorotriazines. In Department of Environmental and Radiologial Health Sciences, p. 78. CSU, Fort Collins.

Przylipiak, A., Kiesel, L., Przylipiak, M., and Runnebaum, B. (1990). Differences in luteinizing hormone release stimulated in rat anterior pituitary cells by leukotriene C4 and by gonadotropin-releasing hormone in vitro. *Experientia* **46**, 298-300.

Ramsey, J. C., and Andersen, M. E. (1984). A physiologically based description of the inhalation pharmacokinetics of styrene in rats and humans. *Toxicol. Appl. Pharmacol.* **73**: 159-175.

Rappaport, S. M., Ting, D., Jin, Z., Yeowell-O'Connell, K., Waidyanatha, S., and McDonald, T. (1993). Application of Raney nickel to measure adducts of styrene oxide with hemoglobin and albumin. *Chem. Res. Toxicol.* **6**(2): 238-244.

Rappaport, S. M., and Yeowell-O'Connell, K. (1999). Protein adducts as dosimeters of human exposure to styrene, styrene-7,8-oxide, and benzene. *Toxicol. Lett.* **108** (2-3): 117-126.

Rayner, J. L., Wood, C. and Fenton, S. E. (2004). Exposure Parameters Necessary for Delayed Puberty and Mammary Gland Development in Long-Evans Rats Expsoed in Utero to Atrazine. *Toxicol Appl Pharmacol* **195**: 23-34.

Razandi, M., Pedram, A., Merchenthaler, I., Greene, G. L., and Levin, E. R. (2004). Plasma membrane estrogen receptors exist and functions as dimers. *Mol Endocrinol* **18**, 2854-65.

Reitz, R., McDougal, J., Himmelstein, M., RJ, N. and Schumann, A. (1988).Physiologically Based Pharmacokinetic Modeling with Methylchloroform: Implications for Interspecies, High Dose/Low Dose and Dose Route Extrapolations. *Toxicol Appl Pharmacol* **95**: 185-199.

Reitz, R. H., McCroskey, P. S., Park, C. N., Andersen, M. E., and Gargas, M. L. (1990). Development of a physiologically based pharmacokinetic model for risk assessment with 1,4-dioxane. *Toxicol. Appl. Pharmacol.* **105**: 37-54.

Rettori, V., and McCann, S. M. (1998). Role of nitric oxide and alcohol on gonadotropin release in vitro and in vivo. *Ann N Y Acad Sci* **840**, 185-93.

Revankar, C. M., Cimino, D. F., Sklar, L. A., Arterburn, J. B., and Prossnitz, E. R. (2005). A transmembrane intracellular estrogen receptor mediates rapid cell signaling. *Science* **307**, 1625-30.

Rhodes, F. M., McDougall, S., Burke, C. R., Verkerk, G. A., and Macmillan, K. L. (2003). Invited review: Treatment of cows with an extended postpartum anestrous interval. *J Dairy Sci* **86**, 1876-94.

Richards, M. W., Wettemann, R. P., and Schoenemann, H. M. (1989). Nutritional anestrus in beef cows: concentrations of glucose and nonesterified fatty acids in plasma and insulin in serum. *J Anim Sci* **67**, 2354-62.

Roberge, M., Hakk, H. and Larsen, G. (2004).Atrazine Is a Competitive Inhibitor of Phosphodiesterase but Does Not Affect the Estrogen Receptor. *Toxicol Lett* **154**: 61-68.

Roberts, W. C. and Abernathy, C. O. (1996). Risk Assessment: Principles and Methodolgies. Toxicology and Risk Assessment: Principles, Methods and Applications. A. M. Fan and L. W. Chang. New York, Marcel Dekker, Inc.: 245-270.

Rochette-Egly, C. (2003). Nuclear receptors: integration of multiple signalling pathways through phosphorylation. *Cell Signal* **15**, 355-66.

Roy, D., Angelini, N. L. and Belsham, D. D. (1999). Estrogen Directly Respresses Gonadotropin-Releasing Hormone (Gnrh) Gene Expression in Estrogen Receptor-Alpha (Eralpha)- and Erbeta-Expressing GT1-7 Gnrh Neurons. *Endocrinology* **140**(11): 5045-5053.

Saadi, M., Gerozissis, K., Rougeot, C., Minary, P., and Dray, F. (1990). Leukotriene C4-induced release of LHRH into the hypophyseal portal blood and of LH into the peripheral blood. *Life Sci* **46**, 1857-65.

Samuelsson, B., Dahlen, S. E., Lindgren, J. A., Rouzer, C. A., and Serhan, C. N. (1987). Leukotrienes and lipoxins: structures, biosynthesis, and biological effects. *Science* **237**, 1171-1176.

Sanderson, J. T., Letcher, R. J., Heneweer, M., Giesy, J. P. and van Den, B. M. (2001).Effects of Chloro-S-Triazine Herbicides and Metabolites on Aromatase Activity in Various Human Cell Lines and on Vitellogenin Production in Male Carp Hepatocytes. *Environ.Health Perspect.* **109**(10): 1027-1031.

Sanderson, J. T., Seinen, W., Giesy, J. P. and van den Berg, M. (2000).2-Chloro-S-Triazine Herbicides Induce Aromatase (Cyp19) Activity in H295r Human

Adrenocrotical Carcinoma Cells: A Novel Mechanism for Estrogenicity? *Toxicological Sciences* **54**: 121-127.

Sarangapani, R., Teeguarden, J., Plotzke, K. P., McKim, J. M., Jr., and Andersen, M. E. (2002). Dose-response modeling of cytochrome p450 induction in rats by octamethylcyclotetrasiloxane. *Toxicol Sci* **67**: 159-172.

Sarkar, D. K., Chiappa, S. A., Fink, G., and Sherwood, N. M. (1976). Gonadotropin-releasing hormone surge in pro-oestrous rats. *Nature* **264**, 461-3.

Savoy-Moore, R. T., Schwartz, N. B., Duncan, J. A., and Marshall, J. C. (1980). Pituitary gonadotropin-releasing hormone receptors during the rat estrous cycle. *Science* **209**, 942-4.

Savoy-Moore, R. T., Schwartz, N. B., Duncan, J. A., and Marshall, J. C. (1981). Pituitary gonadotropin-releasing hormone receptors on proestrus: effect of pentobarbital blockade of ovulation in the rat. *Endocrinology* **109**, 1360-4.

Schaiquevich, P., Niselman, A., and Rubio, M. (2002). Comparison of two compartmental models for describing ranitidine's plasmatic profiles. *Pharmacol Res.* **45**, 399-405.

Schlosser P.M, Bond J.A, Medinsky M.A. (1993). Benzene and phenol metabolism by mouse and rat liver microsomes. *Carcinogenesis.* **14**(12):2477-86.

Schrenk, D., Dekant, W., and Henschler, D. (1988). Metabolism and excretion of S-conjugates derived from hexachlorobutadiene in the isolated perfused rat kidney. *Mol. Pharmacol.* **34** (3): 407-412.

Schultz, I. R., Merdink, J. L., Gonzalez-Leon, A., and Bull, R. J. (1999). Comparative toxicokinetics of chlorinated and brominated haloacetates in F344 rats. *Toxicol Appl Pharmacol* **158**, 103-114.

Sealfon, S. C., Weinstein, H., and Millar, R. P. (1997). Molecular mechanisms of ligand interaction with the gonadotropin-releasing hormone receptor. *Endocr Rev* **18**, 180-205.

Seger, R., and Krebs, E. G. (1995). The MAPK signaling cascade. *Faseb J* **9**, 726-35.

Seglen P.O. (1976). Preparation of isolated rat liver cells. *Methods Cell Biol.* **13**:29-83

Selmanoff, M. (1997). Commentary on the use of immortalized neuroendocrine cell lines for physiological research. *Endocrine* **6**, 1-3.

Semino, G., Lilly, P. D. and Andersen, M. E. (1997).A Pharmacokinetic Model Describing Pulsatile Uptake of Orally-Administered Carbon Tetrachloride. *Toxicology* **117**: 25-33.

Shafer, T. J., Ward, T. R., Meacham, C. A. and Cooper, R. L. (1999).Effects of the Chlorotriazine Herbicide, Cyanazine, on Gaba(a) Receptors in Cortical Tissue from Rat Brain. *Toxicology* **142**(1): 57-68.

Shah, B. H., and Milligan, G. (1994). The gonadotrophin-releasing hormone receptor of alpha T3-1 pituitary cells regulates cellular levels of both of the phosphoinositidase C-linked G proteins, Gq alpha and G11 alpha, equally. *Mol Pharmacol* **46**, 1-7.

Shanker, G., and Aschner, M. (2001). Identification and characterization of uptake systems for cystine and cysteine in cultured astrocytes and neurons: Evidence for methylmercury-targeted disruption of astrocyte transport. *J Neurosci Res* **66**, 998-1002.

Short, R. E., Bellows, R. A., Staigmiller, R. B., Berardinelli, J. G., and Custer, E. E. (1990). Physiological mechanisms controlling anestrus and infertility in postpartum beef cattle. *J Anim Sci* **68**, 799-816.

Shughrue, P. J., Komm, B., and Merchenthaler, I. (1996). The distribution of estrogen receptor-beta mRNA in the rat hypothalamus. *Steroids* **61**, 678-81.

Shughrue, P. J., Lane, M. V. and Merchenthaler, I. (1997).Regulation of Progesterone Receptor Messenger Ribonucleic Acid in the Rat Medial Preoptic Nucleus by Estrogenic and Antiestrogenic Compounds: An in Situ Hybridization Study. *Endocrinology* **138**(12): 5476-84.

Shughrue, P. J., Lane, M. V., Scrimo, P. J., and Merchenthaler, I. (1998). Comparative distribution of estrogen receptor-alpha (ER-alpha) and beta (ER-beta) mRNA in the rat pituitary, gonad, and reproductive tract. *Steroids* **63**, 498-504.

Shughrue, P. J., Lane, M. V., and Merchenthaler, I. F. (1999). Biologically active estrogen receptor-beta: evidence from in vivo autoradiographic studies with estrogen receptor alpha-knockout mice. *Endocrinology* **140**, 2613-20.

Shraga-Levine, Z., Ben-Menahem, D., and Naor, Z. (1996). Arachidonic acid and lipoxygenase products stimulate protein kinase C beta mRNA levels in pituitary alpha T3-1 cell line: role in gonadotropin-releasing hormone action. *Biochem J* **316 (Pt 2)**, 667-70.

Sirica A.E, Pitot H.C. (1979). Drug metabolism and effects of carcinogens in cultured hepatic cells. *Pharmacol Rev.* **31**(3):205-28

Simerly, R. B., Chang, C., Muramatsu, M. and Swanson, L. W. (1990).Distribution of Androgen and Estrogen Receptor Mrna-Containing Cells in the Rat Brain: An in Situ Hybridization Study. *J Comp Neurol* **294**(1): 76-95.

Simerly, R. B., Carr, A. M., Zee, M. C. and Lorang, D. (1996).Ovarian Steroid Regulation of Estrogen and Progesterone Receptor Messenger Ribonucleic Acid in the Anteroventral Periventricular Nucleus of the Rat. *J Neuroendocrinol* **8**(1): 45-56.

Simic, B., Kniewald, J. and Kniewald, Z. (1994).Effects of Atrazine on Reprodcutvie Performance in the Rat. *J. of Applied Toxicol.* **14**(6): 401-404.

Simoneaux, B., Stevens, J. T., Breckenridge, C. B., Hui, X. and Wester, R. (2001).Comparison of the Percutaneous Absorption of ^{14}c-Atrazine in Man to Rodent. *The Toxicologist.*

Simpkins, J. W., Andersen, M. E., Brusick, D. J., Eldridge, J. C., Delzell, E., Lamb, J. C., McConnell, R. F., Safe, S., Tyrey, L. and Wilkinson, C. (2000). Evaluation of a Hormonal Mechanism for Mammary Tumorigenesis of the Chloro-S-Triazine Herbicides: Fourth Consensus Panel Report. Greensboro, NC, Novartis Crop Protection, Inc.: 1-21.

Simpson, E., Mahendroo, M., Means, G., Kilgore, M., Hinshelwood, M., Graham-Lorence, S., Amarneh, B., Ito, Y., Fishcer, C., Michael, M., Mendelson, C. and Bulun, S. (1994).Aromatase Cytochrome P450, the Enzyme Responsible for Estrogen Biosysnthesis. *Endocr Rev* **15**: 342-355.

Skinner, D. C., and Dufourny, L. (2005). Oestrogen receptor beta-immunoreactive neurones in the ovine hypothalamus: distribution and colocalisation with gonadotropin-releasing hormone. *J Neuroendocrinol* **17**, 29-39.

Skynner, M. J., Sim, J. A., and Herbison, A. E. (1999). Detection of estrogen receptor alpha and beta messenger ribonucleic acids in adult gonadotropin-releasing hormone neurons. *Endocrinology* **140**, 5195-201.

Spina, M. B., and Cohen, G. (1989). Dopamine turnover and glutathione oxidation: implications for Parkinson disease. *Proc Natl Acad Sci U S A.* **86**, 1398-400.

Stevens, J. T. and and Sumner, D. D. (1991). Herbicides. Handbook of Pesticide Toxicology. H. J. WH and E. Laws Jr. New York, Academic Press, Inc. **3:** 1317-1391.

Stevens, J. T., Breckenridge, C. B., and Wetzel, L. (1999). A risk characterization for atrazine: oncogenicity profile. *J. Toxicol. Environ. Health A* **56** (2) :69-109.

Stoker, T. E., Robinette, C. L. and Cooper, R. L. (1999).Maternal Exposure to Atrazine During Lactation Suppresses Suckling-Induced Prolactin Release and Results in Prostatitis in the Adult Offspring. *Toxicol. Sci.* **52**(1): 68-79.

Stoker, T. E., Laws, S. C., Guidici, D. L. and Cooper, R. L. (2000).The Effect of Atrazine on Puberty in Male Wistar Rats: An Evaluation in the Protocol for

the Assessment of Pubertal Development and Thyroid Function. *Toxicol.Sci.* **58**(1): 50-59.

Stoker, T. E., Guidici, D. L., Laws, S. C. and Cooper, R. L. (2002).The Effects of Atrazine Metabolites on Puberty and Thyroid Function in the Male Wistar Rat. *Toxicol. Sci.* **67**(2): 198-206.

Stojilkovic, S. S., Reinhart, J., and Catt, K. J. (1994). Gonadotropin-releasing hormone receptors: structure and signal transduction pathways. *Endocr Rev* **15**, 462-99.

Stojilkovic, S. S., and Catt, K. J. (1995). Novel aspects of GnRH-induced intracellular signaling and secretion in pituitary gonadotrophs. *J Neuroendocrinol* **7**, 739-57.

Studer, E. (1998). A veterinary perspective of on-farm evaluation of nutrition and reproduction. *J Dairy Sci* **81**, 872-6.

Suttle, A. B., Pollack, G. M., and Brouwer, K. L. (1992). Use of a pharmacokinetic model incorporating discontinuous gastrointestinal absorption to examine the occurrence of double peaks in oral concentration-time profiles. *Pharm Res* **9**, 350-6.

Suttle, A. B., and Brouwer, K. L. (1995a). Regional gastrointestinal absorption of ranitidine in the rat. *Pharm Res* **12**, 1311-5.

Suttle, A. B., and Brouwer, K. L. (1995b). Gastrointestinal transit and distribution of ranitidine in the rat. *Pharm Res.* **12**, 1316-22.

Tavera-Mendoza, L., Ruby, S., Brousseau, P., Fournier, M., Cyr, D., and Marcogliese, D. (2002a). Response of the amphibian tadpole (Xenopus laevis) to atrazine during sexual differentiation of the testis. *Environ Toxicol Chem.* **21**, 527-31.

Tavera-Mendoza, L., Ruby, S., Brousseau, P., M., F., Cyr, D., and Marcogliese, D. (2002b). Response of the amphibian tadpole Xenopus laevis to atrazine during sexual differentiation of the ovary. *Environ Toxicol Chem.* **21**, 1264-7.

Tennant, M. K., Hill, D. S., Eldridge, J. C., Wetzel, L. T., Breckenridge, C. B. and Stevens, J. T. (1994a).Possible Antiestrogenic Properties of Chloro-S-Triazines in Rat Uterus. *J.Toxicol.Environ.Health* **43**(2): 183-196.

Tennant, M. K., Hill, D. S., Eldridge, J. C., Wetzel, L. T., Breckenridge, C. B. and Stevens, J. T. (1994b).Chloro-S-Triazine Antagonism of Estrogen Action: Limited Interaction with Estrogen Receptor Binding. *J.Toxicol.Environ.Health* **43**(2): 197-211.

Thakur, A. J., Wetzel, L. T., Voelker, R. W. and Wakefield, A. E. (1998). Results of a Two-Year Oncogenicity Study in Fischer 344 Rats with Atrazine, Washington, DC: American Chemical Society.

Thede, B. (1987). Study of ^{14}-C-Atrazine Dose/Response Relationship in the Rat. Greensboro, North Carolina, Ciba - Geigy Corporation: 1-33.

Thede, B. (1988). Comparative Metabolism of Atrazine by Mammalian Hepatocytes: Progress Report. Greensboro, North Carolina, Ciba - Geigy Corporation.

Thomas, P., Pang, Y., Filardo, E. J., and Dong, J. (2005). Identity of an estrogen membrane receptor coupled to a G protein in human breast cancer cells. *Endocrinology* **146**, 624-32.

Thurman R.G., Kauffman F.C. (1979). Factors regulating drug metabolism in intact hepatocytes. *Pharmacol Rev.* **31**(4):229-51.

Timchalk, C., Dryzga, M. D., Langvardt, P. W., Kastl, P. E., and Osborne, D. W. (1990). Determination of the effect of tridiphane on the pharmacokinetics of [^{14}C]-atrazine following oral administration to male Fischer 344 rats. *Toxicology* **61**(1) :27-40.

Toft, D., and Gorski, J. (1966). A receptor molecule for estrogens: isolation from the rat uterus and preliminary characterization. *Proc Natl Acad Sci U S A* **55**, 1574-81.

Traber, P. G., Chianale, J., Florence, R., Kim, K., Wojik, E., and Gumucio, J. J. (1988). Expression of cytochrome P450b and P450c genes in small intestinal mucose of rats following treatment with phenobarbital, polyhalogenated biphenyls, and oraganochlorine pesticides. *J Biol Chem* **263**, 9449-55.

Tran, D. Q., Kow, K. Y., McLachlan, J. A. and Arnold, S. F. (1996).The Inhibition of Estrogen Receptor-Mediated Responses by Chloro-S-Triazine-Derived Compounds Is Dependent on Estradiol Concentration in Yeast. *Biochem.Biophys.Res.Commun.* **227**(1): 140-146.

Trenga, C. A., Kunkel, D. D., Eaton, D. L., and Costa, L. G. F. (1991). Effect of styrene oxide on rat brain glutathione. *Neurotoxicology* **12**, 165-78.

Tsai, M. J., and O'Malley, B. W. (1994). Molecular mechanisms of action of steroid/thyroid receptor superfamily members. *Annu Rev Biochem* **63**, 451-86.

U.S.EPA (2001). Revised Preliminary Human Health Risk Assessment on Atrazine, Registration Branch 3,Health Effects Division,Office of Pesticide Programs.

Vali Pasha, K., and Vijayan, E. (1990). Glutathione and gamma-glutamyl transpeptidase in the adult female rat brain after intraventricular injection of LHRH and somatostatin. *Biochem Int.* **21**, 209-17.

Walters, M. J., Brown, T. J., Hochberg, R. B. and MacLusky, N. J. (1993).In Vitro Autoradiographic Visualization of Occupied Estrogen Receptors in the Rat Brain with an Iodinated Estrogen Ligand. *J Histochem Cytochem* **41**(9): 1279-90.

Wang, H. J., Hoffman, G. E., and Smith, M. S. (1995). Increased GnRH mRNA in the GnRH neurons expressing cFos during the proestrous LH surge. *Endocrinology* **136**, 3673-6.

Wetzel, L. T., Luempert, L. G., III, Breckenridge, C. B., Tisdel, M. O., Stevens, J. T., Thakur, A. K., Extrom, P. J. and Eldridge, J. C. (1994). Chronic Effects of Atrazine on Estrus and Mammary Tumor Formation in Female Sprague-Dawley and Fischer 344 Rats. *J.Toxicol.Environ.Health* **43**(2): 169-182.

Wacher, V. J., Silverman, J. A., Zhang, Y., and Benet, L. Z. (1998). Role of P-glycoprotein and cytochrome P450 3A in limiting oral absorption of peptides and peptidomimetics. *J Pharm Sci.* **87**, 1322-30.

Wiegand, S. J., Terasawa, E., Bridson, W. E., and Goy, R. W. (1980). Effects of discrete lesions of preoptic and suprachiasmatic structures in the female rat. Alterations in the feedback regulation of gonadotropin secretion. *Neuroendocrinology* **31**, 147-57.

Windle, J. J., Weiner, R. I., and Mellon, P. L. (1990). Cell lines of the pituitary gonadotrope lineage derived by targeted oncogenesis in transgenic mice. *Mol Endocrinol* **4**, 597-603.

Wise, P. M. (1982).Norepinephrine and Dopamine Activity in Microdissected Brain Areas of the Middle-Aged and Young Rat on Proestrus. *Biol Reprod* **27**: 526-574.

Wise, P. M. (1984).Estradiol-Induced Daily Luteinizing Hormone and prolactin Surges in Young and Middle-Aged Rats: Correlations with Age-Related Changes in Pituitary Responsiveness and Catecholamine Turnover Rates in Microdissected Areas. *Endocrinology* **115**: 801-809.

Yasin, M., Dalkin, A. C., Haisendleder, D.J., Kerrigan, J. R., and Marshall, J. C. (1995). GnRH pulse pattern regulates GnRH receptor gene expression:augmentation by estradiol. *Endocrinology* **136**, 1559-1564.

Yuan, H., Bowlby, D. A., Brown, T. J., Hochberg, R. B. and MacLusky, N. J. F. (1995).Distribution of Occupied and Unoccupied Estrogen Receptors in the

Rat Brain: Effects of Physiological Gonadal Steroid Exposure. *Endocrinology* **136**(1): 96-105.

Zhou, H. (2003). Pharmacokinetic strategies in decipherine atypical drug absorption profiles. *J Clin Pharmacol* **43**, 211-227.

APPENDICES

APPENDIX 1: (Chapter 2)

A: Abbreviations

Abbreviations used in the total chlorotriainze model and not described in Table 4.1 are defined below:

ACHPL = amount of free (unbound) chlorotriazines in the plasma
AGPL = amount of glutathione conjugates in the plasma
CCH (PL,BD,LIV,BR) = concentration of free (unbound) chlorotriazines in the plasma, body, liver, brain
CGPL = concentration of glutathione conjugates in the plasma
APLBOUND = amount of bound triazine RBC complex
CPLBOUND = concentration of bound triazine RBC complex
ARECRBC = amount of unbound RBC in blood
CRECRBC = concentration of unbound RBC in blood
APPR = amount of plasma protein (albumin)
CPPR = concentration of plasma protein (albumin)
APPRbound = amount of bound triazine plasma protein complex
CPPRbound = concentration of bound triazine plasma protein complex
AMET = metabolism of chlorotriazine pool to glutathione conjugates
AGEXC = total amount of glutathione conjugate pool eliminated
AGURINE = amount of glutathione conjugate pool eliminated into urine
ACHEXC = amount of chlorotriazine pool eliminated into urine
TURINE = total amount of GSH and chlorotriazine pools eliminated into urine
TELIM = total amount of GSH and chlorotriazine pools eliminated into urine and Feces
MWT = molecular weight of ATRA

B: Key differential equations

Key differential equations used in modeling chlorotriazine and GSH conjugates separate from total radioactivity are listed below:

Free Chlorotriazines and GSH conjugates in plasma compartment

(1) Circulating free ATRA/chlorinated metabolite concentration in plasma

```
dACHPL/dt = Qbd*(CCHBD/Pbd)+Qliv*(CCHLIV/liv+ Qbr*(CCHBR/Pbr)
            -Qpl*CCHPL - (dAPLBOUND/dt) - (Kelimch*CCHPL)
            -(Kppr*CCHPL*CPPR*Vpl)
ACHPL = Integral (dACHPL/dt,0)
CCHPL = ACHPL/Vpl
```

(2) Circulating glutathione conjugate concentration in plasma

```
dAGPL/dt = Qbd*(CGBD/Rbd)+Qliv*(CGLIV/Rliv)+ Qbr*(CGBR/Rbr)
      - Qpl*CGPL – dAGEXC/dt
AGPL = INTEG(dAGPL/dt,0)
CGPL = AGPL/Vpl
```

RBC and Plasma Protein Binding
(3a) Circulating concentration of red blood cells

dARECRBC/dt = -Krbc* CCHPL*Vrbc*CRECRBC/MWT
ARECRBC = Integral (dARECRBC/dt,0)
CRECRBC = ARECRBC/Vrbc

(3b) Chlorotriazine binding to red blood cells

dAPLBOUND/dt = Krbc* CCHPL*CRECRB*Vrbc
APLBOUND = Integral (dAPLBOUND/dt,0)
CPLBOUND = APLBOUND/Vrbc

(4a) Circulating concentration of unbound plasma protein (albumin)

dAPPR/dt = Kfpp - (Kepp*CPPR*Vpl) - (Kppr*CCHPL*CPPR*Vpl)
APPR = Integral (dAPPR/dt, APPR0)
CPPR = (APPR/Vpl)

(4b) Chlorotriazine binding to plasma protein (albumin)

dAPPRbound/dt = (Kppr*CCHPL*CPPR*Vpl) – (Ke*CPPRbound*Vpl)
APPRbound = Integral (dAPPRbound/dt, 0)
CPPRbound = APPRbound/Vpl

Metabolism and Elimination
(5) Metabolism of chlorotriazine pool to GSH conjugate pool

dAMET/dt = Kgsh*Vliv*CGSH*(CCHLIV/Pliv)

(6) Elimination of GSH conjugates into urine and feces

dAGEXC/dt = Kelimg*CGPL
AGEXC = INTEG(dAGEXC/dt,0)
AGURINE = AGEXC * PU

(7) Elimination of chlorotriazine pool into urine

dACHEXC = (Kelimch*CCHPL) + (Ke*CPPRbound*Vpl)
ACHEXC = INTEG(dACHEXC,0)

Total amount in urine
URINE = AGURINE + ACHEXC

Total Elimination (amount in urine and feces)
ELIM = AGEXC + ACHEXC

APPENDIX 2. (Chapter 4)

A: Abbreviations

Abbreviations used in the in vitro model and not described in Table 5.2 are defined below:

Catra (ethyl, iso, dact) = concentration of Cl-TRI in flask

B. Key Differential Equations

Differential equations used in modeling chlorotriazine time-course concentrations in flask after initial incubation with ATRA. See Chapter 5 for differential equations describing competitive metabolic inhibiton.

Concentrations of Cl-TRIs in flask

(1) Concentration of ATRA

dCatra'/dt = -METatra;

(2) Concentration of ISO

dCiso/dt = Frac*METatra - METiso;

(3) Concentration of ETHYL

dCethyl/dt = (1-Frac)*METatra - METethyl

(4) Concentration of DACT

dCdact/dt =METiso+ METethyl;

APPENDIX 3. (Chapter 6)

Abbreviations used in the in vivo metabolite model and not described in Table 6.1 are defined below:

A: Abbreviations

ALatra (iso, ethyl, da) = amount chlorotriazine in liver
CLatra (iso, ethyl, da) = concentration of Cl-TRI in liver
ABDatra (iso, ethyl, da) = amount Cl-TRI in body
CBDatra (iso, ethyl, da) = concentraiton of Cl-TRI in body
CPLatra (iso, ethyl, da) = concentration of Cl-TRI in plasma
AMETatra_iso = amt. ATRA metabolized to ISO
AMETatra_ethyl = amt. ATRA metabolized to ETHYL
AELIMatra (ethyl, iso, da) = amt. Cl-TRI eliminated from body

B. Key Differential Equations

Differential equations used in modeling chlorotriazine time-course concentrations after dosing with ATRA.

Ciculating concentration of Cl-TRIs in body/plasma

(5) Circulating concentration of ATRA in body/plasma

dABDatra/dt= QL*(CLatra/PL) + QBR*(CBRatra/PBR) - QPL*CPLatra
CBDatra=ABDatra/VBD
CPLatra = CBDatra/PBD

(6) Circulating concentration of ISO in body/plasma

dABDiso/dt = QL*(CLiso/PL) +QBR*(CBRiso/PBR) - QPL*CPLiso
CBDiso=ABDiso/VBD
CPLiso = CBDiso/PBD

(7) Circulating concentration of ETHYL in body/plasma

dABDethyl/dt = QL*(CLethyl/PL) + QBR*(CBRethyl/PBR) - QPL* CPLethyl
CBDethyl=ABDethyl/VBD
CPLethyl = CBDethyl/PBD

(8) Circulating concentration of 'DACT in body/plasma

dABDda/dt = QL*(CLda/PL) + QBR*(CBRda/PBR) - QPL *CPLda
CBDda=ABDda/VBD
CPLda = CBDda/PBD

Ciculating concentration of Cl-TRIs in liver

(1) Circulating concentration of ATRA in liver

dALatra/dt=QL*(CPLatra - CLatra/PL) - AMETatra_iso' - AMETatra_ethyl' - AELIMatra' +fastloss1+slowloss1+zeroloss1
CLatra=ALatra/VL

(2) Circulating concentration of ISO in liver

ALiso'=QL*(CPLiso - CLiso/PL) +AMETatra_iso' - AMETiso' -AELIMiso' +fastloss3+slowloss3+zeroloss3
CLiso=ALiso/VL

(3) Circulating concentration of ETHYl in liver

dALethyl/dt=QL*(CPLethyl - CLethyl/PL) +AMETatra_ethyl' - AMETethyl' -AELIMethyl' +fastloss2+slowloss2+zeroloss2

CLethyl=ALethyl/VL

(4) Circulating concentration of DACT in liver

dALda'=QL*(CPLda - CLda/PL) +AMETiso' +AMETethyl' -AELIMda'
CLda=ALda/VL

Absorption of Cl-TRIs by multiple uptake processes
abbreviations are defined in Chapter 6
(5) fast-first order loss from gut that includes pre-systemic metabolism of atra
dagutfast/dt = -kafast*agutfast
fastloss1 = -propfast1*agutfast'
fastloss2 = -propfastethyl*agutfast'
fastloss3= -propfastiso*agutfast'
propfast1 = kafast/(krxn+kafast)
propfastethyl= (1-frac)*(krxn/(krxn+kafast))
propfastiso = frac*(krxn/(krxn+kafast))

(6) slow first-order loss from gut that includes pre-systemic metabolsm of atra
dagutslow/dt = if time<tdl1 then 0 else (-kaslow*doseslow* exp(-kaslow*delayslow))
slowloss1 = -propslow1*agutslow'
slowloss2 = -propslowethyl*agutslow'
slowloss3 = -propslowiso*agutslow'
propslow1 = kaslow/(krxn+kaslow)
propslowethyl=(1-frac)*(krxn/(krxn+kaslow))
propslowiso=frac*(krxn/(krxn+kaslow))
delayslow = if time< tdl1 then 0 else (time-tdl1)

(7) zero-order loss from gut that includes pre-systemic metabolism of atra
dagutzero/dt = if time<tdl2 then 0 else (-vgut*agutzero/(kgut+agutzero))
zeroloss1 = -propzero1*agutzero'
zeroloss2 = -propzeroethyl*agutzero'
zeroloss3= -propzeroiso*agutzero'
propzero1= kapprox/(kapprox+krxn)
propzeroethyl=(1-frac)*(krxn/(krxn+kapprox))
propzeroiso=frac* (krxn/(krxn+kapprox))
kapprox=Vgut/(kgut+agutzero)

Saturable Oxidative Metabolism in Liver
(8) ATRA metabolism to ISO
dAMETatra_iso/dt = frac*(VMAXatra*CLatra/PL)/(KMatra + CLatra/PL)

(9) ATRA metabolism to ETHYL

dAMETatra_ethyl/dt = (1-frac)*(VMAXatra*CLatra/PL)/(KMatra + CLatra/PL)

(10) ISO metabolism to DACT

dAMETiso/dt=(VMAXiso*CLiso/PL)/(KMiso*(1+CLatra/PL/KMatra1+CLethyl/PL/KMethyl1) + CLiso/PL)

(11) ETHYL metabolism to DACT

dAMETethyl/dt = (VMAXethyl*CLethyl/PL)/(KMethyl*(1+CLatra/PL/KMatra1+CLiso/PL/KMiso1) + CLethyl/PL)